PETROLOGY OF THE SUTHERLAND COMMONAGE MELILITITE INTRUSIVES

by

K.S. VILJOEN

Thesis submitted in fulfillment of the requirements for the degree of Master of Science in the Department of Geochemistry, University of Cape Town, under the supervision of Professor J.J. Gurney.

December 1988

The copyright of this thesis vests in the author. No quotation from it or information derived from it is to be published without full acknowledgement of the source. The thesis is to be used for private study or non-commercial research purposes only.

Published by the University of Cape Town (UCT) in terms of the non-exclusive license granted to UCT by the author.

University of Cape Town

DECLARATION

I hereby declare that all the work presented in this thesis is my own, except where otherwise stated in the text.

K.S. Viljoen
December, 1988

ABSTRACT

The petrology of the Sutherland Commonage olivine melilitite intrusives have been investigated using petrographic and chemical methods.

The occurrence consists of a ring dyke which surrounds a centrally located sill complex. The rock of the ring dyke is a typical melilitite which consists of olivine in a groundmass of melilite, clinopyroxene, opaque spinel, nepheline and perovskite.

The sill complex is a multiple intrusion and is comprised of a lower green melilitite and an overlying (and younger) grey melilitite. The green melilitite is deuterically altered and the original mineralogy is destroyed to a large extent. The grey melilitite contains autoliths of the green and is a fairly typical monticellitic melilitite in which phenocrysts of olivine are set in a groundmass of melilite, monticellite, opaque spinel, nepheline and perovskite.

Microprobe analyses of clinopyroxenes indicate that they are aluminous titanian diopsides and salites which exhibit complex zonation patterns. They record magmatic conditions ranging from the intrusive stage to a final phase of magmatic evolution during which a vapour phase evolved after the majority of the groundmass minerals had crystallised.

The chemistry of olivine phenocrysts suggests that the parent magma to the Commonage intrusives accumulated in a temperature-zoned reservoir at the base of the lithosphere. Large, unzoned olivine phenocrysts crystallised in this chamber. Subsequent rupture of the chamber and ascent of magma led to supercooling and the crystallisation of abundant, strongly zoned phenocrysts of smaller size. Olivine crystallisation continued until the magma reached crustal levels.

It is inferred from the chemistry of chromites and magnetites that the magma in the ring dyke was more evolved than those in the sill complex and that very oxidising conditions prevailed in the grey melilitite during the crystallisation of magnetite in this intrusive type. The high fO_2 may have resulted from the degassing of CO_2 after intrusion.

Major and trace elements have been analysed for in eleven whole rock samples and the $^{87}Sr/^{86}Sr$ ratio was determined for seven of the same samples. The results of the geochemical study suggest that the Commonage melilitites were derived by the melting of a recently metasomatised region of the asthenosphere, probably under the influence of an ocean-island-type hotspot situated in the lower mantle.

ACKNOWLEDGEMENTS

I am indebted to a number of people for their help, advice and encouragement whilst writing this thesis. I would like to thank the following people:

J.B. Hawthorne, C.R. Clement and M. Skinner for permitting me to work on this project, and for arranging funding from De Beers Consolidated Mines.

M. Otter and R. Rickard who instructed me in the usage of the electron microprobe.

S. Newton and R. Sweeney for their advice and help in whole rock XRF analysis.

T. Clark for instruction in chemical methods, filament preparation and mass spectrometer calisthenics at the isotope laboratory of the Bernard Price Institute. His help in this respect was instrumental to the completion of this work.

J. Bristow and H. Welke for arranging access to the BPI isotope laboratory.

R. Moore, S. Shee, M. Field and H. Grütter for proofreading this thesis and trenchant comments.

L. Colgan for her help, encouragement and companionship.

W. Mbolweni for cheerfully producing a seemingly endless stream of doubly polished thin sections.

S. Hastie and S. Vermaas for draughting all the diagrams.

F. Joseph for developing and printing all the photographic plates.

The people of Sutherland for their hospitality and the Town Council for allowing me to work on the Commonage.

Various patrons of the Star for their cheerful companionship when academia became a burden.

CONTENTS

LIST OF TABLES

LIST OF FIGURE CAPTIONS

1 INTRODUCTION

1.1 Location

The olivine melilitite occurrence investigated occurs on a low escarpment to the north-west of Sutherland, a small Karoo town in the Cape Province, R.S.A. (figure 1.1).

1.2 Previous work on the Sutherland Commonage intrusives

The field relations and petrography of the Commonage were first investigated by Rogers and Du Toit (1903, 1904). Taljaard (1936) presented detailed petrographic descriptions of a number of samples and also the first chemical analyses. The geology and petrography of the Commonage rocks were also the subject of an M.Sc. study by Gerard (1958), and K-Ar dating and paleomagnetic studies were carried out by Duncan (et al., 1978). Limited mineral chemistry and whole-rock chemical data were presented in general studies on the petrology of melilitites from the R.S.A. by McIver and Ferguson (1979), Dawson (et al., 1985) and Boctor and Yoder (1986).

1.3 Objectives of the present study

Olivine melilitites have superficial similarities to kimberlites and this has led some investigators (e.g. McIver and Ferguson, 1979; Moore and Erlank, 1979 and Raeside and Helmstaedt, 1982) to believe that the parent magmas of these rocks are genetically related. As will be shown in the review presented below, many significant differences exist between these rock types, and olivine melilitites are thought to represent a seperate and unrelated group of rocks to

Figure 1.1 Location of the study area

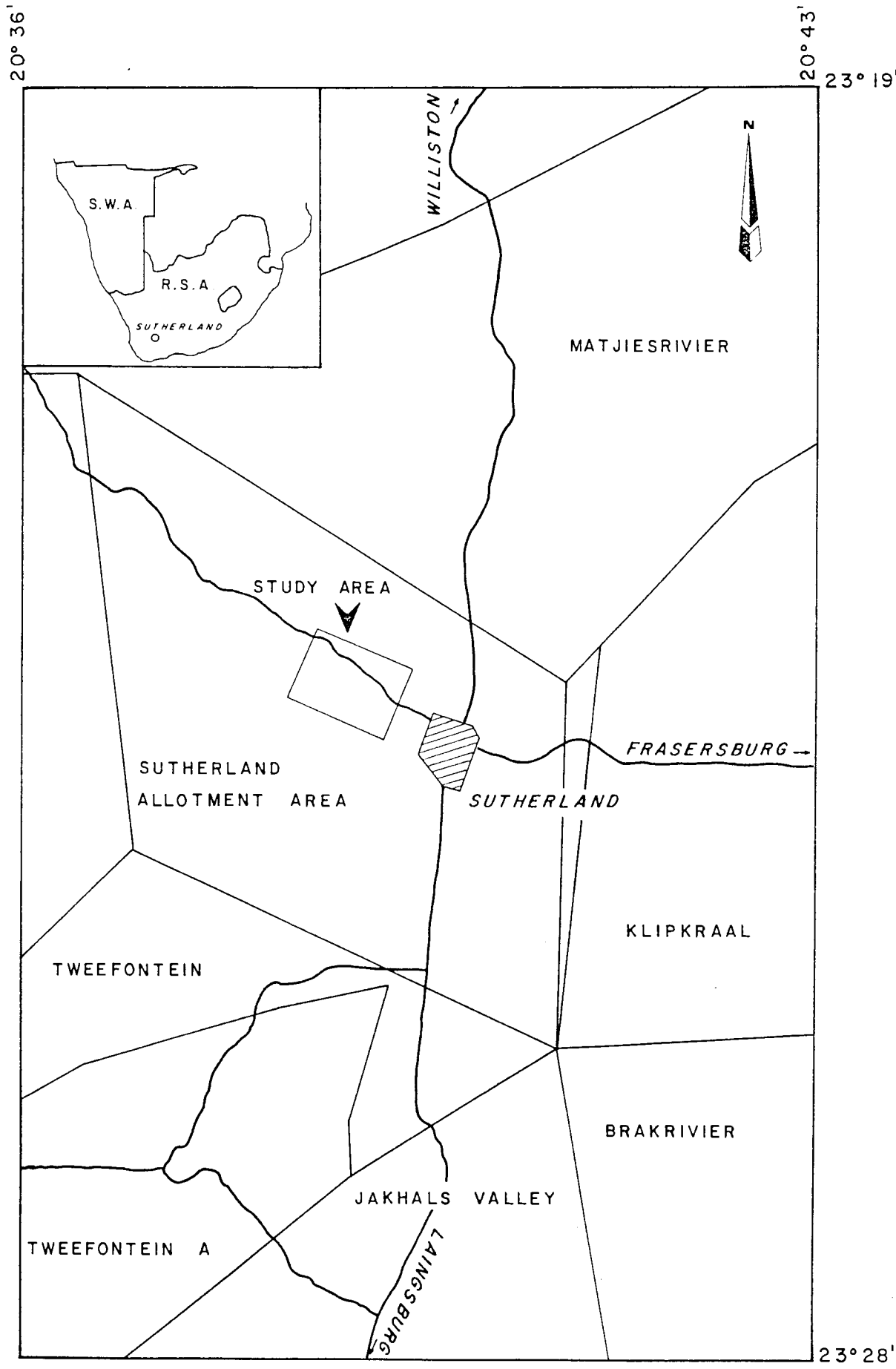

kimberlites.

At present a reasonably comprehensive volume of data on the characteristics of kimberlites exist (e.g. Clement, 1982; Shee, 1986; Mitchell, 1986 and Skinner, 1988). The petrology of olivine melilitites, on the other hand, is comparatively poorly known. The Commonage intrusives are classic olivine melilitites, and the occurrence could potentially serve as a type locality for melilitites in general and is therefore worthy of detailed study. All the previous studies of the Commonage melilitites were done on small sample suites for which information on sample localities and detailed petrography were not given.

This thesis therefore represents a study of the petrology of the Sutherland Commonage olivine melilitite intrusives. The objectives of this study include:

(1)An update on the geology and petrography of the intrusives;

(2)An analysis of the evolutionary trends of clinopyroxene, olivine and spinel mineral chemistry data;

(3)An analysis of whole-rock chemistry and an interpretation of the interrelationship of rock types;

(4)An evaluation of trace elements and strontium isotopes as petrogenetic indicators for the origin of these rocks;

(5)An evaluation of the influence of late stage processes on the mineralogical variability of melilitites.

1.4 A review of the characteristics of olivine melilitites; comparison to kimberlites (adapted from Shee, 1986)

1.4.1 Introduction

The following review of the geology and mineralogy of olivine melilitites is based on studies of several occurrences. South African localities include the Garies and Gamoep clusters in Namaqualand (Moore, 1979; Moore and Erlank, 1979; Moore, 1981; McIver, 1981; Moore, Erlank and Duncan,1982 and Moore, 1983) and the Sutherland Commonage and Saltpetre Kop occurrences in the Cape Province (Moore, 1979; McIver and Ferguson, 1979 and Boctor and Yoder, 1986). Two Canadian occurrences have been studied, these are the Marathon dykes, Ontario (Platt and Mitchell, 1979 & 1982) and the Ile Bizard intrusion, Montreal, Quebec (Raeside and Helmstaedt, 1982; Mitchell, 1983). Olivine melilitites occur as rare rocks scattered over Western Europe and their mineralogy, geology and isotopic character has been investigated by Hernandez (1976); Velde and Thiebault (1973); Wimmenauer (1967); Shrbeny and Machacek (1974); Frechen (1963) and Alibert (et al., 1983). An olivine melilitite intrusion in an oceanic setting occurs on the Malaita Island, Solomon Islands. This occurrence has been studied by Dawson (et al., 1978); Nixon and Boyd (1979); Nixon (et al., 1980) and Bielski-Zyskind (et al., 1984).

1.4.2 Petrography

Olivine melilitites characteristically contain euhedral olivine phenocrysts and magnetite macrocrysts set in a fine grained matrix of clinopyroxene, melilite, phlogopite, serpentine, calcite, apatite, melanite-schorlomite garnet, nepheline, perovskite and spinel. They characteristically

have porphyritic or microporphyritic textures, but rare examples containing relatively large anhedral olivine macrocrysts which impart a macrocrystic texture to the rock do occur (Moore, 1979). This is in contrast to the macrocrystic textures commonly observed in kimberlites. The olivine phenocrysts in olivine melilitites have complex multiple growth or resorbed textures (hopper crystals) compared to the euhedral phenocrysts commonly occurring in kimberlites. Olivines in some melilitites have been corroded and embayed by reaction with the surrounding liquid, producing rims of phlogopite followed by melilite and other matrix minerals. In other cases the olivine phenocrysts show a reaction relationship with monticellite or melilite. Minerals such as melilite, nepheline and melanite-schorlomite garnet are not observed in kimberlites. It is now recognised that melilite has a limited stability field and that under certain physical conditions (excess water, temperature < 750°C and pressures < 7 Kb) monticellite will crystallise rather than melilite (Yoder, 1968). Boctor and Yoder (1986) noted that although the effect of pressure on the stability of Ti-rich melanite-schorlomite garnet is not known, its occurrence in association with melilite in the groundmass suggests that it formed at low pressures.

1.4.3 Xenoliths and megacrysts

Ultramafic xenoliths and megacrysts of presumed upper mantle origin do occur in some olivine melilitites but are not usually abundant or common. Moore (1979) noted the presence of spinel harzburgite xenoliths and olivine megacrysts in the Zwartheuwel and Hoedkop olivine melilitites in the Gamoep

cluster. They also occur as rare constituents of other Gamoep pipes but were not found in any of the Garies pipes. Rare garnet lherzolites from the Hoedkop pipe yield equilibration pressures of 25 Kb and temperatures of 937°C (Moore, 1979) which are considerably lower than those obtained from similar xenoliths in kimberlite pipes e.g. garnet lherzolites from Bultfontein have calculated temperatures and pressures of 860°C - 1228°C and 36,2 - 54,4 Kb (Lawless, 1978). McIver and Ferguson (1979) reported the presence of hornblende, biotite and ilmenite megacrysts in carbonate-rich intrusions around Saltpetre Kop and abundant coarse (several centimetres) amphibole, clinopyroxene, ilmenite and brown mica megacrysts in the associated Silverdam pyroclastics. The Ile Bizard intrusion near Montreal contains megacrysts of aluminous clinopyroxene, phlogopite and Mg-titanomagnetite (Raeside and Helmstaedt, 1982) which do not resemble the megacryst suite commonly found in kimberlites. Peridotites (dunites, harzburgites and lherzolites) and websterites occur in the Ile Bizard occurrence. Many of these xenoliths contain phlogopite and/or amphibole. The few xenoliths with the requisite mineralogy yielded equilibration temperatures of 880 - 980°C and pressures of 21 - 28 Kb, which again are shallower than those found in kimberlites. Garnet lherzolite xenoliths, spinel lherzolite xenoliths and megacrysts of pyrope, augite, augite-ilmenite, subcalcic diopside and bronzite from the Malaita olivine melilitite have been studied by Nixon and Boyd (1979). The deep-seated garnet lherzolites equilibrated approximately at pressures of 18 - 33 Kb and temperatures of 850 - 1100°C. The xenoliths and megacrysts from the Malaita occurrence yield a higher geothermal gradient than those

obtained for continental kimberlite-derived nodules.

In summary, olivine melilitites do not generally contain abundant mantle-derived xenolithic material. The xenoliths that are recovered tend to have equilibrated at lower pressures than those recovered from kimberlites.

1.4.4 Chemistry of olivine

Moore (1979) studied the olivine melilitites in Namaqualand, South Africa and analysed many olivine macrocrysts and phenocrysts. He noted the presence of two compositionally distinct types of olivine macrocrysts - more forsteritic macrocrysts (Fo_{91}) are indistinguishable from those in kimberlites whilst the second group ($Fo_{70.8 - 81.5}$) are much more iron-rich than olivine macrocrysts in kimberlites. The olivine phenocrysts in these olivine melilitites are typically skeletal in appearance, a feature which is not commonly observed in kimberlites. Moore (1979) concluded that the olivine phenocrysts were quench or hopper crystals. These hopper olivines are much more iron-rich ($Fo_{80.5 - 85.5}$) than olivine phenocrysts in kimberlites ($Fo_{87 - 94}$).

McIver and Ferguson (1979) note that the olivine phenocrysts in the Saltpetre Kop olivine melilitites have been corroded and embayed by reaction with the surrounding liquid, producing rims of phlogopite followed by melilite, magnetite, perovskite, minor monticellite and anorthite. Platt and Mitchell (1982) have studied ultramafic dyke rocks (lamprophyres) from McKellar Harbour, Ontario in Canada. The

rocks which are termed the Marathon dykes (Platt and Mitchell, 1979) consist of phenocrysts of olivine and titanian phlogopite set in a groundmass of titanian phlogopite, spinel, apatite, perovskite, carbonate and altered laths thought to be relic melilite. The presence of these laths allows classification of the Marathon dykes as olivine melilitites. The relatively iron-rich compositions of the olivine phenocrysts ($Fo_{81 - 87}$) is consistent with this interpretation. The compositions of olivine phenocrysts ($Fo_{84.1 - 85.8}$) from Malaita (Nixon et al., 1980) are similar to those of olivine in other olivine melilitites mentioned above. The olivine macrocrysts (Fo_{91}) consist of strained grains and are thought to represent disaggregated lherzolite xenoliths. The composition of the macrocrysts are similar to the olivine macrocrysts in kimberlites.

It is clear from the examples cited that the compositions of olivine phenocrysts in olivine melilitites are consistently more iron-rich than olivine phenocrysts in kimberlites. The relatively forsterite-poor compositions of the olivine phenocrysts in olivine melilitites could be explained if they crystallised from a relatively evolved (differentiated) magma and/or if the magma formed by partial melting of a more fertile peridotite (garnet lherzolite) containing more iron-rich olivines.

1.4.5 Major element chemistry

Olivine melilitites have compositions which have similarities and differences to those of kimberlites. As a group the olivine melilitites have high TiO_2, Al_2O_3, Fe_2O_3,

MnO, CaO and Na_2O and low MgO and CO_2 contents compared to kimberlites. They have similar SiO_2 contents to Group 2 kimberlites and similar K_2O contents to Group 1 kimberlites.

1.4.6 Trace element chemistry

Olivine melilitites have higher S, V, Cu, Zn, Zr and Y and lower Cr, Rb, Ni and Ba contents than kimberlites. Sr, Co and Nb contents are similar. REE abundances are much lower than in kimberlites.

1.4.7 Radiogenic isotopes

Relatively few isotopic studies have been carried out on olivine melilitites. Moore (1979) reported initial $^{87}Sr/^{86}Sr$ ratios of between 0.70338 - 0.70403 for t > Namaqualand olivine melilitites, and Marsh (et al., 1981) determined the Nd and Sr isotopic systematics of specimens of olivine melilitite from the Garies and Gamoep clusters in Namaqualand. The initial $^{87}Sr/^{86}Sr$ ratios of the latter group fall in the range 0.70325 - 0.70385, and although Marsh et al. (op. cit.) did not cite initial $^{143}Nd/^{144}Nd$ ratios, they noted that both the Sr and Nd isotopes are consistent with the olivine melilitites being derived from a source that is depleted in Rb/Sr and Nd/Sm relative to bulk earth values. In this respect the Namaqualand olivine melilitites resemble Group 1 kimberlites (Smith, 1983). Alibert (et al., 1983) reported that European melilitites had $^{87}Sr/^{86}Sr$ ratios in the range of 0.703223 - 0.706536 and $^{143}Nd/^{144}Nd$ ratios in the range 0.512688 - 0.513004 indicating derivation from a depleted isotopic source. When the isotopic data is plotted on an initial Sr-Nd diagram (figure 1.2) most analyses plot within

the mantle array of O'Nions (et al., 1977). Alibert et al. (op. cit.) noted that some samples had distinctly high $^{87}Sr/^{86}Sr$ ratios which they attributed to late-stage contamination of the melilitites by a crustal component. The Malaita olivine melilitite has initial $^{87}Sr/^{86}Sr$ in the range 0.70455 - 0.70467 and $^{143}Nd/^{144}Nd$ in the range 0.511956 - 0.512802 (Bielski-Zyskind et al., 1984). The Malaita melilitite plots within the Group 1 kimberlite field on the plot of initial Sr vs. Nd isotope ratios. All studies of olivine melilitites to date indicate that they are derived from sources which are isotopically similar to Group 1 kimberlites i.e. depleted in Rb/Sr and Nd/Sm relative to Bulk Earth.

1.4.8 Genesis of olivine melilitites

The geochemistry of olivine melilitites is consistent with formation by partial melting of a garnet lherzolite source. The fact that olivine melilitites in South Africa occur in the outer margins of the Namaqua-Natal mobile belt (Moore, 1979 and Skinner, 1988), the absence of diamonds and the absence of deep seated mantle derived xenoliths all indicate that the olivine melilitites originated at relatively shallow levels in the upper mantle. This is in keeping with the high geothermal gradient in the outer parts of mobile belts. Isotopically olivine melilitites have similar characteristics to Group 1 kimberlites and ocean island basalts and are thought to have their source areas in the convecting asthenosphere. The relatively low pressures at which olivine melilitites form could in part be responsible for their less magnesian compositions than kimberlites (c.f. Takahashi and Scarfe,

Figure I.2 Sr and Nd isotopic data for kimberlites, melilitites, lamproites and ocean basalts.

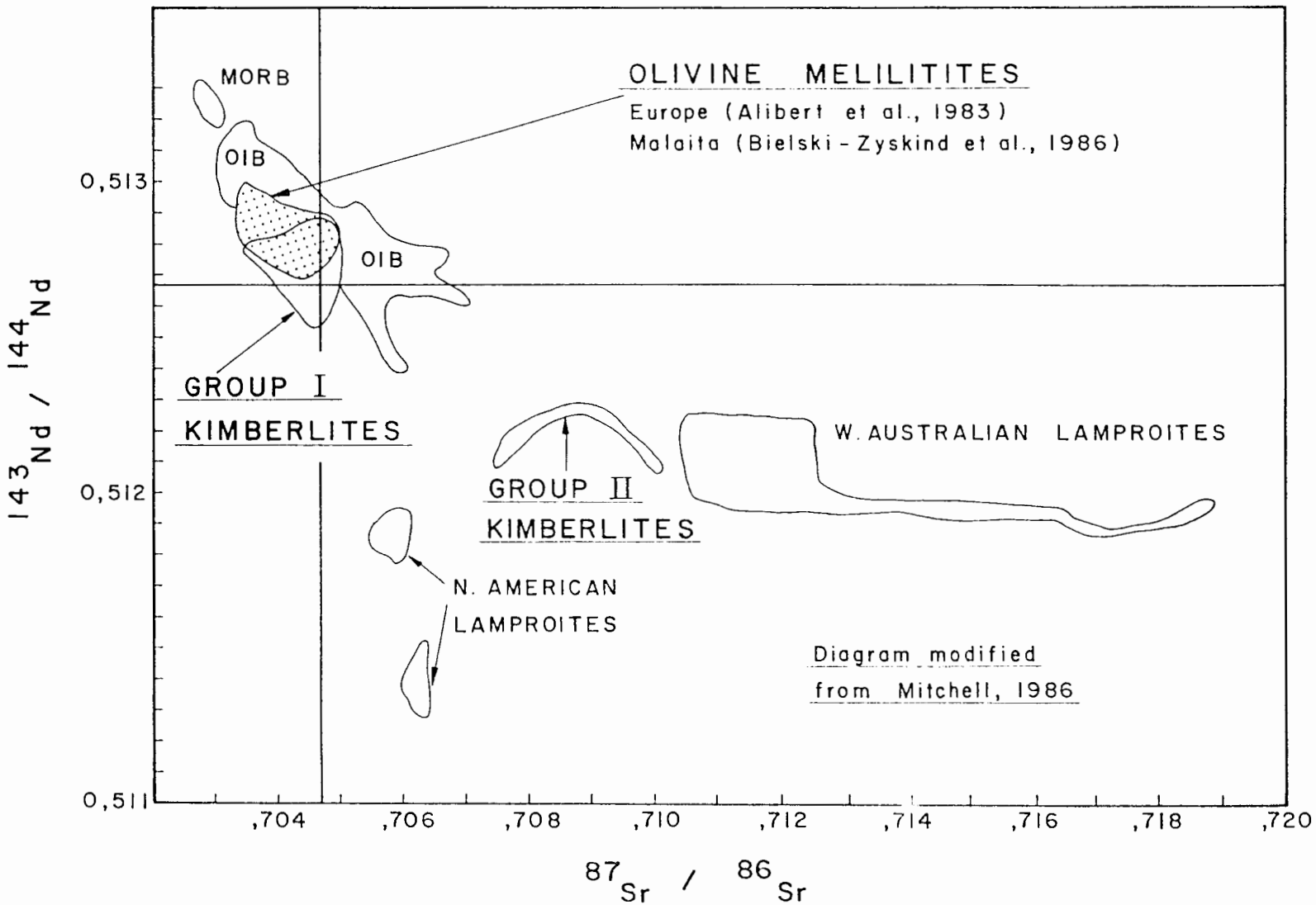

1985).

2 GEOLOGY AND PETROGRAPHY

2.1 Previous studies

Rogers and Du Toit (1903 & 1904) were the first to research the field relations of the Commonage melilitite intrusives. They concluded that the complex consists of a central pipe which is surrounded by a ring dyke. Subsequently Taljaard (1936) interpreted the central area of the intrusion as a sill complex. This was confirmed by the work of Gerard (1958) who also proved the existence of a ring dyke by means of a geophysical survey. The following description of the field geology of the melilitites are largely a synthesis of observations by Gerard (op. cit.) and those of the author.

2.2 Geology and petrography of the intrusives

2.2.1 Introduction

The melilitites intrude the Adelaide subgroup of the Beaufort Group which is a sequence of sedimentary rocks assigned to the Karoo sequence. The rocks are of Phanerozoic age and consist essentially of greenish-grey mudstones and sandstones (SACS, 1980). The alternation of resistant layers of sandstone with more easily weathered mudstones impart a terraced appearance to the terrain.

The igneous rocks are susceptible to spheroidal weathering, exposure is generally poor and most of the areas examined comprise of a small outcrop surrounded by a wide field of loose boulders. The intrusion consists of an outer ring dyke (areas one to ten on the main map in the annexure at the back

of the thesis) which partially encircles a centrally located sill complex (areas eleven to sixteen). See figure 2.1 for an idealised sketch of the shape of the intrusive complex.

Both the dyke and the sill complex was drilled by a De Beers Consolidated Mines drill crew in order to obtain fresh, in situ material but in both cases the resultant core proved to be unsuitable for analytical work due to deep, intense weathering of the intrusives. The positions of the respective boreholes are indicated on the main map in the back pocket.

2.2.2 The ring dyke

Where exposed the contact with the country rock is vertical and at right angles to the flat lying sediments. Lateral spreading of the dyke is evident in a number of places, and this is probably due to the melilitite magma intruding bedding planes between mudstone and overlying sandstone. This is particularly evident in areas one to three where a small sill-like body developed (see the main map). The borehole at area 7 passed through melilitite at surface into underlying shale, suggesting that horizontal spreading of the dyke also occurred at this outcrop. The presence of melilitite outcrop in the stream bed to the east of area four seems to indicate that the ring dyke in this area separated into two individual dykes. The exposure in the stream bed parallels the course of the stream which would suggest that the water preferentially carved into the igneous rock. The contacts of the melilitite with the surrounding shales (where exposed) were vertical.

Close to the contact with the country rock the melilitite

Figure 2.1 Morphology of the Sutherland Commonage melilitite intrusives

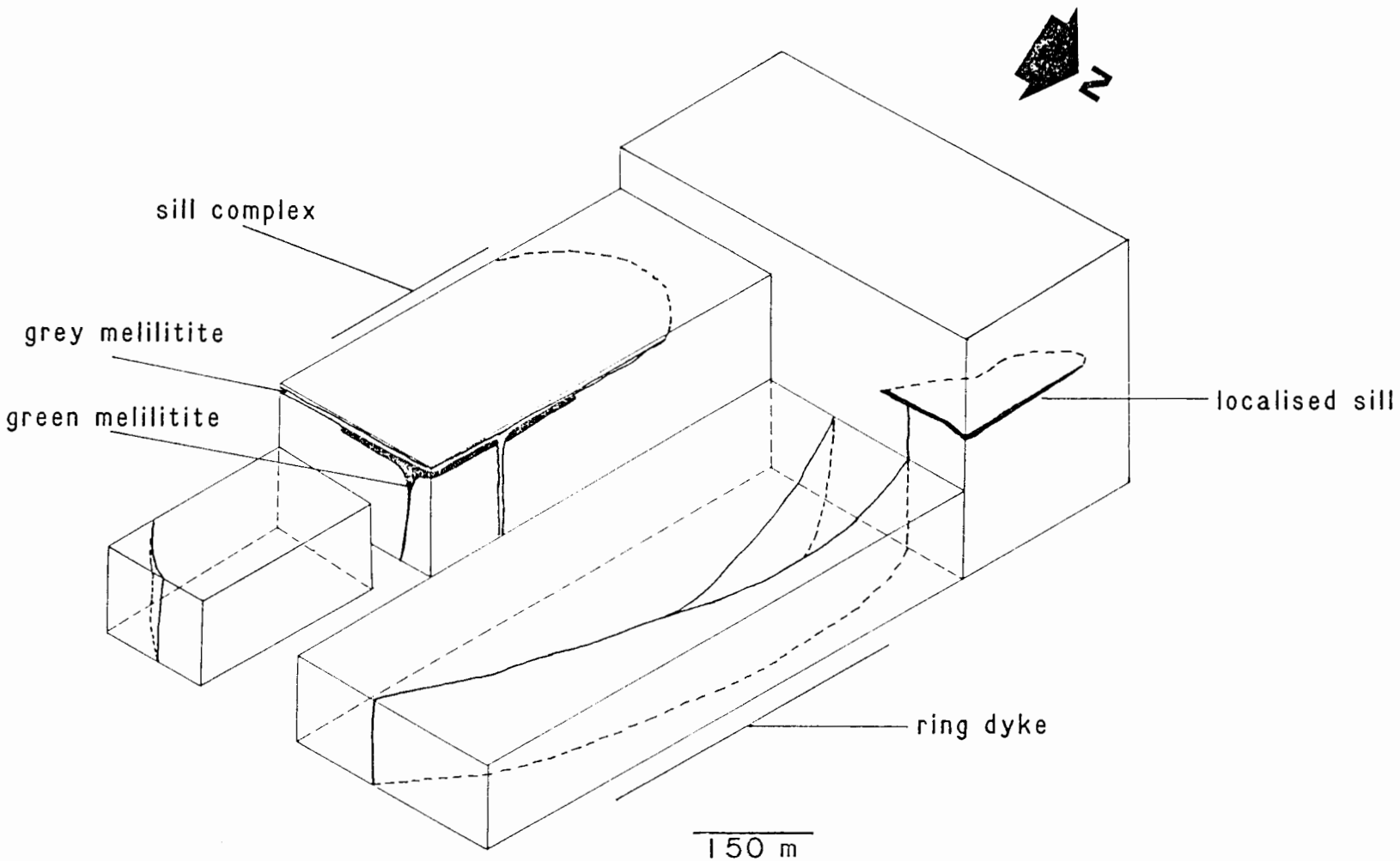

in the ring dyke is fine grained and exhibits a smooth uniform surface. This material is obviously chilled and in a number of cases glass is observed in the groundmass. Towards the central zone of the dyke the colour of the melilitite gradually changes from black to a distinctive mottled grey due to the development of zeolite filled vesicles which are macroscopically visible. The degree of vesicularity is highest in areas where the dyke has intruded horizontally along sediment bedding planes and is most pronounced in area three (see the main map and figure 2.2).

In hand specimen the glass bearing rocks are black, fine grained and generally somewhat weathered. One of the samples collected consists of angular fragments of magmatic rock cemented by a carbonate matrix.

In thin section the glassy chill is characterised by olivine phenocrysts and smaller grains of melilite, opaque spinel and perovskite in a base of brown isotropic glass (plate 2.1a). A few aggregates of colourless clinopyroxene are seen in sample 155, but these are probably the result of assimilation of crustal xenoliths. This feature is often seen in kimberlites, where clinopyroxene is produced due to the contamination of the silicate melt by crustal material (Skinner, pers comm).

In hand specimen the crystalline chill is extremely hard, fine grained and exhibits a greyish black colour. In some cases a network of grey veins are seen on exposed surfaces.

Figure 2.2 Idealised scetch of a sill developed in the ring dyke

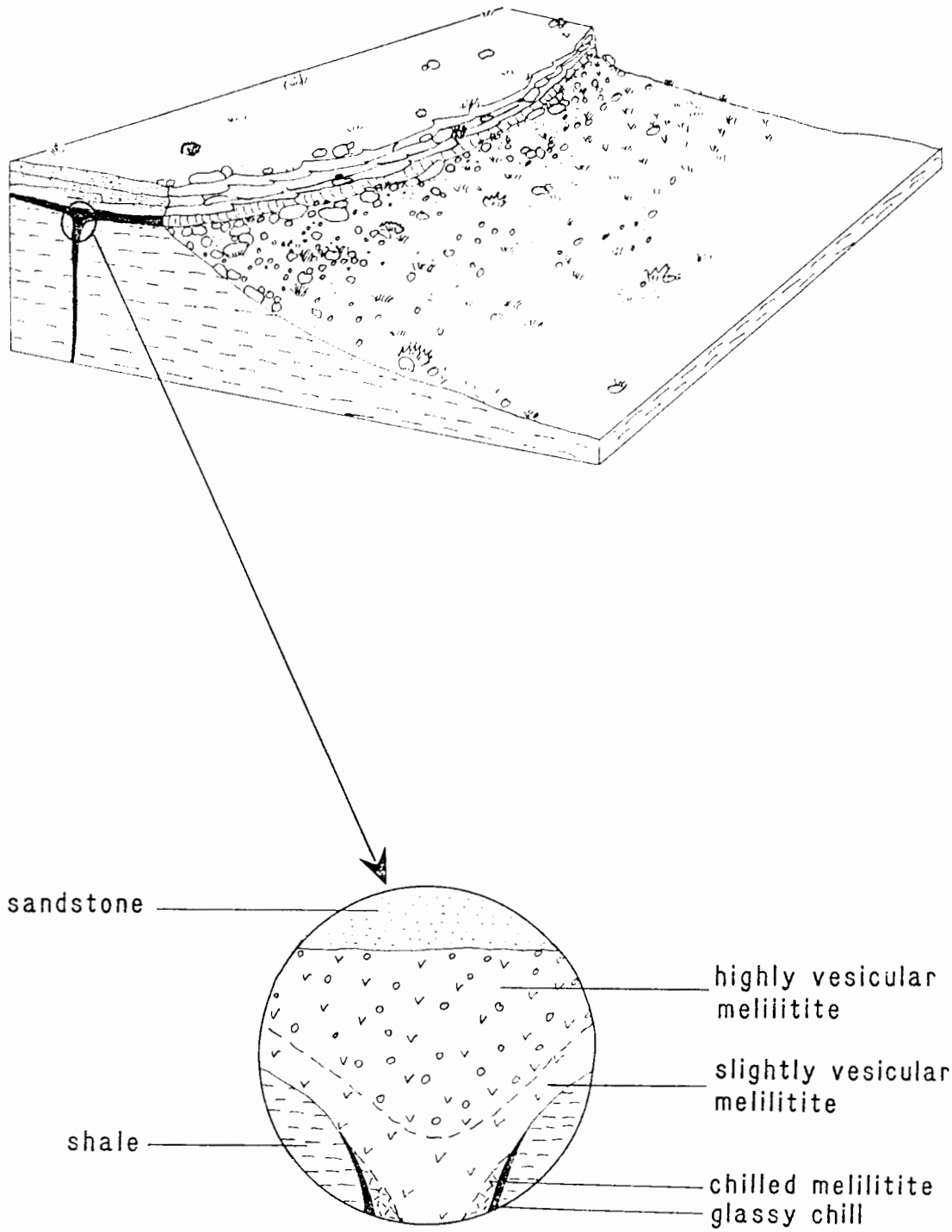

PLATE 2.1

A - Glass-bearing melilitite sampled at the contact of the ring dyke with the country rock. Note the euhedral melilite which in a number of cases partially encloses opaque spinel and perovskite.
Sample 155
Scale bar=0.05mm

B - Euhedral melilite, phlogopite, clinopyroxene, opaque spinel, perovskite and interstitial nepheline in the groundmass of crystalline chill from the ring dyke.
Sample 55
Scale bar=0.05mm

C - Olivine (partially replaced by phlogopite), opaque spinel and perovskite in a fibrous base consisting of zeolites and clay minerals. Green melilitite.
Sample 191
Scale bar=0.1mm

D - Olivine plus abundant granular monticellite, opaque spinel, perovskite and rare apatite. Grey melilitite.
Sample 212
Scale bar=0.05mm

a

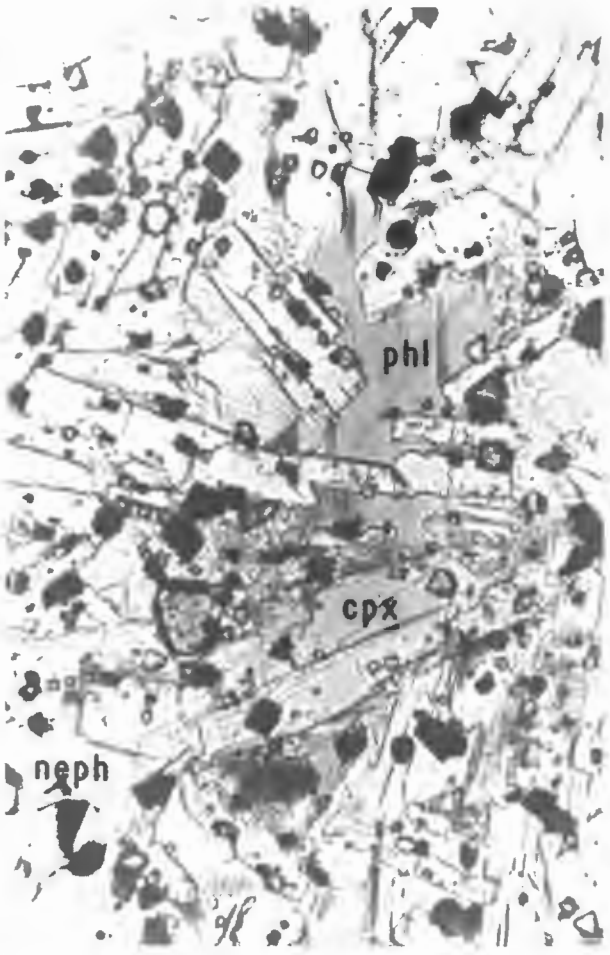

b

c

d

Petrographic examination shows olivine phenocrysts in a matrix of melilite, clinopyroxene, phlogopite, opaque spinel, perovskite and apatite (plate 2.1b). Nepheline forms the base. Principal mineralogical differences between samples result from modal variations in the proportions of nepheline, clinopyroxene and phlogopite. The grey veins seen in hand specimen consist of extremely small clinopyroxene microlites and euhedral opaque spinels in a base of nepheline. These veins simply grade into the rest of the groundmass. In addition a number of specimens show small spherical vesicles (not visible in hand specimen) which are filled by nepheline and clinopyroxene. These veins and vesicles are probably the result of late crystallization residua expelled from the groundmass during the final stages of crystallisation. Modal analyses of typical samples are presented in table 2.1.

The vesicular variety of melilitite is a most distinctive grey rock which is characterised by the presence of macroscopically visible white vesicles. The number and size of the vesicles present is highly variable and range from samples showing a few small white spots (approximately 1mm in size) to specimens in which vesicles are abundant, have irregular shapes and vary in size up to 1cm.

The vesicular rocks consist of olivine phenocrysts in a matrix of melilite, phlogopite, apatite, clinopyroxene, perovskite and opaque spinel. Nepheline and fibrous zeolites form the base. The abundance of vesicles in hand specimen can be correlated with mineralogical differences seen in thin section. It is generally found that samples showing few

Table 2.1 Modal analyses of chilled rocks

(volume percent)

	Ring Dyke				Sill Complex
Sample Number	30	169	256	259	197
OLIVINE MACROCRYSTS	1	0	0	0	0
OLIVINE PHENOCRYSTS	22	23	23	26	28
PHLOGOPITE	8	<2	4	2	<2
CLINOPYROXENE	14	26	26	23	16
MELILITE	19	23	20	18	21
PEROVSKITE	5	4	4	10	7
OPAQUE MINERALS	11	14	20	12	15
NEPHELINE	18	8[1]	3[1]	10[1]	11[1]
APATITE	1	tr	1	1	0

CONVENTION

0.1–0.4 = trace
0.5–0.7 = <1
0.8–1.2 = 1
1.3–1.4 = >1
1.5–1.7 = <2
1.8–2.2 = 2 etc

>5 VOLUME PERCENT

5.0–5.4 = 5
5.5–6.4 = 6 etc

(1) The count is probably too low as nepheline occur interstitially in a mat of clinopyroxene microlites.

vesicles are characterised by relatively fresh nepheline and melilite. Highly vesicular samples by contrast often exhibit clinopyroxenes which are partially altered to actinolite,and exhibit lath-shaped pseudomorphs after melilite which consist of a fibrous mass of zeolites and clay minerals. Nepheline is usually also extensively altered to a brownish, fibrous, often isotropic material which is probably a mixture of hydronepheline, analcite and zeolites. Modal analyses demonstrate the variability of the mineral content of the vesicular rocks (table 2.2).

The vesicles show wide variations in shape but are generally oval or circular in cross section. They are commonly filled by sheaths of fibrous zeolites with a minor component of yellowish garnet. In some cases carbonate is developed in the centres. A number of vesicles show an intermediate border consisting of coarse clinopyroxene and nepheline. This mineralogy is similar to that of the grey veins and ocelli seen in the chilled rocks from the dyke contact. The groundmass minerals bordering on the vesicles are often coarser than in the normal groundmass. This coarse growth is probably a consequence of the concentration of heat and volatile rich residual liquids in the vesicle. Similar features have been recognised in lamprophyres from western Otago, New Zealand (Cooper, 1979) and Labrador (Foley, 1984). It is suggested that the vesicles are segregations of residual liquids drawn into gas vesicles as a consequence of the reduction of the vapour phase volume during cooling. The carbonate core seen in a few of the vesicles is interpreted as the condensed vapour phase (Cooper, op. cit.).

Table 2.2 Modal analyses of vesicular rocks

(volume percent)

	Ring Dyke							
Sample Number	80	100	167	260	83*	154*	257*	258*
OLIVINE MACROCRYSTS	0	0	0	0	0	0	0	0
OLIVINE PHENOCRYSTS	17	26	37	31	21	28	26	26
PHLOGOPITE	6	8	5	8	>4	2	>4	8
CLINOPYROXENE	10	5	3	8	15	4	3	14
MELILITE	16[1]	8	14	7[1]	6[1]	5[1]	4[1]	9[1]
PEROVSKITE	4	3	>2	4	<4	8	9	5
OPAQUE MINERALS	12	8	6	10	12	8	8	8
NEPHELINE	tr	10	5	6	6	6	4	>4
APATITE	7	9	<2	>2	8	tr	>2	>2
ZEOLITES	4	4	1	<4	11	6	5	5
CARBONATE	tr	0	0	0	0	0	0	0
AMPHIBOLE	0	0	0	0	0	>4	0	0
GARNET	0	0	0	0	0	1	0	0
GROUNDMASS[2]	24	19	26	19	12	28	34	18

* Samples which show a high degree of vesicularity

(1) Lath-shaped pseudomorphs counted as melilite

(2) Brown, often isotropic base which probably consists of altered nepheline

2.2.3 The sill complex

This intrusion evidently formed by the horizontal spreading of the melilitite magma at the contact between a layer of mudstone and overlying sandstone. The horizontal sandstone capping is brecciated in places and indurated by veins and lenses of carbonate which are probably associated with the magmatic event. Extensive bleaching of the sandstone is commonly observed. Evidence for baking and melting of sediments surrounding the sill is seen at the southern outcrop area.

The rocks of the sill complex are dominated by two types of melilitite which respectively exhibit a distinctive green and grey colour in hand specimen. The grey melilitite overlies the green melilitite and is probably a younger intrusion, as it contains small, spherical autoliths of the green melilitite. Where exposed the contact between the two intrusives is irregular but approximately horizontal. Flow differentiation of the coarse constituents is seen in the grey melilitite at the contact with the underlying green melilitite. The green melilitite was noted to be aphanitic along the lower contact with the underlying sediments, and this may be due to flow differentiation.

In thin section the green melilitite shows a highly variable olivine content. Numerous olivine phenocrysts together with less common macrocrysts (terminology of Clement,1982) are seen. These are set in a groundmass which displays a high degree of deuteric alteration. Recognisable

minerals in the groundmass include phlogopite (which is often bleached and chloritised), apatite, perovskite, opaque spinel, garnet, fibrous zeolites and carbonate (plate 2.1c). Secondary clay minerals, chlorite and serpentine fill interstitial areas. The zeolites, carbonate, garnet, serpentine and clay minerals probably formed during the deuteric event. The mineralogy is highly variable as shown by modal analysis (table 2.3).

The grey melilitite is characterised in hand specimen by a distinctive grey colour and the presence of numerous olivine and magnetite macrocrysts up to 1cm in size.

In thin section the rock consists of olivine phenocrysts and macrocrysts plus a few magnetite macrocrysts set in a finer-grained matrix. The matrix is dominated by monticellite, perovskite and opaque spinel, but also contains minor phlogopite, melilite, apatite and a few translucent spinels (plate 2.1d). These are set in a base of nepheline and rare carbonate. A number of specimens exhibit flow orientation of the coarser components. Altered, angular country rock fragments (up to 1cm in size) are seen in all the samples examined (plate 2.2c). They are totally replaced by an assemblage of nepheline, phlogopite, monticellite and dust-like opaque spinels. Autoliths of green melilitite consists of fresh olivine set in a matrix of partially chloritised phlogopite, yellowish garnet, abundant apatite and opaque spinel, fibrous zeolites, monticellite, perovskite and minor carbonate (plate 2.2d). The border of the autoliths are characterised by the development of abundant opaque spinel.

Table 2.3 Modal analyses of the green melilitite

(volume percent)

	Sill Complex						
Sample Number	193	205	261	262	264	209*	263*
OLIVINE MACROCRYSTS	0	7	3	0	0	0	13
OLIVINE PHENOCRYSTS	18	23	24	17	28	22	20
PHLOGOPITE	8	9	4	8	7	3	5
MELILITE	0	0	0	0	0	3	0
PEROVSKITE	5	6	5	8	7	12	<4
OPAQUE MINERALS	<4	>2	1	2	1	10	4
MONTICELLITE	–	–	–	–	–	35	7
APATITE	10	10	20	14	15	>2	>4
GARNET	0	3	3	0	0	1	1
CARBONATE	3	0	4	<2	0	1	0
ZEOLITES	0	0	8	17	8	0	1
GROUNDMASS [1]	53	40	28	32	35	11	41

(1) Fibrous, greenish base which consists of clay minerals, zeolites and chlorite

* Samples taken at the contact with the overlying grey melilitite

PLATE 2.2

A - Abundant euhedral grains of clinopyroxene plus a few opaque spinels and lath shaped ilmenites in a base of nepheline. Olivine nephelinite.

Sample 192

Scale bar=0.2mm

B - Country rock which experienced melting due to the intrusion of the sill complex. Note the abundance of euhedral grains of K-feldspar.

Sample 188

Scale bar=0.5mm

C - Country rock xenolith in the grey melilitite. Note the concentric arrangement of dust-like opaque spinels.

Sample 171

Scale bar=0.5mm

D - Autolith of the green melilitite in the grey melilitite.

Sample 211

Scale bar=0.2mm

a

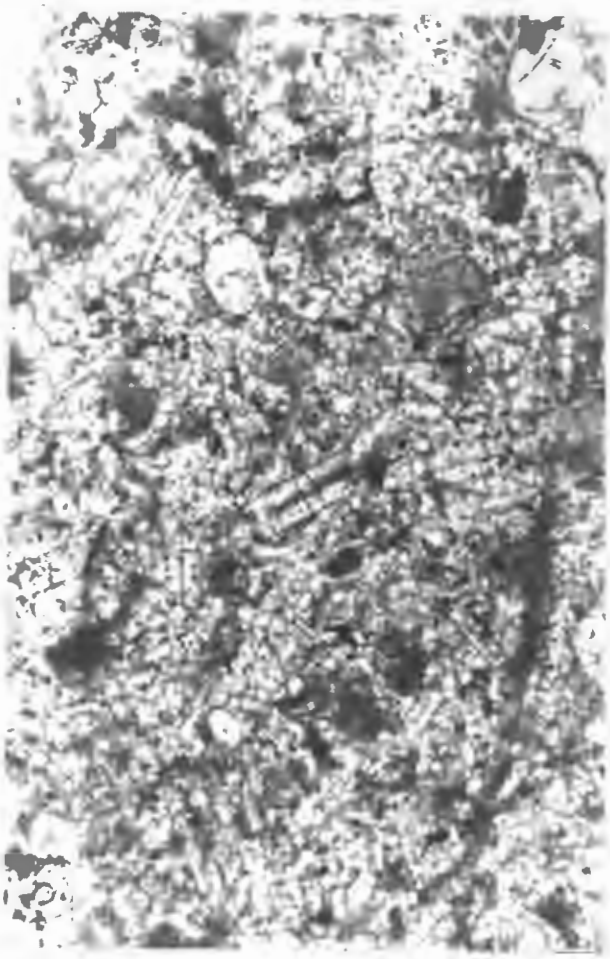

b

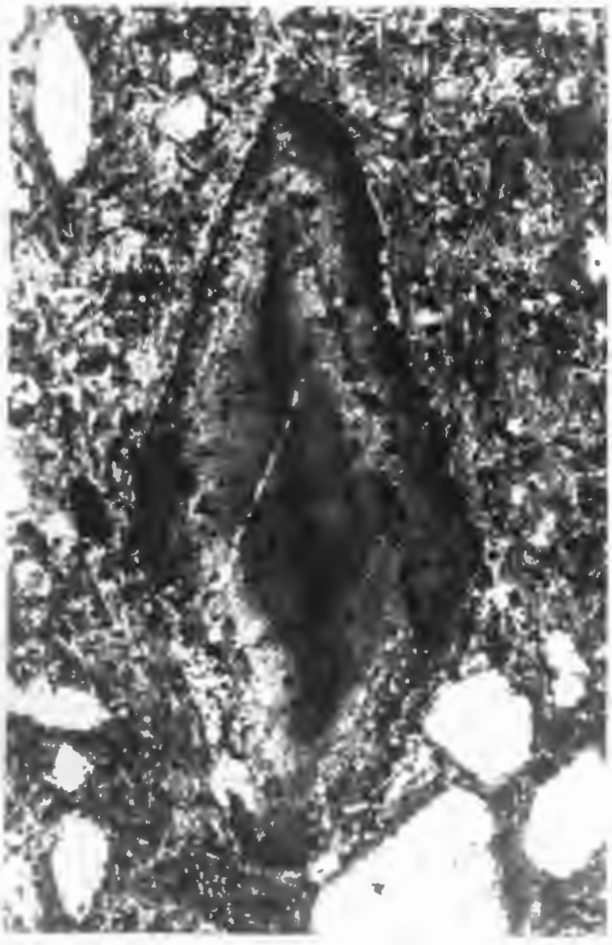

c

d

Modal analyses of typical specimens of the grey melilitite are given in table 2.4.

The green melilitite in direct contact with the grey melilitite shows petrographic evidence of metamorphism and a degree of metasomatism. Monticellite (which is generally never seen in the green melilitite) occur in samples taken at the contact and is often present as big poikilitic plates.

Rocks similar in appearance to those from the ring dyke are also seen in the vicinity of the sill complex but are never found in situ. In addition a small localised outcrop of an olivine nephelinite is present at area fifteen. This material appear to be restricted to the top part of the sill and was found by Gerard (op. cit.) to take the form of veins intruding into the overlying sandstone. Gerard also described a friable yellow "tuff" in the immediate vicinity of the sill complex. However, close examination of this material suggests that it is more likely to be an intensely weathered analogue of the green melilitite.

The olivine nephelinite occurring in area 15 shows a distinctive mottled appearance in hand specimen due to the presence of dark, clinopyroxene rich areas which is enclosed in a fine grained, greyish surround of nepheline.

In thin section the rock consists of olivine phenocrysts set in a matrix of clinopyroxene, phlogopite, opaque minerals and apatite (plate 2.2a). Nepheline is in some cases partially replaced by fibrous zeolites and forms the base.

Table 2.4 Modal analyses of the grey melilitite (volume percent)

	Sill Complex			
Sample Number	171	211	265	266
OLIVINE MACROCRYSTS	1	0	12	1
OLIVINE PHENOCRYSTS	25	26	24	33
MONTICELLITE	36	31	36	43
MELILITE	7	<4	5	2
PHLOGOPITE	0	3	1	0
PEROVSKITE	<4	5	8	>4
OPAQUE MINERALS	12	6	6	8
APATITE	0	2	tr	tr
NEPHELINE	0	0	4[1]	5[1]
CARBONATE	0	1	0	0
ZEOLITES	0	3	0	0
GROUNDMASS	15[2]	19[2]	0	0
CR-XENOLITHS	1	0	3	3

(1) The count is probably too low as nepheline occur interstitially to small, closely-packed grains of monticellite

(2) Brown, often isotropic base which probably consists of altered nepheline

The rock is texturally unusual and is probably equivalent to the ijolite and pegmatite described by Gerard (1958). Modal abundances are presented in table 2.5.

2.3 Thermal effects on the country rock

The ring dyke appears to have had little thermal effect on the country rock as metamorphism is usually limited to bleaching of the sediments in the immediate vicinity of the contact.

The intrusion of the sill complex led to the melting and assimilation of country rock by the melilitite magma in a number of places. In hand specimen these "mixed" rocks are black and fine grained. They contain carbonatised xenoliths of unaffected country rock. The rocks bear a striking resemblance to basaltic lava and have in the past often been described as such (Rogers and Du Toit, 1903 & 1904; Gerard, 1958).

In thin section these rocks consist of feldspar microlites set in a base of isotropic glass (plate 2.2b). Subrounded, partially melted grains of quartz are often seen and further attest to the origin of the rock by melting of the country rock. A number of thin sections also show some melilite which exhibits an unusual dark blue birefringence.

2.4 Lower crustal xenoliths

A large number of lower crustal xenoliths were collected. These xenoliths consist of two pyroxenes plus plagioclase and exhibit an equilibrium texture. Gerard (1958) also recognised

Table 2.5 Modal analyses of the olivine nephelinite

(volume percent)

	Sill Complex	
Sample Number	192	267
OLIVINE MACROCRYSTS	0	0
OLIVINE PHENOCRYSTS	16	24
NEPHELINE	27	17
ZEOLITES	11[1]	>4[1]
CLINOPYROXENE	43	49
PHLOGOPITE	<2	1
OPAQUE MINERALS	1	4
APATITE	1	0

(1) Fibrous mineral which replace nepheline

garnet in one of his samples. A few of the xenoliths are layered, showing white plagioclase rich bands which alternate with darker pyroxene rich zones.

3 MINERALOGY

3.1 Olivine

Olivine is ubiquitous in all the samples examined. It is generally very fresh and alteration (when present) is limited to replacement by serpentine along the edges of grains. Four varieties of olivine are distinguished on petrographic grounds:

a)Large (1-8mm), generally rounded and corroded grains are termed macrocrysts (after Clement, 1982). These grains show signs of strain such as deformation bands and are in many cases recrystallised (plate 3.1a and 3.1b) and overgrown by a later generation of olivine (plate 3.3a). They often contain abundant fluid inclusions (plate 3.1c) which impart a turbid appearance to the grains. A number of the grains include euhedral apatite and are intergrown with magnetite macrocrysts (figure 3.1). These olivines are rare in the dyke rocks (0-1 vol%) but are more abundant in the green and grey melilitites of the sill complex, where they reach abundances of up to 13 vol%.

b)The term simple phenocryst applies to any subhedral to euhedral grain larger than approximately 0.5mm. These grains do not show any evidence of multiple growth or pronounced hopper shapes and are not strained (figure 3.2a).

c)Microphenocrysts are generally smaller than 0.5mm, but are equivalent of simple phenocrysts (figure 3.2a and plate 3.2d).

d)Complex phenocrysts are grains which either consist of aggregates of subhedral to euhedral grains (which form multiple growth aggregates-see figure 3.2d, 3.2e and plate

Figure 3.1 Intergrowths of olivine macrocrysts with magnetite and apatite

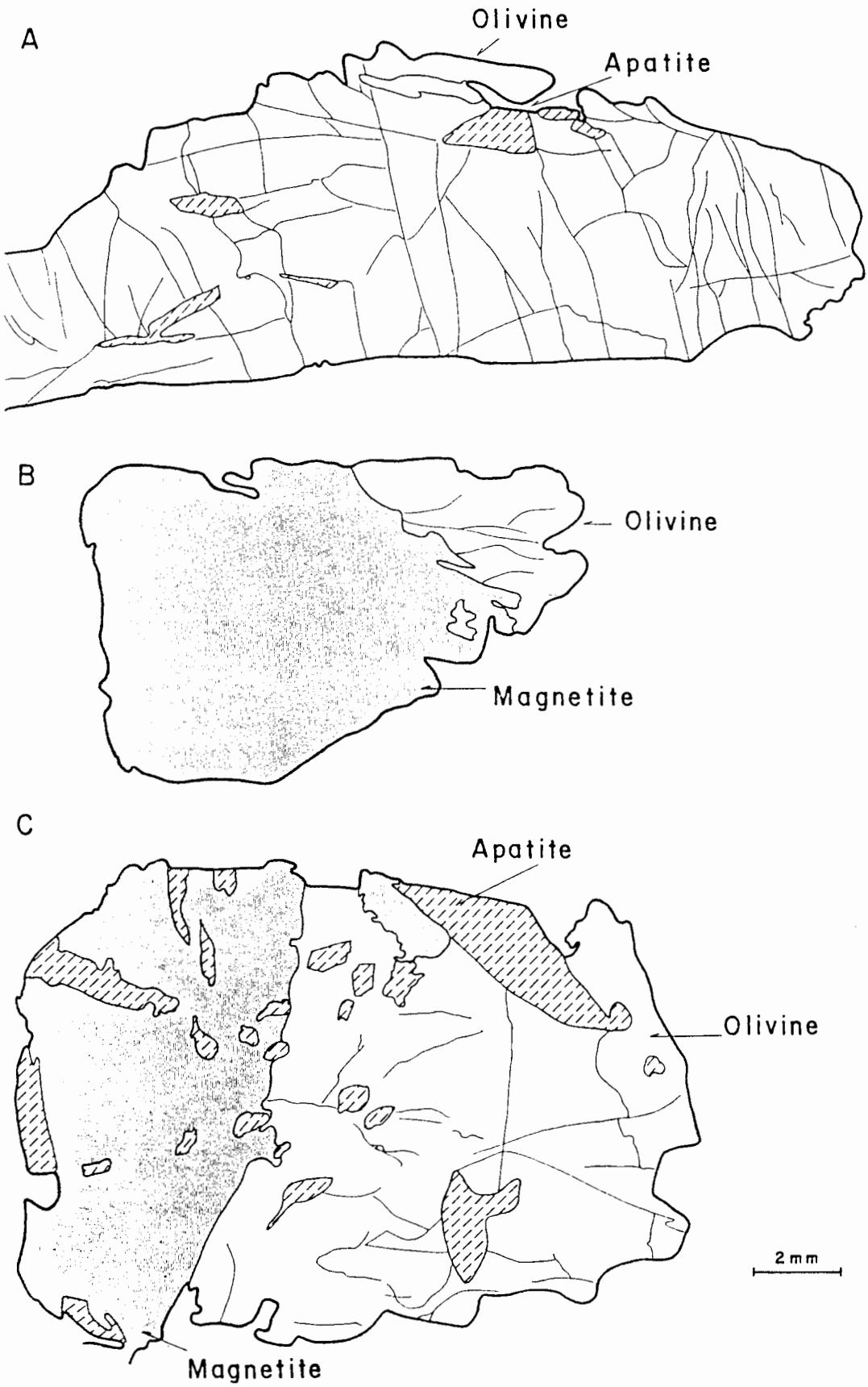

PLATE 3.1

A - Anhedral olivine macrocryst.

Sample 208

Scale bar=0.5mm

B - Same as (a) but under crossed nichols. Note the pronounced recrystallisation features.

C - Anhedral olivine macrocryst. Note the corrosional shape and the abundance of fluid inclusions.

Sample 55

Scale bar=0.5mm

D - Typical complex olivine phenocryst (hopper shape).

Sample 36

Scale bar=0.5mm

a

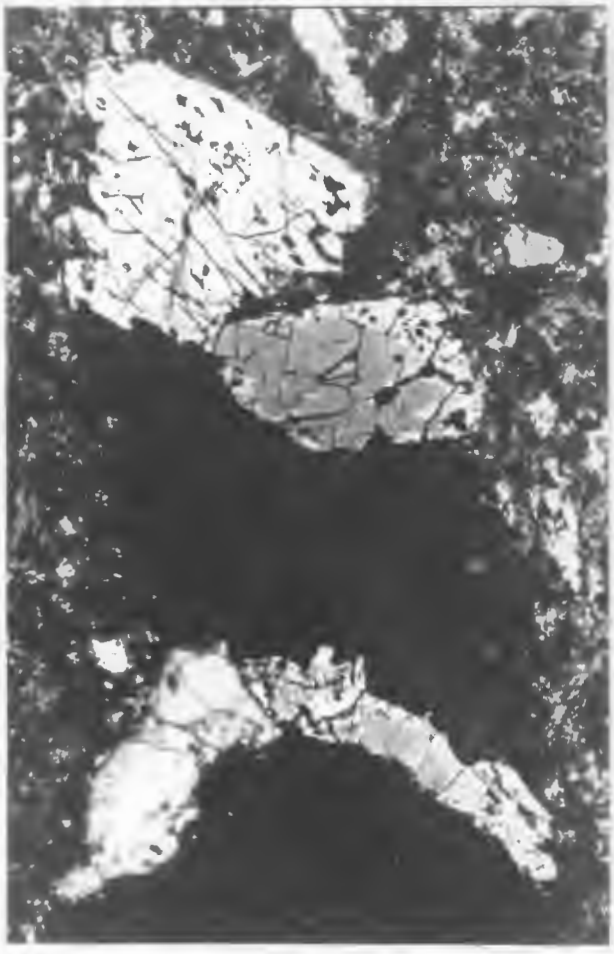

b

c

d

3.2b, 3.2c) or single crystals showing pronounced corrosional (figure 3.2b and plate 3.2a) or hopper shapes (terminology of Moore, 1978-see figure 3.2c and plate 3.1d). These crystals show a wide range of sizes ranging from approximately 0.5mm in size to grains several millimetres across.

Phenocryst abundances are highly variable and range from 16 to 37 vol%. Small inclusions of translucent reddish brown and opaque chromite are present in complex, simple and microphenocrysts (plate 3.2d) but are generally not seen in macrocrysts. This suggests that the olivine macrocrysts are unrelated to the melilitite magma and consequently probably represent xenocrysts.

The larger complex and simple phenocrysts often exhibit circular inclusions which typically consist of abundant serpentine and minor zeolite with one or more of the minerals phlogopite, opaque spinel (generally titanomagnetite), clinopyroxene and grossular garnet. These inclusions might represent liquids (melt) trapped during olivine growth or alternatively are artifacts of embayments with respect to the plane of the thin section (or both). Moore (1978) described similar inclusions in melilitites from Bushmanland and considered them to be melt inclusions trapped during a phase of rapid olivine growth.

3.2 Phlogopite

Groundmass phlogopite is not represented in the glass bearing melilitite, but is commonly seen in the other petrographic variants. Modal abundances vary by up to 9 vol%

Figure 3.2 Morphology of the Commonage olivines

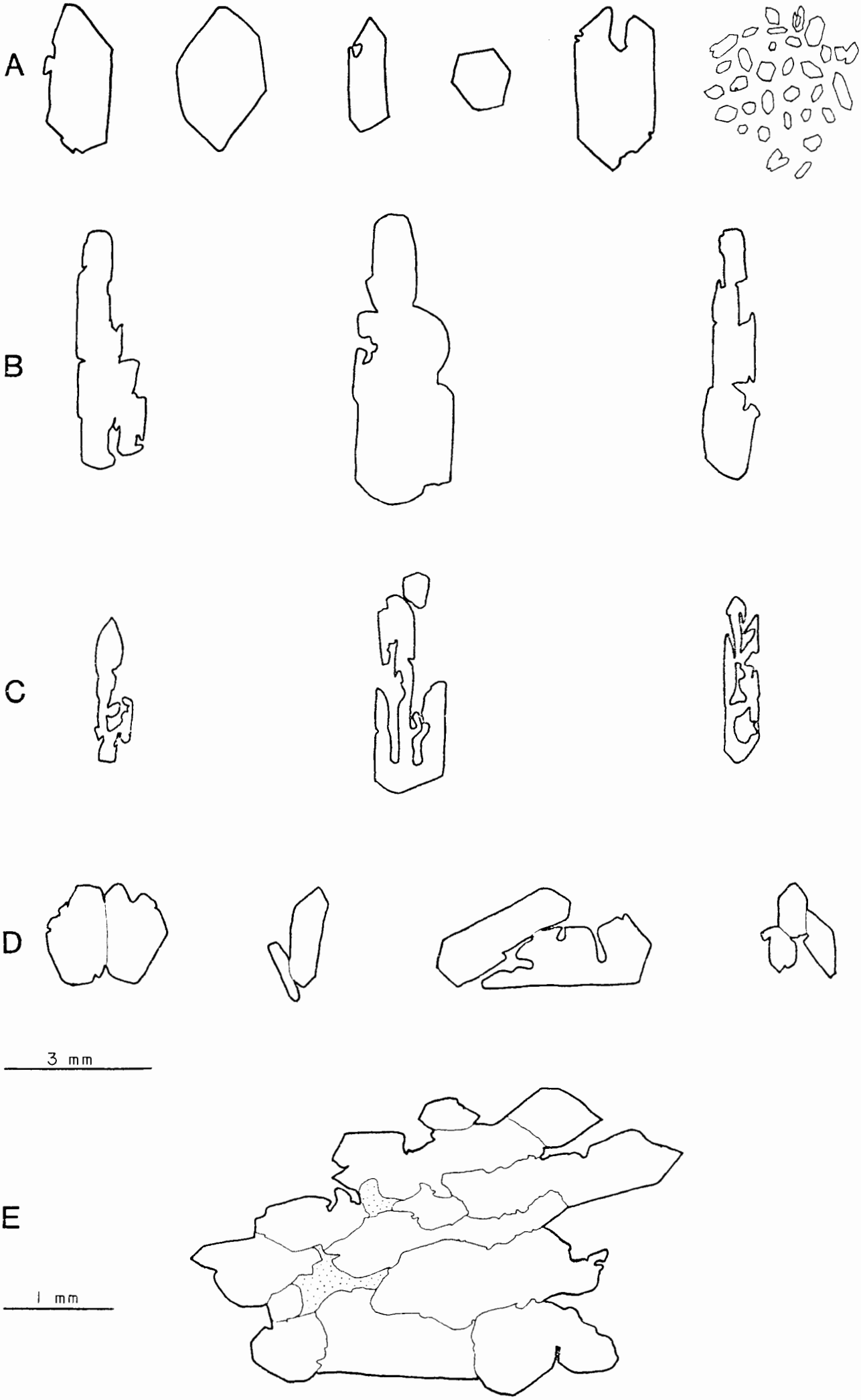

PLATE 3.2

A - Olivine phenocryst showing corroded crystal faces.

Sample 30

Scale bar=0.5mm

B - Multiple growth aggregate consisting of two olivine phenocrysts.

Sample 69

Scale bar=0.5mm

C - Multiple growth aggregate of olivine phenocrysts.

Sample 30

Scale bar=0.2mm

D - Typical olivine microphenocryst. Note the small chromite inclusions.

Sample 69

Scale bar=0.1mm

a

b

c

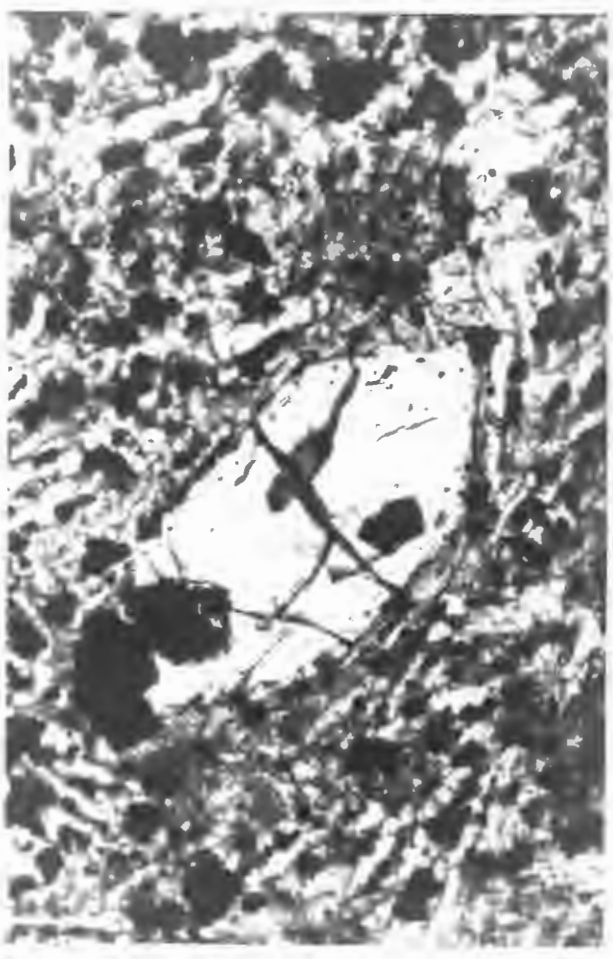

d

PLATE 3.3

A - Pronounced second generation olivine overgrowth on an olivine macrocryst. Ring dyke.
Sample 179
Scale bar=0.5mm
Crossed nichols

B - Euhedral melilite showing inclusions of opaque spinel and perovskite. Note the interstitial nepheline.
Sample 30
Scale bar=0.05mm

C - Typical alteration of melilite in a vesicular rock from the ring dyke. Note the interstitial nepheline which is partially replaced by fibrous zeolites.
Sample 83
Scale bar=0.05mm

D - Melilite in the grey melilitite. The irregular shape of the grains are due to marginal replacement by monticellite (not clear in photograph).
Sample 211
Scale bar=0.05mm

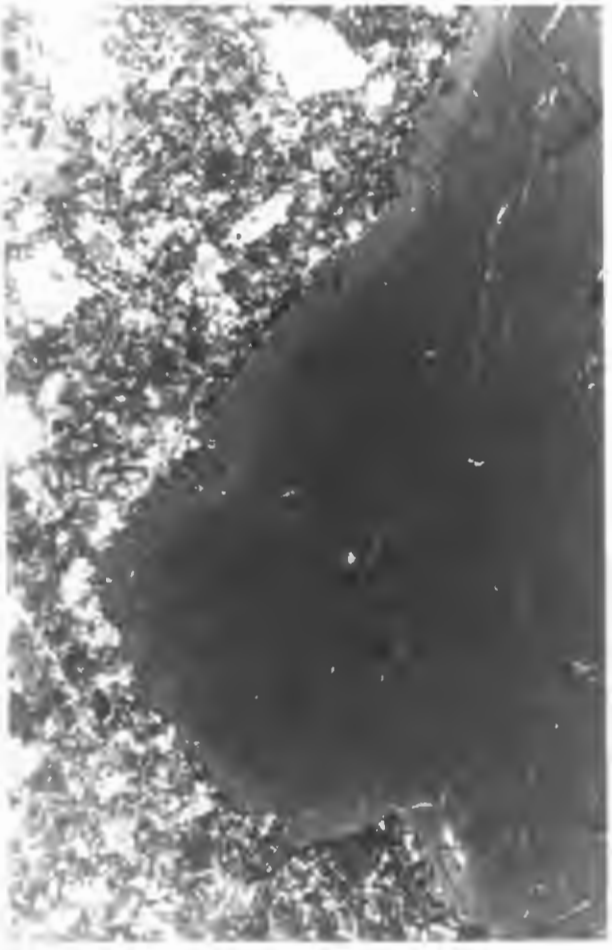

a

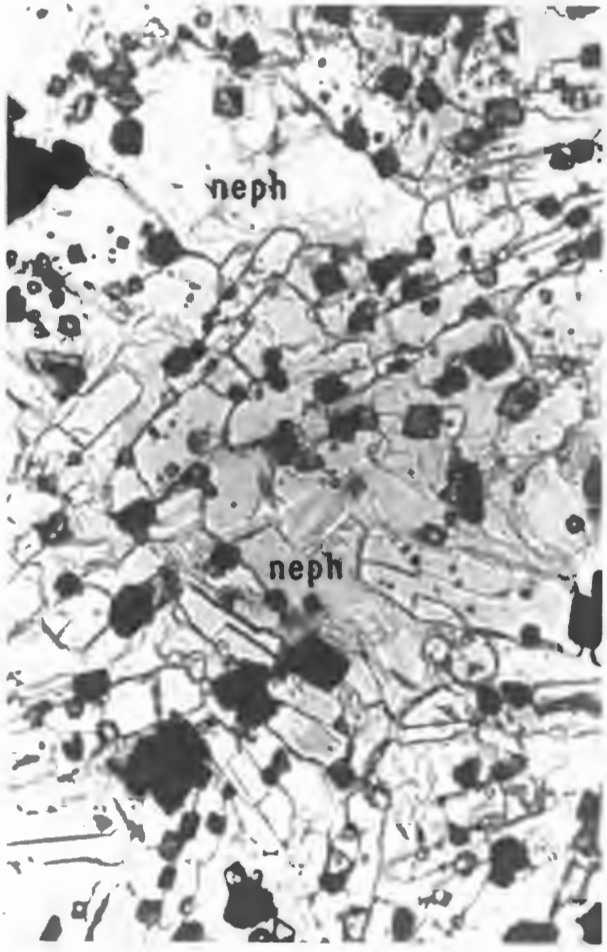

b

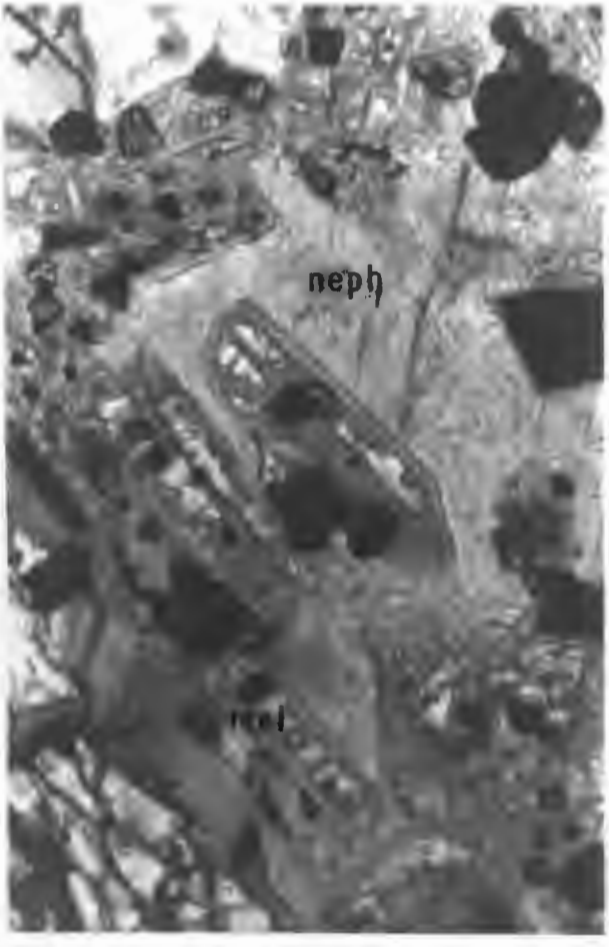

c

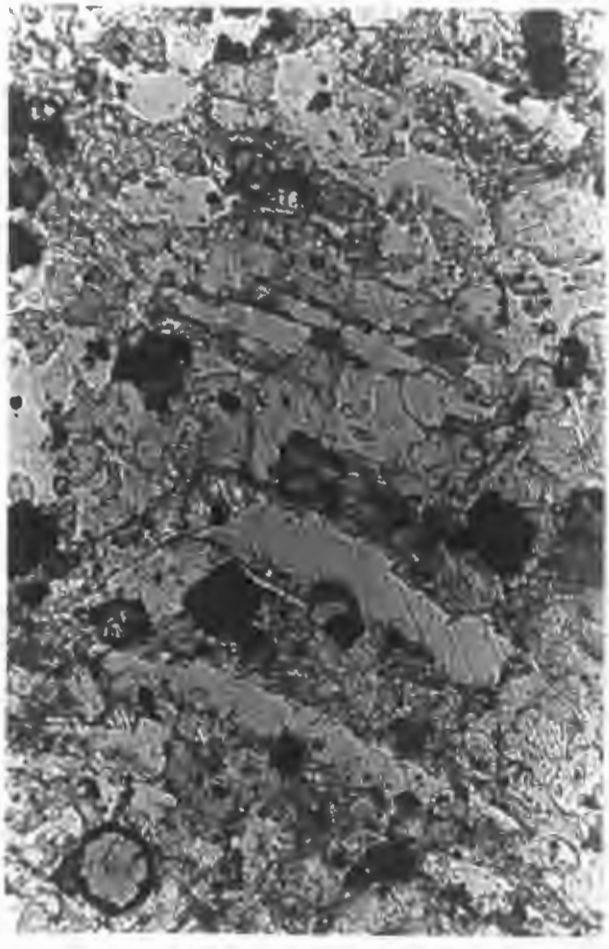

d

and are generally highest in the green melilitite and the vesicular rocks.

A number of macrocrysts, of up to 1cm in size, are seen in the grey melilitite. These grains exhibit a yellowish brown colour and show a reaction rim of granular monticellite and dust-like opaque spinels (plate 3.4d). This phlogopite is probably xenocrystic and could be derived from disaggregated "glimmerite" nodules described by Gerard (1958).

Typical groundmass phlogopite occurs as irregular, pleochroic plates (X=pale yellowish brown; Y=Z=reddish brown) showing normal pleochroism. The grains are up to 0.3mm in size and are more euhedral in the vicinity of nepheline-clinopyroxene veins and vesicles in the crystalline chill and vesicular rocks respectively. In many cases these grains display a thin rim of reversely pleochroic, mahogany-red tetraferriphlogopite which probably represents a late stage overgrowth or is the product of reaction of the phlogopite with a residual, oxidising liquid. Groundmass phlogopite in the green melilitite is often chloritised and difficult to recognise. However, in the grey melilitite it generally shows a pale yellow colour and is commonly observed poikilitically enclosing finer grained monticellite implying late stage crystallisation. Phlogopites in the nephelinite are generally strongly pigmented, show normal pleochroism (X=pale yellow; Y=Z=mahogany red) and are generally small (<0.13mm). Phlogopite hosts inclusions of apatite, opaque spinel, perovskite, melilite and, where present, clinopyroxene and monticellite (plate 3.4b and 3.4c).

Plate 3.4

A - Granular clinopyroxene replacing melilite.

Sample 83

Scale bar=0.1mm

B - Bleached phlogopite in the groundmass of the deuterically altered green melilitite. Note the apatite inclusions.

Sample 193

Scale bar=0.1mm

C - Phlogopite replacement of olivine.

Sample 100

Scale bar=0.1mm

D - A large phlogopite macrocryst in the grey melilitite. Note the dark reaction rim. This consists of monticellite and small, dust-like opaque spinels.

Sample 26

Scale bar=0.5mm

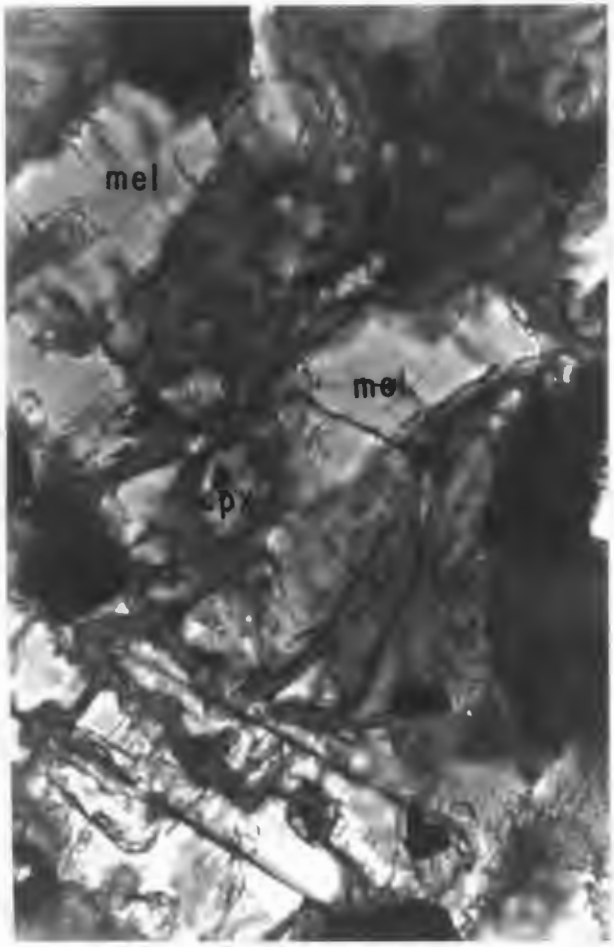

a

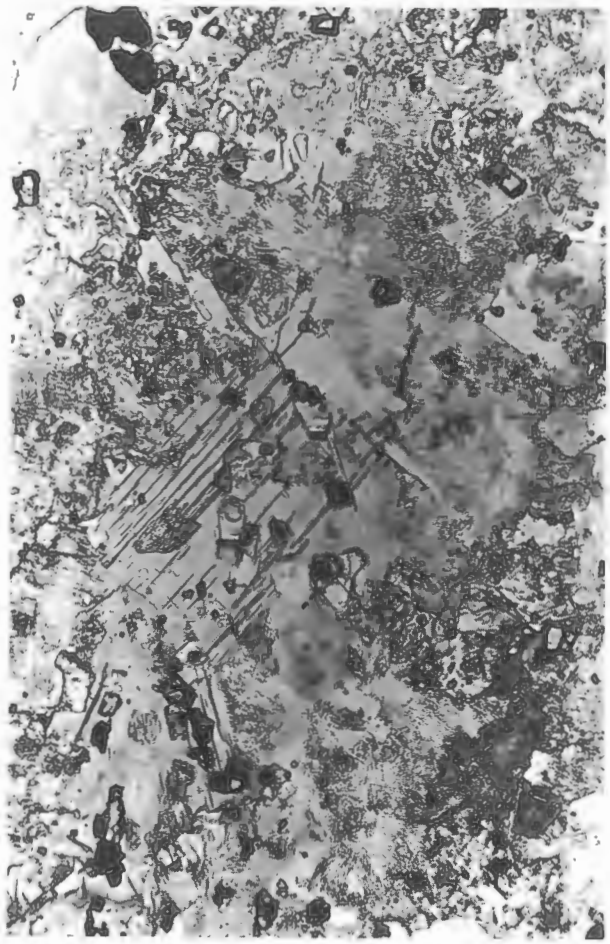

b

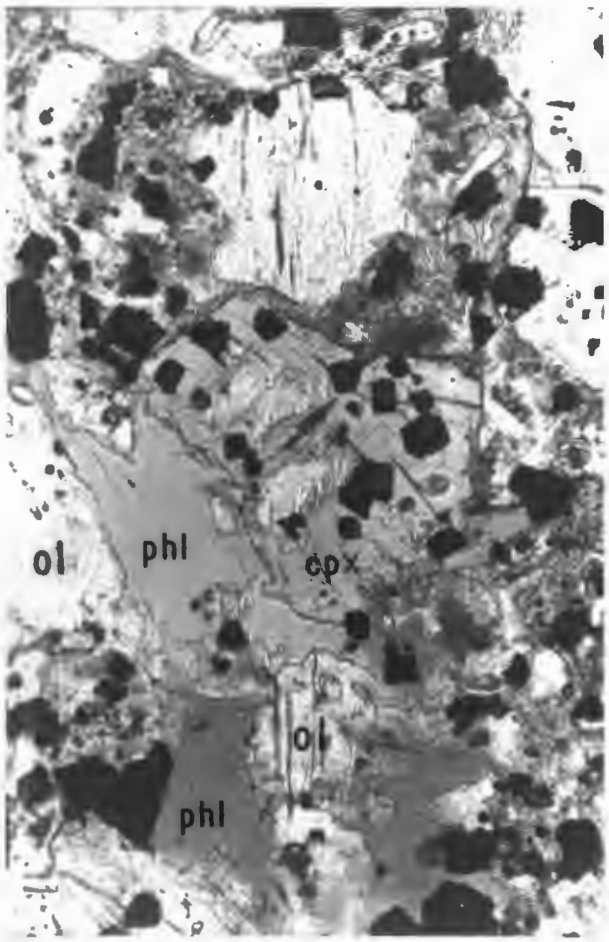

c

d

Olivine is in many cases rimmed and partially replaced by phlogopite. Numerous descriptions of this association are to be found in the literature. Melilitic intrusives in which this reaction is observed includes Haystack Butte, Montana (Buie, 1941), a number of intrusions in the Highwood Mountains of Montana (Larsen et al., 1941; Ross, 1926), Ile Cadieux, Quebec (Bowen, 1922), the Bushmanland swarm of intrusives, R.S.A.(Taljaard, 1936), Bitterfontein, R.S.A.(McIver, 1981) and Saltpetre Kop, R.S.A. (Boctor, 1986). It is also seen in lamproites (Mitchell, 1985) and Group 2 kimberlites (M. Skinner, pers. comm.). The reaction therefore appears to be commonly present in ultramafic alkaline igneous rocks. The experimental study of Luth (1967) in the system $KALSiO_4$-$MgSiO_4$-H_2O showed that forsterite reacts with the residual liquid to produce phlogopite. The melting relations at pressures of up to 30 Kb for an orendite composition have been investigated by Barton and Hamilton (1982). At pressures below 12 Kb a reaction between olivine and liquid to produce phlogopite was also observed.

Phlogopite reaction rims on olivine are not seen in the glass bearing chilled rocks, which suggest that the reaction took place after the melilitite magma intruded into crustal levels - that is, after emplacement. The reaction is also markedly more advanced in the slower cooled rocks which has the global implication that olivine-poor or olivine-free melilitic rocks which are rich in phlogopite may have lost olivine by reaction with the magma.

3.3 Melilite

Melilite is a characteristic groundmass phase in the chilled and vesicular rocks (plate 3.3b). Modal abundances vary from 4 to 23 vol%. It is rare in the grey melilitite and is generally not seen in samples of the green melilitite. Melilite is absent from the groundmass of the nephelinite.

Groundmass melilite is subhedral to euhedral and up to 0.25mm in size. It often shows flow orientation. In the vesicular rocks melilite is often partially or completely replaced by fibrous zeolites and clay minerals (plate 3.3c). Peg structures are commonly developed. Late replacement of melilite by groundmass clinopyroxene have also been observed. In the grey melilitite, melilite is generally quite fresh with minor replacement by monticellite (plate 3.3d). Melilite includes perovskite and opaque spinel.

3.4 Clinopyroxene

Clinopyroxene is a common groundmass constituent in samples from the ring dyke (but is absent from glass bearing chill), chilled and vesicular rocks from the sill complex and the nephelinite. It is absent from the groundmass of the green and grey melilitite but a number of olivine phenocrysts in both rock types show corrosion hollows which enclose relict clinopyroxene (plate 3.5d). In such cases the clinopyroxene is seperated from the groundmass by a "plug" of phlogopite which suggests that clinopyroxene was originally a groundmass constituent in these rocks but was subsequently lost either by deuteric alteration (in the case of the green melilitite) or some kind of monticellite forming reaction in the grey

PLATE 3.5

A - Euhedral clinopyroxenes in the groundmass of a vesicular rock from the ring dyke.

Sample 160

Scale bar=0.5mm

B - Clinopyroxene associated with zeolite in a vesicle.

Sample 83

Scale bar=0.5mm

C - Clinopyroxene partially replaced by amphibole. Highly vesicular rock from the ring dyke.

Sample 159

Scale bar=0.1mm

D - A small clinopyroxene enclosed in a corrosional hollow in olivine. Grey melilitite.

Sample 26

Scale bar=0.5mm

a

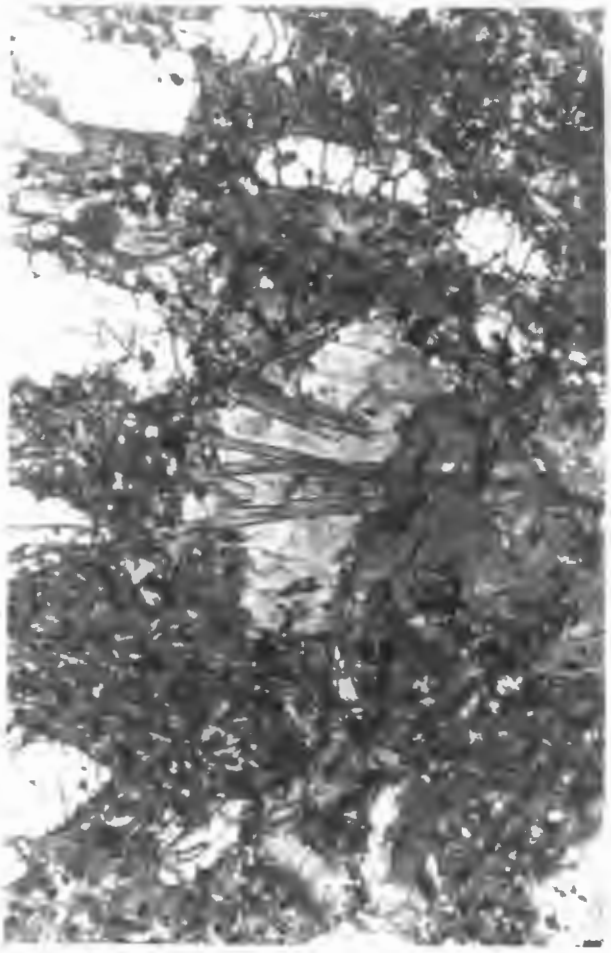

b

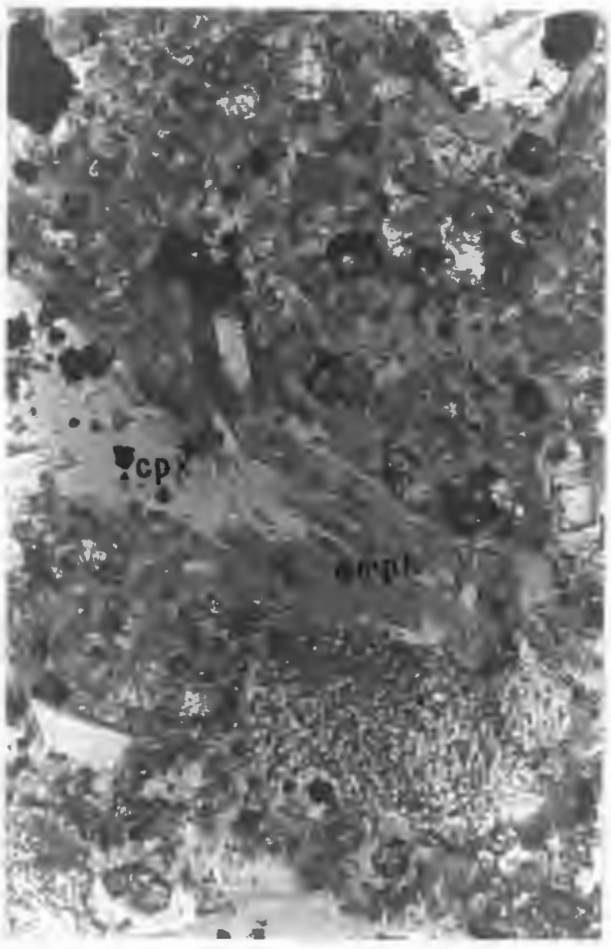

c

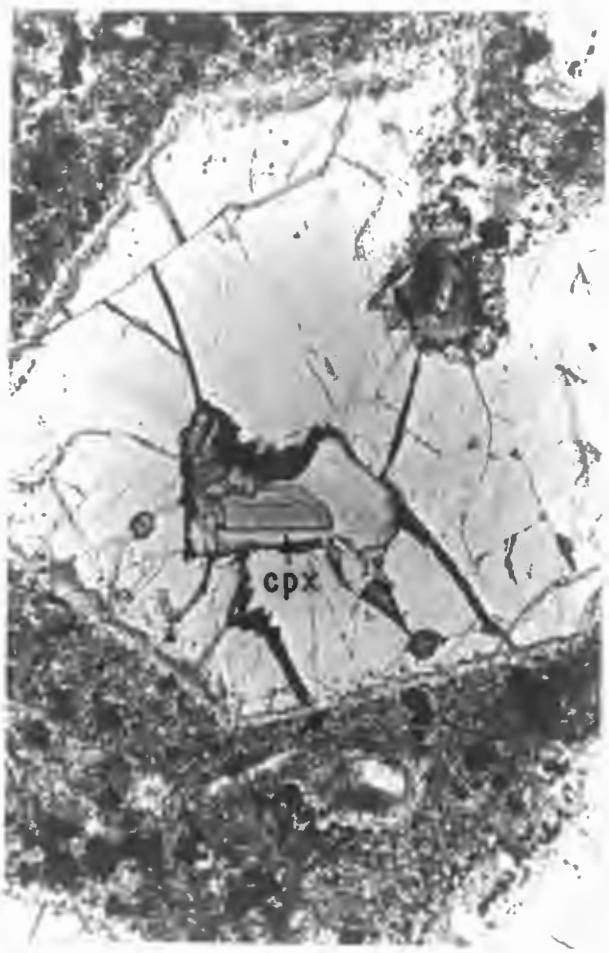

d

melilitite. This line of thought is further developed in chapter 8.

The modal concentration of clinopyroxene in the chilled and vesicular rocks is extremely variable, ranging from about 3 to 26 vol%. It is generally less abundant in the vesicular rocks.

Grain shapes range from blebs filling the interstices between laths of melilite in the crystalline chill to euhedral crystals and glomeroporphyritic aggregates in samples of vesicular material (plate 3.5a). Average grain sizes increase from smaller than 0.25mm in the chilled rocks to euhedral crystals of up to 0.75mm in vesicular samples. Pyroxenes in the vesicular specimens attain their largest dimension when they occur in the border zone of vesicles (plate 3.5b and 3.9a). Tiny pyroxene microlites are present in nepheline- and clinopyroxene-filled veins in samples of chilled melilitite.

The pyroxenes range in colour from neutral through pale yellowish green to light olive green. This correlates with increasing titanium content. Fine oscillatory zoning is commmon. Twinning is less common and is mostly of a bisegmental type. In a number of cases the clinopyroxenes in the nepheline rich outer zone of vesicles shows a thin rim of strongly pleochroic aegirine-augite.

The presence of melilite and absence of pyroxene in samples of glass bearing chill suggests that pyroxene crystallisation commenced after melilite and that it is a post intrusion

phase. In the wholly crystalline rocks clinopyroxene often hosts inclusions of melilite and in a few cases clinopyroxene appears to be replacing melilite (plate 3.4a). Larger grains host inclusions of opaque spinel, perovskite and apatite. The association of abundant clinopyroxene with nepheline in the outer rim of vesicles in which no olivine and melilite and very little opaque spinel is seen, attests to the extended period of crystallisation of this mineral and implies that it is partly contemporaneous with nepheline.

Clinopyroxene in the nephelinite accounts for approximately 45% of the rock volume. It is present as colourless, euhedral basal sections and prisms which range in size from smaller than 0.02mm to 0.25mm. The grains generally show well developed oscillatory zoning.

3.5 Monticellite

Primary groundmass monticellite is present in the grey melilitite in amounts ranging from about 31 to 43 vol%. The grains are typically small (up to 0.03mm in size), rounded and/or anhedral. Individual monticellite grains are closely packed in the groundmass and usually seperated from each other by a thin divide of nepheline (plate 3.6a). The larger olivines in the grey melilitite are in most cases partially replaced along the edges by granules of monticellite, while smaller grains are generally completely replaced (plate 3.6d). In a number of cases these monticellite replacements consist of large single crystals of monticellite (plate 3.6b), although polycrystalline aggregates may also occur.

PLATE 3.6

A - Small, granular monticellites in the groundmass of the grey melilitite. Note the grains enclosed in phlogopite.
Sample 209
Scale bar=0.1mm

B - A large, irregularly shaped monticellite in the grey melilitite. The grain probably replaced an olivine macrocryst.
Sample 178
Scale bar=0.5mm

C - Small, euhedral perovskites.
Sample 209
Scale bar=0.1mm

D - Euhedral perovskites in the groundmass of the grey melilitite. Note how the grains define the shape of an olivine phenocryst which is now completely replaced by monticellite.
Sample 24
Scale bar=0.2mm

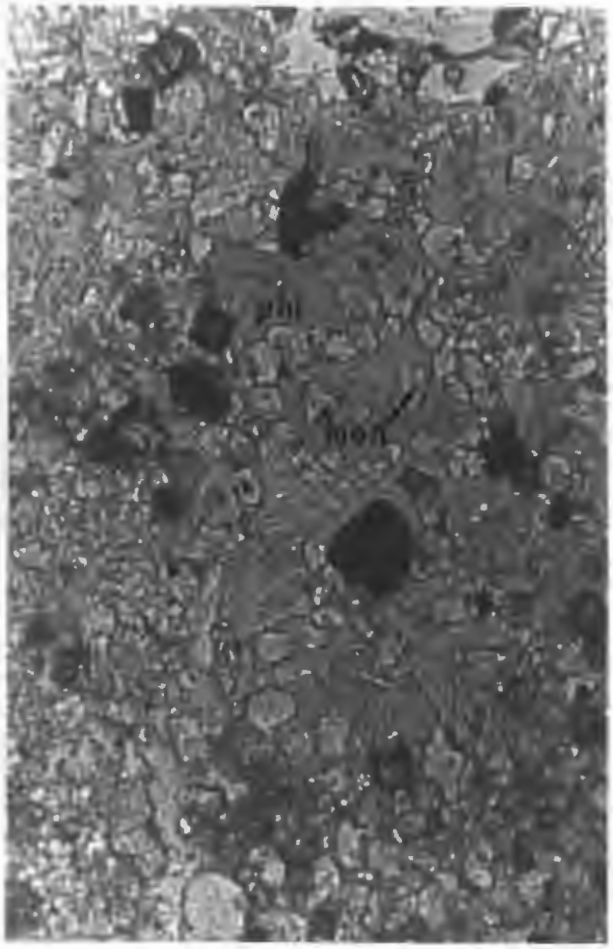

a

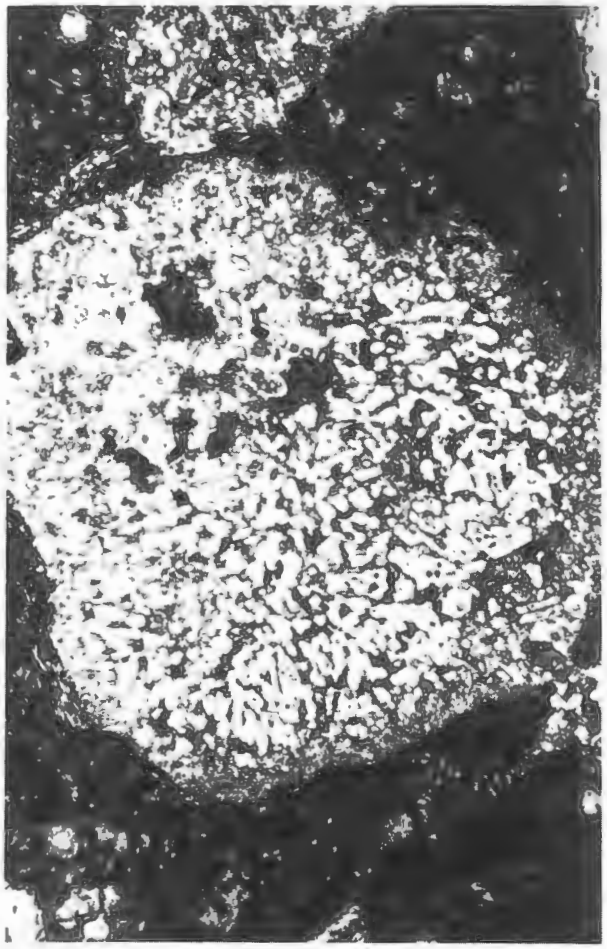

b

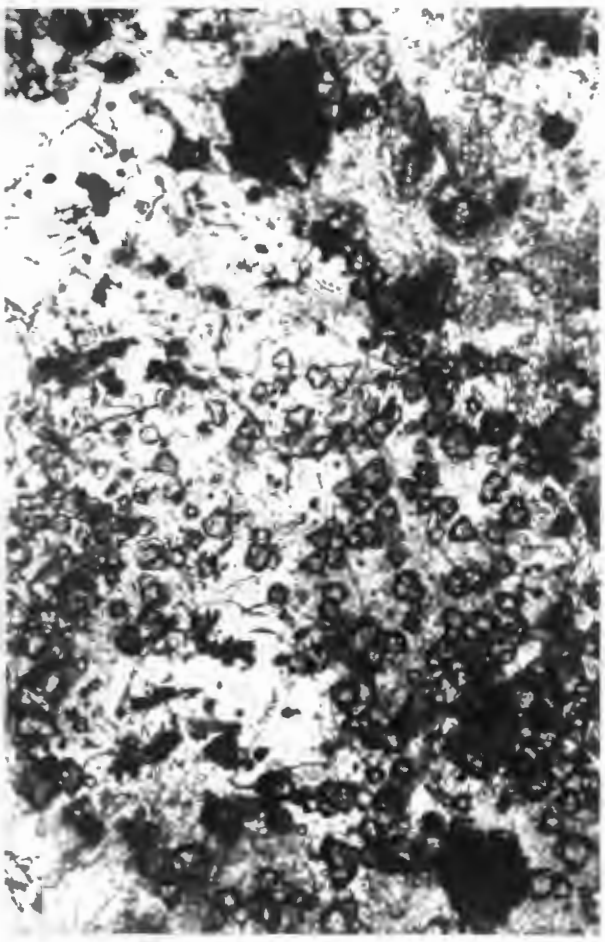

c

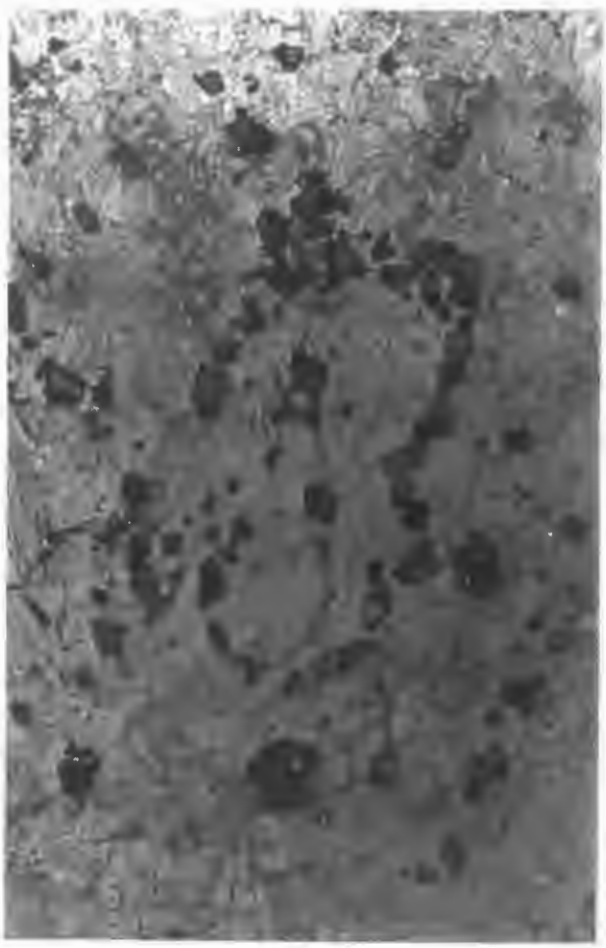

d

Large plates (up to 0.25mm) of metasomatic monticellite are seen in samples of the green melilitite taken close to the contact with the overlying grey melilitite. Modal abundances are variable but are generally higher in samples taken at the contact. This monticellite probably crystallised after deuteric alteration occurred as these grains include blebs and clots of groundmass phases including zeolites and clay minerals.

Small, square inclusions of possible kalsilite are seen in monticellites in the grey melilitite which are similar to inclusions described from Haystack Butte, Montana (Hearn, 1979).

3.6 Spinel

Spinels were examined in reflected and transmitted light. They are ubiquitous in almost all the rocks examined and occur as transparant to translucent, reddish brown chromites ("coloured spinels"), opaque chromites and opaque titanomagnetites. Chromites are generally rare in the nephelinite and spinels are rare or absent in vesicles.

Coloured spinels occur as discrete subhedral to euhedral grains in the groundmass and as tiny euhedral inclusions in olivine phenocrysts. The grains occurring in the groundmass are typically large (up to approximately 0.1mm in size) and are in many cases mantled by titanomagnetite (plate 3.7g and 3.7h). They are occasionally mantled by opaque chromite which is in turn mantled by titanomagnetite. The coloured spinels sometimes show evidence of resorption such as rounding and

PLATE 3.7

A - Titanomagnetite overgrown on a chromite core.

Sample 26

Scale bar=0.05mm

Reflected light

B - Euhedral chromite partially enclosed in an olivine phenocryst. Note the magnetite overgrowth where the grain was exposed to the surrounding liquid.

Sample 83

Scale bar=0.05mm

Reflected light

C - Cluster of chromites overgrown by titanomagnetite.

Sample 9

Scale bar=0.05mm

Reflected light

D, E & F - Titanomagnetite overgrowths on chromite cores.

Samples 163 (D & E) and 24 (F).

Scale bars=0.05mm

Reflected light

G & H - Reddish-brown translucent chromites overgrown by titanomagnetite.

Samples 26 (G) and 211 (H).

Scale bars=0.05mm.

Transmitted and reflected light

a

b

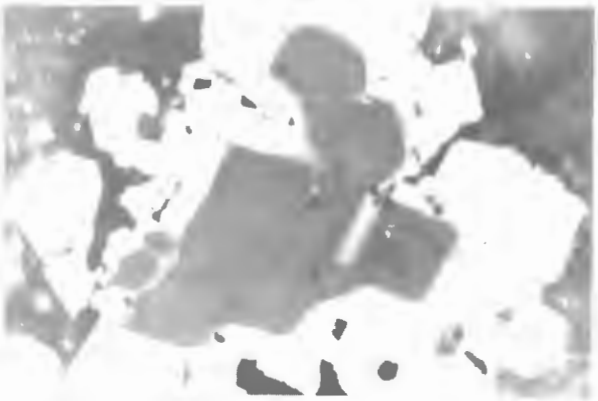

c

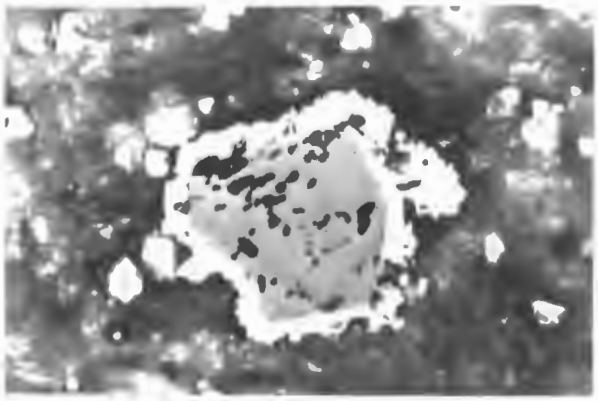

d

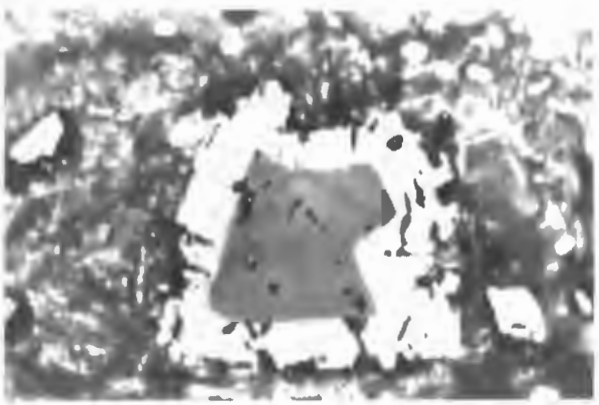

e

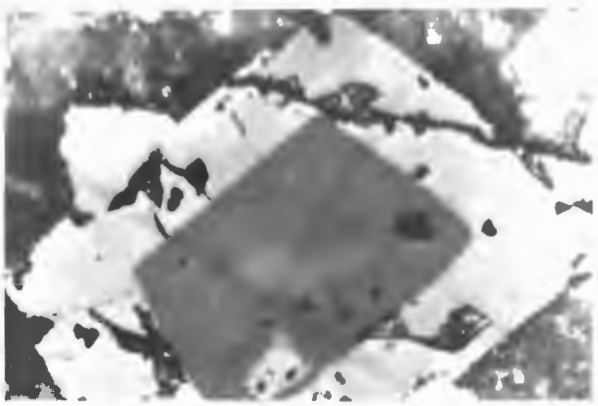

f

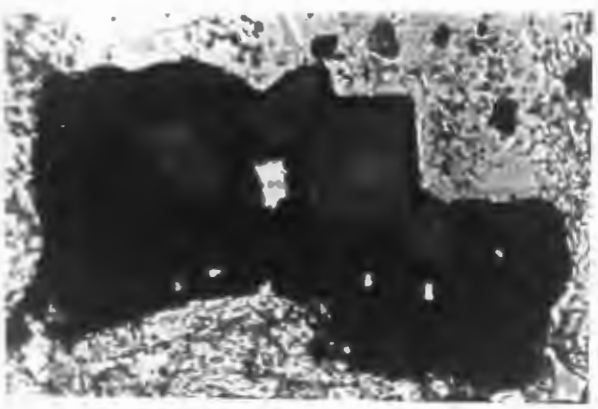

g

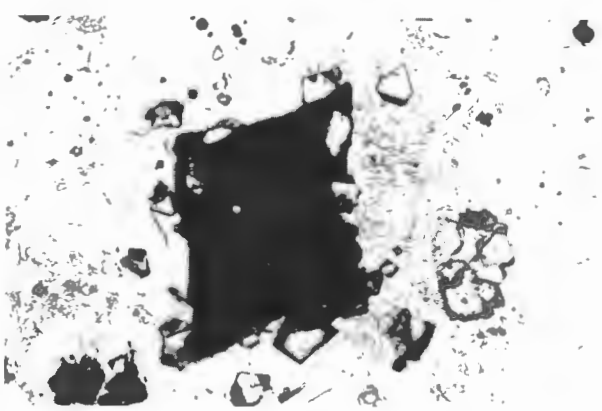

h

corrosion of the edges of grains. Coloured spinels are generally more abundant in the grey melilitite than in any of the other rock types, and they bear a superficial resemblance to the spinels described from the Wesselton Sills by Shee (1985), who concluded that they were derived from spinel harzburgites (i.e. they are xenocrysts).

Opaque chromites form cores to titanomagnetite overgrowths (plate 3.7c-f), are partly or completely enclosed in olivine phenocrysts (plate 3.7a, 3.7b and 3.8a) and are in a few cases seen as mantles on coloured spinels. Resorption features similar to those observed for the coloured spinels are rarely seen. It is quite possible that the opaque chromites enclosed in olivine are actually coloured but are too thick to transmit light and therefore appear to be opaque.

Titanomagnetite occurs as discrete, often euhedral grains and as mantles to the coloured and opaque chromites. Discrete grains are generally smaller (up to 0.06mm) than the aggregates which are cored by chromite (up to 0.13mm in size). Anhedral, optically homogenous magnetite macrocrysts up to 1cm in size are commonly seen in the grey melilitite and are occasionally present in specimens from the ring dyke and the green melilitite. A number of these macrocrysts are intimately intergrown with olivine and subhedral to euhedral, elongate grains of apatite.

3.7 Perovskite

Perovskite is not seen in the nephelinite but a few cloudy aggregates showing high birefringence (sphene?) are present.

Sphene is a common deuteric alteration product of perovskite. Perovskite is otherwise ubiquitous in rocks from the ring dyke and the sill complex. Modal abundances vary between 1 and 12 vol%.

Perovskite grains exhibit a brownish yellow colour, are generally euhedral and range in size from tiny octahedra to grains up to 0.06mm in size (plate 3.6c). They tend to occur as a necklace around olivines in the green and grey melilitites (plate 3.6d). Perovskites are not present in the zeolite or carbonate filled centre of vesicles but are, in a few cases, seen in the outer clinopyroxene-nepheline zone where they exhibit a purplish colour, possibly due to higher iron content.

3.8 Ilmenite

Ilmenite macrocrysts up to 5mm in size are a rare constituent of the Commonage melilitites. Where present they are anhedral, optically homogenous grains which are rimmed by irregular overgrowths of perovskite and titanomagnetite. Groundmass ilmenite is exceedingly rare and has only been observed in the nephelinite where it is lath-shaped and up to 0.5mm in size.

3.9 Nepheline

Groundmass nepheline forms the base in the crystalline and vesicular rocks, the grey melilitite and the nephelinite. It was probably present in the green melilitite but is now not seen due to the effects of pervasive deuteric alteration. Nephelines in the nepheline-clinopyroxene filled veins and

outer rims of vesicles are in many cases euhedral (plate 3.8b). In the vesicular rocks and the nephelinite it is commonly altered to turbid hydronepheline or turbid brownish, isotropic analcite and is often replaced by fibrous zeolites.

Nepheline obviously crystallised late as it hosts inclusions of almost all the groundmass minerals (excluding zeolites, garnet and carbonate).

3.10 Apatite

Skeletal and/or euhedral apatite (plate 3.8b and 3.8c) is present in all the rocks examined. Modal abundances are highly variable, ranging from trace concentrations to 20 vol% in the green melilitite.

Euhedral apatite inclusions are present in olivine macrocrysts (figure 3.1).

3.11 Garnet

Yellowish, high relief grains of grossular garnet up to 0.13mm in size are often seen in association with zeolites in vesicles (plate 3.9b, 3.9c and 3.9d). It is also present in the groundmass of highly vesicular rocks and the green melilitite where it accounts for approximately 1 to 3% of the rock volume. It is in many cases moulded onto coexisting zeolites in the vesicles which suggests that it crystallised late from a volatile rich fluid.

3.12 Zeolites

Zeolites occur in vesicles (plate 3.8d), and are

PLATE 3.8

A - Small euhedral chromites completely enclosed in an olivine phenocryst.

Sample 30

Scale bar=0.1mm

B - Euhedral and skeletal apatite enclosed in nepheline.

Sample 50

Scale bar=0.05mm

C - Apatite associated with carbonate, zeolites and garnet in the groundmass of the green melilitite.

Sample 193

Scale bar=0.2mm

D - Note the fibrous inward-growing zeolite which lines the wall of a carbonate filled vesicle. Vesicular rock from the ring dyke.

Sample 80

Scale bar=0.2mm

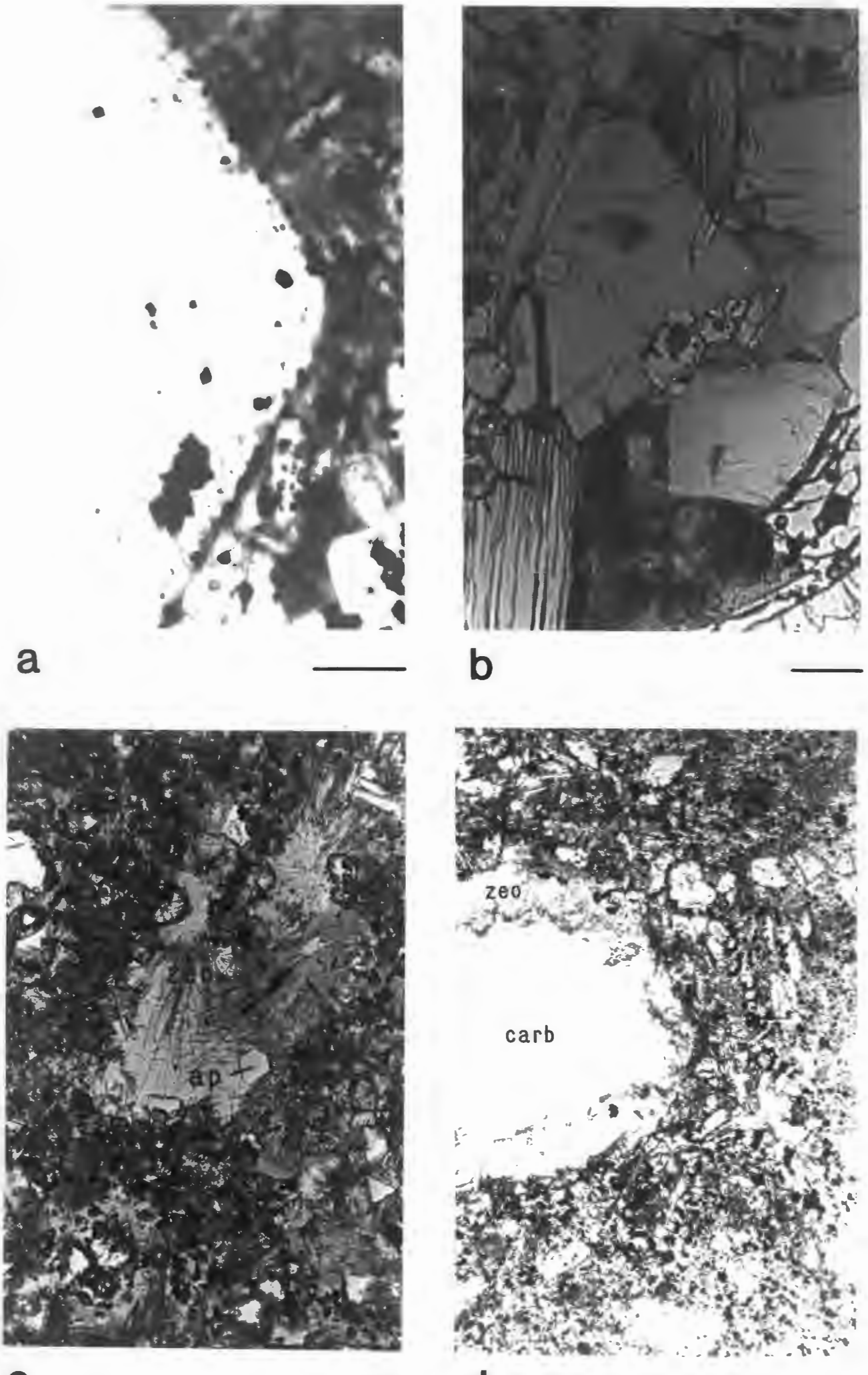
a
b
ap
c
zeo
carb
d

disseminated through the groundmass of the green melilitite, where they are associated with the breakdown of nepheline. Slender needles showing high relief and occurring as clusters and sheaths in vesicles are probably natrolite (plate 3.9b). Low relief, fibrous thomsonite has also been recognised by Gerard (1958) and Boctor and Yoder (1986). McIver and Ferguson (1979) recorded the presence of laumontite in the grey melilitite.

3.13 Amphibole

A green fibrous amphibole partially replaces clinopyroxenes in the highly vesicular rocks (plate 3.5c). The grains exhibit weak pleochroism from pale green to brownish green and are probably actinolite which formed by the late stage replacement of clinopyroxene under water rich conditions.

3.14 Carbonate, chlorite and clay minerals

Coarse grains of possible primary carbonate are seen in a few cases in the cores of vesicles (plate 3.8d) and is also disseminated through the groundmass of a number of samples. It is generally more abundant in the green melilitite than in the other rock types examined.

A little interstitial serpentine is seen in the groundmass of the green melilitite. The olivines in this rock type are also in many cases partially replaced by serpentine and it is therefore considered to be of predominantly deuteric origin.

Greenish pleochroic chlorite and abundant unidentified clay minerals are ubiquitous in the groundmass of the green

melilitite and are probably also of deuteric derivation.

PLATE 3.9

A - Typical zeolite filled vesicle. Note the clinopyroxene laths at the edge of the vesicle and the coarsely crystalline nature of the surrounding groundmass.

Sample 80

Scale bar=0.5mm

B - Small grains of grossular garnet associated with fibrous zeolite and carbonate in a vesicle.

Sample 162

Scale bar=0.1mm

C - Garnet in the groundmass of the green melilitite. Note the darker coloured cores of the crystals.

Sample 209

Scale bar=0.1mm

D - Numerous grains of garnet associated with serpentine in a corrosional hollow in olivine.

Sample 162

Scale bar=0.1mm

a

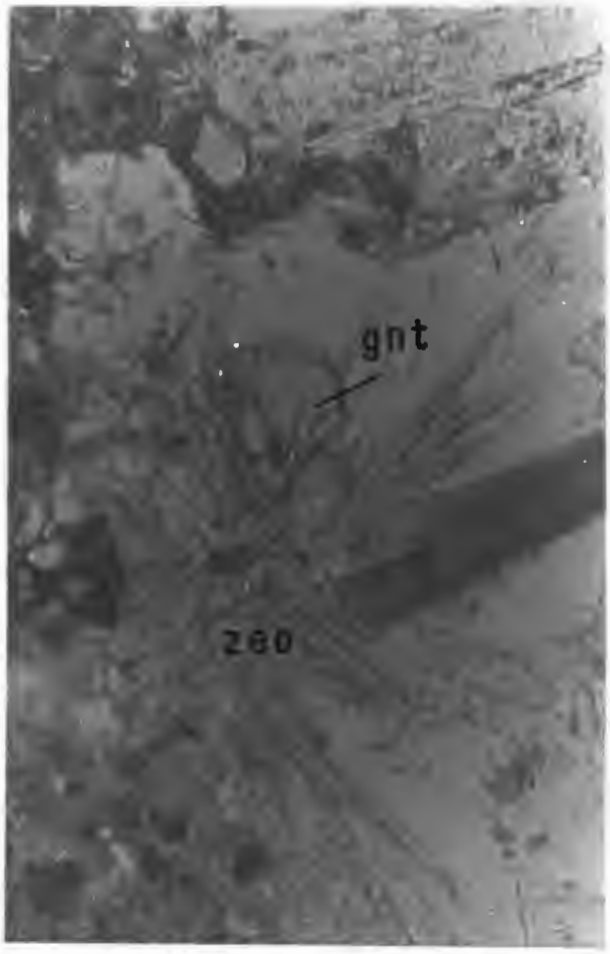

b

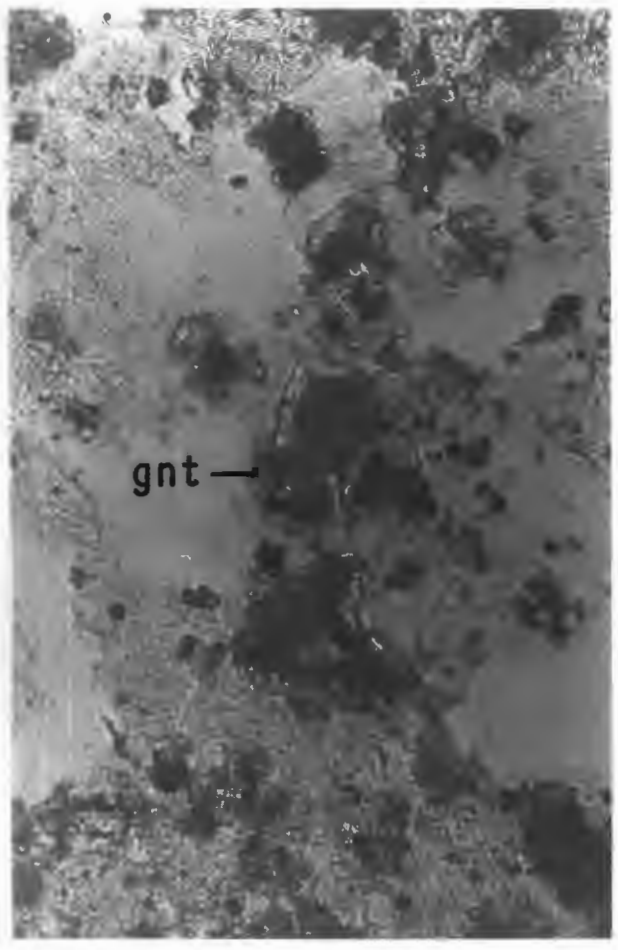

c

d

4 PYROXENE MINERAL CHEMISTRY

4.1 Introduction

Groundmass clinopyroxene is an abundant phase in the ring dyke and the olivine nephelinite. It is extremely rare in the green and grey melilititites of the sill complex as often only one grain is observed in every 10 thin sections examined (see chapter 3). It was consequently decided to concentrate only on clinopyroxene in samples from the ring dyke and the olivine nephelinite.

Chemical variations of clinopyroxenes were studied for the following reasons:

1) They indirectly monitor the chemical evolution of a typical melilitite magma, particularly with respect to SiO_2, TiO_2, Al_2O_3, FeO, MgO, CaO, and Na_2O. The rocks from the ring dyke are ideally suited to such a study since they exhibit a variety of groundmass textures, ranging from a glass-bearing chill to slowly-cooled, coarse vesicular rocks, all of which contain clinopyroxene.

2) To monitor the evolution of the magma which crystallised the olivine nephelinite.

3) To compare the clinopyroxene mineral chemistry of the Commonage rocks with those of other undersaturated alkaline ultrabasic intrusives.

4.2 Variations in clinopyroxene chemistry at the Commonage

Four rock samples from the ring dyke and one sample of olivine nephelinite were selected for detailed study of their

constituent clinopyroxenes. Samples taken from the ring dyke are as follow:

Sample 155 - area 1 A glass-bearing chilled melilitite from the dyke contact.

Sample 30 - area 2 A fine grained but wholly crystalline rock from the dyke contact.

Samples 83 and 160 - area 3 and 8 Two highly vesicular, coarse grained melilitites from small sill-like bodies associated with the ring dyke.

Sample 267 - area 15 One typical olivine nephelinite was selected for detailed study. Details of each of these rocks are presented in appendix 8.

Microprobe analyses of the Sutherland Commonage clinopyroxenes are given in appendix 4 and compositional ranges are summarised in table 4.1.

Compositional trends shown by core and rim analyses are illustrated graphically in Ca-Mg-Fe diagrams (figures 4.1 and 4.2), plots of Al_2O_3 and TiO_2 versus the ferrosilite percentage (ring dyke only-figures 4.3 and 4.4) or the wollastonite percentage (olivine nephelinite only-figures 4.5 and 4.6) and Na-Mg-(Fe^{2+}+Mn) diagrams (figures 4.9 and 4.10). Detailed microprobe scans were done on five clinopyroxenes in the ring dyke and one clinopyroxene from the olivine nephelinite. Zonation patterns in these grains are presented in figures 4.11(a-f).

Comparison of figures 4.1 and 4.2 with the pyroxene classification scheme of Poldervaart and Hess (1951) show that

Table 4.1 Summary of Sutherland Commonage clinopyroxene compositional data

(a) Clinopyroxenes in the ring dyke

	min(wt%)	max(wt%)	mean(wt%)
SiO_2	42.62	53.88	50.37
TiO_2	0.41	5.13	2.09
Al_2O_3	0.13	6.99	1.93
Cr_2O_3	0.00	0.20	0.01
FeO	3.86	8.44	5.99
MnO	0.00	0.24	0.15
MgO	11.65	16.27	14.47
CaO	22.57	24.47	23.69
Na_2O	0.31	0.92	0.65
K_2O	0.00	0.06	0.01

(b) Clinopyroxenes in the olivine nephelinite

	min(wt%)	max(wt%)	mean(wt%)
SiO_2	41.05	53.96	48.94
TiO_2	0.43	5.42	2.45
Al_2O_3	0.40	10.99	4.35
Cr_2O_3	0.00	0.20	0.04
FeO	5.28	8.40	6.50
MnO	0.00	0.21	0.12
MgO	11.22	16.32	13.94
CaO	21.75	24.23	23.42
Na_2O	0.29	0.80	0.43
K_2O	0.00	0.27	0.01

Figure 4.1 Ca - Mg - Fe plot for groundmass clinopyroxenes in the ring dyke

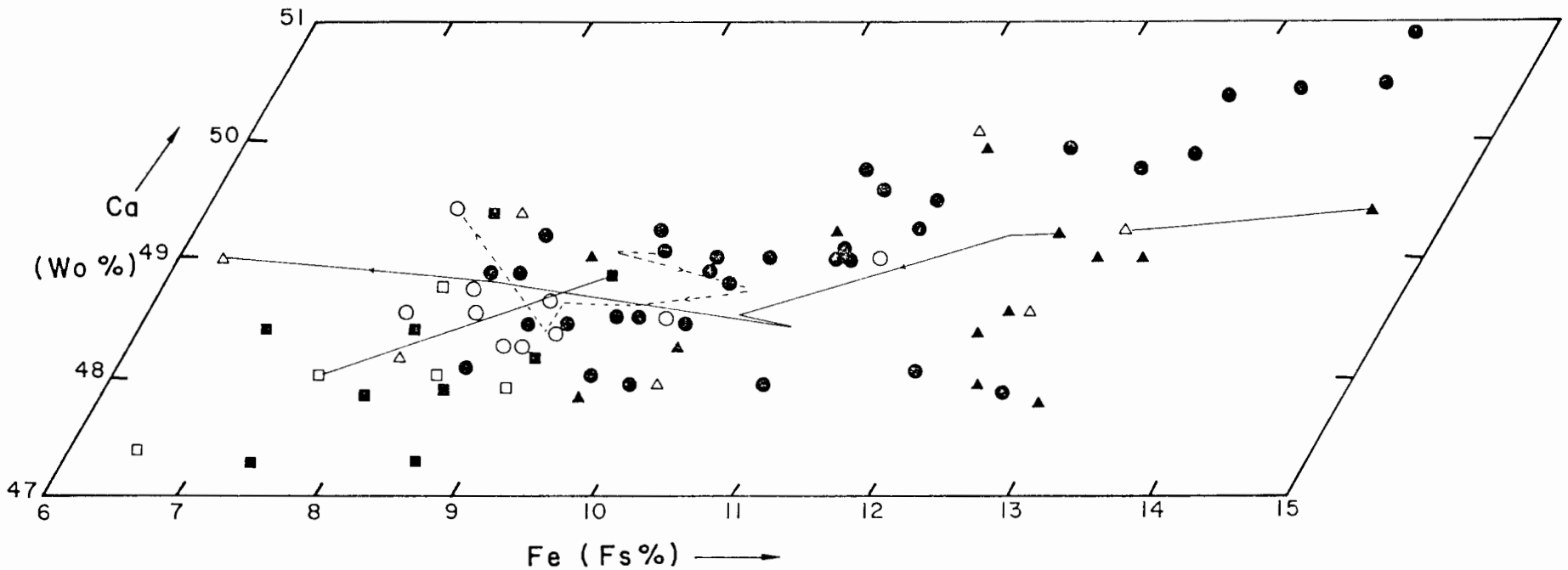

- ● groundmass cores
- ○ groundmass rims
- ▲ cores } clinopyroxenes
- △ rims } in vesicles
- ■ cores } clinopyroxenes
- □ rims } in glass-rich chill

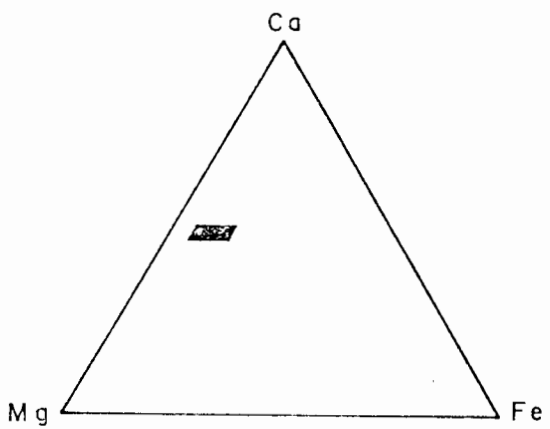

Figure 4.2 Ca - Mg - Fe plot for groundmass clinopyroxenes in the olivine nephelinite

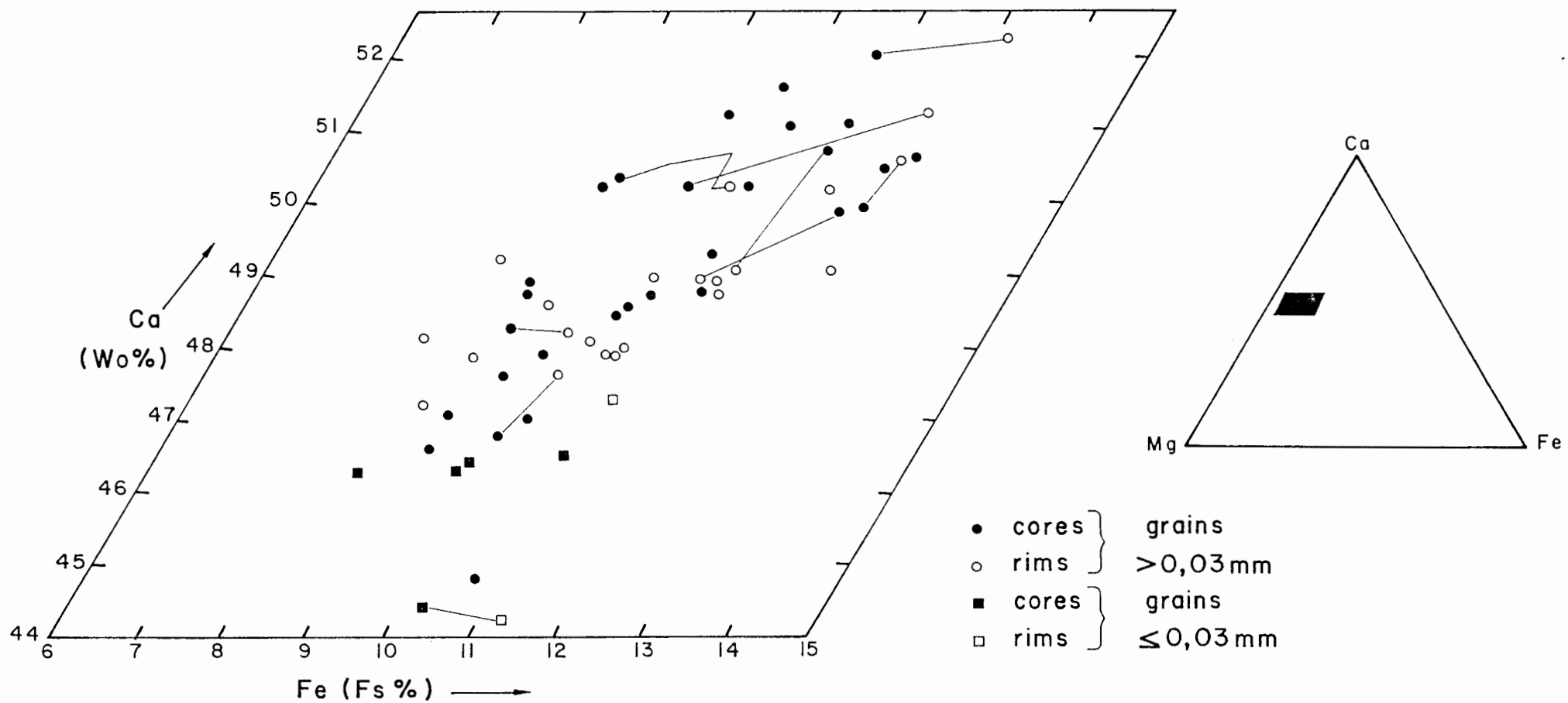

Figure 4.3 Plot of Wt % Al_2O_3 versus the ferrosilite % for groundmass clinopyroxenes in the ring dyke

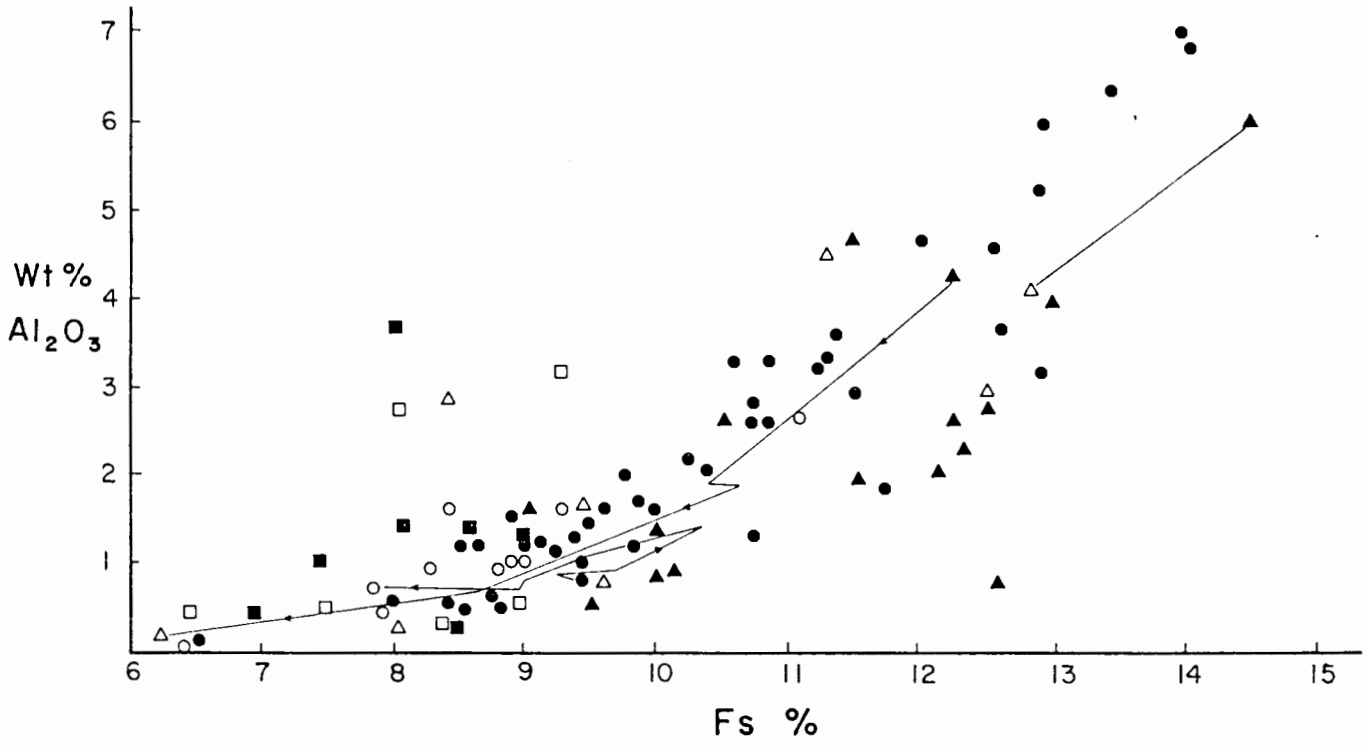

- ● groundmass cores
- ○ groundmass rims
- ▲ cores } clinopyroxenes
- △ rims } in vesicles
- ■ cores } clinopyroxenes
- □ rims } glass-rich chill

Figure 4.4 Plot of Wt % TiO_2 versus the ferrosilite % for groundmass clinopyroxenes in the ring dyke

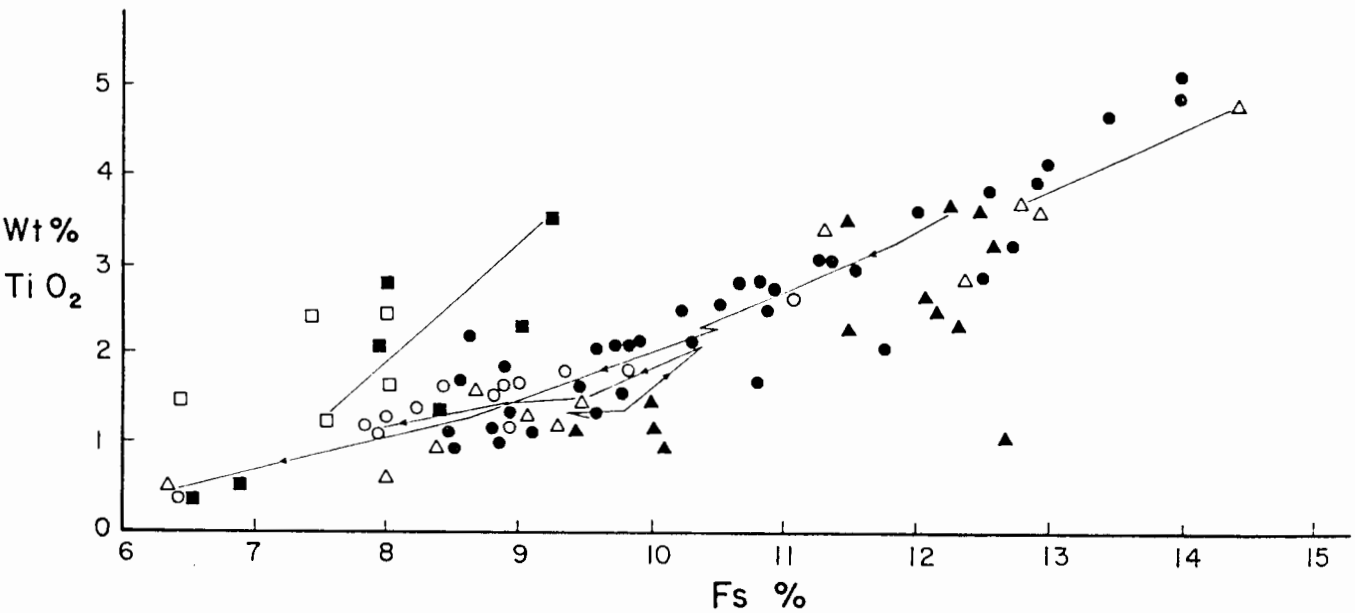

symbols as in figure 4.3

Figure 4.5 Plot of Wt % Al_2O_3 versus the wollastonite % for groundmass clinopyroxenes in the olivine nephelinite.

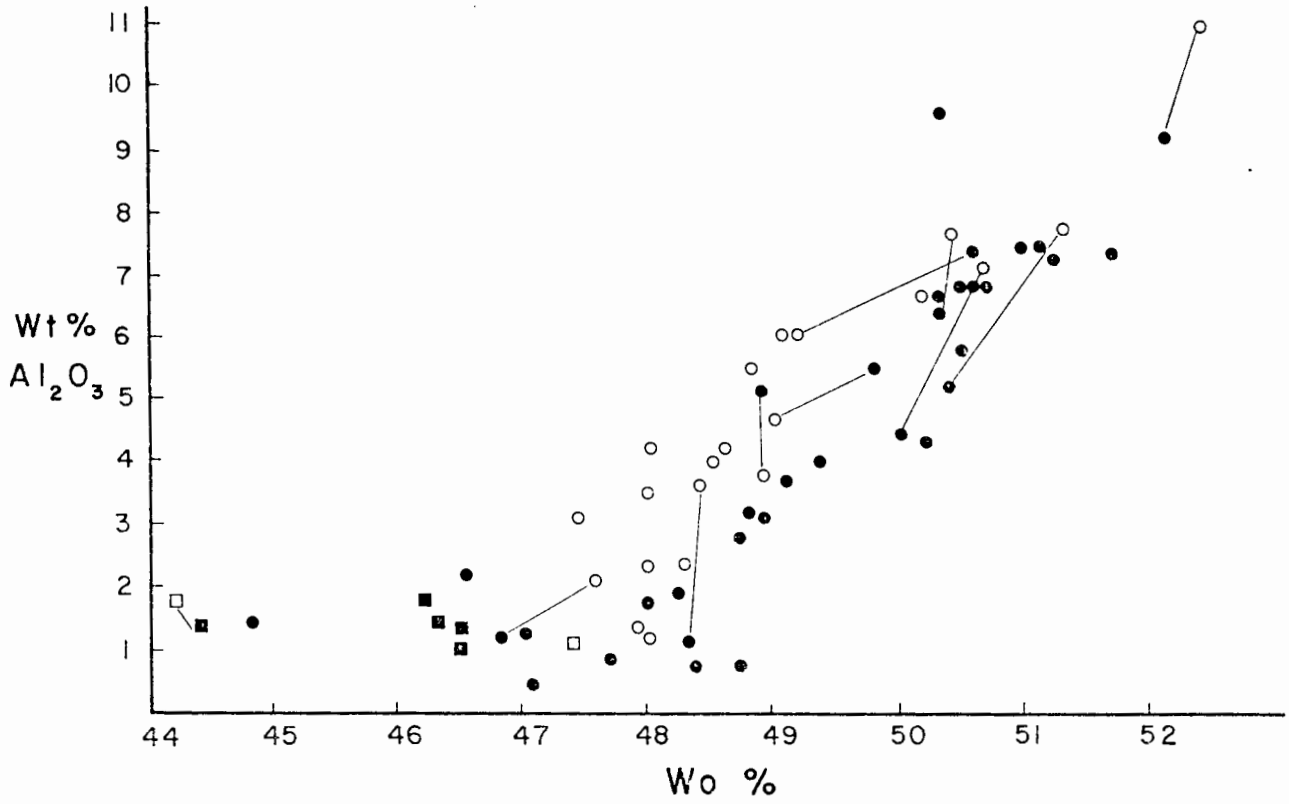

Figure 4.6 Plot of Wt % TiO_2 versus the wollastonite % for groundmass clinopyroxenes in the olivine nephelinite

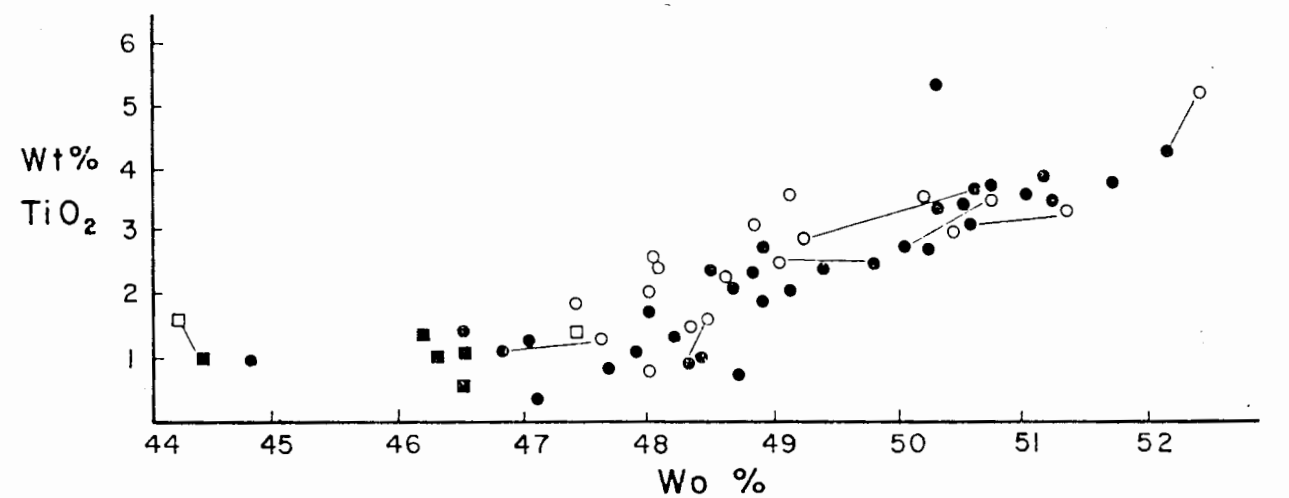

symbols as in figure 4.5

all the pyroxenes fall in the diopside or salite fields. Other noteworthy features of the Commonage pyroxenes are the presence of significant quantities of Al_2O_3 (up to 10.99 wt%) and TiO_2 (up to 5.42 wt%), and the low Cr_2O_3 (<0.20 wt%), MnO (<0.24 wt%) and K_2O (average wt%=0.01) concentrations (table 1).

Pyroxenes in the ring dyke show a wide range in ferrosilite content, ranging from approximately 6% to 14.5%. Wollastonite contents varies from 47% to 51% (figure 4.1). The grains are continuously zoned and generally exhibit a trend of increasing SiO_2 and MgO from core to rim, and decreasing FeO, TiO_2 and Al_2O_3 (figures 4.4, 4.7, 4.8 and 4.11a-e). The behaviour of CaO is often erratic (figure 4.11a) but it is in broad terms generally constant from core to rim in normal groundmass grains and increases from core to rim in grains in vesicles (figures 4.1 and 4.11d-e). Na_2O contents remain constant from core to rim, or may show slight enrichment in the rims (figure 4.9 and 4.11a-e).

Pyroxenes in the olivine nephelinite, by comparison exhibit a relatively restricted range in ferrosilite contents (8% to 14%) but exhibits a wider range of wollastonite contents, ranging from 44% to 52.5% (figure 4.2). These clinopyroxenes show a pattern of increasing FeO, Al_2O_3, TiO_2 and Na_2O, and decreasing MgO and SiO_2 from their cores to rims (figure 4.2, 4.5, 4.6, 4.8 and 4.11f). The behaviour of CaO and SiO_2 are highly variable and do not show any recognisable pattern.

4.3 Comparison of the Sutherland Commonage clinopyroxenes with

Figure 4.7 Plot of Wt% SiO versus the ferrosilite % for groundmass clinopyroxenes in the dyke

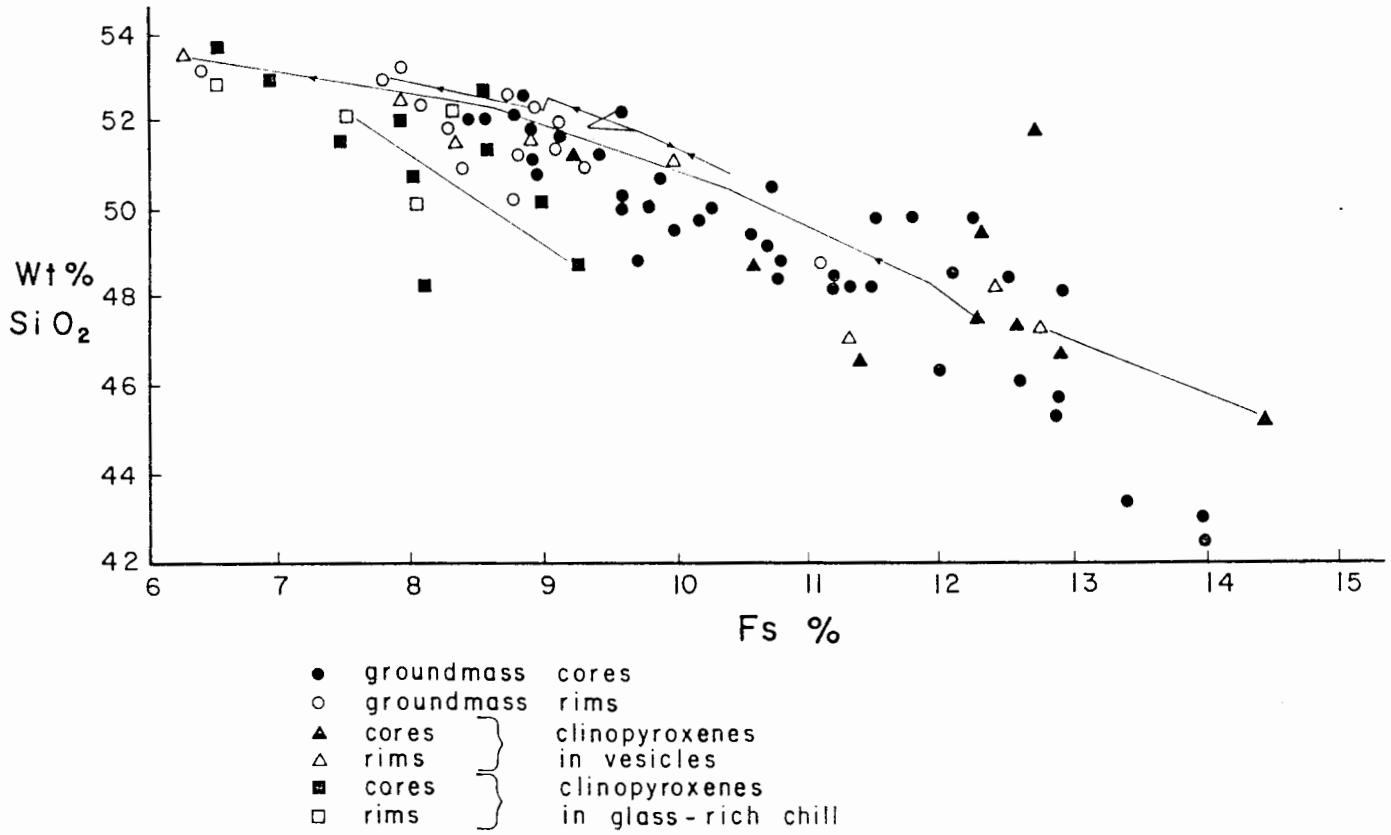

Figure 4.8 Plot of Wt% SiO_2 versus the wollastonite % for groundmass clinopyroxenes in the olivine nephelinite

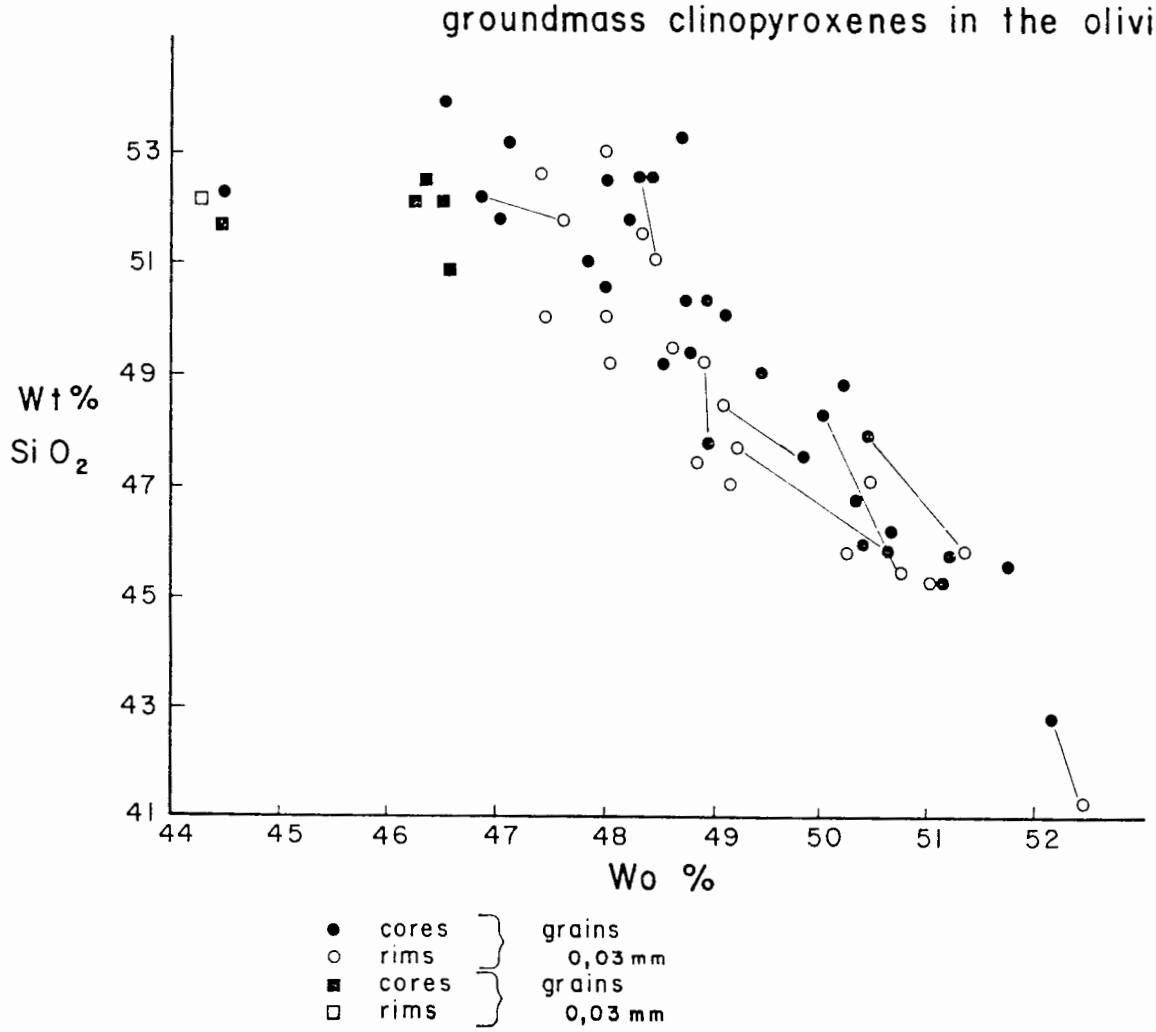

Figure 4.9 Na - Mg - (Fe^{2+} + Mn) plot of groundmass clinopyroxenes in the ring dyke

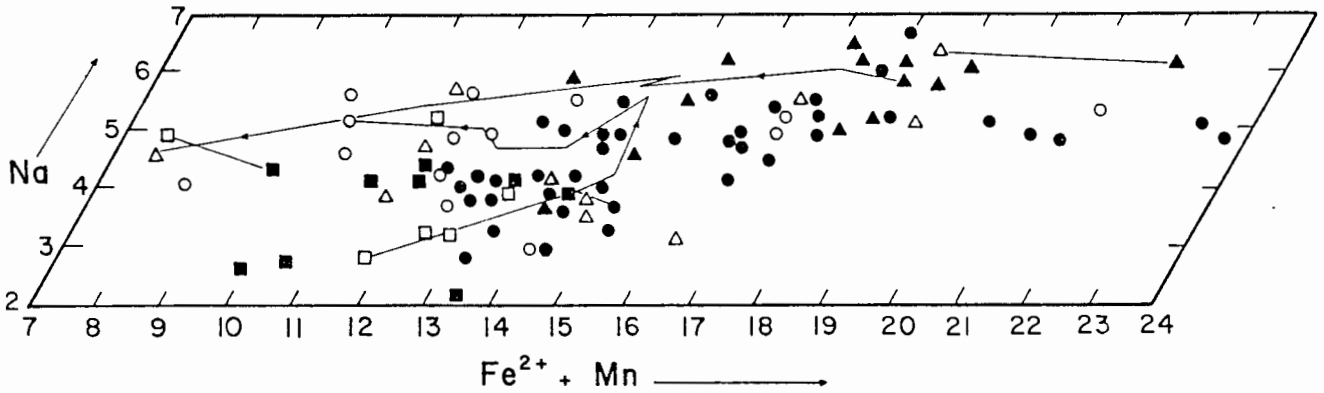

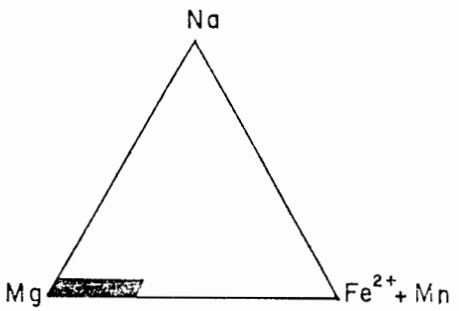

- ● groundmass cores
- ○ groundmass rims
- ▲ cores } clinopyroxenes
- △ rims } in vesicles
- ■ cores } clinopyroxenes
- □ rims } in glass-rich chill

Figure 4.10 Na - Mg - (Fe^{2+} + Mn) plot of groundmass clinopyroxenes in the olivine nephelinite

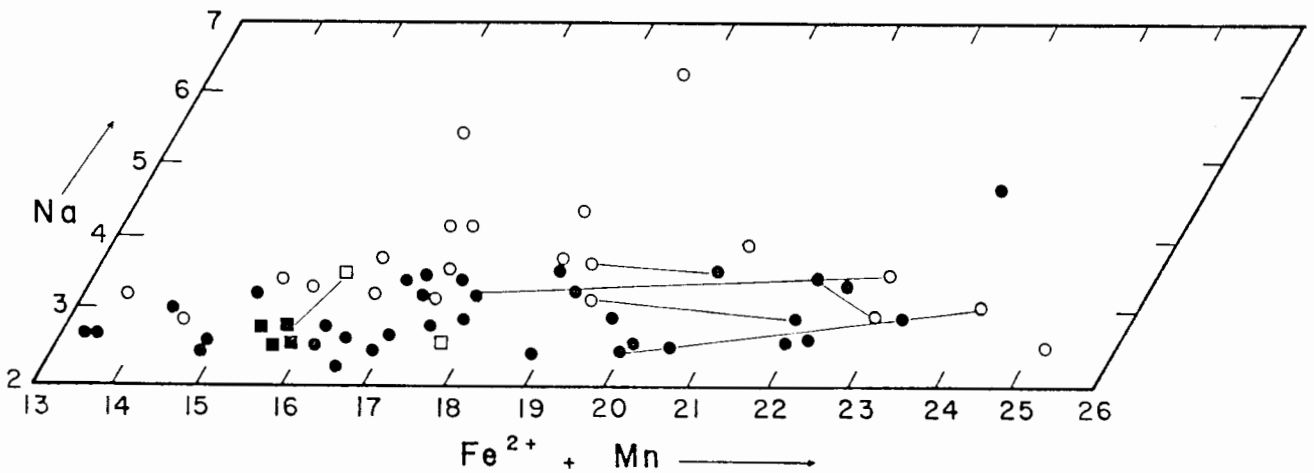

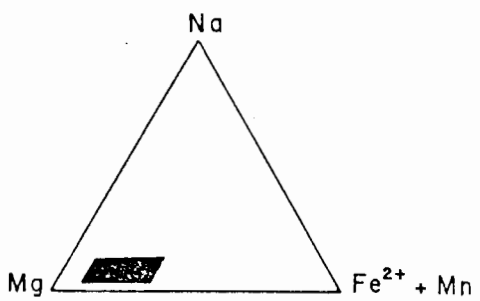

- ● cores } grains
- ○ rims } > 0,03mm
- ■ cores } grains
- □ rims } ≤ 0,03mm

Zonation of Sutherland clinopyroxenes

Figure 4.11 (a)

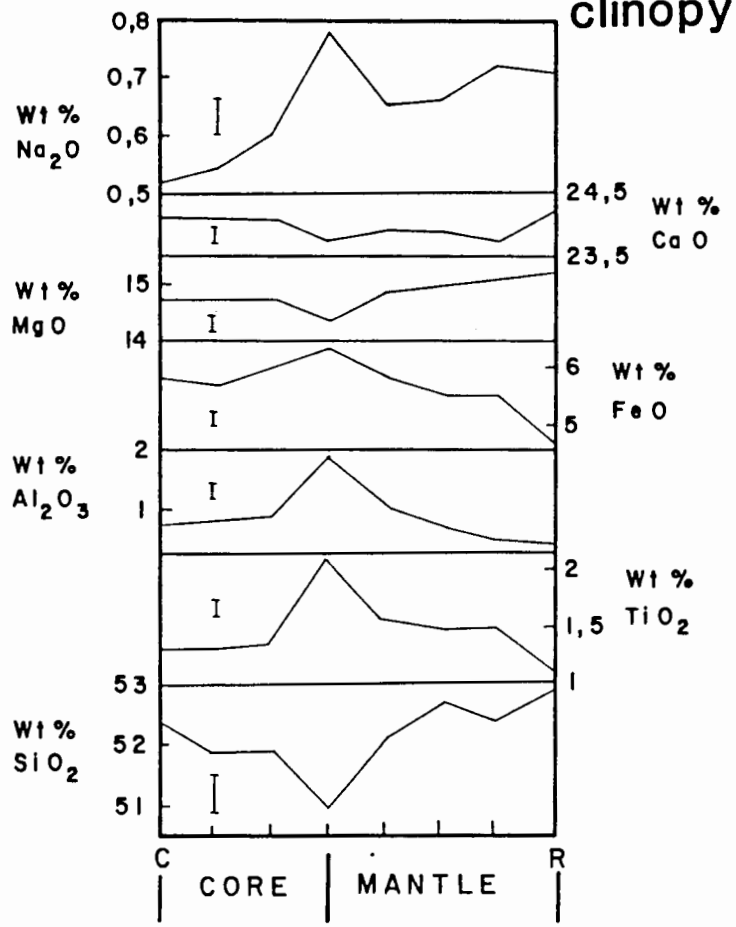

vertical bars – experimental error

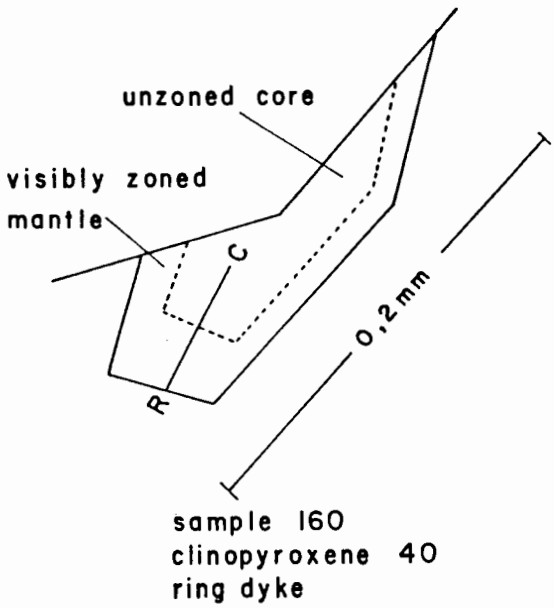

sample 160
clinopyroxene 40
ring dyke

Figure 4.11 (b)

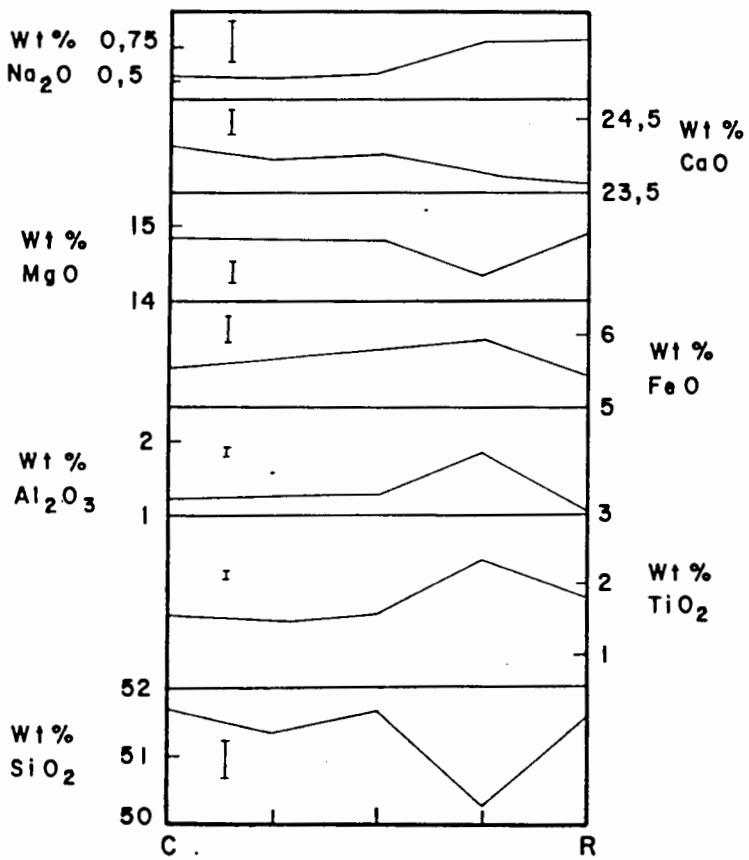

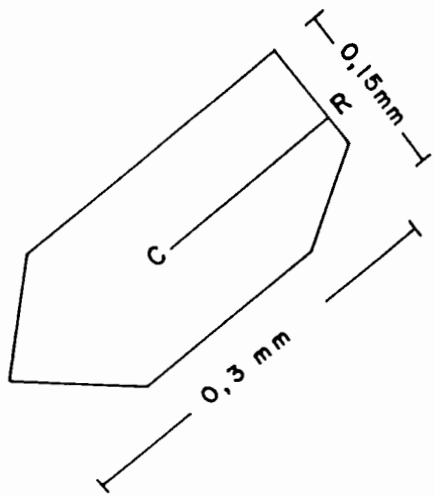

sample 160
clinopyroxene 43
ring dyke

Figure 4.11 (c)

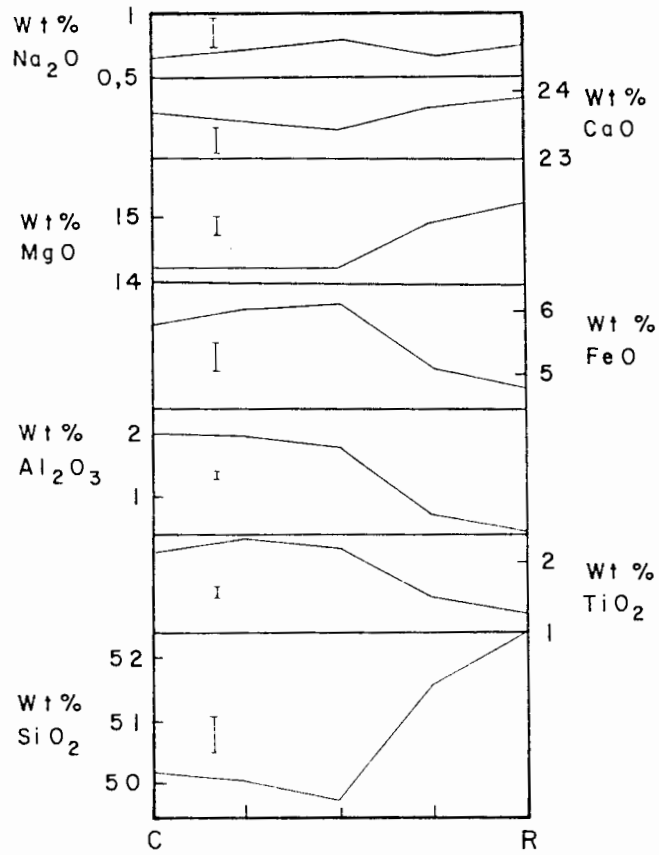

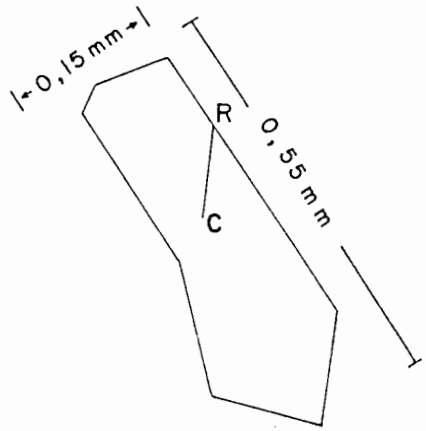

sample 160 (ring dyke)
clinopyroxene 44

Figure 4.11 (d)

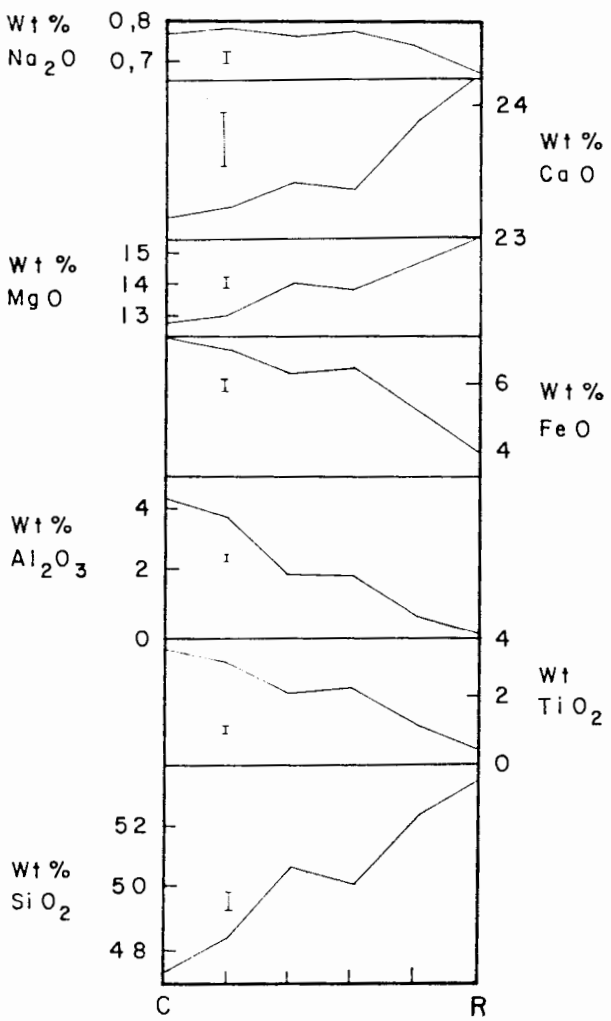

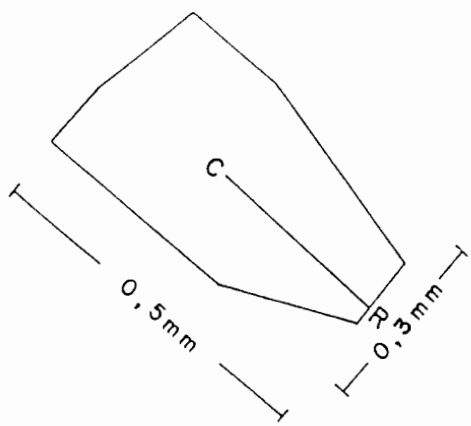

sample 160
clinopyroxene 41
(in vesicle)
ring dyke

Figure 4.11 (e)

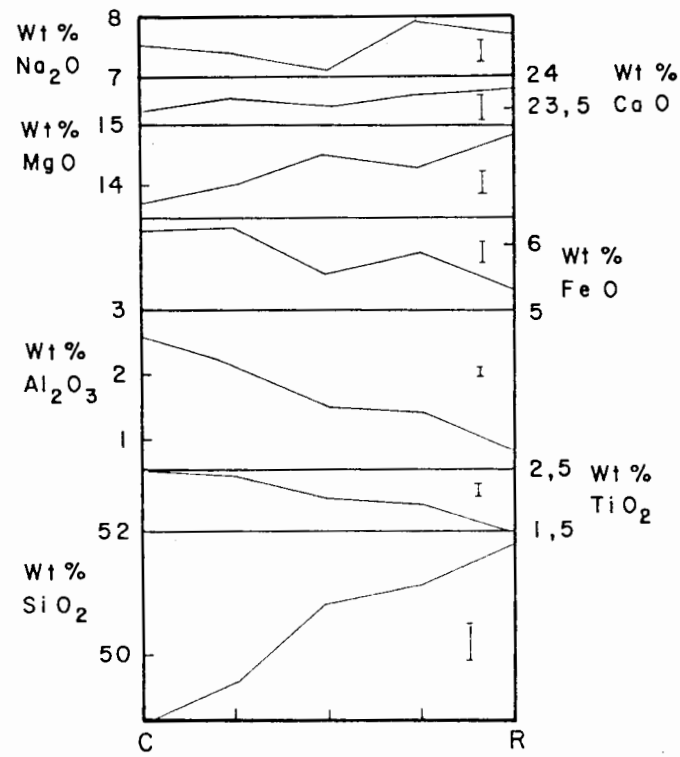

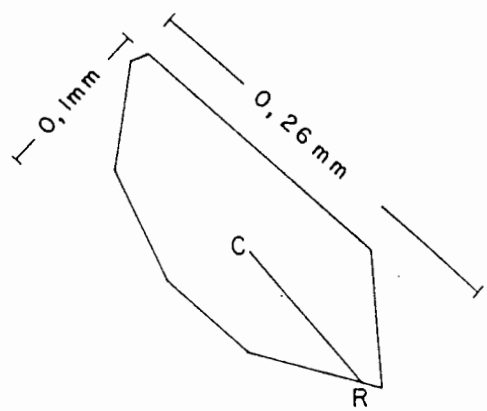

sample 160 (ring dyke)
clinopyroxene 42
(in vesicle)

Figure 4.11 (f)

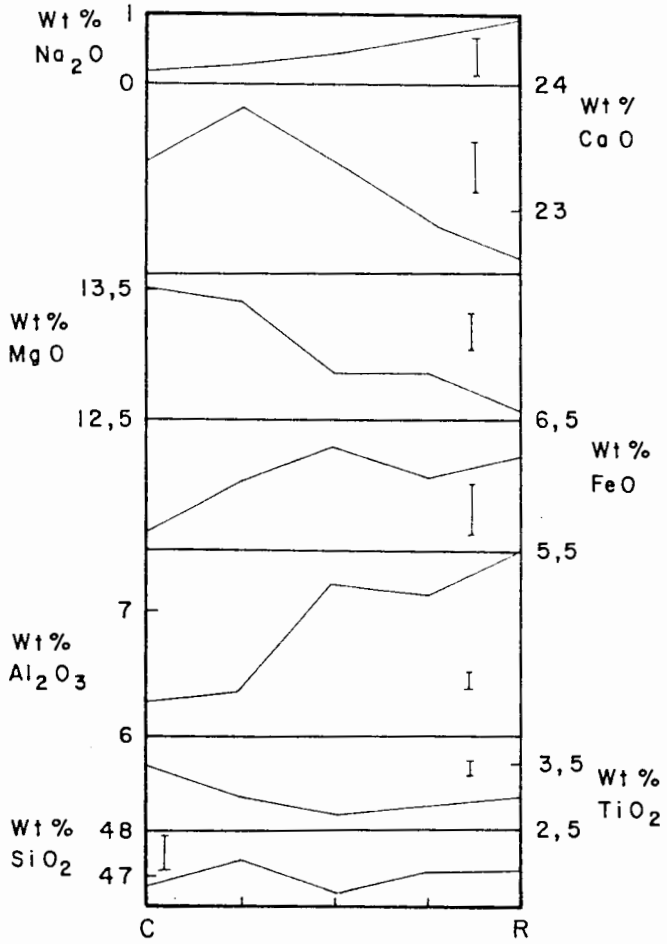

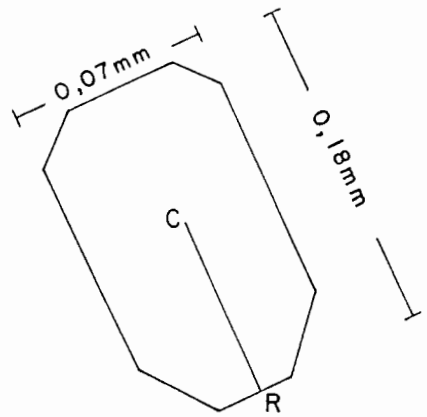

sample 267
(ol. nephelinite)
clinopyroxene 51

those from other alkaline rocks

The results of a literature survey on CaO, MgO, FeO, SiO_2, TiO_2 and Al_2O_3 concentrations in phenocryst and groundmass clinopyroxenes from selected alkaline igneous rocks are summarised in table 4.2 and figure 4.12. Melilitites for which compositional data are available include localities in the African Rift Valley (Dawson et al., 1985), Italy (Durazzo et al., 1984), Republic of South Africa (Boctor and Yoder, 1986; McIver,1981; Colgan et al., 1988), Western Australia (Robey et al., 1988), Argentina (Meyer and Villar, 1984), Solomon Islands (Nixon et al., 1980) and Greenland (Hansen, 1980). Analyses of clinopyroxenes in a few nephelinites, one ijolite, one basanite and several alkali basalts are also included to allow a more general comparison.

Clinopyroxenes from the above mentioned rock types are characterised by a wide range in SiO_2 (37.31% to 54.10%), TiO_2 (0.24% to 8.73%) and Al_2O_3 concentrations (0.20% to 13.64%). In general the clinopyroxenes from Sutherland Commonage (this study) show similar concentrations of these elements. Maximum Al_2O_3 contents (10.99 wt%) of pyroxenes from the Commonage olivine nephelinite approach the highest value recorded for melilitites in the literature (11.06 wt% Al_2O_3-Durazzo et al., 1984).

Commonage clinopyroxenes also show a large field of compositional overlap with other melilitites, nephelinites and alkali basalts when plotted on a Ca-Mg-Fe diagram (figure 4.12).

Table 1.2 Compositional ranges of SiO_2, TiO_2 and Al_2O_3 in phenocryst and groundmass clinopyroxenes from selected sodic alkaline rocks

Locality	Rock Type	SiO_2	TiO_2	Al_2O_3	Reference
Eastern Rift, North Tanzania	Melilitite	48.30-52.30	1.49-3.42	1.09-4.81	Dawson et al., 1985
Toro-Ankole field, S.W. Uganda	Melilitite	48.80-51.60	1.36-2.79	1.69-3.10	Dawson et al., 1985
Mt. Queglia, Abbruzzo, Italy	Melilitite	38.25-48.01	2.43-6.76	4.05-11.06	Durazzo et al., 1984
Saltpetre Kop, R.S.A.	Melilitite	52.45	0.24	0.74	Boctor and Yoder, 1986
Zandkopsdrift, R.S.A.	Melilitite	42.58-50.86	1.20-5.42	0.98-7.42	Boctor and Yoder, 1986
Biesiesfontein, R.S.A.	Melilitite	46.98-47.75	3.32-3.70	4.10-4.82	Boctor and Yoder, 1986
Bitterfontein, R.S.A.	Melilitite	47.42-50.40	1.47-3.52	1.65-4.51	Melver, 1981
Emtilombo, R.S.A.	Melilitite	51.40-51.67	1.83-2.48	0.62-1.31	Colgan et al., 1987
Norseman, W. Australia	Aillikite	47.47-49.04	2.26-3.87	2.48-2.59	Robey et al., 1987
Los Alisos, N. Argentina	Alnoite	52.10-53.90	0.38-1.48	0.20-1.11	Meyer and Villar, 1984
Malaita, Solomon Islands	Alnoite	42.50-49.50	2.50-5.20	3.70-8.60	Nixon et al., 1980

Table 4.2 (Cont.)

Locality	Rock Type	SiO_2	TiO_2	Al_2O_3	Reference
Gardiner Complex, E. Greenland	Melilitolite	49.48-51.23	1.33-2.01	2.16-3.28	Nielsen, 1980
Frederikshåbs Isblink, S.W. Greenland	Ol-Nephelinite	42.40-48.05	2.47-4.92	5.25-9.34	Hansen, 1980
	Nephelinite	44.08-49.06	1.00-3.54	1.64-7.34	
	Melilitite	43.98-46.17	2.21-3.12	4.92-6.51	
Fen Complex, Norway	Ijolite	47.00-52.30	0.30-2.50	1.10-5.90	Mitchell, 1980
Maui, Hawaii	Basanite	43.20-49.00	2.10-4.70	4.60-10.00	Fodor et al., 1975
Moiliili, Oahu, Hawaii	Ol-Nephelinite	49.80-51.90	1.43-2.67	0.55-2.84	Wilkinson and Stolz, 1983
Massif Central, France	Alkali Basalt	44.30-48.80	1.28-3.32	5.72-9.93	Wass, 1979
Southern Highlands, New South Wales	Alkali Basalt	42.40-50.00	1.74-5.71	4.27-11.00	Wass, 1979
Skien, Norway	Alkali Basalt	43.30-54.10	0.40-4.10	1.00-8.30	Segalstadt, 1979
Tahiti	Alkali Basalt	37.31-48.21	2.36-8.73	6.38-13.64	Tracy and Robinson, 1977
Tenerife, Canary Islands	Alkali Basalt	43.80-46.30	3.80-4.80	6.40-8.20	Scott, 1976
Hocheifel, W. Germany	Alkali Basalt	45.53-47.00	2.02-2.84	7.72-8.69	Huckenholz, 1973

Figure 4.12 Ca-Mg-Fe plot for various melilitites and nephelinites

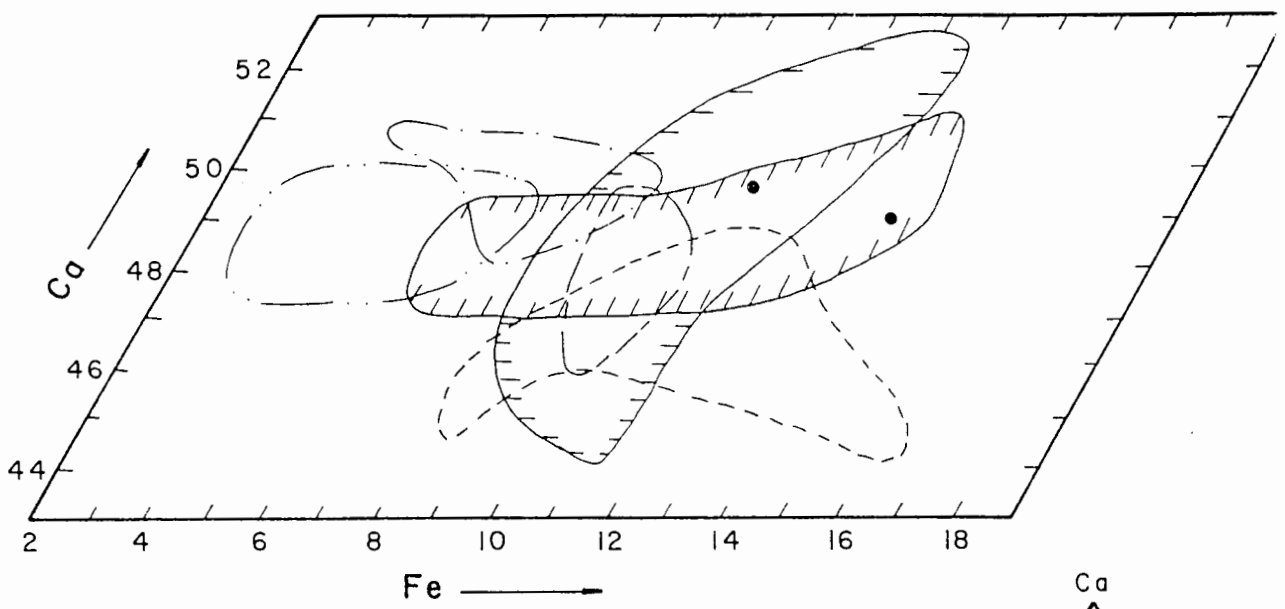

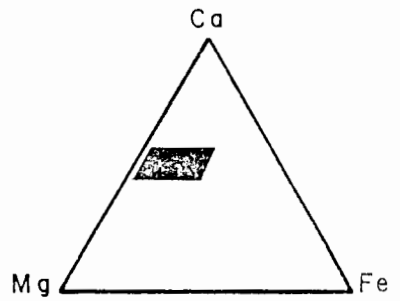

Sutherland Commonage (ring dyke)
Sutherland Commonage (ol-nephelinite)
Emtilombo, R.S.A. (Colgan et al., 1988)
Norseman, W.A. (Robey et al., 1988)
Eastern Rift, Tanzania (Dawson et al., 1985)
Los Alisos, Argentina (Meyer & Villar, 1984)
Bitterfontein, R.S.A. (Mc Iver, 1981)

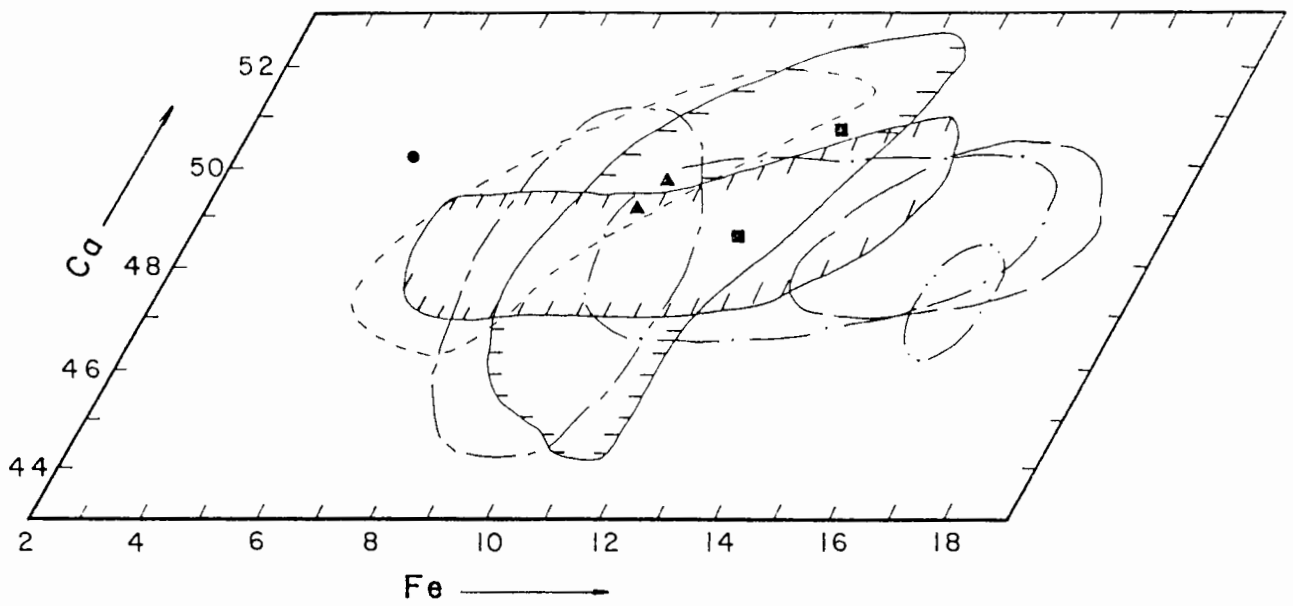

Sutherland Commonage (ring dyke)
Sutherland Commonage (ol-nephelinite)
Malaita, Solomon Islands (Nixon et al., 1980)
Moilili, Oahu, Hawaii (Wilkinson & Stolz, 1983) (ol-nephelinite)
Ol-nephelinite
Nephelinite
Melilite
} Friderikshåbs Isblink S.W. Greenland (Hansen, 1980)
Saltpetre kop, R.S.A.
Sandkopsdrift, R.S.A.
Biesiesfontein, R.S.A.
} Boctor & Yoder, 1986)

4.4 Discussion of the crystal chemistry of the Commonage pyroxenes

The simplest structural formula for calcic clinopyroxenes (such as those in the Commonage rocks) may be taken as diopside ($CaMgSi_2O_6$) where Ca is in the large (M_2) octahedral site, Mg is in the (M_1) octahedral site, and Si is tetrahedrally coordinated. Simple substitutions of Fe^{2+} and Mn^{2+} for Mg in (M_1) give rise to the compositional variations described in the pyroxene quadrilateral, plotted as proportions of $CaSiO_3$, $MgSiO_3$ and $(Fe,Mn)SiO_3$ and usually calculated from atomic proportions of Ca, Mg and (Fe+Mn).

When pyroxenes from the Commonage are plotted in this fashion, a number of analysis are seen to have $CaSiO_3$ values greater than 50% (figure 4.1 and 4.2). This is postulated to result from the exclusive substitution of "non-quadrilateral" components such as Ti, Al, Cr and Fe^{3+} for Fe^{2+} and Mg in the (M_1) site (Tracy and Robinson, 1977).

The purpose of this section is therefore to investigate the nature of Ti and Al substitution in the Commonage pyroxenes. Cr^{3+} is not considered because of its low abundance and Fe^{3+} is excluded since the microprobe cannot distinguish Fe^{3+} from Fe^{2+} (and most proposed methods of recalculation often produce inaccurate results).

The main components of pyroxenes containing "non-quadrilaterals" are $CaMgSi_2O_6$ (Di), $CaFe^{2+}Si_2O_6$ (Hd), $CaTiAl_2O_6$ (Ti-pyroxene component, Tp), $CaAl_2SiO_6$ (Ca-Tschermaks component, CATS), $CaFe^{3+}AlSiO_6$ (ferri-aluminum

Tschermak's component, FATS), $NaFe^{3+}Si_2O_6$ (Ac) and $Mg_2Si_2O_6$ (En) (Onuma and Yagi, 1971).

Inspection of cation values in appendix 4 should reveal that a number of clinopyroxenes in the olivine nephelinite apparently have Si^{4+}-contents smaller than the amount necessary to fill the tetrahedral site (which is normally filled by Si^{4+} and which should have a total of 2). This is probably due to the introduction of Al^{3+} into the tetrahedral site because of the inability of Si^{4+} to completely fill the tetrahedral site (Carmichael et al., 1974). The presence of Al^{3+} in the tetrahedral site is not unique to the Commonage clinopyroxenes but appear to be commonly present in clinopyroxenes from undersaturated alkaline igneous rocks such as alkali basalts, nephelinites, basanites and other olivine melilitites (Tracy and Robinson, 1977; Scott, 1976; Huckenholz, 1973; Wass, 1979; Fodor et al., 1975; Segalstadt, 1979; Magonthier et al., 1976; Onuma, 1983).

Low silica activity in the magma from which the pyroxenes crystallise is evidently a prerequisite for the introduction of Al^{3+} into the tetrahedral site (Yoshikawa, 1977; Carmichael et al., 1970; Gupta et al., 1973; Magonthier et al., 1976). If the amount of silicon available to the clinopyroxene is not sufficient to fill up the tetrahedral position, the rest of the position is occupied by Al^{3+} and not Fe^{3+} and Ti^{4+} (Onuma and Akasaka, 1980). This relationship is certainly borne out by the plot of total Al^{3+} versus Si^{4+} (figures 4.13 and 4.14) for clinopyroxenes from both the ring dyke and the olivine nephelinite. Note the strong negative correlation between

Figure 4.13 Plot of Al^{3+} versus Si^{4+} for groundmass clinopyroxenes in the ring dyke (normalised to 4 cations)

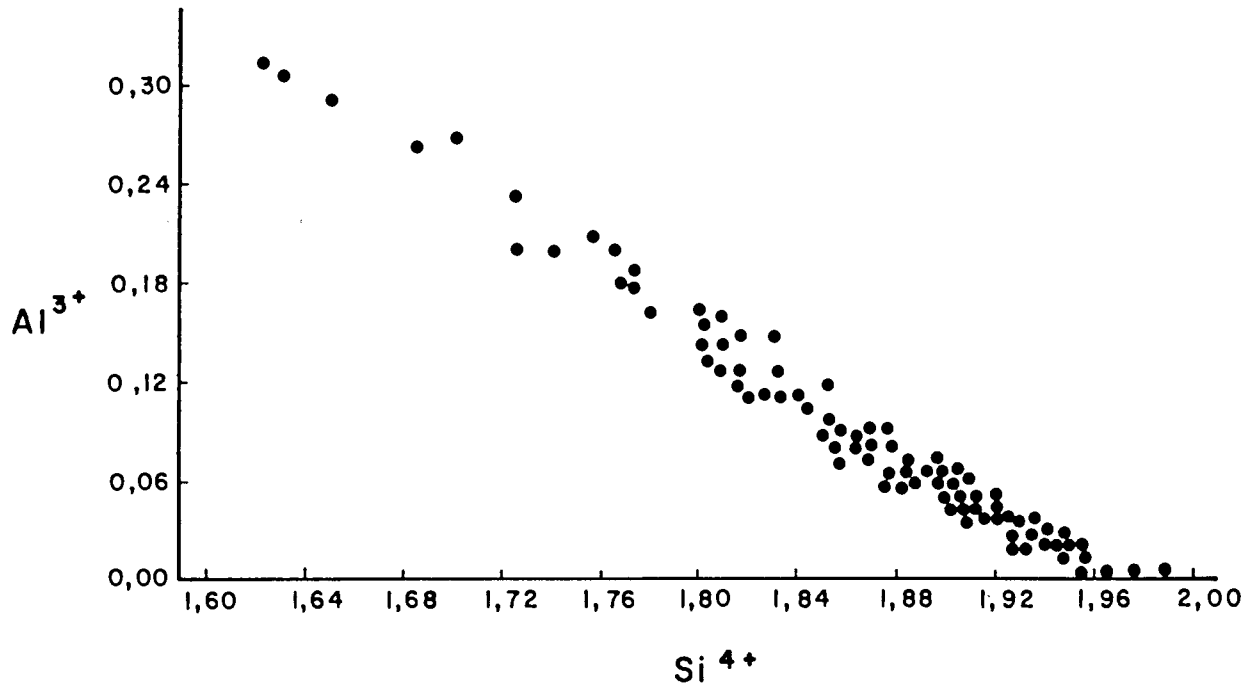

Figure 4.14 Plot of Al^{3+} versus Si^{4+} for groundmass clinopyroxenes in the olivine nephelinite (normalised to 4 cations)

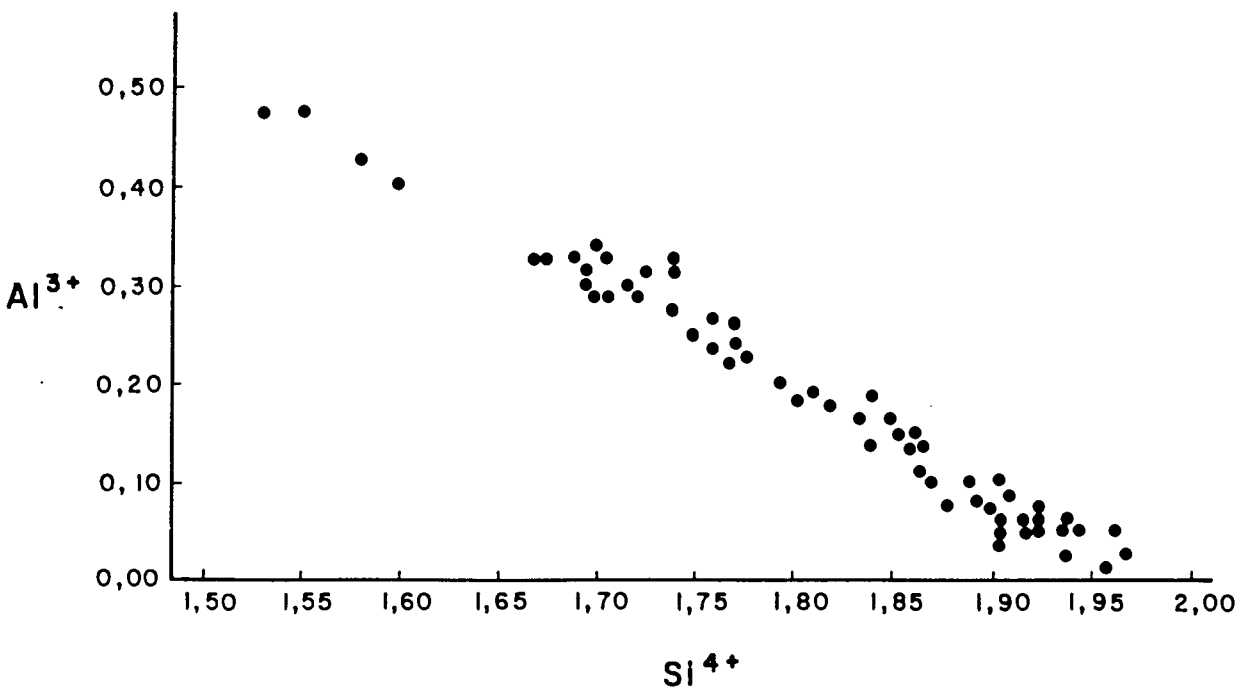

these two elements.

The Al^{3+} ions in the tetrahedral position must be accompanied by Ti^{4+}, Al^{3+} and Fe^{3+} ions in the octahedral position in order to maintain electrical neutrality. Clinopyroxenes crystallising from alkalic magmas (such as the Commonage melilitite) are usually rich in TiO_2 and hence Al^{3+} ions in tetrahedral positions are largely compensated for by Ti^{4+} ions in the (M1) octahedral position (Kushiro, 1960).

It is also conceivable, however, that the high TiO_2 concentrations of alkalic magma results in the high titanium content and consequently high aluminium content in the clinopyroxenes. This implies that the molecular concentration of TiO_2 in the magma determines the amount of titanium and aluminium in the clinopyroxenes, but this is considered to be unlikely (Kushiro, 1960).

The clinopyroxenes from undersaturated rocks (such as the Commonage melilitites), are rich not only in the CATS component but also in Tp and FATS components, and usually also contains a small amount of acmite, usually less than 5% (Onuma and Yagi, 1975). In this regard the low Na_2O content of all the pyroxenes at the Commonage (table 4.1) should be noted.

In relatively recent studies of Al- and Ti-rich pyroxenes (Tracy and Robinson, 1977; Scott, 1976) diagrams have been presented showing Ti^{4+} plotted against Al^{3+}, and slopes of linear trends on such diagrams have been used to suggest titanium substitution mechanisms. Such a plot for the

Figure 4.15 Plot of Ti^{4+} versus Al^{3+} for groundmass clinopyroxenes in the ring dyke (normalised to 4 cations)

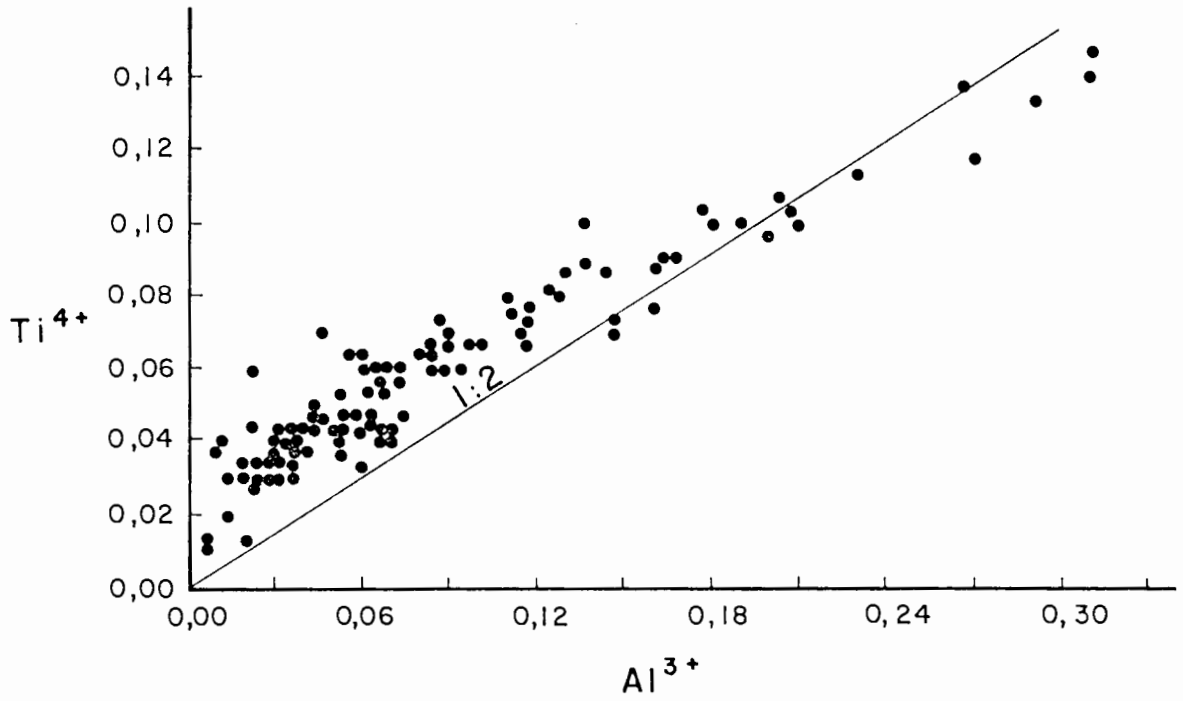

Figure 4.16 Plot of Ti^{4+} versus Al^{3+} for groundmass clinopyroxenes in the olivine nephelinite (normalised to 4 cations)

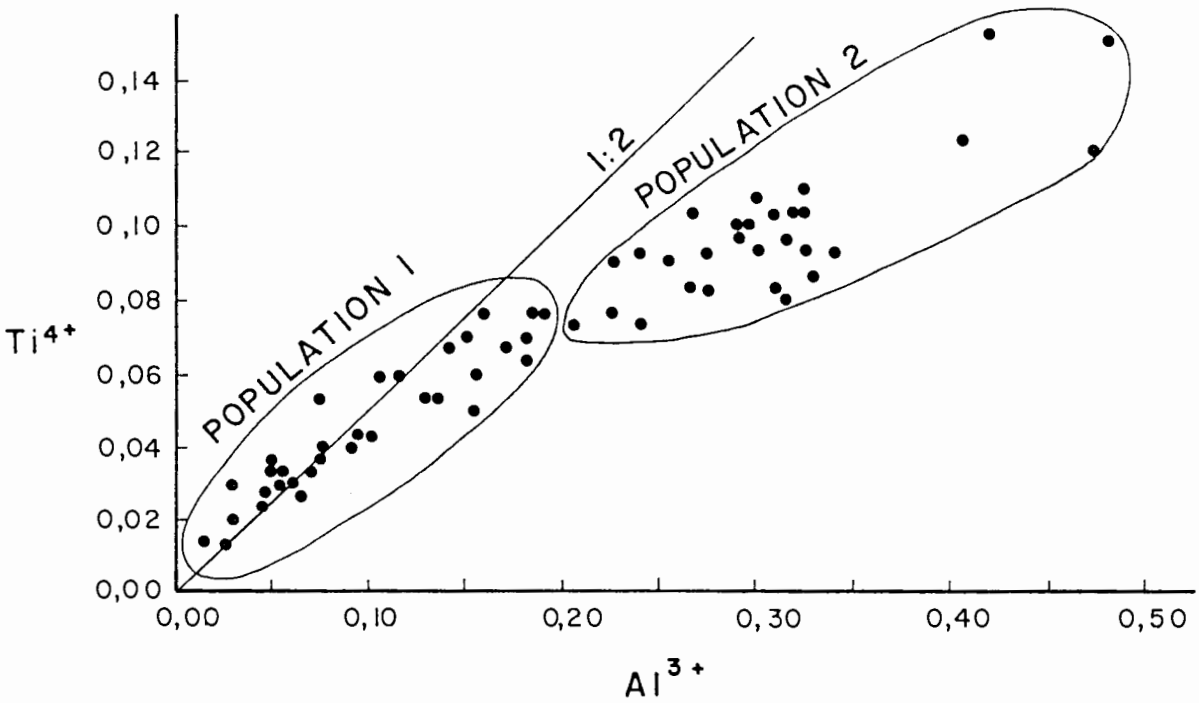

Commonage clinopyroxenes in the ring dyke (figure 4.15) shows a varying slope, but displays a linear trend with a slope approximating 1/2 (statistically determined slope = 0.8/2) suggesting substitution toward an $R^{2+}TiAl_2O_6$ composition.

Clinopyroxenes in the olivine nephelinite by comparison appear to show two subpopulations on a Ti-Al plot. Population 1 (figure 4.16) corresponds to comparatively low Al-pyroxenes which seem to cluster around a line with slope of 1/2, again suggesting substitution towards an $R^{2+}TiAl_2O_6$ composition. Population 2, however, show a general excess of Al^{3+} for a given amount of Ti^{4+} which suggest that more aluminium than is necessary to fill up the tetrahedral site is present in these clinopyroxenes. This Al^{3+} is most likely present as octahedrally coordinated aluminium in the (M1) octahedral site. Two types of coupled substitutions involving Al^{3+} in the tetrahedral and the (M1) octahedral site is therefore considered important for the Commonage pyroxenes:

Trend 1

$$Ti^{4+}(oct) + 2Al^{3+}(tet) = R^{2+}(oct) + 2Si^{4+}(tet)$$

This substitutional couple is present in pyroxenes from both the ring dyke and the olivine nephelinite.

Trend 2

$$Al^{3+}(oct) + Al^{3+}(tet) = R^{2+}(oct) + Si^{4+}(tet)$$

This couple is present only in the high Al pyroxenes present in the olivine nephelinte.

These substitutions imply that the sum of Ti^{4+} and (Mg+Fe) in the (M1) octahedral site should remain constant at 1.0 minus any other cations present in (M1), and that the data should form a line with a slope of -1.0 in a plot of Ti^{4+} versus (Mg+Fe) (Tracy and Robinson, 1977). Figures 4.17 and 4.19 however, shows a slope of -0.95 (and a large amount of scatter) for pyroxenes from the ring dyke and a slope of -0.53 for pyroxenes from the olivine nephelinite, which implies a more complex relationship. Plots of $(Ti^{4+}+Fe^{2+})$ versus Mg^{2+} for pyroxenes in both rock types (figures 4.18 and 4.20) shows linear trends with slopes of -1.0 (ring dyke) and -0.7 (olivine nephelinite) respectively. This supports a substitution of the type: $Fe^{2+}+Ti^{4+}+2Al^{3+}=2Mg+2Si$ for pyroxenes in the ring dyke, equivalent to an idealised end-member $CaFe^{2+}_{0.5}Ti^{4+}_{0.5}AlSiO_6$ (Tracey and Robinson, op cit.). The absence of a significant improvement in slope when clinopyroxenes from the olivine nephelinite are plotted in this manner suggest that early crystallisation of oxides (which did not occur in the nephelinite-see section 4.5) control the relationship between Fe^{2+}, Ti^{4+} and Mg^{2+} in the melt and consequently also in the crystallising pyroxenes. The relationship between these elements as displayed by clinopyroxenes in the ring dyke is therefore considered to be an artefact of early oxide crystallisation and is probably not a function of crystal chemistry.

4.5 Petrologic significance of clinopyroxene compositional trends

Figure 4.17 Plot of Ti^{4+} versus $(Fe^{2+} + Mg^{2+})$ for groundmass clinopyroxenes in the ring dyke (normalised to 4 cations)

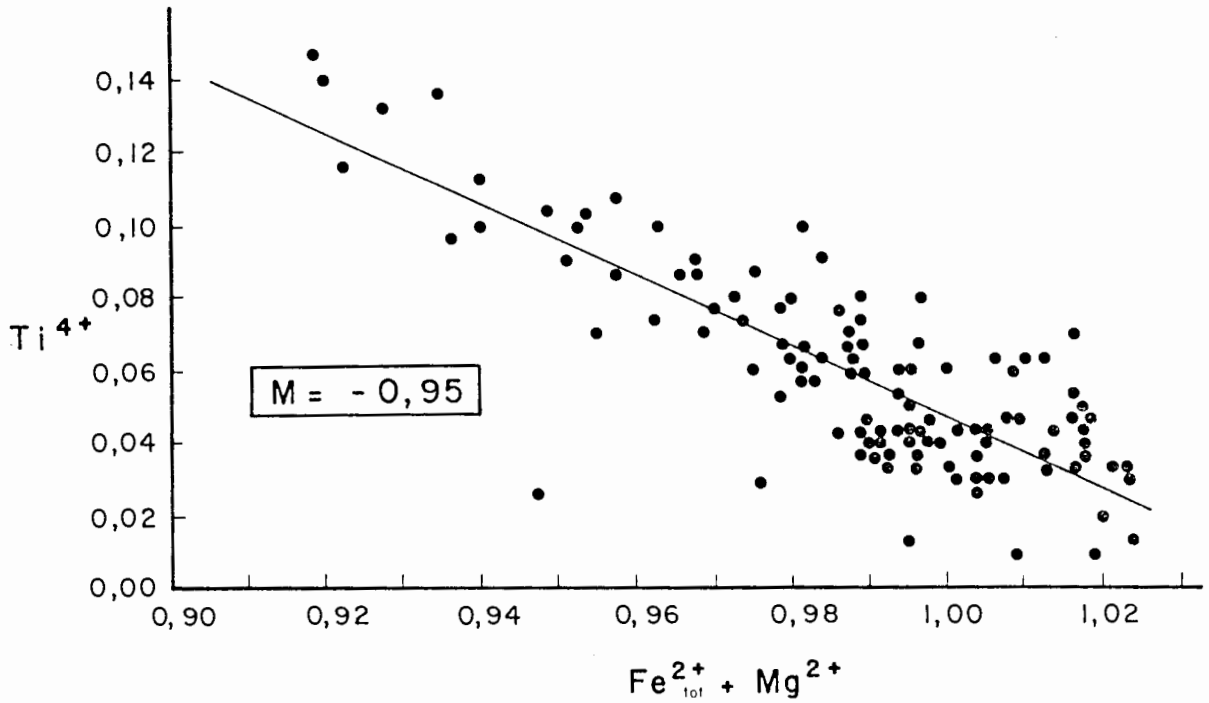

Figure 4.18 Plot of $(Ti^{4+} + Fe^{2+})$ versus Mg^{2+} for groundmass clinopyroxenes in the ring dyke (normalised to 4 cations)

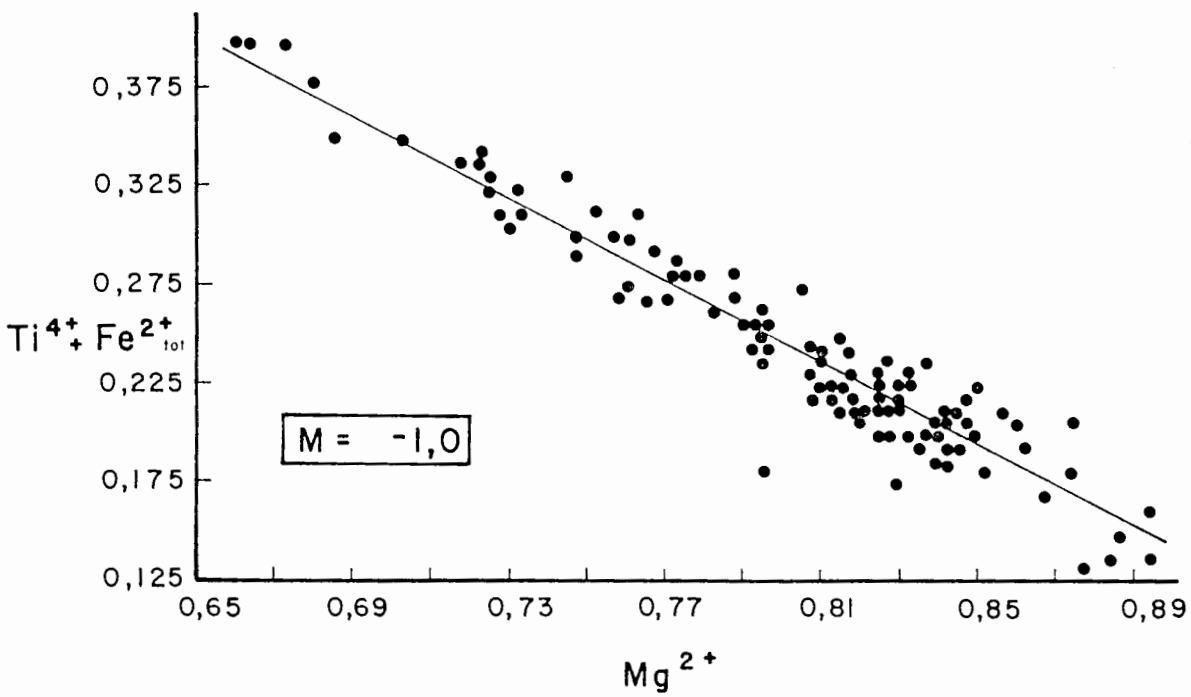

Figure 4.19 Plot of Ti^{4+} versus $(Fe^{2+} + Mg^{2+})$ for groundmass clinopyroxenes in the olivine nephelinite (normalised to 4 cations)

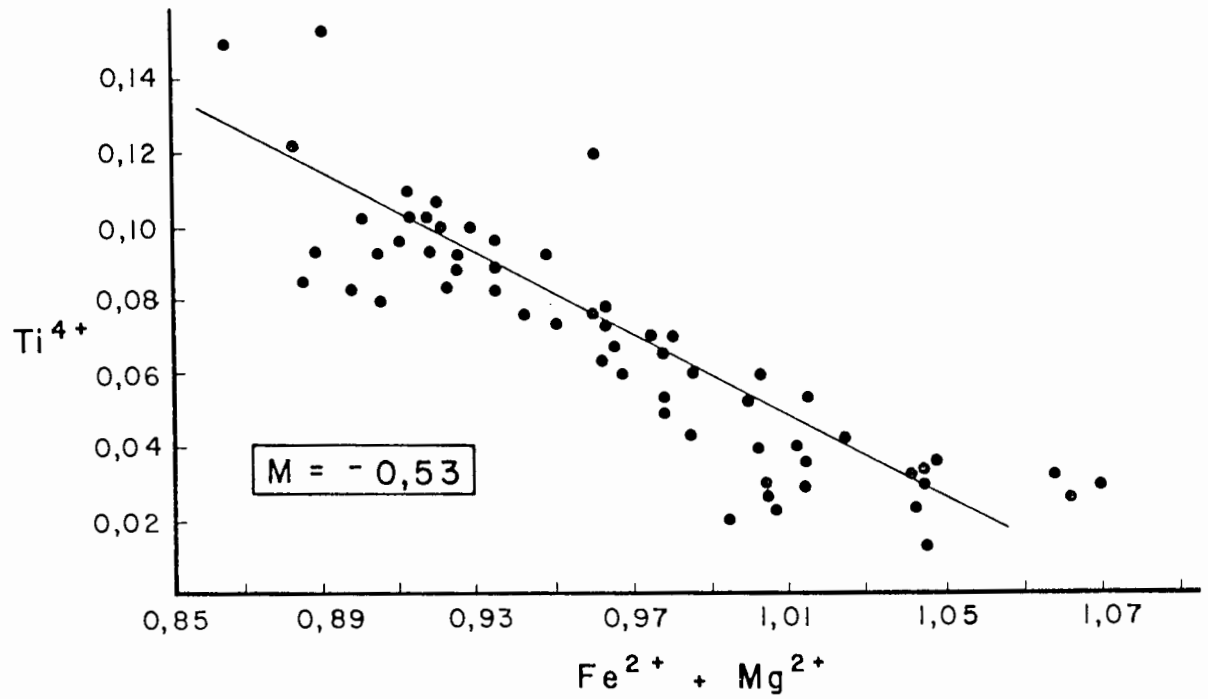

Figure 4.20 Plot of $(Ti^{4+} + Fe^{2+})$ versus Mg^{2+} for groundmass clinopyroxenes in the olivine nephelinite (normalised to 4 cations)

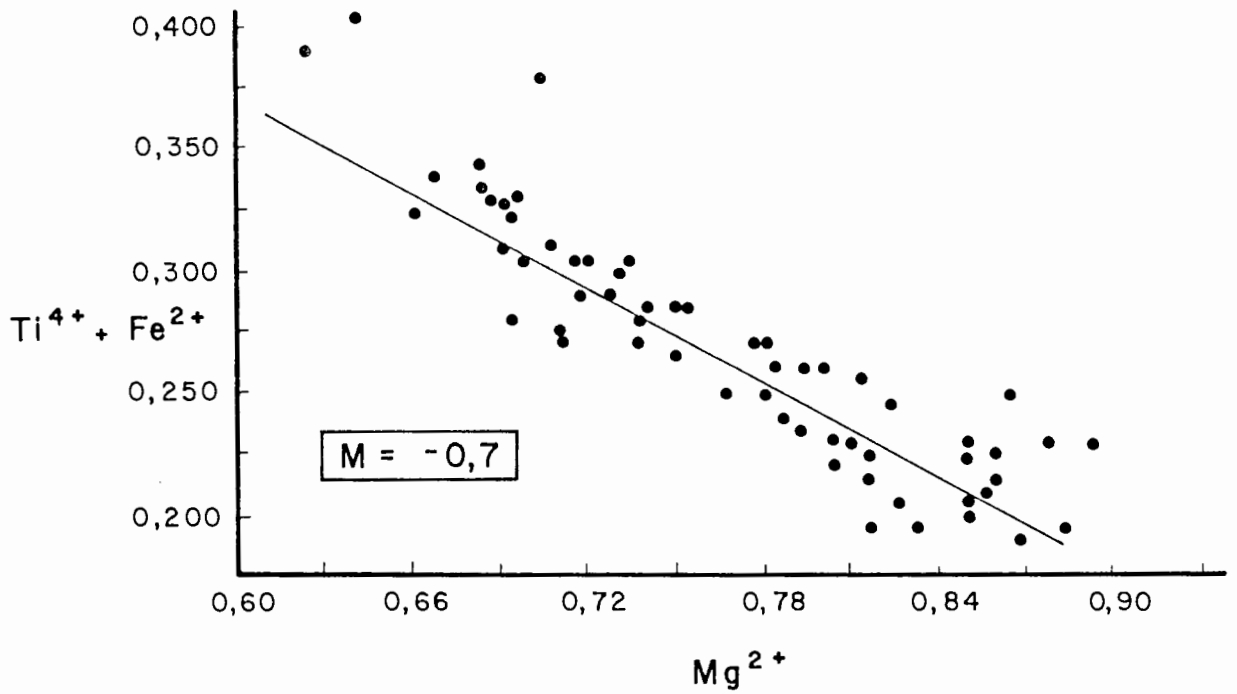

4.5.1 MgO, FeO and CaO

All the pyroxenes in the ring dyke show an overall trend of decreasing Fe/Mg ratio with progressive crystallisation, suggesting that the magma from which these pyroxenes crystallised was gradually being depleted in iron by a co-precipitating Fe-rich phase (figures 4.1 and 4.11a-e). A likely candidate is probably magnetite as it is an abundant groundmass phase and is also common as inclusions in pyroxenes. Analysis of pyroxenes in glass rich, chilled melilitite from the dyke contact have unusually low Fe/Mg ratios which suggest that they precipitated from a primitive, unevolved magma. The anomalous composition of these pyroxenes suggest that their crystallisation was brought about by a process (other than falling temperature) which induced pyroxene crystallisation. This is supported by the observation that they occur as unusually coarse grained aggregates of grains in melilite free areas in the groundmass.

Detailed microprobe scans across clinopyroxenes in the groundmass of the ring dyke (figures 4.11a-c) show that the pyroxenes usually exhibit a constant to slightly increasing Fe/Mg ratio from the core to an intermediate position (approximately half-way). It is only beyond this point that the iron concentration starts to decrease. This trend is taken to indicate that large amounts of magnetite started to crystallise only after an extended period of pyroxene crystallisation (during which small amounts of magnetite precipitated). This is supported by the presence of magnetite in glass rich chill at the dyke contact. Acceleration of magnetite crystallisation was probably caused by a sharp

increase in fO_2 during the later stages of pyroxene crystallisation. Cores of clinopyroxenes in vesicles show surprisingly high Fe/Mg ratios which suggest that these grains formed relatively early (figure 4.1). This is unusual since the vesicles show evidence of late crystallisation as they are filled by zeolites and are generally surrounded by coarse-grained groundmass minerals. It is therefore possible that the position of a vesicle is "determined" early in the pyroxene crystallisation sequence by the random concentration of patches of relatively unevolved residual liquid in open areas in a mesh of rare clinopyroxene and abundant melilite laths.

Calcium concentrations in pyroxenes from the ring dyke decrease with progressive crystallisation (figure 4.1). Relatively low concentrations are recorded in pyroxenes from the glass rich chill, which confirms that they crystallised from a primitive, unevolved liquid. The composition of these pyroxenes might also be an indication that a hiatus occured before the majority of "normal" groundmass pyroxenes started to crystallise. During this interval the magma must have evolved towards a higher calcium content since early normal groundmass clinopyroxenes (i.e. high Fe/Mg) are far more calcic than the clinopyroxenes in the glassy margin of the ring dyke. Pyroxenes in vesicles exhibit marginally lower concentrations of CaO compared to the early groundmass clinopyroxenes (with similar Fe/Mg ratios). This relative calcium depletion of these pyroxenes is probably due to the influence of melilite. A local concentration of heat and volatiles in the general environment of a developing vesicle

would lead to an accelarated rate of melilite crystallisation in this localised microcosm, resulting in more rapid calcium depletion than in the surrounding, evolving groundmass. The almost flat calcium trend shown by pyroxenes with ferrosilite contents lower than 10.5% strongly suggest that melilite crystallisation probably also buffered the availability of calcium in the residual liquid during the later stage of groundmass clinopyroxene crystallisation.

Pyroxenes in the olivine nephelinite show a trend of increasing iron and decreasing magnesium with progressive crystallisation (figure 4.2), implying that magnetite crystallisation in the parent magma was probably delayed until a very late stage, presumably as a result of low oxygen fugacity. This would also explain the more iron-rich nature of nephelinite pyroxenes compared to those in the ring dyke. However, small pyroxenes (up to 0.03mm) in the nephelinite indicate that during the final stage of clinopyroxene crystallisation the fO_2 must have increased considerably as these grains possess some of the lowest Fe/Mg ratios. Massive Fe^{2+}-depletion of the liquid by almost instantaneous crystallisation of large amounts of magnetite would be a likely scenario.

Calcium variations in clinopyroxenes from the olivine nephelinite are erratic and difficult to explain (figures 4.2 and 4.11f). However, grains of up to 0.03mm in size are all depleted in calcium relative to the larger grains which can probably be ascribed to decreasing calcium contents in the residual liquid with progressive crystallisation. CaO

contents in the crystallising nephelinite magma also dropped to lower levels than in the parent magma of the ring dyke, presumably due to more extensive pyroxene crystallisation. The similar wollastonite content of early pyroxenes suggest that both magmas evolved to comparable calcium concentrations before clinopyroxene crystallisation commenced.

4.5.2 SiO_2, Al_2O_3 and TiO_2

Clinoyroxenes in the ring dyke and the olivine nephelinite show a similar range in SiO_2 contents (table 4.1, figures 4.7 and 4.8). Pyroxenes in the ring dyke show a regular, almost linear increase in SiO_2 content from core to rim (figures 4.7 and 4.11a-e). Core-rim variations in pyroxenes from the nephelinite are, by comparison, somewhat erratic and more difficult to explain (figures 4.8 and 4.11f). However, clinopyroxenes in both rock types do seem to reflect a trend of increasing silica activity in the residual liquid with progressive crystallisation. This trend is considered to be a direct consequence of the simultaneous crystallisation of clinopyroxene, melilite (only in the ring dyke), perovskite and magnetite which depleted the parent magma in elements such as CaO, FeO, Al_2O_3 and TiO_2, thereby enriching the residual liquid in SiO_2.

Clinopyroxenes in the glassy, chilled contact of the ring dyke have higher SiO_2 contents than early (high Fe/Mg ratio) groundmass pyroxenes from more slowly cooled areas in the dyke. This possibly indicates that these grains might have crystallised from a silica enriched magma, presumably as a consequence of contamination of the dyke contact by

assimilated country rock.

Clinopyroxenes in the ring dyke show decreasing contents of Al_2O_3 and TiO_2 from their cores to their rims and exhibit an overall drop in Al_2O_3 and TiO_2 throughout the pyroxene crystallisation interval (figures 4.1, 4.3, 4.4 and 4.11a-e). This pattern of decreasing Al_2O_3 and TiO_2 with progressive crystallisation of pyroxene is repeated in the olivine nephelinite but here core-rim variations are somewhat more erratic and complex (figures 4.2, 4.5, 4.6 and 4.11f).

The decrease in Al_2O_3 and TiO_2 contents of the pyroxenes with progressive crystallisation probably reflects the postulated increase in a_{SiO_2} of the magma (see the section on crystal chemistry for a full discussion). However, early pyroxenes in the olivine nephelinite are characterised by extremely high Al_2O_3 contents when compared to those in the ring dyke. These early aluminous pyroxenes might have crystallised from a magma which was originally very rich in Al_2O_3 or, alternatively, was not partially depleted in Al_2O_3 by an aluminous phase (such as melilite, which is an abundant phase in the ring dyke but is never seen in the olivine nephelinite). An alternative explanation is that these aluminous pyroxenes crystallised under higher pressure than any of the pyroxenes in the ring dyke. Increasing pressure favours octahedrally coordinated Al in the magma and consequently allows the incorporation of Al in the octahedral (M1) site of the pyroxenes (Wass, 1979). This scenario implies that pyroxene crystallisation in the nephelinite commenced at an earlier stage than in the ring dyke,

presumably during the ascent of the magma through the lower crust as these pyroxenes are known to be unstable at pressures higher than 10 kilobar and at fO_2 conditions approximating the magnetite stability field (Onuma and Yagi, 1975).

The anomalously high TiO_2 and Al_2O_3 contents of pyroxenes in glass rich chill at the dyke contact is probably caused by rapid crystallisation. High cooling rates lead to elevated aluminium and titanium levels in clinopyroxenes (Magonthier and Velde, 1976; Tracy and Robinson, 1977).

4.5.3 Na_2O

Na_2O contents of pyroxenes in the ring dyke decrease from core to rim and also become more depleted with progressive crystallisation (figures 4.9 and 4.11a-e). Cores of pyroxenes in vesicles have somewhat higher Na_2O contents than typical groundmass grains, probably reflecting a higher Na_2O content in the residual liquid from which they crystallised. Pyroxenes in the glass-rich chill are low in Na_2O which is in keeping with crystallisation from a primitive liquid. Note that two trends are apparant in figure 4.9. Early groundmass clinopyroxenes do not show any decrease in sodium with decreasing Fe/Mg ratio. Late groundmass clinopyroxenes (low Fe/Mg ratios) by comparison, are depleted in sodium. This strongly suggests that abundant nepheline started to crystallise towards the close of the pyroxene crystallisation interval in the ring dyke.

Clinopyroxenes in the olivine nephelinite show an increase in Na_2O from cores to rims, but no evolutionary pattern with

progressive crystallisation is evident (figure 4.10). Sodium concentrations of these clinopyroxenes are generally lower than in pyroxenes from the ring dyke, suggesting that the nephelinite is less sodic or that the more abundant nepheline in the nephelinite restricted the availability of sodium in the residual liquid.

The low Na_2O content of pyroxenes from both rock types is noteworthy, considering the sodic nature of the magmas from which they crystallised (see Chapter 7). However, in alkaline rocks such as melilitites and nephelinites the main control on the presence of the acmite molecule in pyroxene probably depends on the concentration of CaO in the magma. Studies on experimental systems and natural clinopyroxenes suggest that when fO_2 is higher than the magnetite-wustite transition (i.e. magnetite stability field), pyroxene becomes acmitic if the accompanying liquid has $Na>Fe^{3+}+Al$ or aluminous in the case of $Na<Fe^{3+}+Al$ (Okta et al., 1977; Onuma and Yagi, 1975; Huckenholz, 1973). If $Na<Fe^{3+}+Al$ and enough CaO is present in the liquid then Fe^{3+} enters into pyroxene in the form of $CaFe^{3+}AlSiO_6$ and sodium forms nepheline, resulting in relatively sodium-depleted clinopyroxenes.

4.6 Conclusion

In conclusion, the following points, resulting from attempts to interpret the mineral chemistry of groundmass clinopyroxenes in the ring dyke and the olivine nephelinite, are stressed.

1)It is apparent that both magmas evolved towards higher

silica activity with progressive crystallisation.

2)The parent magma of the nephelinite was more reduced than that of the ring dyke.

3)Higher fO_2 in the ring dyke parent led to the early crystallisation of magnetite which depleted the residual liquid in iron. Comparatively lower fO_2 in the nephelinite delayed magnetite crystallisation which resulted in a trend of increasing iron in the residual liquid.

4)Calcium concentrations in the dyke magma were buffered by the crystallisation of melilite. The absence of a trend of calcium control in the nephelinite suggests that melilite never crystallised in this rock type.

5)The nephelinite parent magma was more aluminous than the parent to the ring dyke. Alternatively, pyroxene crystallisation in the nephelinite commenced while the magma was still rising to crustal levels.

5)Vesicles in the ring dyke started to form at an intermediate stage of groundmass crystallisation, possibly due to the random, localised concentration of residual fluids in vacant areas in a crystalline mesh formed by lath-shaped grains of melilite and early clinopyroxenes.

6)The glassy margin of the ring dyke represents a very early, unevolved magma whose composition predates a major portion of the pyroxene crystallisation interval. However, it

was contaminated by the assimilation of siliceous country rock, and microprobe analysis of the glass will therefore not be a reliable estimate of its primary composition.

5 OLIVINE MINERAL CHEMISTRY

5.1 Introduction

Olivine is an abundant mineral phase in all the intrusives at Sutherland Commonage. It is evidently one of the earliest phases to crystallise, a feature considered to be typical of alkaline ultrabasic magmas in general (Deer et al., 1982). The only mineral which might precede olivine in the crystallisation sequence is chrome spinel, as tiny euhedral grains of chromite are commonly found as inclusions in olivine. A systematic study of olivine mineral chemistry could therefore provide a wealth of information about early processes in the evolution of the Commonage melilitite magma.

The petrography of olivine is discussed in detail in chapter 3 and is briefly reiterated here for purposes of discussion. Four varieties of olivine are distinguished on petrographic grounds:

a)Large (1 - 8mm), generally rounded and corroded grains are termed macrocrysts. These grains often contain abundant fluid inclusions, are intergrown with euhedral apatite and magnetite and in many cases show distinct olivine overgrowths.

b)The term phenocryst applies to any subhedral to euhedral grain larger than 0.5mm in size.

c)Microphenocrysts are subhedral or euhedral olivines smaller than 0.5mm in size.

d)Complex phenocrysts are grains which either consist of aggregates of subhedral to euhedral grains (to form multiple growth aggregates) or single crystals showing pronounced corrosional or "hopper" shapes. These crystals show a wide

range of sizes, ranging from approximately 0.5mm to grains several millimetres across.

The main part of the present research is centred on olivines in the ring dyke since the grains are very fresh and their rims are not destroyed by late-stage processes such as deuteric alteration, which is a common problem in rocks from the sill complex. Cores and rims were analysed and the size and shape of each olivine was recorded. Cores (and rims where possible) of olivines in the green and grey melilitites and the olivine nephelinite in the sill complex were also determined in order to compare the olivine compositions within the different intrusive types. Forty eight, fifteen, eighteen and fourteen olivines were analysed in the ring dyke, the green and grey melilitites and the olivine nephelinite respectively. These analyses are to be found in appendix 5. Forsterite, nickel, calcium and manganese contents are summarised by means of histograms in figures 5.1 to 5.4.

Detailed microprobe traverses were done across typical olivines from each petrographic olivine group, and the scans are presented in figure 5.8(a-j). The location of single analyses in grains whose chemistries are considered to contribute significantly to the petrogenetic picture are given in figure 5.9(a-e).

5.2 Mineral chemistry

5.2.1 Introduction

One of the first objectives of the olivine study was to

determine whether there is any compositional difference between the various petrographic olivine groups. It soon became clear that there are no gross disparate chemical difference between phenocrysts, microphenocrysts and complex phenocrysts. Macrocrysts, on the other hand, proved to be a distinctive olivine type since the grains are characterised by much lower forsterite contents, while nickel concentrations are generally below a detection limit of 0.05 wt% (figures 5.1 to 5.4). Manganese concentrations are also unusually high compared to the rest of the olivines. They are chemically identical to the high iron-low nickel (HILN) olivines which were described by Moore (1979) in olivine melilitites from Namaqualand. The chemistry of olivine phenocrysts and olivine macrocrysts (hereafter referred to as HILN olivines) are therefore discussed separately.

5.2.2 Phenocryst and microphenocryst mineral chemistry

Olivine phenocrysts and microphenocrysts at the Commonage are forsteritic (up to $Fo_{89,5}$) and have detectable levels of nickel, calcium and manganese (figures 5.1 to 5.4).

These olivines show a significant variation in forsterite content, ranging from approximately Fo_{81} to $Fo_{89,5}$. Phenocryst cores are generally more forsteritic than phenocryst rims, are enriched in nickel (compared to rim analyses) and are depleted in calcium and manganese (figures 5.1 to 5.4).

Cores of phenocrysts larger than approximately 2.5mm in size are characteristically high in forsterite and nickel and

Figure 5.1 Variation in forsterite content in cores and rims of olivines at Sutherland Commonage

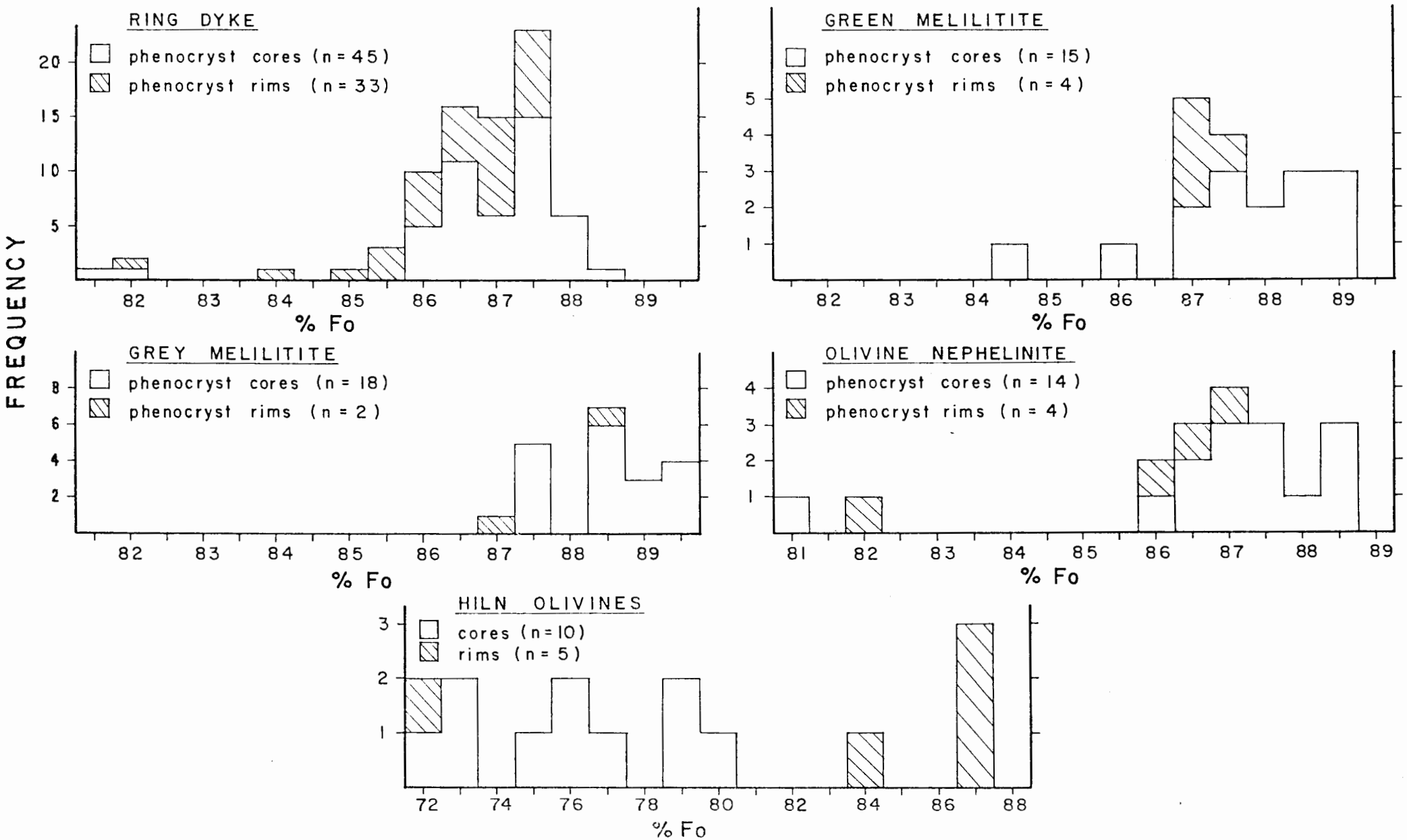

Figure 5.2 Variation in NiO in cores and rims of olivines at Sutherland Commonage

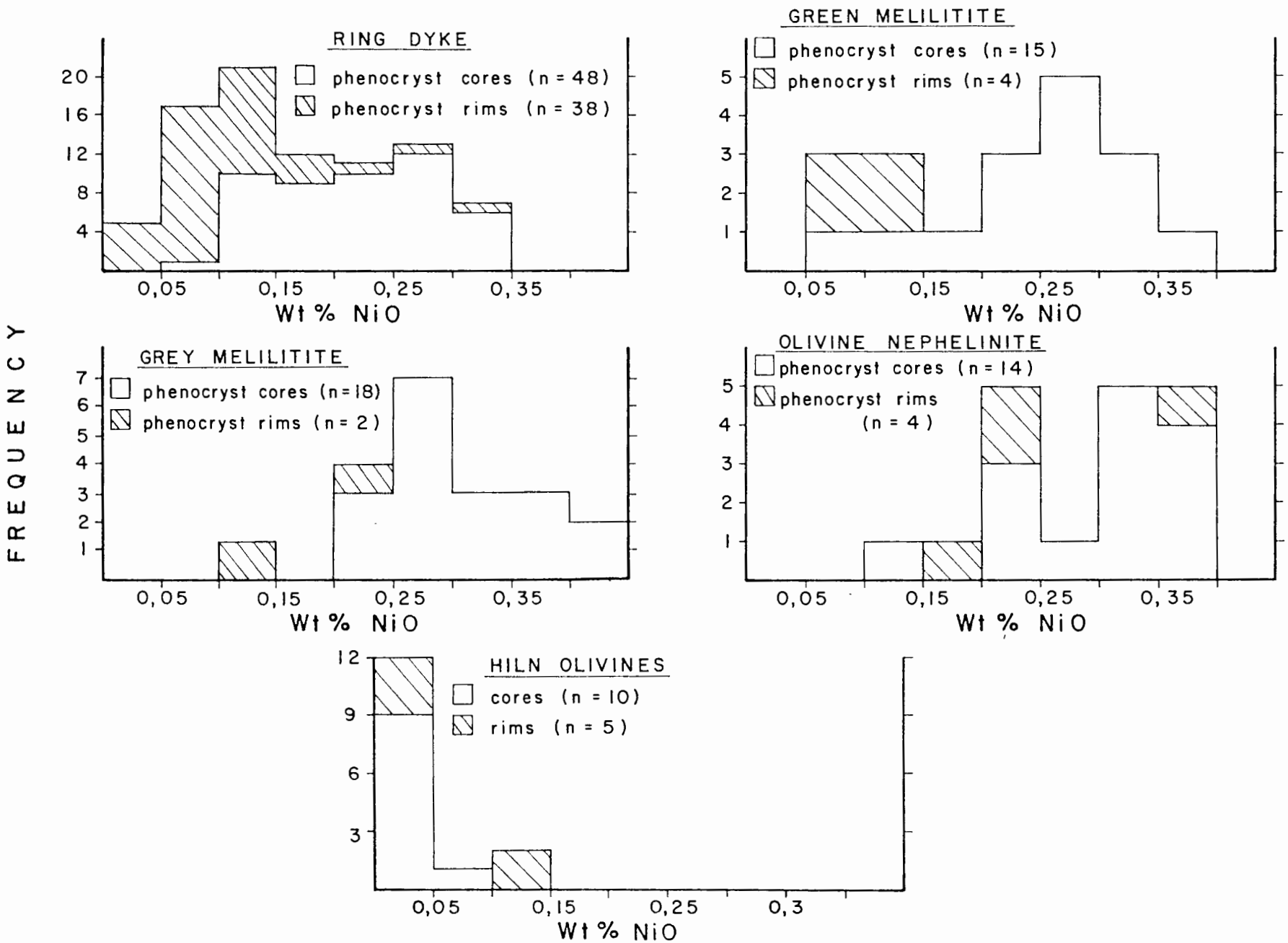

Figure 5.3 Variation in CaO in cores and rims of olivines at Sutherland Commonage

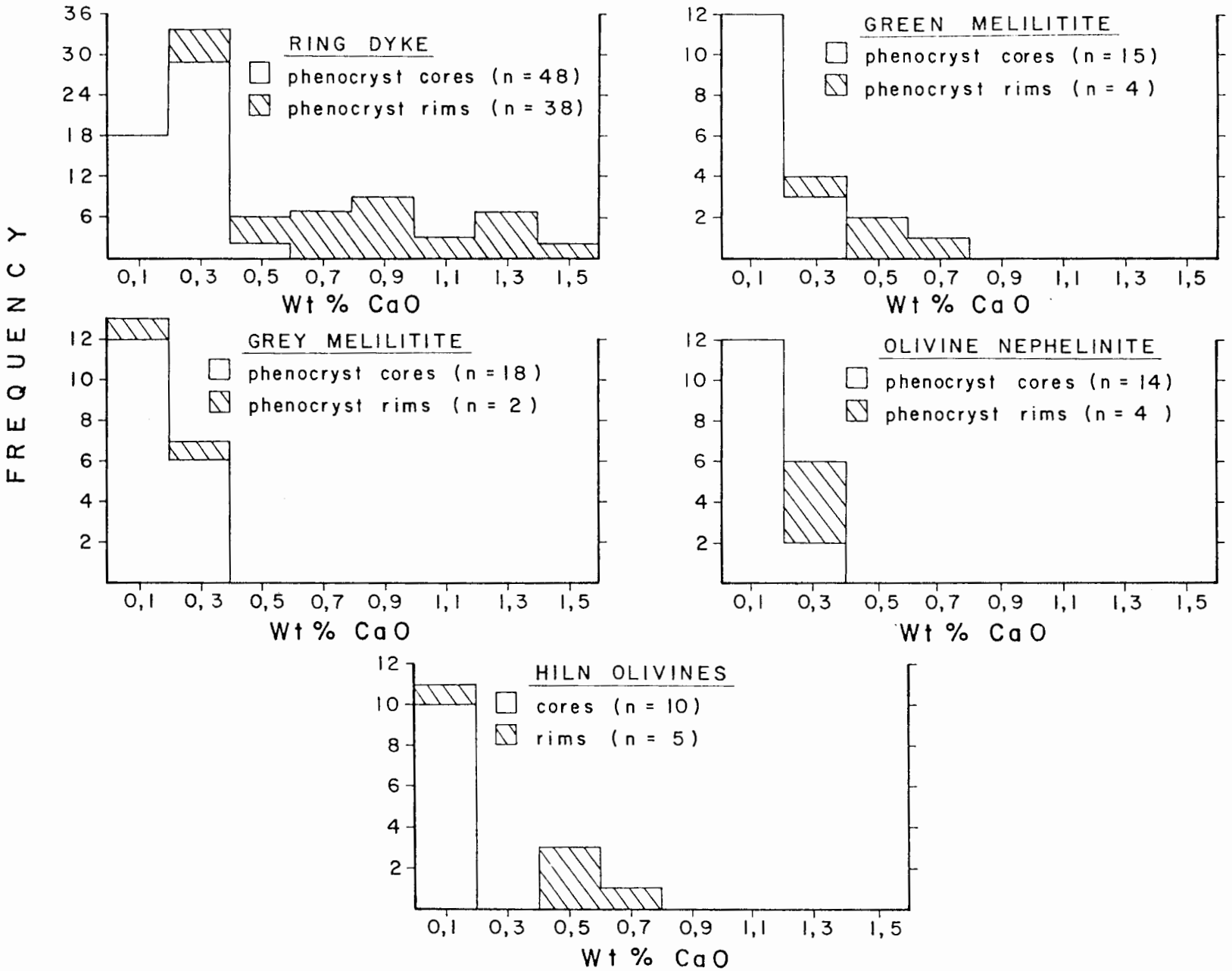

Figure 5.4 Variation in MnO in cores and rims of olivines at Sutherland Commonage

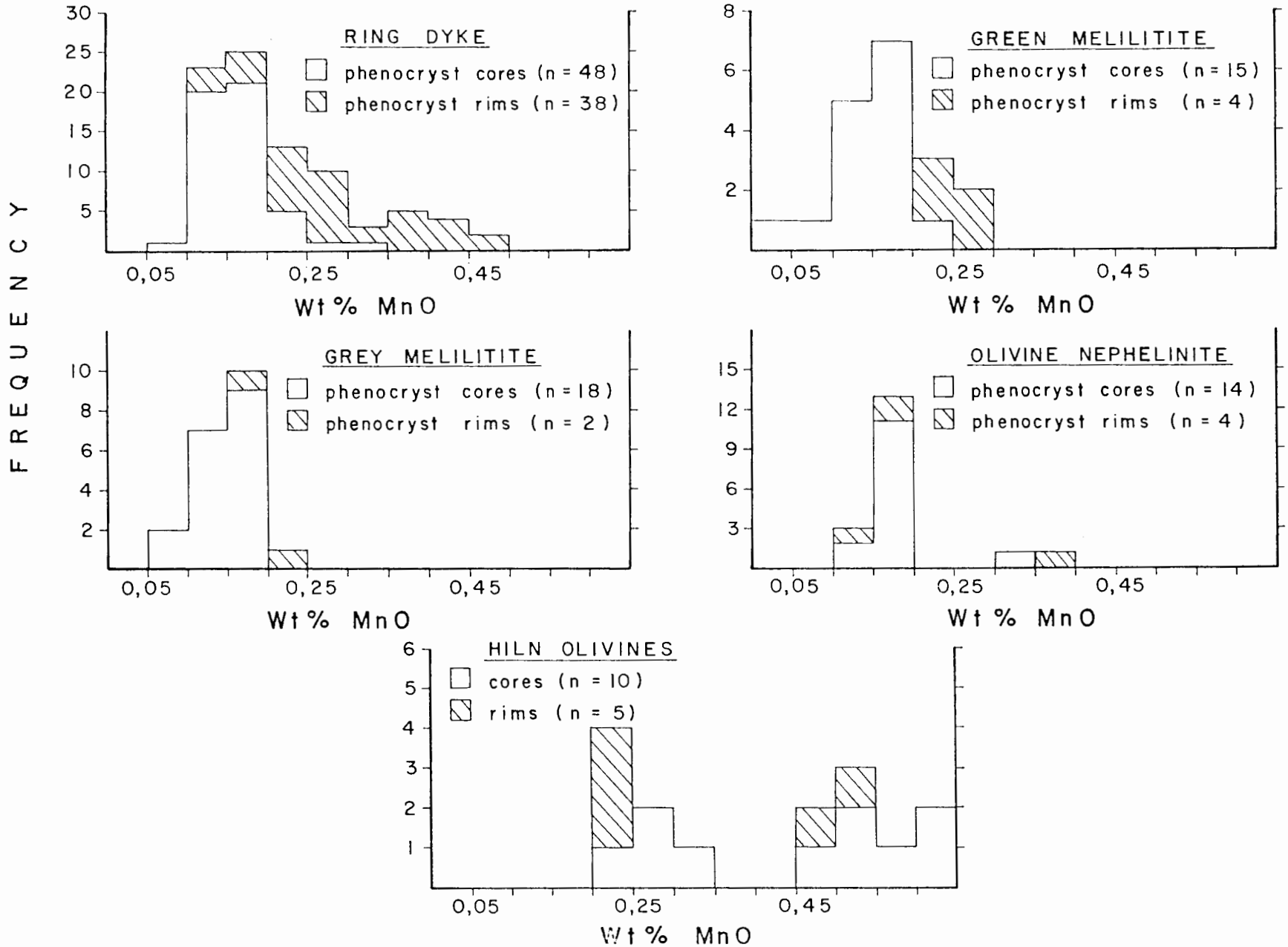

have low concentrations of calcium and manganese. Smaller phenocrysts (including microphenocrysts) by comparison show much wider compositional spread, trend towards lower forsterite levels and nickel concentrations and have higher levels of calcium and manganese (figures 5.5 to 5.7; manganese data not shown).

A variety of zonation patterns are present. Unzoned grains predominate (figures 5.8a, 5.8f, 5.8g and 5.8h), but a number of distinctly zoned olivines were also observed (figures 5.8b and 5.8c). Unzoned grains generally consist of a well developed, homogenous core and are mantled by a thin rim (usually about 50 micron wide) which can be normally or reversely zoned with respect to forsterite. Nickel concentrations are always lower in the rims and calcium and manganese concentrations are often at elevated levels when compared to the core. These thin rims appear to be a common feature of all the olivines analysed in this study. Good examples of normally and reversely zoned rims are illustrated in figure 5.10.

A typical normally zoned olivine phenocryst is illustrated in figure 5.8(b). Note that the actual core of the grain is probably somewhat asymmetric in relation to the euhedral outline. Calcium content in this grain rises steadily at a distance of about 140 microns from the core and reaches an apparent plateau at 210 microns. At approximately 250 microns from the core the calcium, manganese and forsterite content show a rapid increase, probably due to the omnipresent "edge effect" described above.

Figure 5.5 Plot of phenocryst size versus forsterite core composition for olivines in the ring dyke

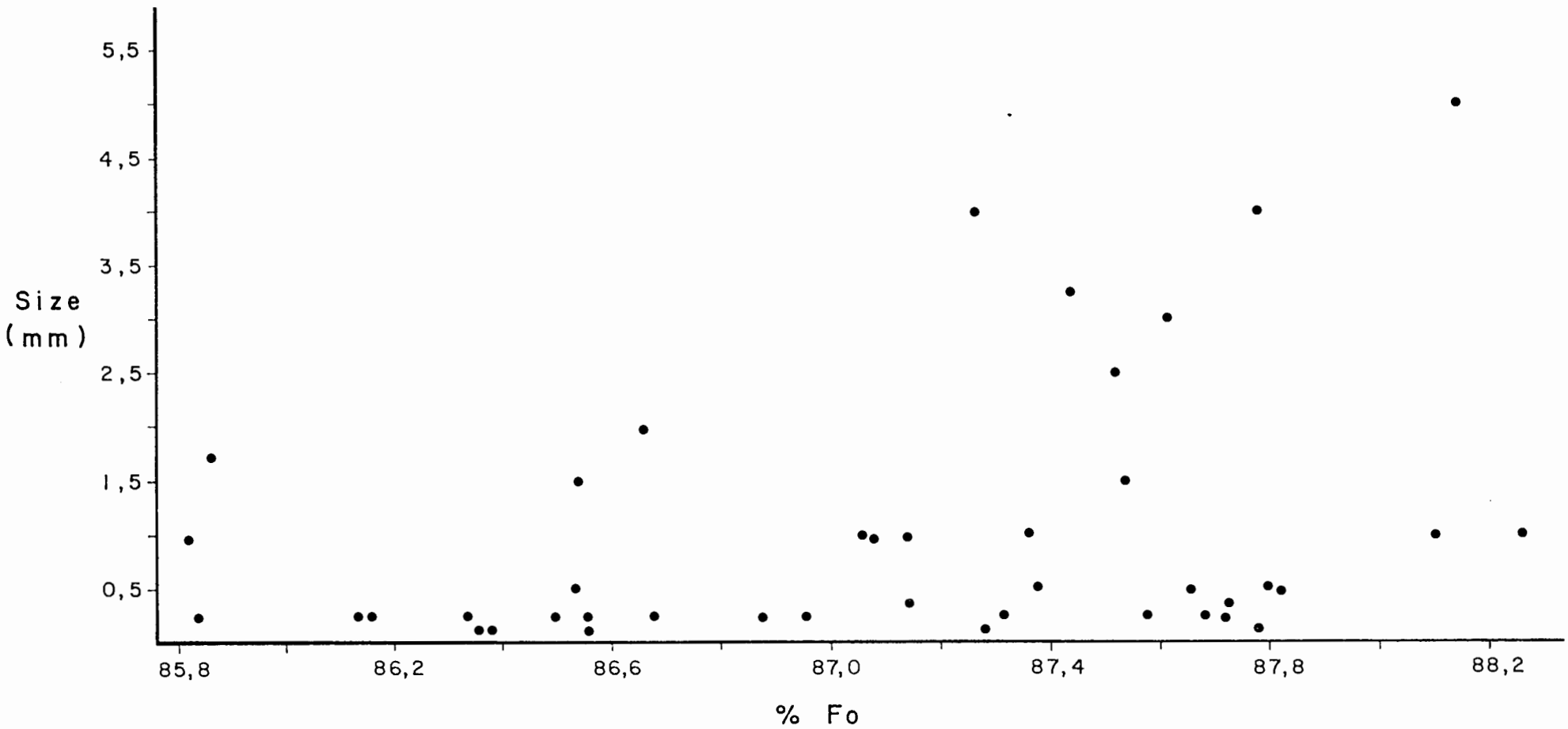

Figure 5.6 Plot of phenocryst size versus NiO core composition for olivines in the ring dyke

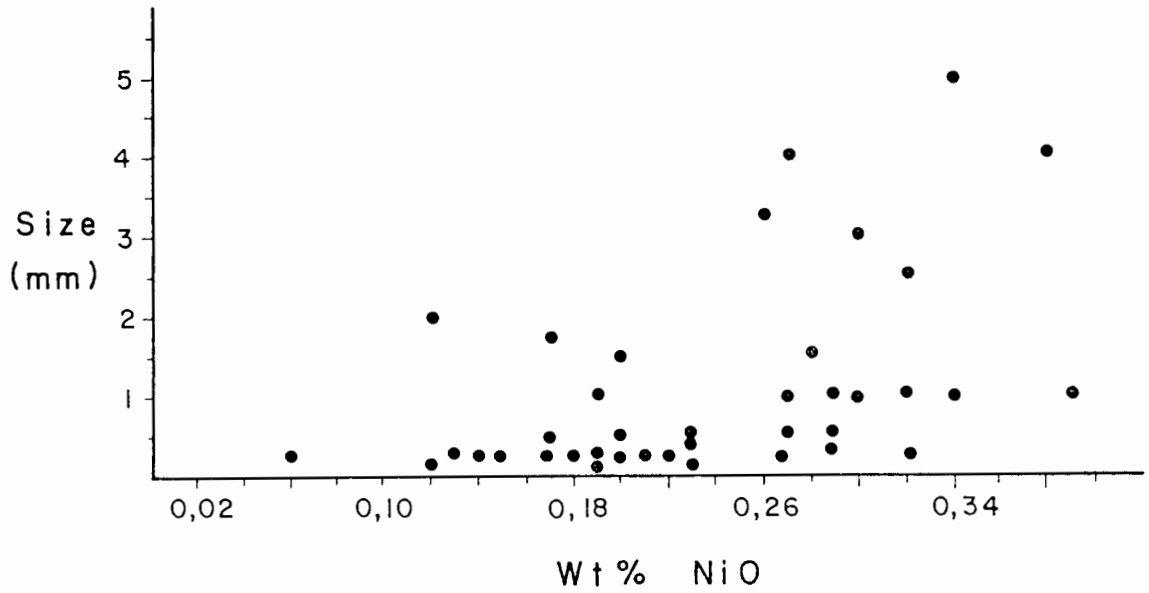

Figure 5.7 Plot of phenocryst size versus CaO core composition for olivines in the ring dyke

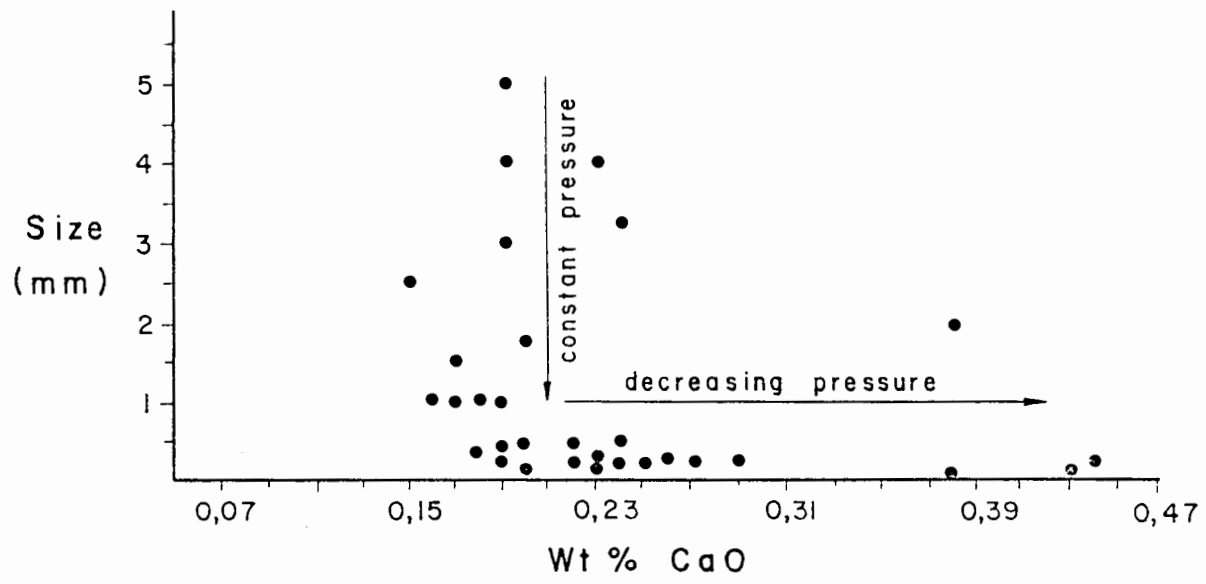

Reversely zoned grains are also present (figure 5.8c). Olivine 42 in the ring dyke is a very small microphenocryst which show an asymmetric pattern of steadily increasing forsterite from the core to a position 40 micron from the rim, after which it shows a sharp decrease in forsterite content, presumably a reflection of the "edge effect". The apparent increase in nickel in this zone is simply due to the fact that the nickel concentration in the analysis 40 microns from the rim is below a detection limit of 0.05 wt%. The rim analysis recorded 0.06 wt% NiO and the fluctuation is therefore within analytical error. It is important to realise that nickel contents in both the normally and reversely zoned grains discussed above show a steady decrease in nickel content from core to rim, irrespective of the forsterite zonation pattern. However, this is not always the case as will be shown in the following section.

5.2.3 Mineral chemistry of complex phenocrysts

Chemically the hopper olivines and multiple growth aggregates of the complex phenocryst group are indistinguisable from olivine phenocrysts and microphenocrysts (figure 5.10). Hopper olivines are usually not zoned and also exhibit the "edge effect" described in section 2.3 (figure 5.9d). In broad terms the same can be said of the multiple growth aggregates, but a number of features make them worthy of more detailed description.

The majority of the multiple growth aggregates are of bisegmental type and do not show a change in composition

Figure 5.8 (a)
Sample 256 (ring dyke)
Olivine phenocryst 40

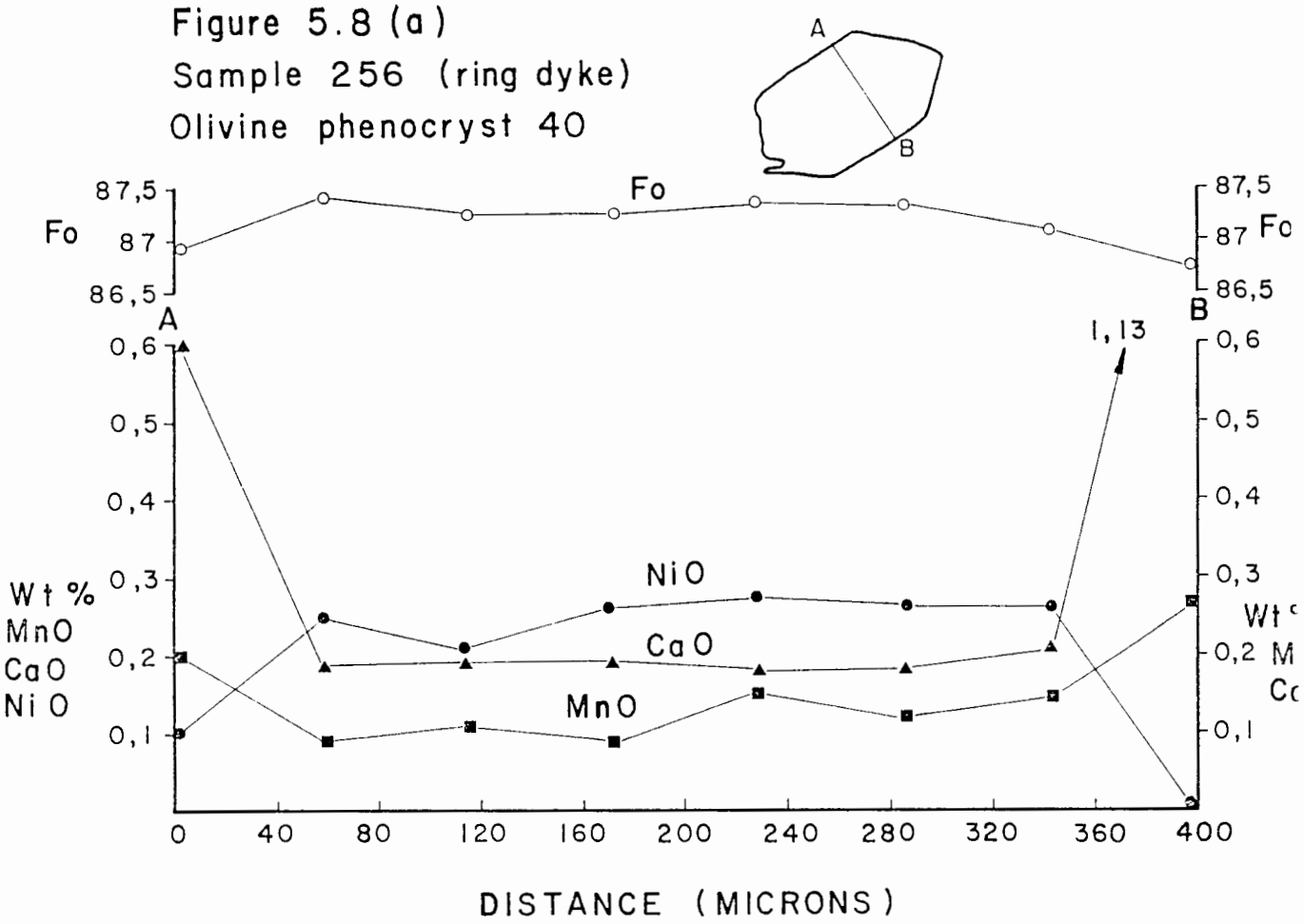

Figure 5.8 (b)
Sample 256 (ring dyke)
Olivine phenocryst 43

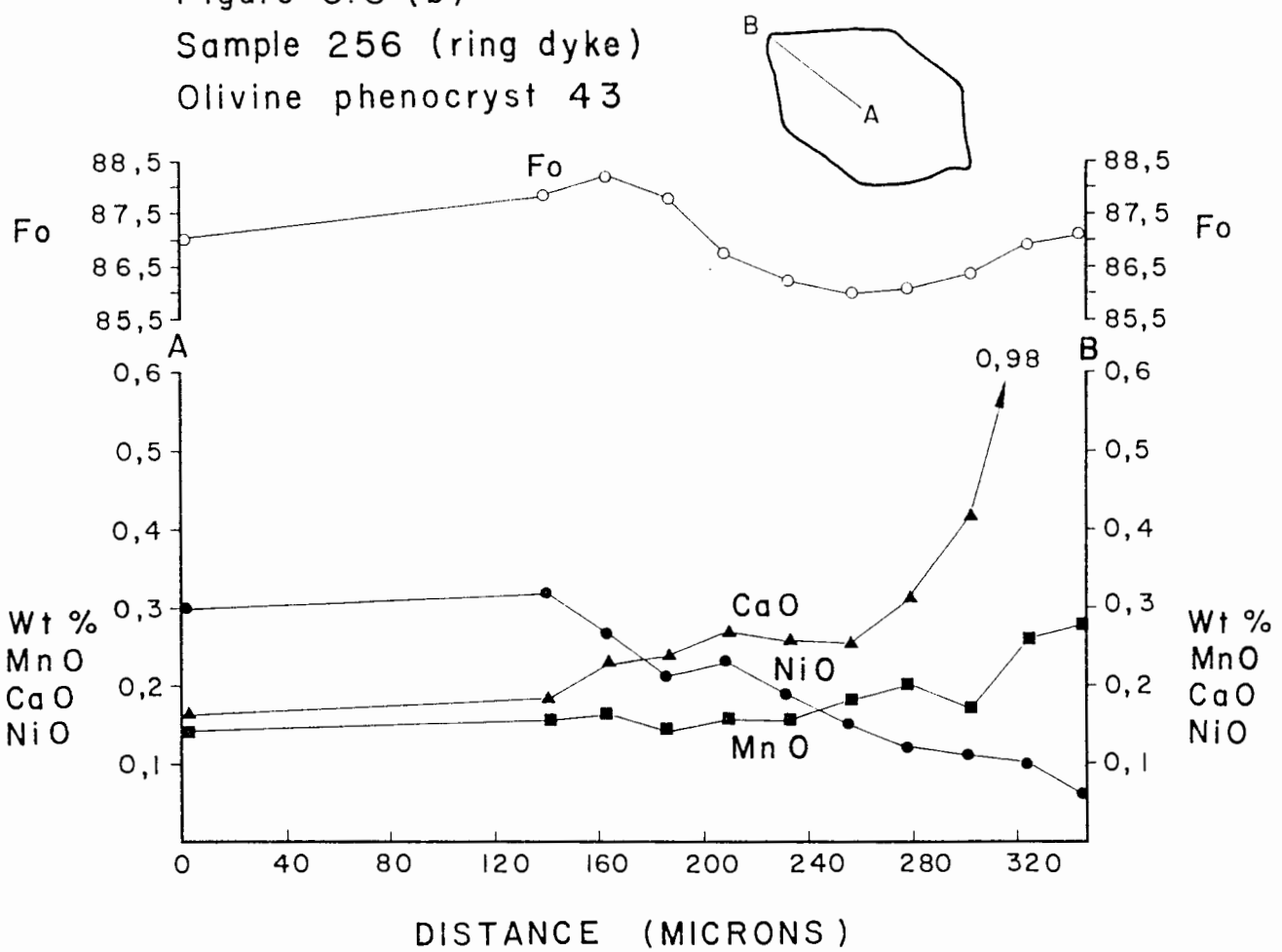

Figure 5.8 (c)
Sample 256 (ring dyke)
Olivine phenocryst 42

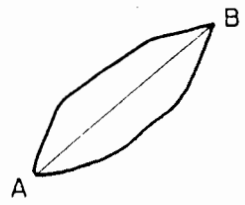

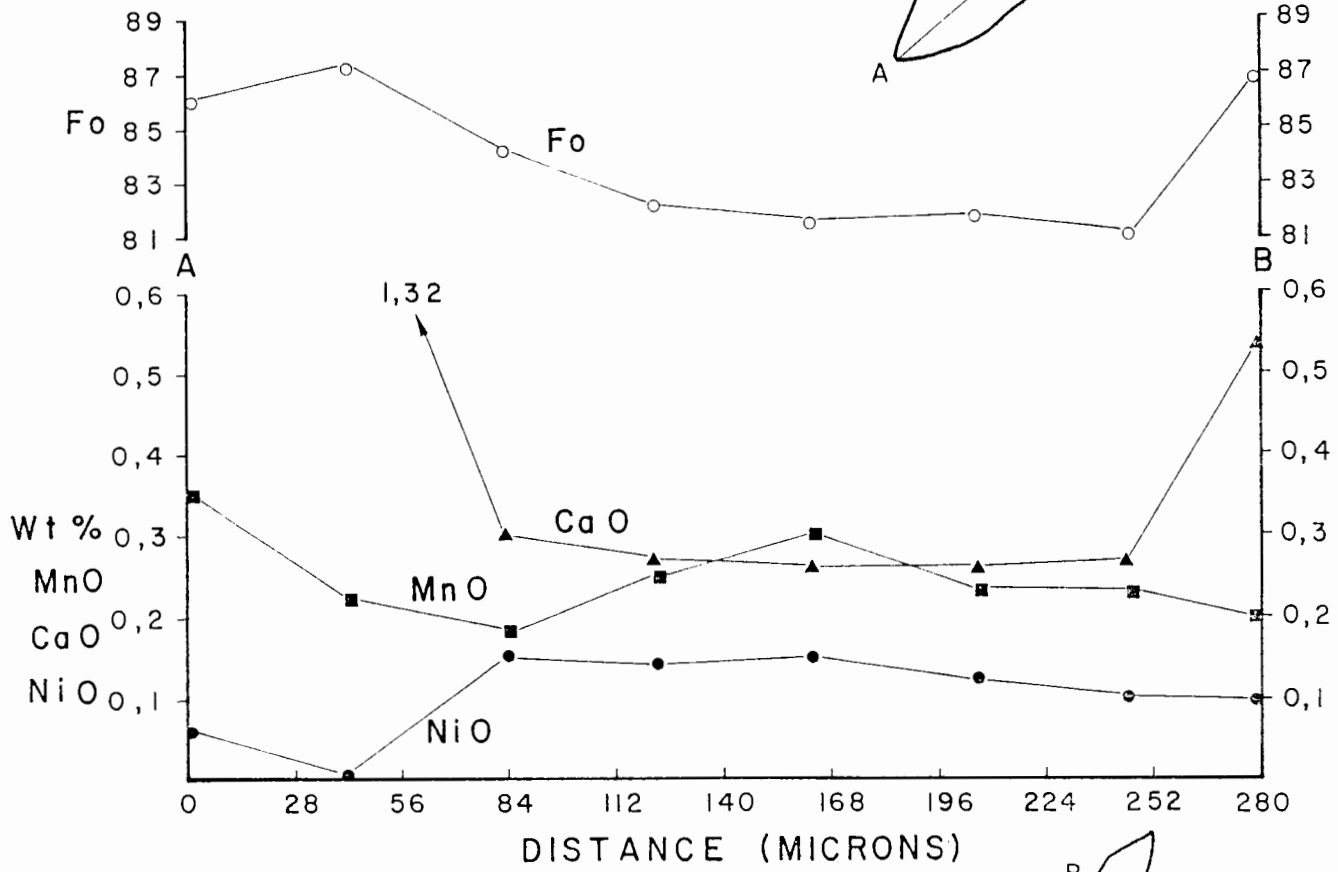

Figure 5.8 (d)
Sample 256 (ring dyke)
Olivine phenocryst 41

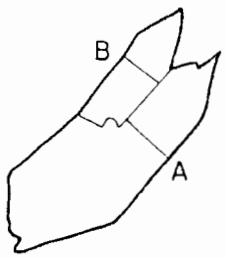

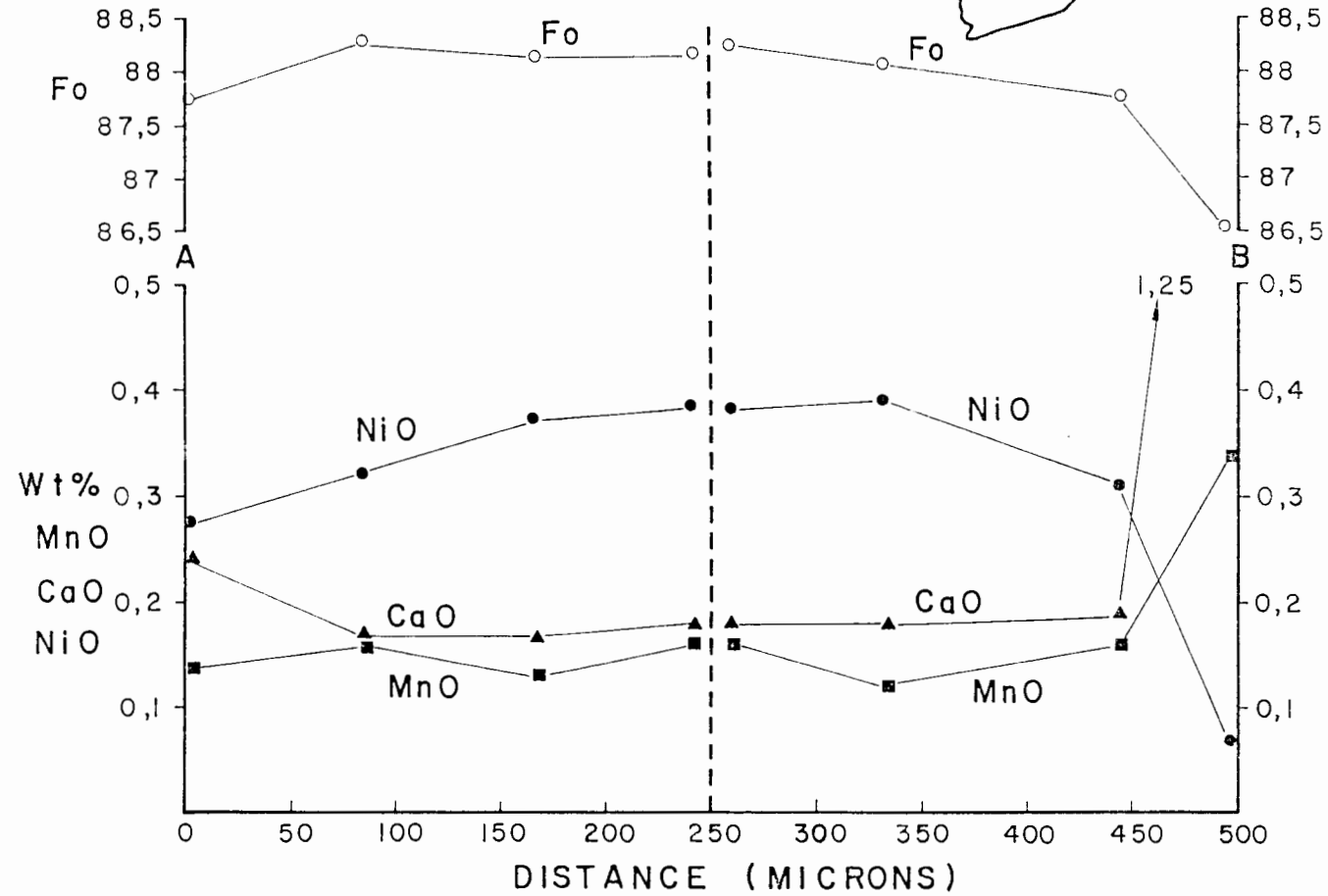

Figure 5.8 (e)
Sample 256 (ring dyke)
Olivine phenocrysts 44-50

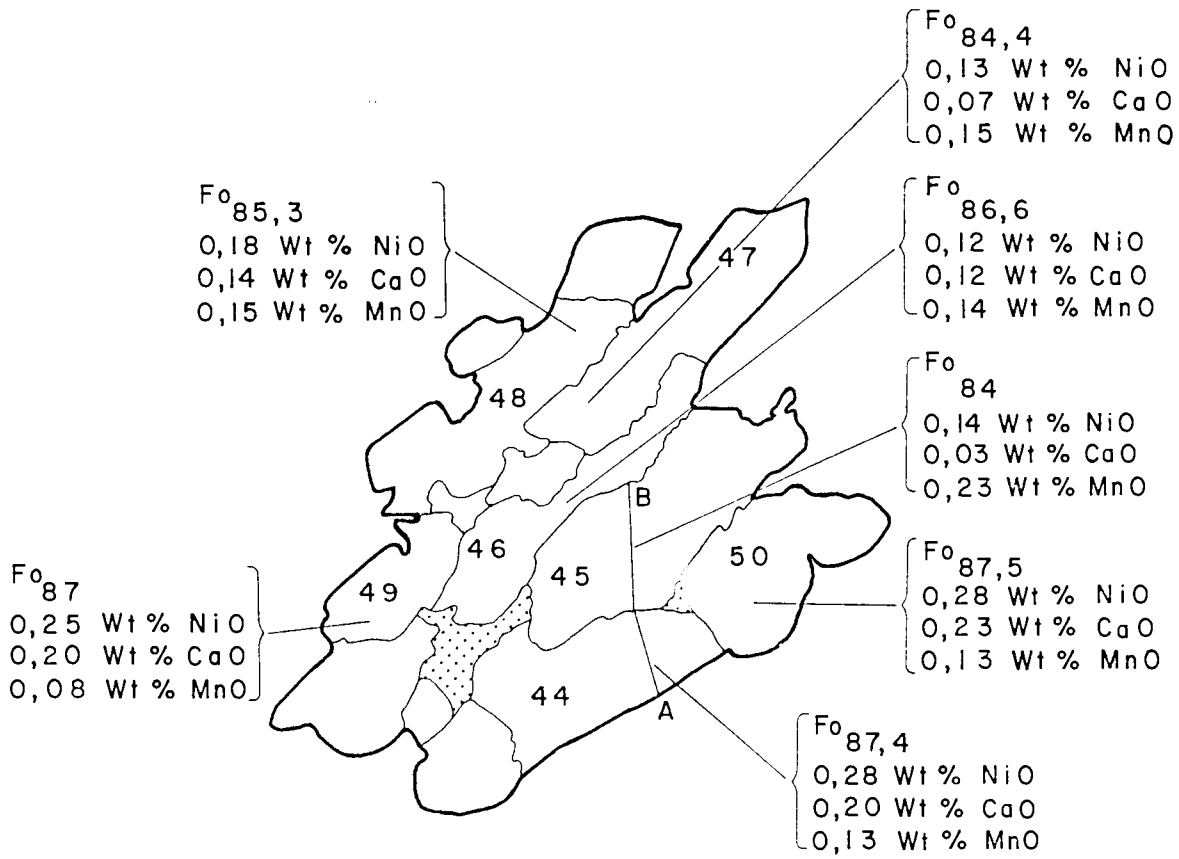

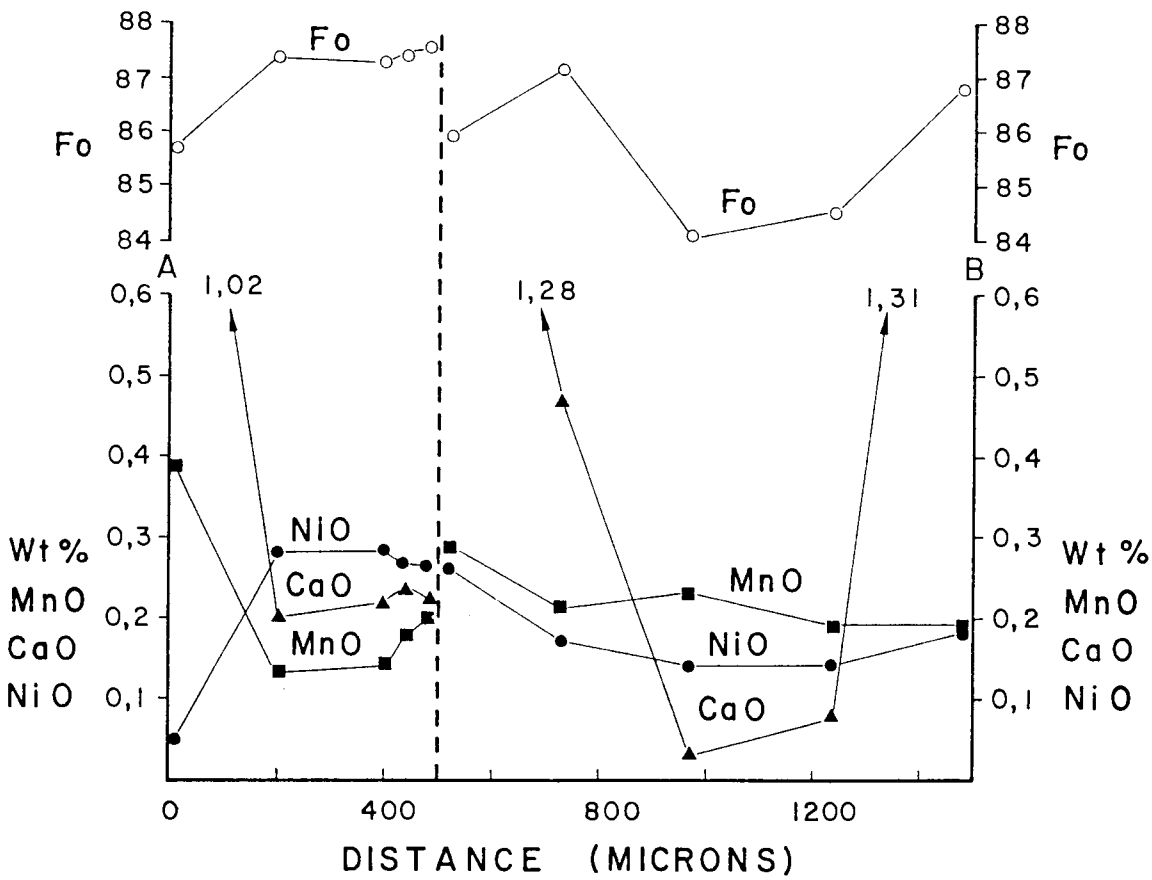

Figure 5.8 (f)

Sample 256 (ring dyke)
Olivine phenocryst 1

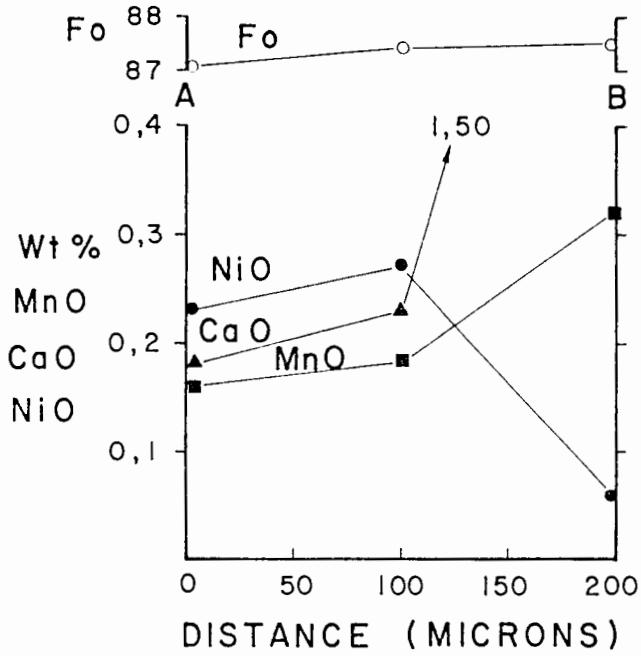

Figure 5.8 (g)

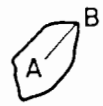

Sample 256 (ring dyke)
Olivine phenocryst 2

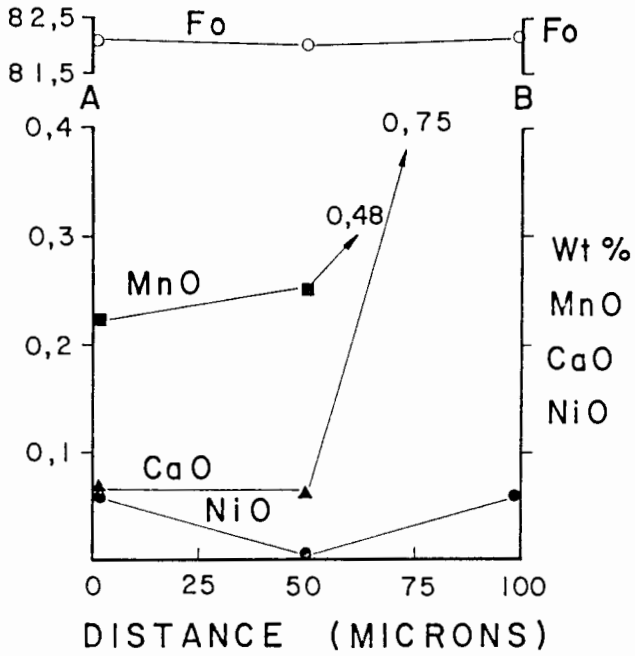

Figure 5.8 (h)

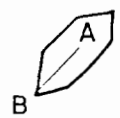

Sample 267 (olivine nephelinite)
Olivine phenocryst 15

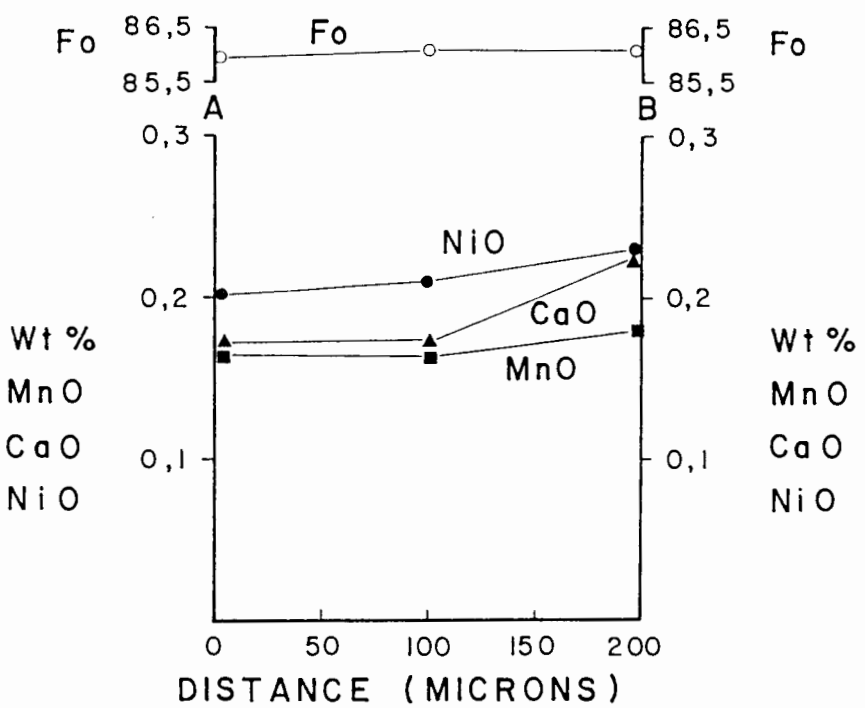

Figure 5.8 (i)
Sample 205 (green melilitite)
HILN olivine 16

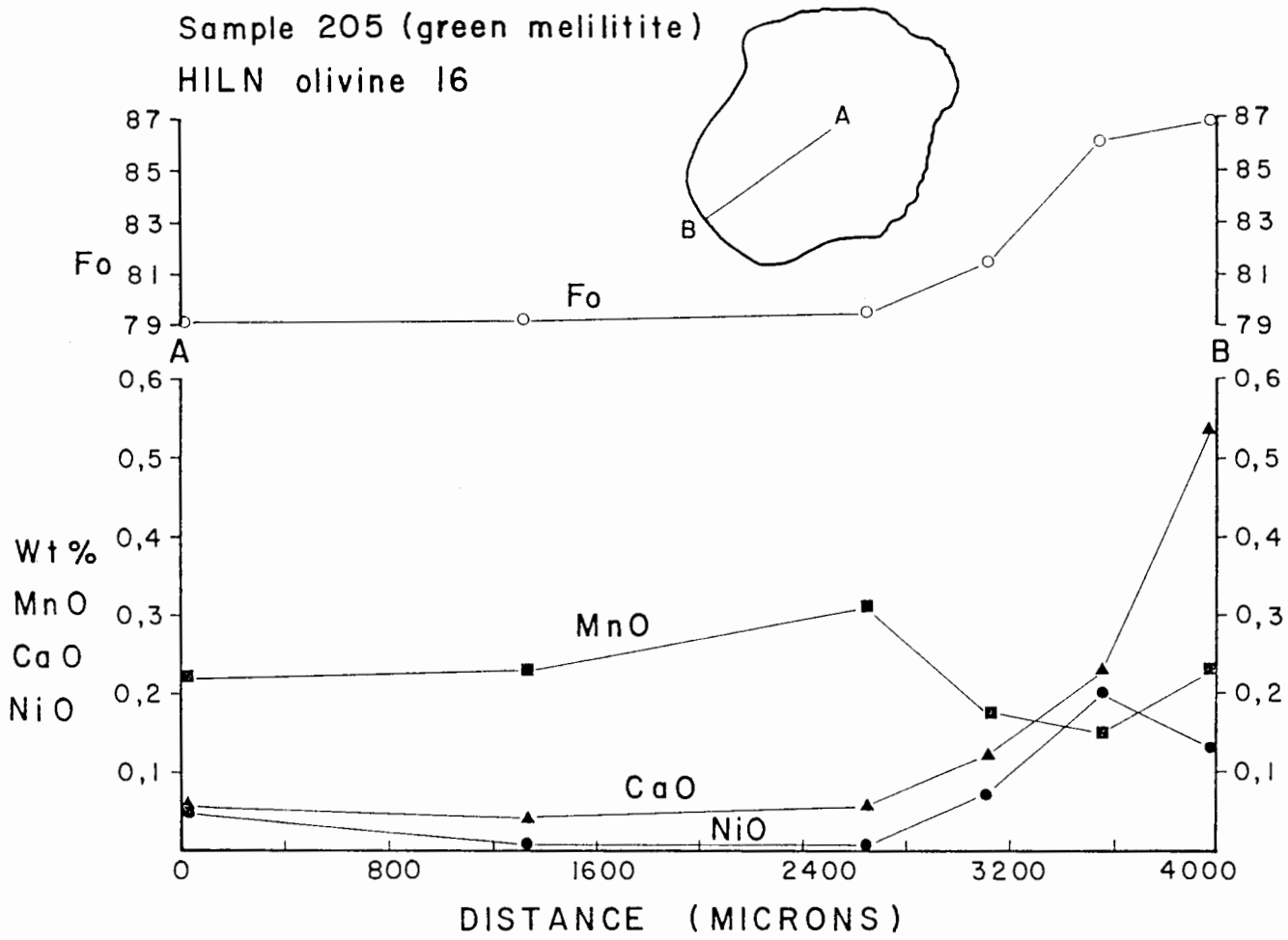

Figure 5.8 (j)
Sample 30 (ring dyke)
HILN olivine 1

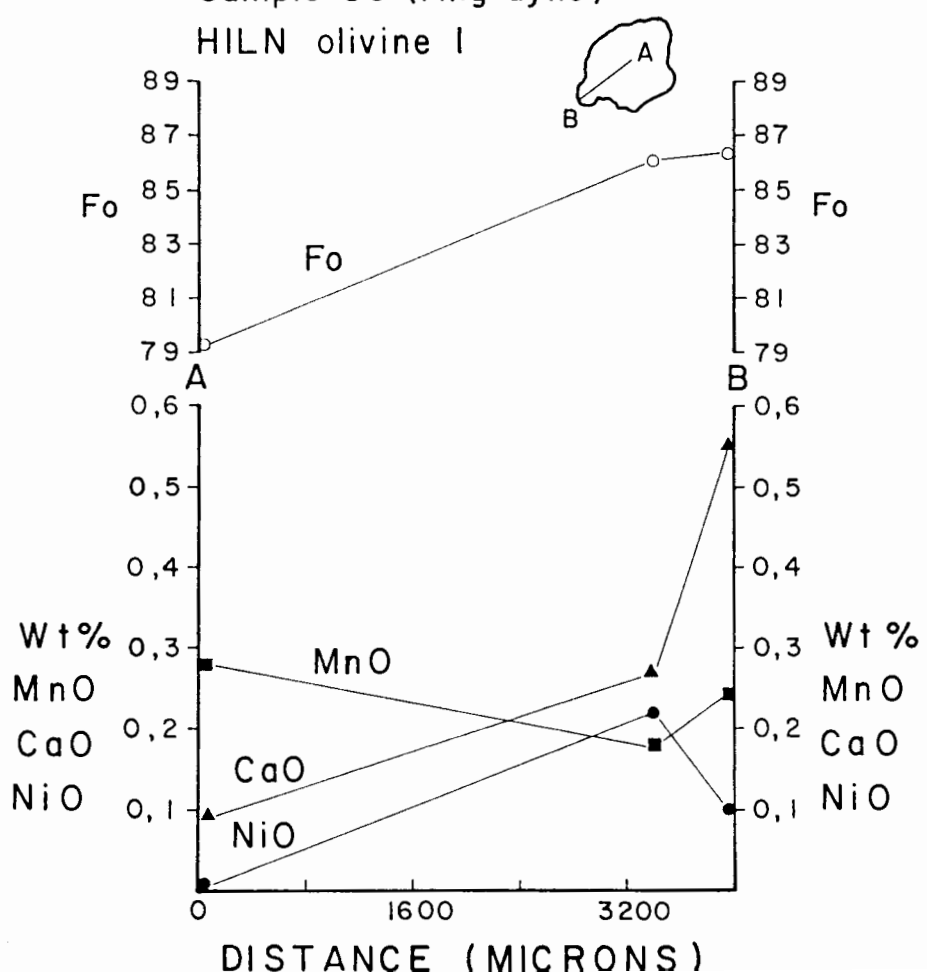

Figure 5.9

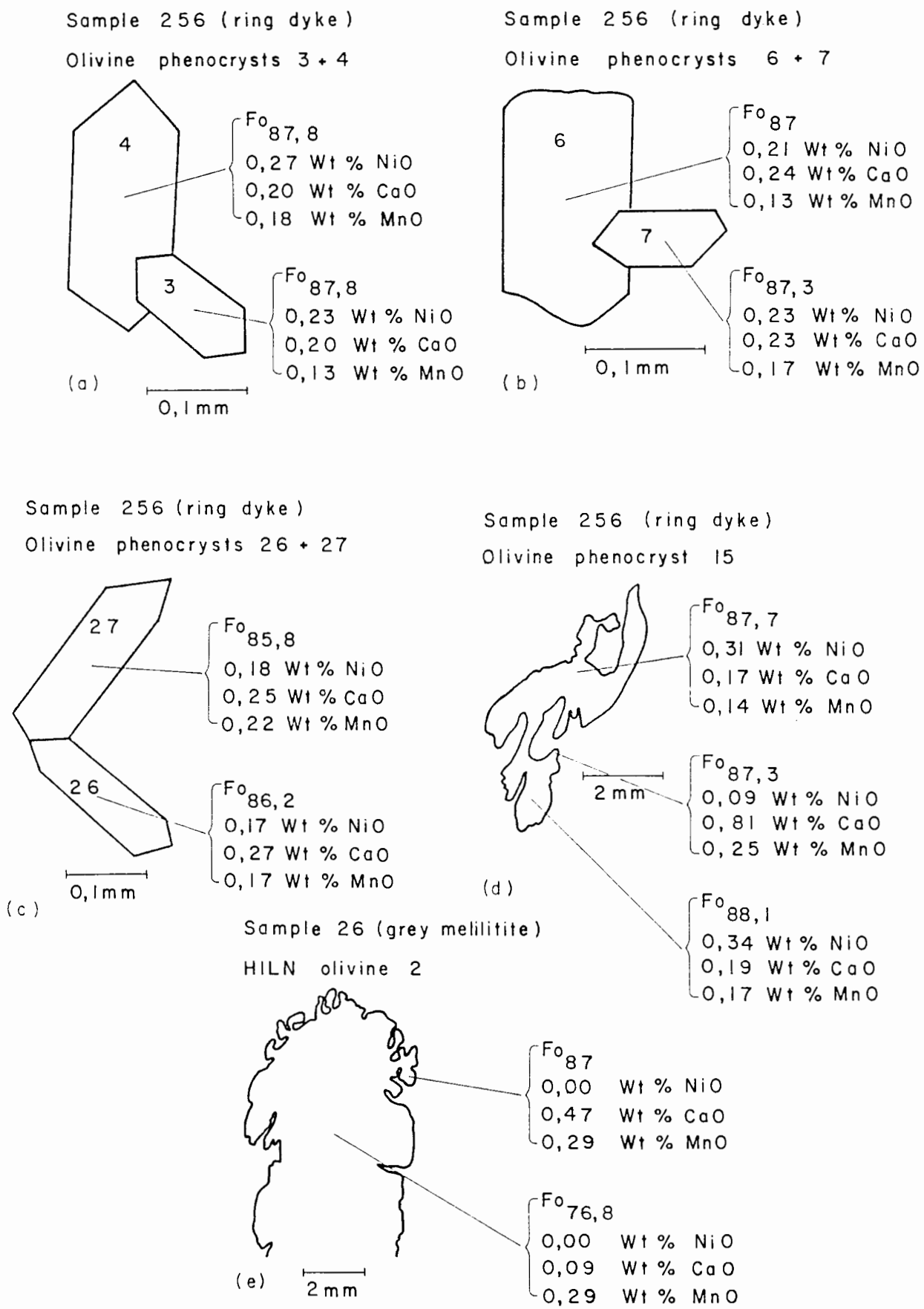
Sample 256 (ring dyke)
Olivine phenocrysts 3 + 4
4
3
Fo87,8
0,27 Wt % NiO
0,20 Wt % CaO
0,18 Wt % MnO
Fo87,8
0,23 Wt % NiO
0,20 Wt % CaO
0,13 Wt % MnO
(a)
0,1mm
Sample 256 (ring dyke)
Olivine phenocrysts 6 + 7
6
7
Fo87
0,21 Wt % NiO
0,24 Wt % CaO
0,13 Wt % MnO
Fo87,3
0,23 Wt % NiO
0,23 Wt % CaO
0,17 Wt % MnO
0,1mm
(b)
Sample 256 (ring dyke)
Olivine phenocrysts 26 + 27
27
26
Fo85,8
0,18 Wt % NiO
0,25 Wt % CaO
0,22 Wt % MnO
Fo86,2
0,17 Wt % NiO
0,27 Wt % CaO
0,17 Wt % MnO
0,1mm
(c)
Sample 256 (ring dyke)
Olivine phenocryst 15
Fo87,7
0,31 Wt % NiO
0,17 Wt % CaO
0,14 Wt % MnO
2mm
Fo87,3
0,09 Wt % NiO
0,81 Wt % CaO
0,25 Wt % MnO
Fo88,1
0,34 Wt % NiO
0,19 Wt % CaO
0,17 Wt % MnO
(d)
Sample 26 (grey melilitite)
HILN olivine 2
Fo87
0,00 Wt % NiO
0,47 Wt % CaO
0,29 Wt % MnO
Fo76,8
0,00 Wt % NiO
0,09 Wt % CaO
0,29 Wt % MnO
(e)
2mm

Figure 5.10 Plot of NiO versus forsterite for olivine phenocrysts in the ring dyke

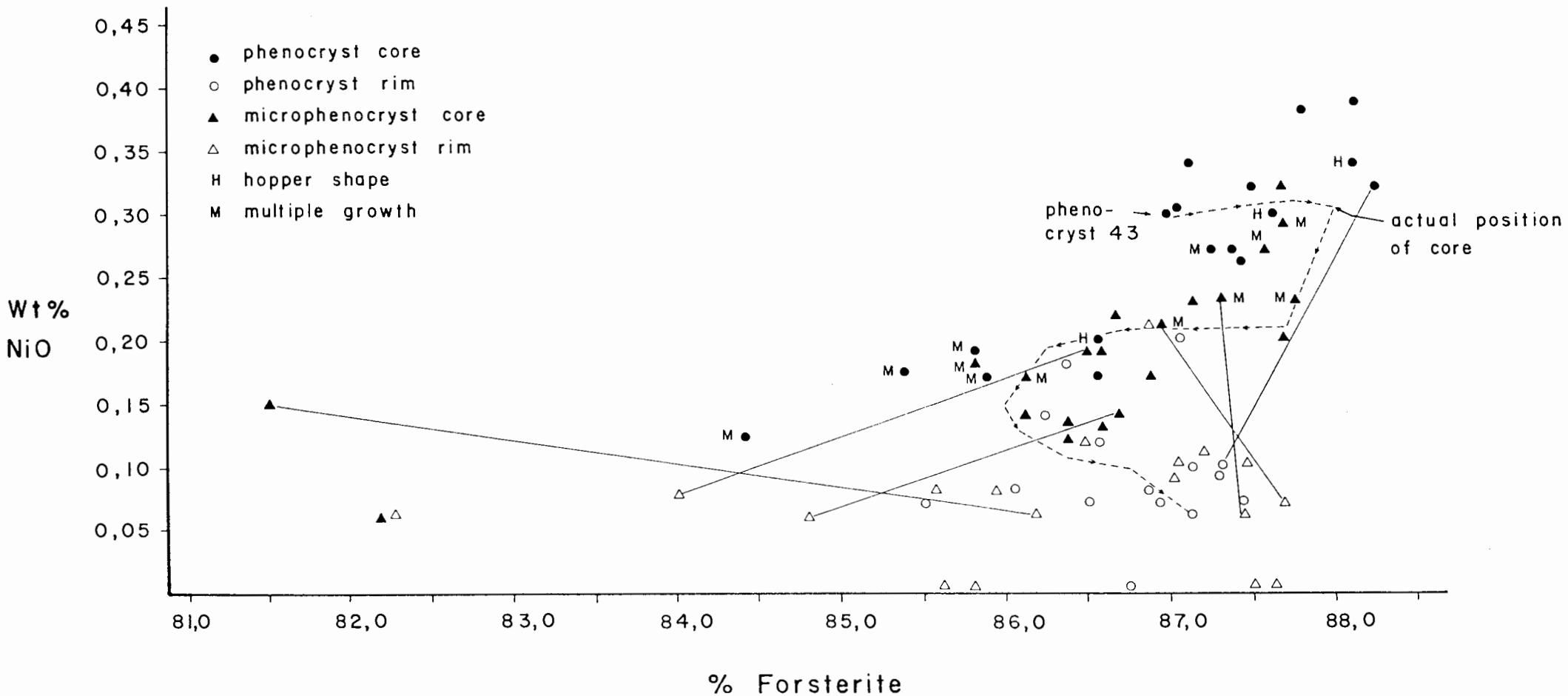

across the interface between the two grains (figure 5.8d). The cores of grains sharing an interface generally have identical compositions (figures 5.9a, 5.9b and 5.9c).

Exceptions however, do occur. Olivines 44 to 50 in the ring dyke occur in an exceptionally large multiple growth aggregate which consists of thirteen optically identifiable individuals (figure 5.8e). Grain 44 in this cluster is a typical unzoned olivine. It abuts against a reversely zoned grain (olivine 45) which shows increasing forsterite and nickel from core to rim. This olivine also exhibits an "edge effect" but here the nickel content is still higher at the rim. This strongly suggests that the "edge effect" influences the forsterite, manganese and calcium contents of olivine rims, but has no effect on nickel concentrations. The absence of an edge effect in grain 44 is presumably due to slight inaccuracy in the determination of the analytical position since this phenomenon is most marked at the extreme outer edge of grains. Spot analyses on a number of the remaining grains in the cluster show that a wide range of olivine chemistries are present (figure 5.8e).

5.2.4 Chemistry of the HILN olivines

As was mentioned in section 2.1, the HILN olivines are compositionally unusual when compared with the other olivine types at the Commonage. Core compositions are characterised by very low forsterite contents (Fo_{71} to Fo_{80}), and nickel contents are generally below a detection limit of 0.05 wt%. By increasing the counting time on the nickel peak to four minutes, two grains yielded <0.02 wt% and 0.03 wt% nickel

respectively. Calcium concentrations in the cores overlap with those of core analyses of phenocrysts. Manganese concentrations in HILN olivine cores are exceptionally high, often up to 0.06 wt% (see figures 5.1 to 5.4).

The olivine overgrowths on these grains (see chapter 3) are generally more forsteritic and have higher calcium and nickel contents than core analysis (figures 5.1 to 5.4, figures 5.8i-j and figure 5.9e), while manganese concentrations are lower in the mantles than in the cores. These overgrowths are compositionally identical to phenocrysts, and a marked "edge effect" is again noticeable in the outermost rims of all the grains.

HILN olivine cores are generally compositionally homogenous (figure 5.8i). By contrast, mantles with olivine phenocryst compositions show reverse zoning, but this might simply be due to elemental diffusion across the contact between the olivine core and the overgrown mantle.

5.2.5 A comparison between olivine compositions at the Commonage and literature data

Olivine compositional data for melilitites are relatively scarce, but a useful summary was compiled by Shee (1986). The Commonage olivine phenocrysts are generally more forsteritic than olivines from melilitites in Namaqualand (up to $Fo_{85.5}$), R.S.A.; Malaita ($Fo_{85.82}$), Solomon Islands, and the Marathon Dykes (Fo_{87}), Canada. The Commonage phenocrysts are however, virtually identical to those from the neighbouring Saltpetre Kop intrusion (thirty kilometres away) which implies that the

two intrusions are probably cogenetic (McIver and Ferguson, 1979).

HILN olivine compositions reported by Moore (1979) from melilitites in Namaqualand are identical to those recorded for the Commonage. Perusal of the Saltpetre Kop data presented by McIver and Ferguson (1979) suggest that HILN olivines are also present at this locality, but that forsterite contents may vary to as low as Fo_{65}. Gurney (et al., 1979) reported chemical analysis of olivine megacrysts from the Monastery kimberlite which are similar to melilitite HILN olivines. The grains have forsterite and nickel contents as low as $Fo_{78,3}$ and 0.06 wt% NiO respectively.

5.3 Discussion

5.3.1 Olivine phenocrysts

This study of the phenocryst chemistry indicates that a wide variety of early processes occurred in the melilitite magma. Features of the olivines which may have an important bearing on the petrogenesis of the intrusions are:

1)Unzoned, euhedral phenocrysts are present.

2)A number of olivines show normal and reverse zoning with respect to forsterite content. Nickel content in these olivines decreases irrespective of the forsterite zonation pattern.

3)A few phenocrysts show reverse zonation patterns coupled with increasing nickel concentrations.

4)Microphenocrysts are often reversely zoned with respect to forsterite but show decreasing nickel from core to rim.

5)Large phenocrysts generally have high forsterite and nickel contents coupled with low calcium concentrations while phenocrysts smaller than 2.5 mm in size are often less forsteritic, lower in nickel and exhibit higher calcium and manganese contents.

6)Hopper olivines are not zoned.

7)Multiple growth aggregates consists either of compositionally identical grains or comprise of phenocrysts with widely disparate chemistries.

8)A pronounced "edge effect" is present in the outer 50 micron of all olivines. In this zone the forsterite, calcium and manganese contents often show a sharp increase while nickel is not affected.

9)Olivines in the sill complex are slightly more forsteritic than those in the ring dyke.

Large phenocrysts with high nickel and forsterite core compositions must have crystallised from a relatively primitive, unevolved magma. Their unzoned nature suggest that they crystallised under equilibrium conditions. During this process the precipitating olivines should still deplete the magma in magnesium and nickel, and normally zoned olivines could result. Maaløe and Hansen (1982) calculated theoretical olivine zonation patterns under the assumption that there is insignificant diffusional exchange between crystals and melt, and that crystallisation is fractional. They found that the calculated zonation pattern depends on the temperature at which the olivines nucleate and on the number of growing crystals in the magma. If the olivines are few and large, then the crystals will be essentially unzoned, primarily

because the remaining liquid is still relatively voluminous and undepleted. This is in keeping with the petrographic study of the Commonage rocks which shows that olivine phenocrysts larger than 2.5 mm in size are extremely rare in comparison to smaller phenocrysts and microphenocrysts.

It is evident from figures 5.5 and 5.6 that these large, early crystallising phenocrysts exhibit a range in forsterite and nickel contents in their cores in spite of the absence of zoning. One would expect these grains to have identical compositions if they crystallised from a single batch of magma under equilibrium conditions. Clement (1982) and Shee (1986) ascribed a range in core compositions of olivine phenocrysts in the Wesselton kimberlite to the mixing of separate batches of magma. The present author is hesitant to apply this explanation to the Commonage phenocrysts as there is no evidence for stepped zonation patterns in early olivine phenocrysts at Sutherland Commonage. Stepped zonation patterns would be expected if, for arguments sake, grains in a low Fe/Mg magma were to carry on crystallising in a "mixed" magma with a higher Fe/Mg ratio. It is therefore envisaged that all the early, large, euhedral, unzoned phenocrysts crystallised in one magma chamber which was temperature zoned. The presence of large, unzoned hopper phenocrysts with pronounced corrosional morphologies (figure 5.9d) indicates that there was probably some movement of magma and suspended crystals in the chamber. Transportation of phenocrysts from areas in the chamber with lowish ambient temperature to the central, hotter core will lead to the corrosion and resorption of these grains, and pronounced hopper shapes should form.

Movement of high temperature grains to a low temperature environment should lead to overgrowth formation, but if the grains are already large then the amount of material needed to form recognisable overgrowths will probably be excessive and the inferred slow growth rate (deduced from the large size and euhedral nature of these olivines) should therefore preclude the formation of thick mantles of different composition. In other words, chemically different mantles might have formed but are not recognised because they were very thin.

Normally zoned phenocrysts indicate a period of extensive and rapid olivine precipitation during which the magma was extensively depleted in magnesium and nickel (for example, the zonation pattern of olivine 43 when plotted in figure 5.10 covers almost the whole field defined by the phenocryst compositions). This increase in the rate of olivine nucleation is presumably due to the supercooling of the magma which was caused by the rupture of the magma chamber and the movement of the liquid into a cooler area of the mantle. It is conceivable that the degree of supercooling was not constant throughout the bulk of the magma from which the olivines were crystallising. The experimental work of Donaldson (1976) indicates that the small, euhedral olivine phenocrysts as well as multiple growth aggregates of the bisegmental type (e.g. the olivines in figures 5.9a-e) crystallised in areas in the magma with comparatively low degrees of supercooling, while crystals with pronounced hopper shapes crystallised in regions with a higher degree of supercooling. It is important to note that the present author therefore assumes that hopper shaped olivines can form by

corrosion and rapid growth.

The unzoned nature of the hopper olivines and the presence of identical core compositions for individual grains in multiple growth aggregates is therefore also considered to be a consequence of relatively rapid olivine nucleation.

Decreasing pressure appears to favour the incorporation of calcium in crystallising olivines (Stormer, 1973; Ferguson, 1978). If this is so, then the trend of increasing calcium content with decreasing grain size (figure 5.7) substantiates a model in which the early forsteritic olivines crystallised at depth under conditions of virtually constant pressure while the smaller phenocrysts and microphenocrysts precipitated from a magma which experienced a steady drop in pressure, presumably due to the upward movement of the liquid. The calcium plateau shown by the olivine in figure 5.8(b) which is at a higher calcium concentration than the core of the grain provides additional support for a pressure decrease during the crystallisation of the more evolved compositions. Note, however, that there is no distinct break in the curve relating phenocryst size to calcium content (figure 5.7). This is taken to indicate that olivine did not crystallise in two distinct generations (one at high pressure and the other at lower pressure) but rather that olivine crystallisation was a continuous, uninterrupted process.

It appears that the melilitite magma in the ring dyke incorporated a small volume of melt with a lower Fe/Mg ratio and lower nickel content. Olivine 45 (figure 5.8e) occurs in

an unusually large multiple growth aggregate. It shows marked reverse forsterite and nickel zonation and is in contact with an unzoned olivine (olivine 44) with higher average forsterite and nickel content. The zonation pattern of phenocryst 45 trends towards the composition of olivine 44 which indicates that phenocryst 45 was incorporated into the magma from which olivine 44 was crystallising. The volume of incorporated magma must have been small since phenocryst 44 does not reflect a marked change in the composition of the magma from which it was crystallising. The incorporation of a magma with a low Fe/Mg ratio would also explain the presence of the two low forsterite olivines in figure 5.10. It is proposed that the sudden rupture of the magma chamber in which the earliest phenocrysts crystallised and the ascent of the contained liquid might have created volume instabilities in the surrounding mantle. This could be the driving force behind the movement of other pockets of melt (unrelated to the main melilitite magma) into the same conduit.

The consistent chemical features in the rims of all the olivines at Sutherland Commonage (the "edge effect") is presumably due to very late stage processes. Boyd and Clement (1977) and Shee (1986) suggested that the edge effect might be due to late stage diffusional exchange between the residual magma and the olivines. The effect is probably most pronounced for calcium as it reaches extremely high levels in the rims of all the olivines at Sutherland Commonage. The commonly observed increase in forsterite content in olivine rims might be due to overlap of magnetite crystallisation with the final stage of olivine precipitation (Moore, 1979) or it

is simply a consequence of diffusion of magnesium from a Mg-enriched residual fluid (the result of extensive magnetite precipitation) into the olivine lattice. Overlap of the crystallisation of olivine and magnetite would also explain the reverse forsterite zonation (coupled with decreasing nickel contents) seen in a few of the microphenocrysts.

Lower maximum forsterite composition of olivine phenocryst in the ring dyke compared to phenocrysts from the sill complex can be taken as evidence that the ring dyke is derived from a separate, more evolved magma. Alternatively the difference could be related to the loss of large, highly forsteritic olivines from the dyke magma by flow differentiation of the coarser constituents during emplacement.

5.3.2 Olivine-spinel equilibria

The partitioning of Mg^{2+} and Fe^{2+} between coexisting spinel and olivine is sensitive to the prevailing temperature and is therefore a potentially useful geothermometer (Irvine, 1965). The equilibrium distribution of iron and magnesium between these two minerals can be expressed as follows:

$$1/2Fe_2SiO_4 + Mg(Cr_xAl_yFe^{3+}_z)_2O_4 = 1/2Mg_2SiO_4 + Fe(Cr_xAl_yFe^{3+}_z)_2O_4$$

where x, y and z are the atomic fractions of the respective trivalent cations (Roeder et al., 1979). The equilibrium constant for this reaction is:

$$K_D = (FeO/MgO)^{sp}/(FeO/MgO)^{ol}$$

Figure 5.11 Plot of Ni concentration versus Mg-number (atomic ratio of $Mg/Mg+Fe^{2+}$) for rocks of the karoo volcanic province in relation to the HILN olivine parent

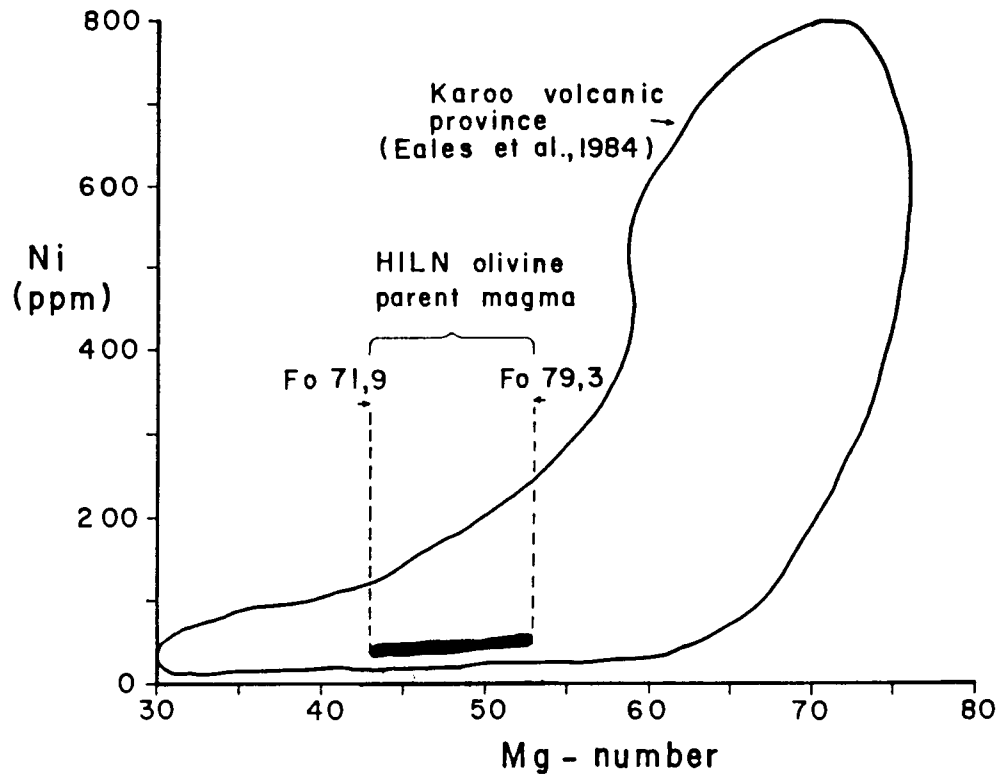

Figure 5.12 Plot of (Fe/Mg) ratios in coexisting olivine phenocrysts and chrome spinels

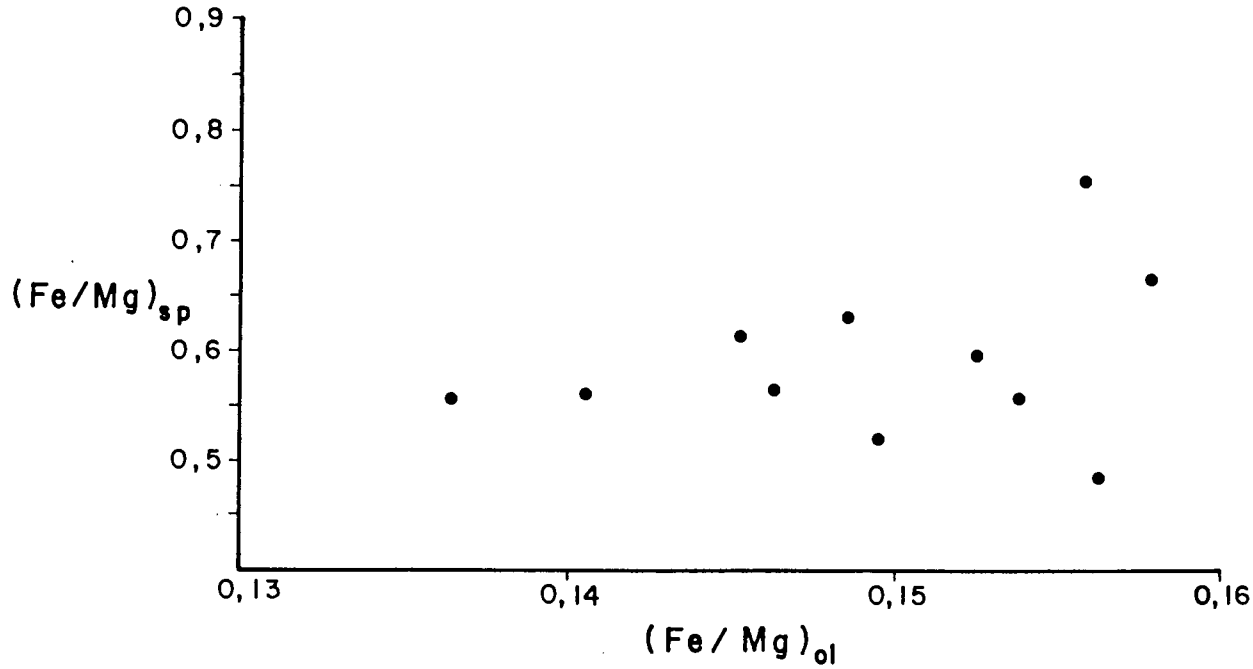

An attempt was therefore made to obtain a temperature of olivine crystallisation by analysing 10 olivine-spinel pairs in two samples from the ring dyke. The (Fe/Mg) ratios of these coexisting pairs are plotted in figure 5.12. It is evident that there is no correlation and that olivine-spinel pairs in the Commonage melilitites therefore do not represent equilibrium assemblages.

It is considered that these spinels probably crystallised early and were subsequently encapsulated during the olivine crystallisation interval. Alternatively their formation might be due to relatively rapid olivine growth. In the latter case the melt around the growing olivine phenocryst is enriched in aluminium, chrome and iron. The spinel crystals initially nucleate near the olivine phenocrysts, and the olivine crystals continue growing after the formation of spinel. Shortly afterwards the growth of olivine is retarded near the spinel, probably because the growth of spinel depletes the melt in iron. The resulting change in growth rate in the area close to the spinel causes an embayment. During further olivine growth the olivine crystal encloses the spinel. These spinel inclusions thus formed from a liquid with a composition differing from that of the bulk liquid (Maaløe and Hansen, 1982), hence the absence of equilibrium between olivine-spinel pairs.

5.3.3 Origin of the HILN olivines

Moore and Erlank (1979) described HILN olivines identical to those at the Commonage from melilitites in Namaqualand.

They concluded that these olivines crystallised under conditions of low oxygen activity from a carbonate-rich magma, and that olivine-melt partition for the transition elements were higher than those appropriate to carbonate free magmas of equivalent composition. In their model the HILN olivines crystallised after the crystallisation of olivine megacrysts (not present at the Commonage) but before the crystallisation of hopper olivines (Moore's term for multiple growth aggregates). It is therefore possible to envisage that the HILN olivines at the Commonage were the first olivine population to crystallise, that they crystallised from a reduced magma and that phenocryst crystallisation occurred at a later stage from a more oxidised magma.

However, several features of the Commonage HILN olivines negate such a scenario:

1)They are intergrown with magnetite and apatite which strongly suggest that they are not related to the melilitite magma since phenocrysts do not show these intergrowths. Furthermore, the presence of magnetite indicates that they crystallised in a relatively oxidising environment, probably under fO_2 conditions which were higher than the wüstite-magnetite buffer.

2)HILN olivines at the Commonage do not contain any detectable aluminium and chrome, while phenocrysts record concentrations of up to 0.06 wt% and 0.15 wt% respectively. If (as postulated by Moore and Erlank) the magma from which these grains crystallised was sufficiently reduced to render high concentrations of Fe^{2+}, Mn^{2+} and Ni° (and therefore resulting in olivines with low Fo, high MnO and low NiO

contents) then the magma should also have high concentrations of Al^{2+} and Cr^{2+} and the resulting olivines should contain higher concentrations of these two elements than the later crystallising olivine phenocrysts.

It is therefore proposed that the HILN olivines are xenocrysts which are not related in any way to the melilitite magma. The presence of magnesium and nickel enriched overgrowths with phenocryst compositions surrounding the HILN olivines suggests that these grains were incorporated in the magma during the phenocryst crystallisation interval.

It is possible to estimate the chemical composition of a magma through the use of mineral-melt partition coefficients (Cox et al., 1981). In particular, the distribution of magnesium and iron between olivine and coexisting liquids can be represented by the following equation:

$$1/2(Mg_2SiO_4)_{ol} + 1/2(Fe_2SiO_4)_{liq} = 1/2(Mg_2SiO_4)_{liq} + 1/2(FeSiO_4)_{ol}$$

The distribution coefficient for this equation can be written as follow:

$$K_D = (X_{FeO}/X_{MgO})^{ol}(X_{MgO}/X_{FeO})^{liq}$$

Roeder and Emslie (1970) found that for a variety of basaltic compositions and a wide range of temperatures and oxygen fugacities the K_D is equal to 0.3 at one atmosphere pressure, and is independent of temperature and oxygen fugacity.

Maximum and minimum Fe/Mg ratios in the parent liquid was therefore calculated for the parental magma to the HILN olivines by assuming a K_D of 0.3 between the limits $Fo_{71,9}$ and $Fo_{79,3}$. These ratios were then recalculated to the atomic ratio of $Mg/Mg+Fe^{2+}$. The result indicates that the HILN olivines could have crystallised from a magma similar to the basalts with higher Fe/Mg ratios which occur in the Karoo Volcanic Province (figure 5.11).

Similar calculations based on the distribution of nickel between olivine and a basaltic melt (Hart and Davis, 1978) predicts a nickel content of 20 ppm in the HILN olivine parent (assuming 6 wt% MgO in the parent melt and 0.04 wt% NiO in a HILN olivine of Fo_{79} composition). Increasing the magnesium concentration in the parent magma to 10 wt% still results in a nickel concentration of 40 ppm. This calculated nickel concentration therefore indicates that the HILN olivines crystallised from an evolved magma, a deduction which is substantiated by the unusually high manganese contents of these olivines.

It is therefore proposed that the HILN olivines are xenocrysts unrelated to the melilitite magma. This model requires that the Commonage intrusives ascended through a cumulate layer in the crust or upper mantle, which was formed by the fractional crystallisation of a basaltic magma, presumably related to the Karoo volcanic event.

Furthermore, basaltic melts probably have olivine on the

liquidus only up to pressures of about 10 kbar (Maaløe, 1985; Wyllie, 1971; Yoder, 1976; Cox et al., 1981), suggesting that the postulated cumulate layer occurs at depths of less than about 30 kilometres. If so, then olivine was still a crystallising phase in the melilitite magma while it was intruding into crustal levels, since the distinct olivine mantles with phenocryst compositions on the HILN olivines would otherwise not have formed.

5.4 Conclusion

It is clear that the ring dyke magma had a complex early history. Olivine compositions provide good evidence that this magma probably resided in a deap seated, convecting and laterally extensive magma chamber which was zoned with respect to temperature. A few large olivine phenocrysts crystallised in the different temperature regimes in this chamber from a primitive, unevolved liquid.

At some stage the chamber ruptured and the contained magma started to ascend to the surface while olivine continued to crystallise, but at an accelerated rate due to supercooling of the magma. Rapid olivine crystallisation presumably led to the precipitation and incorporation of small chromites in the crystallising olivines. Calcium contents of these olivines indicate that there was probably not a hiatus in olivine crystallisation after rupture of the deep seated magma chamber. During this stage the magma incorporated a small volume of a more evolved magma with lower Fe/Mg ratio and lower nickel content.

The ascending magma disrupted an olivine-bearing cumulate layer which resided somewhere between the base of the crust and the surface. This layer formed by the fractionation of a basaltic magma which could have been associated with Karoo volcanism. The presence of olivine mantles with phenocryst compositions on these xenocrysts imply that olivine crystallisation in the melilitite magma occurred up to crustal levels.

The final stage of olivine crystallisation and the earliest stage of magnetite precipitation might have overlapped. This, in combination with late stage diffusional processes influenced the rim compositions of all the olivines at Sutherland Commonage.

6 SPINEL MINERAL CHEMISTRY

6.1 Introduction

Spinel compositions have been subjected to detailed examination since they are potentially an important tool in petrogenetic studies as pointed out by Irvine (1967). In view of the extensive substitution of Cr, Al, Fe^{2+}, Fe^{3+} and Mg in various structural sites, spinels proves to be as informative about the earliest stages of crystallisation in basic and ultrabasic igneous rocks as pyroxenes are in the middle and late stages (Sigurdsson and Schilling, 1976; Ridley, 1977; Boctor and Meyer, 1979; Fisk and Bence, 1980; Pasteris, 1980; Sack, 1982; Thy, 1983; Jones and Wyllie, 1985; Tompkins and Haggerty, 1985). Spinel compositions are a complex function of the original bulk magma composition, general fractionation trends (controlled by pressure, temperature and fO_2) which in turn affect melt chemistry, types and abundances of coprecipitating phases, the degree of resorption of early crystallising spinels and equilibration between the core and mantle of chromite-magnetite clusters.

Petrographic examination indicates that the Commonage melilitites contain four textural varieties of spinel:

1) Large (0.1 to 0.2mm in size), often anhedral orange-red translucent chromites.
2) Subhedral to euhedral opaque groundmass chromites which average approximately 0.05mm in size.
3) Groundmass magnetites which occur as discrete, euhedral grains and as overgrowths on chromites.
4) Anhedral magnetite macrocrysts up to 1cm in size.

These grains are intimately intergrown with olivine xenocrysts (see chapter 5) and are therefore considered to be unrelated to the melilitite magma.

6.2 Compositions

Typical analyses of Commonage spinels are given in table 6.1 and the complete set of analyses are lodged in appendix 6. Ferric iron was calculated by the method of Finger (1972). The major element compositional variation is illustrated using the reduced spinel prism (Haggerty, 1973) in figure 6.1(a-d) and figure 6.2. This graphical means of depicting spinel compositional variation (Johnston prism) was used by Irvine (1965) to study the value of chrome spinel as a petrogenetic indicator. Haggerty's (1972) study of lunar spinels required modification of the Johnston prism to take into account the highly reducing conditions under which lunar spinels formed. The Fe^{3+}-bearing spinels, $MgFe_2O_4$ (magnesioferrite) and Fe_3O_4 (magnetite) placed at the oxidised prism apex were replaced by Mg_2TiO_4 (magnesian ulvöspinel) and Fe_2TiO_4 (ulvöspinel). Utilisation of the reduced spinel prism does not illustrate possible variations in the $MgFe_2O_4$ and Fe_3O_4 contents of spinels, however, all elements analysed are plotted. Spinel compositions were plotted by the method of Pasteris (1980).

The spinel prism is based upon the extensive solid solution between spinel end-members. The base of the prism is defined by solid solutions involving $FeCr_2O_4$ (chromite), $MgCr_2O_4$ (picrochromite), $FeAl_2O_4$ (hercynite) and $MgAl_2O_4$ (spinel). Chemical variation is defined by changes in the Cr/(Cr+Al) and Fe/(Fe+Mg) ratios (total iron calculated as Fe^{2+}). The apices

Table 6.1 Typical electron microprobe analyses of spinels, wt%

Oxide	Mg-Al chromite		Ti-Mg chromite			Titanomagnetite			Mag-macrocrysts
	1	2	3	4	5	6	7	8	9
SiO_2	0.00	0.00	0.06	0.00	0.00	0.24	0.03	0.00	0.00
TiO_2	1.56	1.89	3.11	2.98	3.70	22.21	16.95	9.00	5.41
Al_2O_3	37.23	26.38	19.62	22.47	21.56	1.06	0.94	1.52	0.53
Cr_2O_3	23.39	33.15	35.63	32.46	29.36	0.09	0.47	2.40	0.00
FeO	11.24	13.08	14.87	14.43	16.85	47.84	38.35	31.16	34.08
Fe_2O_3	6.88	8.26	11.25	11.04	13.01	24.92	36.08	49.26	58.32
MnO	0.21	0.17	0.16	0.39	0.34	1.02	1.20	0.85	0.37
MgO	17.77	15.78	14.69	14.92	13.56	1.81	4.44	4.70	1.06
CaO	0.06	0.00	0.20	0.07	0.17	0.33	0.15	0.12	0.00
	98.34	98.71	99.60	98.77	98.55	99.52	98.62	99.02	99.76

Figure 6.1 Sutherland spinel compositions plotted in the reduced spinel prism

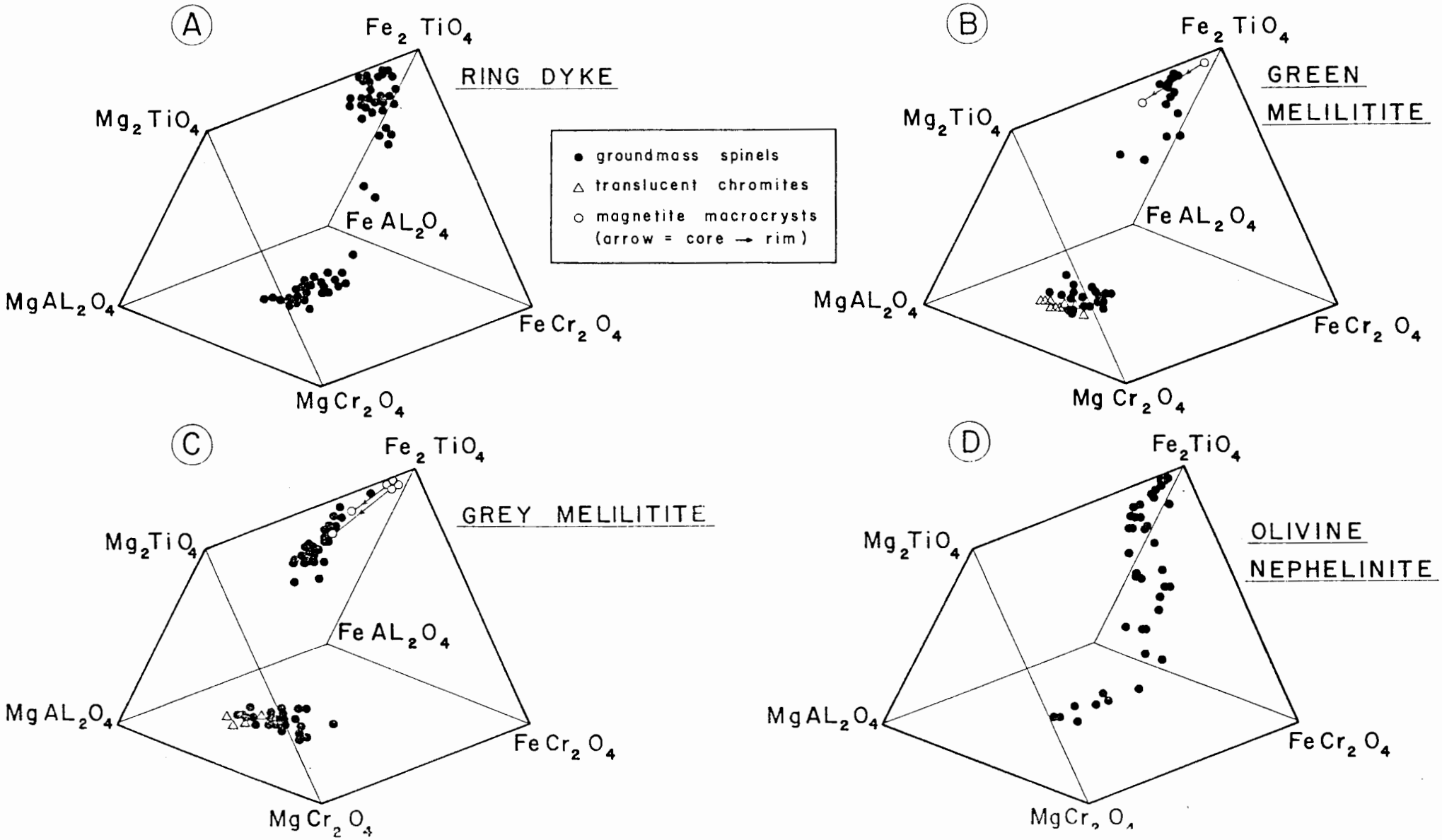

Figure 6.2 Compositional space within the reduced spinel prism occupied by the Sutherland spinels

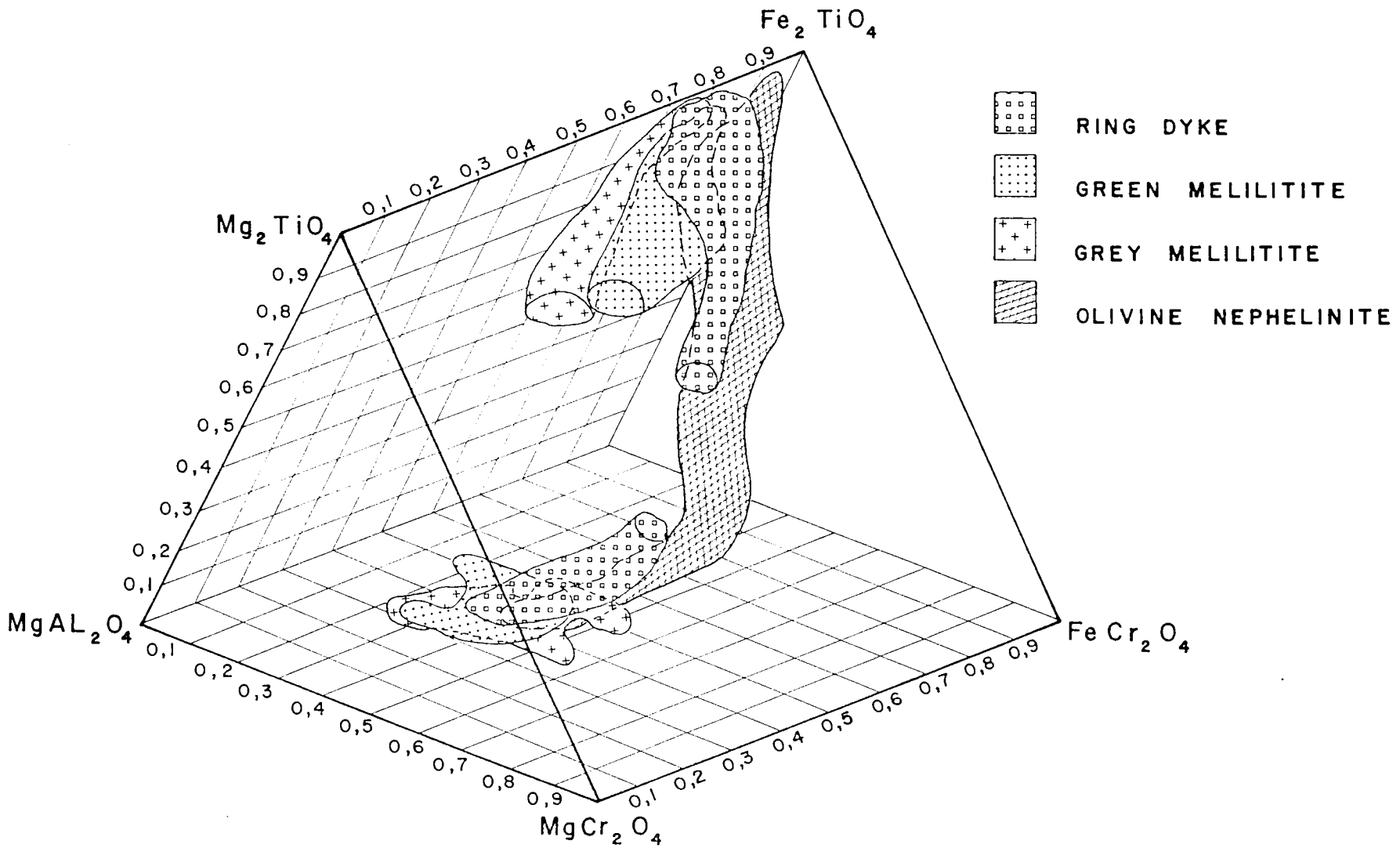

of the prism are defined by solid solutions between Mg_2TiO_4 (magnesian ulvöspinel) and Fe_2TiO_4 (ulvöspinel). Chemical variation between the two endmembers is defined by changes in the Fe/(Fe+Mg) ratio. Geochemical variation between the base and apex of the prism is defined by changes in the Ti/(Ti+Al+Cr) ratio. For an accurate representation of molecular proportions of spinel end-member molecules this ratio should be calculated as 2Ti/(2Ti+Al+Cr) (Mitchell, 1986).

Spinels from the Commonage vary in chemistry from aluminous magnesian chromites to titanian magnesian chromites to titanomagnetites. The macrocrystic translucent orange-red chromites are best described (in terms of their chemistry) as aluminous magnesian chromites. They typically contain less than 2 wt% TiO_2 (table 6.1) and exhibit a wide range in Cr/(Cr+Al) ratios (0.25-0.5) but a restricted range in Fe/(Fe+Mg) ratio's (0.25-0.35). Individual grains are typically homogenous.

Groundmass spinels display a normal magmatic trend consisting of chrome-rich cores and titanomagnetite rims. The spinels evolve from Cr_2O_3-rich, TiO_2-poor compositions to Cr_2O_3 poor, TiO_2-rich compositions with a corresponding increase in total iron, the Fe^{3+}/Fe^{2+} ratio (due to increasing fO_2) and a sharp decrease in magnesium and aluminium contents (table 6.1 and figure 6.1). There is usually a marked break in chemistry between groundmass chromites and groundmass titanomagnetites. This feature is most pronounced in the melilitites of the sill complex (figures 6.1b and 6.1c) but is

absent in the olivine nephelinite (figure 6.1d).

Magnetite macrocrysts are depleted in MgO and TiO_2 relative to groundmass titanomagnetites (table 6.1).They are in many cases also overgrown by groundmass titanomagnetite (figure 6.1b and c).

Aluminous magnesian chromites are found only in the green and grey melilitites of the sill complex. Titanian magnesian chromites are present in all the intrusions. Those in the ring dyke and the olivine nephelinite show a restricted range in Cr/(Cr+Al) ratios and trend towards higher Fe/(Fe+Mg) ratios than grains from the sill complex melilitites (figure 6.2). The latter chromites are enriched in MgO, Cr_2O_3 and Al_2O_3 but are depleted in TiO_2 relative to those from the ring dyke and the olivine nephelinite (figures 6.3 and 6.4).

Groundmass titanomagnetites from the various intrusions exhibit compositions which plot as distinct fields with a minimum amount of overlap in the reduced spinel prism (figure 6.2). Titanomagnetites from the sill complex melilitites have lower Fe/(Fe+Mg) ratio's and are depleted in TiO_2 and Fe^{2+} (as opposed to Fe^{3+}) compared to grains from the ring dyke and the olivine nephelinite (figures 6.5 and 6.6).

6.3 Spinel in heavy mineral concentrate

Three 5kg samples from the ring dyke, the green melilitite and the grey melilitite were partly digested in acid and separated in bromoform by assistants to O. Garvie of the Anglo American Research Laboratories (AARL). The resultant heavy

Figure 6.3 Plot of Wt % MgO versus Wt % TiO_2 for Sutherland chromites

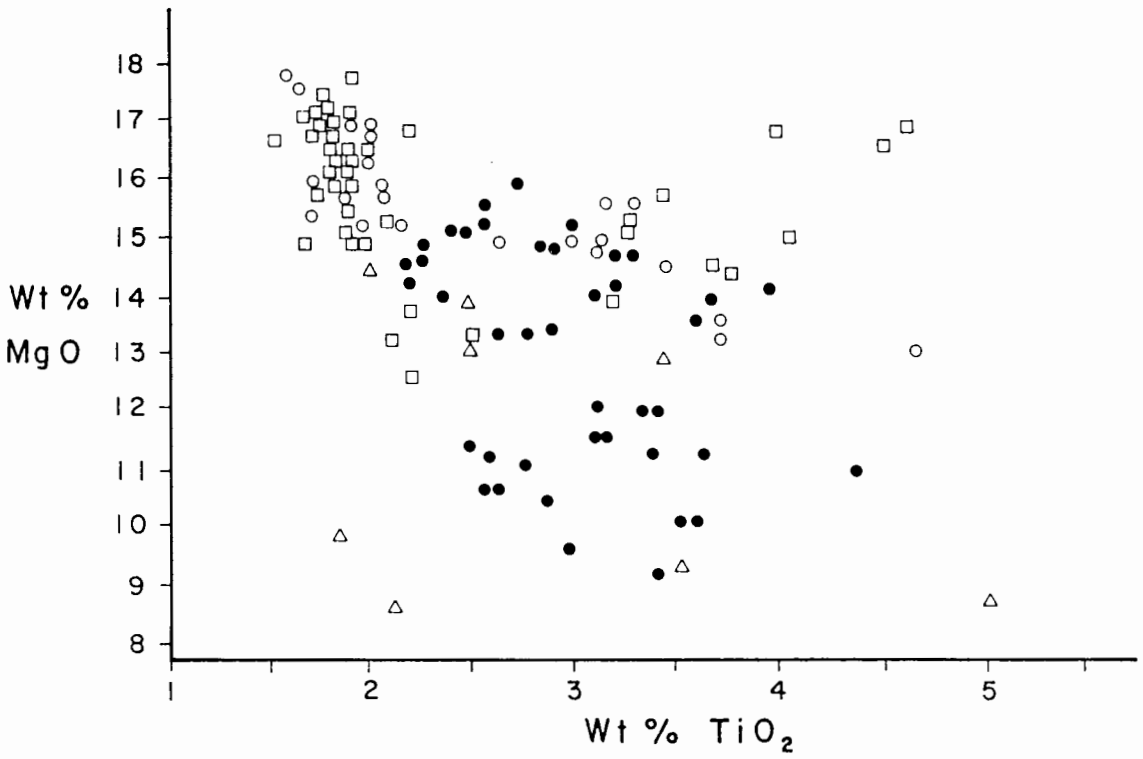

Figure 6.4 Plot of Wt % Cr_2O_3 versus Wt % AL_2O_3 for Sutherland chromites

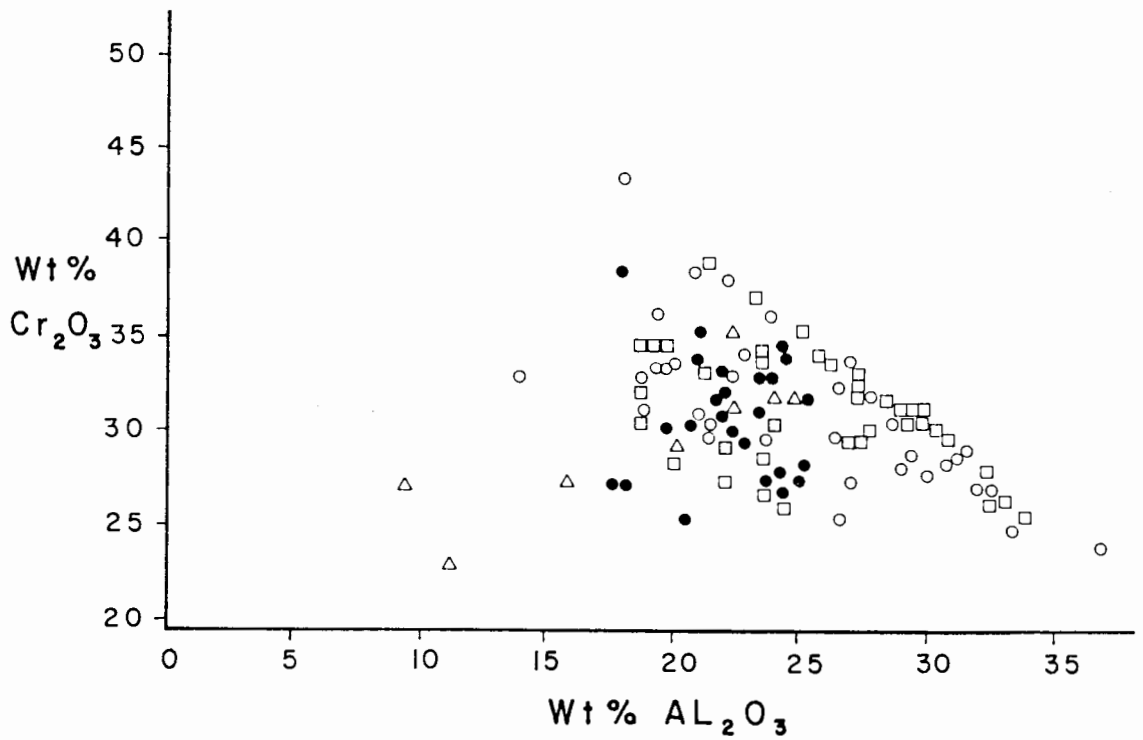

Symbols as in figure 6.3

Figure 6.5 Plot of Wt % FeO (total) versus Wt % TiO_2 for Sutherland magnetites

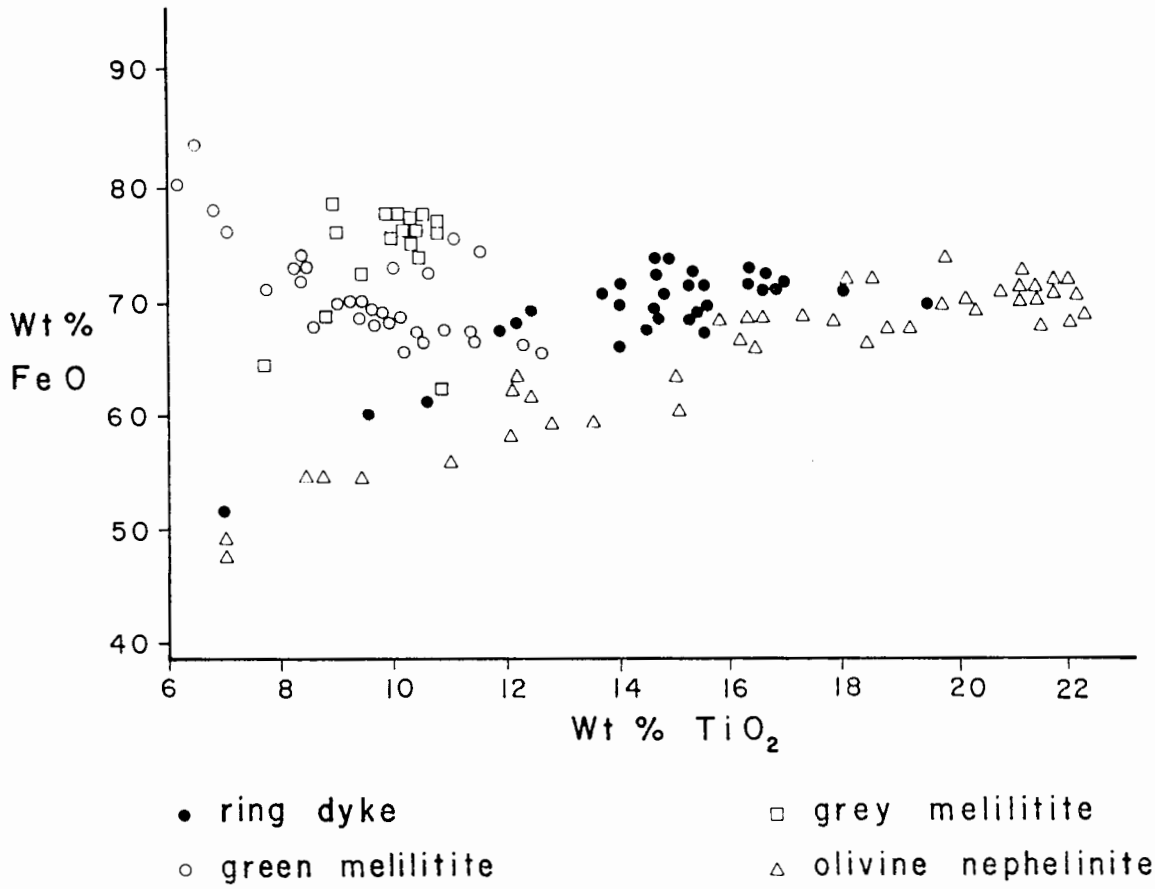

Figure 6.6 Plot of Fe^{2+}/Fe^{3+} versus $Fe^{2+}/Fe^{2+} + Mg$ (molar ratios) for Sutherland magnetites

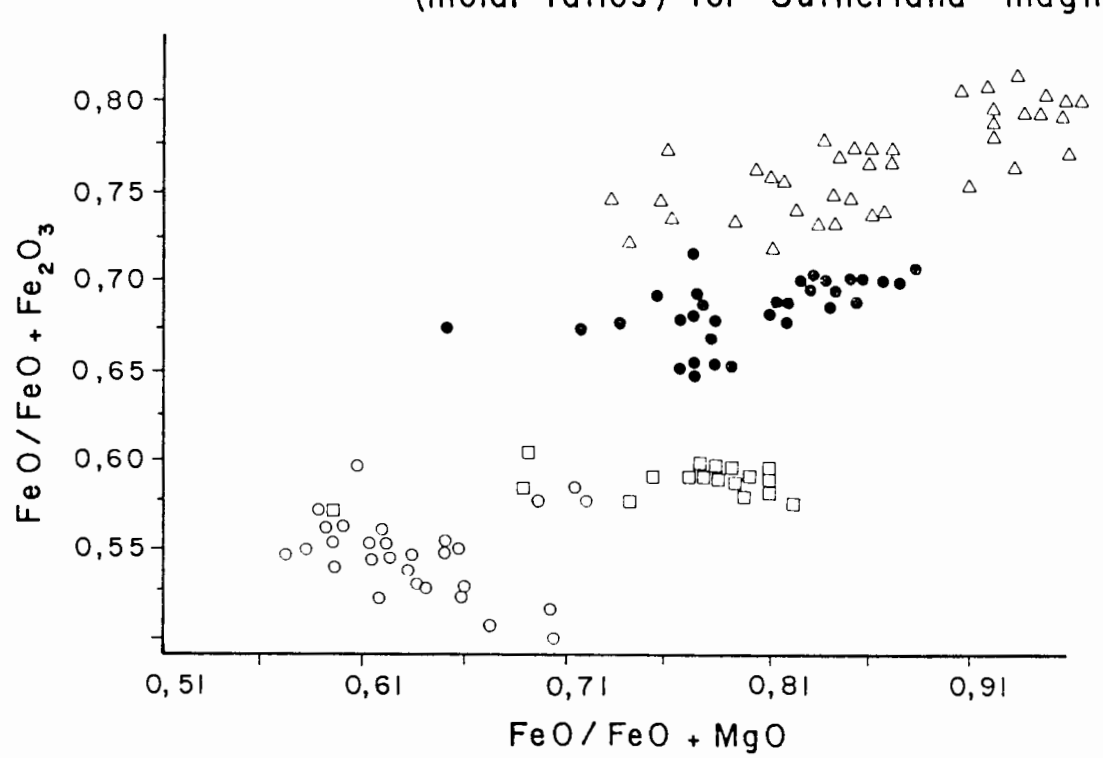

Symbols as in figure 6.5

mineral concentrate were sieved into different size fractions. Spinels were then picked from the concentrate by staff at AARL and analysed on a JEOL microprobe. Close examination of these analyses show that the compositions of the concentrate chromites are identical to the chromites analysed by the present author. Since the concentrate chromites do not contribute to a clearer picture of spinel compositions (i.e they do not define any new compositional fields and show total overlap with the presently defined spectrum of chromite compositions) it was decided to exclude these analyses from the present study-primarily to prevent undue clutter on the diagrams.

6.4 Dicussion and conclusion

The iron-rich nature of the magnetite macrocrysts coupled with the unusual compositions of the olivines with which they are intergrown (see chapter 5) strongly suggests that these grains are of xenocrystic derivation.

The composition of chromian spinel might be sensitive to pressure (Irvine, 1967; Sigurdsson and Schilling, 1976; Haggerty, 1976; Fisk and Bence, 1980; Thy, 1983). In particular, the Al-Cr substitution might be pressure controlled (Sigurdsson and Schilling, 1976; Fisk and Bence, 1980) but no clear experimental support is available. However, the effect of high pressure can be expected to increase octahedral sites in the melt and consequently to decrease Cr-contents in the spinel structure (Thy, 1983). This implies that the Cr/(Cr+Al) ratio of liquidus spinels vary inversely with pressure (Sigurdsson and Schilling, 1976;

Thy, 1983) and that the aluminous magnesian chromites are early, high-pressure phenocrysts. An alternative model is that these grains are xenocrysts derived from disaggregated mantle material. For example, chromites in spinel lherzolite xenoliths from the Nanorluk intrusion at Somerset Island, Canada, have Cr/(Cr+Al) and Fe/(Fe+Mg) ratios of 0.20-0.53 and 0.23-0.66 respectively (Jago, 1982). Data for the Sutherland aluminous magnesian chromites fall well into this field and could for all intents and purposes be derived from a similar type of mantle material.

The compositions of groundmass chromites and magnetites strongly suggest that the green and grey melilitites represent less evolved magmas than the ring dyke and the olivine nephelinite. Pasteris (1980) believes that increasing Fe/(Fe+Mg) ratios in the spinel suites present in various sequential intrusions in the De Beers kimberlite pipe reflect increasing degrees of differentiation of a single batch of parent magma from which the various De Beers kimberlites are sequentially derived. If so, then the Commonage groundmass spinels indicate that the green and grey melilitites represent an early magma pulse from the source region and the ring dyke a later pulse. Considering the location of the nephelinite at the top of the sill complex the highly evolved nature of the spinels in the olivine nephelinite might indicate that this intrusion could have formed by the continued differentiation of one of the sill complex magmas.

The progressive decrease in oxygen fugacity from the green melilitite to the olivine nephelinite as defined by the

$FeO/(FeO+Fe_2O_3)$ ratio (figure 6.6) is a puzzling feature of the Sutherland melilitite intrusives. It is considered that the sill complex melilitites might have been gas-charged intrusives which originally contained higher concentrations of CO_2 than the ring dyke or the nephelinite since they were the first magmas to be derived from the source region. Thus the increased fO_2 in the sill complex melilitites could have been caused by the degassing (after intrusion) of large volumes of CO_2. Mathez (1984) proposed that the degassing reaction

$$CO_3^{=}{}_{(m)} = CO_{(v)} + O^{=}_{(m)} + 1/2O_{2(m)}$$

results in a drastic increase in the oxygen content of the magma. This consequently leads to elevated oxygen fugacity in the melt and an increase in the Fe^{3+}-content of crystallising spinels.

Early release of the sill complex melilitites from the source region depleted later magma pulses (such as the ring dyke) in CO_2. Lower CO_2-content led to the production of lower oxygen concentrations upon degassing, hence the lower fO_2 during magnetite crystallisation in the ring dyke.

7 GEOCHEMISTRY

7.1 Introduction

Moore (1979), Duncan (et al., 1978) and McIver and Ferguson (1979) presented whole-rock analyses of the Commonage melilitites. In all cases details of sample localities and complementary petrography are not given and it was therefore decided to analyse a variety of well-characterised specimens from the various intrusions for major and trace elements.

Eleven whole-rock analyses have been made using X-ray fluorescence techniques. Details of analytical procedures are given in appendix 2 and the analyses are listed in table 7.1. $^{87}Sr/^{86}Sr$ isotope ratios were determined for seven samples, as no previous analyses of this type had been performed in the past. The results are given in table 7.2. The green melilitite was not selected for isotopic analysis because this intrusive type shows evidence of extensive deuteric alteration (see chapter 2).

7.2 Chemistry

7.2.1 Major and trace element variations

Standard variation diagrams for the Commonage melilitites, in which major and trace elements are plotted against MgO, are shown in figures 7.1 and 7.2.

The rocks are strongly undersaturated and show a range of approximately 5% MgO. In general the grey melilitite is enriched in MgO, Fe_2O_3, MnO, CaO and P_2O_5 compared to the rest

Table 7.1(a) Major element compositions of the Commonage melilitites

SAMPLE	256	257	258	259	260	261	262	263	265	266	267
SiO_2	36.40	34.96	34.67	35.49	34.85	33.89	33.45	33.07	32.19	31.55	41.21
TiO_2	3.47	3.36	3.60	3.68	3.44	3.21	3.21	3.16	3.00	2.98	2.35
Al_2O_3	7.84	7.12	7.95	8.15	6.78	7.25	7.18	7.24	6.94	6.93	10.33
Fe_2O_3	12.83	12.49	12.70	13.03	12.78	11.42	12.13	12.08	13.68	13.81	9.91
MnO	0.21	0.22	0.25	0.21	0.23	0.21	0.23	0.22	0.27	0.31	0.15
MgO	18.39	18.20	15.30	16.17	18.55	18.88	18.98	18.31	19.54	19.17	14.99
CaO	14.85	14.84	15.43	15.81	15.64	13.69	14.03	15.34	17.18	18.15	12.16
Na_2O	3.30	0.86	1.96	3.35	1.30	0.80	0.68	0.65	2.80	3.11	4.55
K_2O	1.93	1.63	1.57	2.30	1.02	2.32	2.53	2.19	1.31	1.31	0.22
P_2O_5	0.92	0.91	1.03	1.03	0.80	0.92	1.15	1.32	1.42	1.78	0.58
H_2O^-	0.07	0.48	0.63	0.13	0.42	0.61	0.45	0.38	0.14	0.12	0.32
LOI	0.21	4.48	4.92	0.76	4.14	6.60	5.23	5.35	1.53	0.87	4.57
Total	100.42	99.55	100.01	100.13	99.96	99.80	99.24	99.32	100.02	100.09	101.33

Total iron as Fe_2O_3.

256 Ring dyke (chill)
257 Ring dyke (highly vesicular)
258 "
259 Ring dyke (chill)
260 Ring dyke (vesicular)
261 Sill complex (green melilitite)
262 Sill complex (green melilitite)
263 Sill complex (green melilitite)
265 Sill complex (grey melilitite)
266 Sill complex (grey melilitite)
267 Sill complex (olivine nephelinite)

Table 7.1(b) Trace element compositions of the Commonage melilitites

SAMPLE	256	257	258	259	260	261	262	263	265	266	267
Ba	1110	994	1040	823	782	1170	1220	1550	969	850	472
Sc	30	26	25	30	22	27	29	31	28	28	21
La	58	53	61	64	61	54	62	61	108	130	47
Ce	108	95	108	118	109	94	104	104	181	227	104
Nd	54	49	53	56	54	46	52	48	84	106	51
Co	81	79	73	74	84	80	82	78	79	74	65
Cr	831	776	689	766	898	853	882	792	841	837	626
V	273	254	265	269	228	195	248	304	182	182	176
Nb	126	118	130	136	120	132	138	139	184	209	69
Zr	304	257	289	247	219	232	250	306	269	311	237
Y	26	24	28	27	23	22	24	24	32	36	25
Sr	1176	1350	1006	1240	1308	571	841	1784	1599	1744	361
Rb	60	69	60	65	45	67	74	79	41	37	15
Th	12	13	13	13	14	11	12	15	25	26	9

*** All values in ppm ***

Table 7.2 Strontium isotope composition of samples from Sutherland Commonage

NUMBER	DESCRIPTION	Rb(ppm)	Sr(ppm)	$^{87}Rb/^{86}Sr$	$^{87}Sr/^{86}Sr_{(meas)}$	$^{87}Sr/^{86}Sr_{(init)}$
256	Ring dyke-chill	60	1176	0.1472	0.70489(4)	0.70473
258	Ring dyke-vesicular	60	1006	0.1735	0.70444(7)	0.70426
259	Ring dyke-chill	65	1240	0.1503	0.70351(7)	0.70335
260	Ring dyke-vesicular	45	1308	0.1003	0.70452(8)	0.70441
265	Sill complex-grey melilitite	41	1599	0.0741	0.70456(9)	0.70448
266	Sill complex-grey melilitite	37	1744	0.0621	0.70333(7)	0.70326
267	Sill complex-ol-nephelinite	15	361	0.1176	0.70485(8)	0.70472

numbers in parentheses - 2 sigma uncertainty

Figure 7.1 Major oxide (wt %) variation diagrams

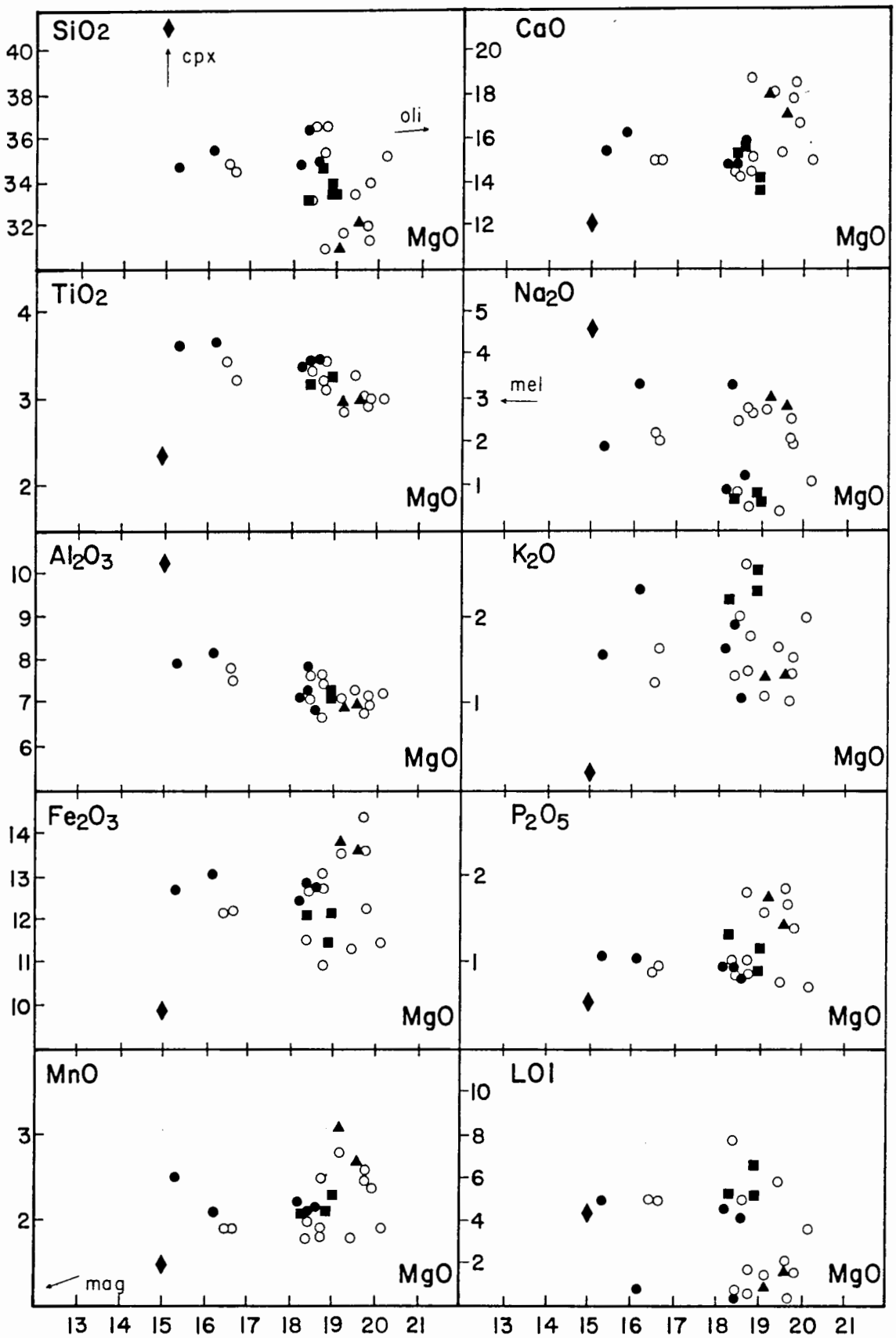

Figure 7.2 Trace element variation in the Commonage melilitites with MgO (wt %) as the abscissa

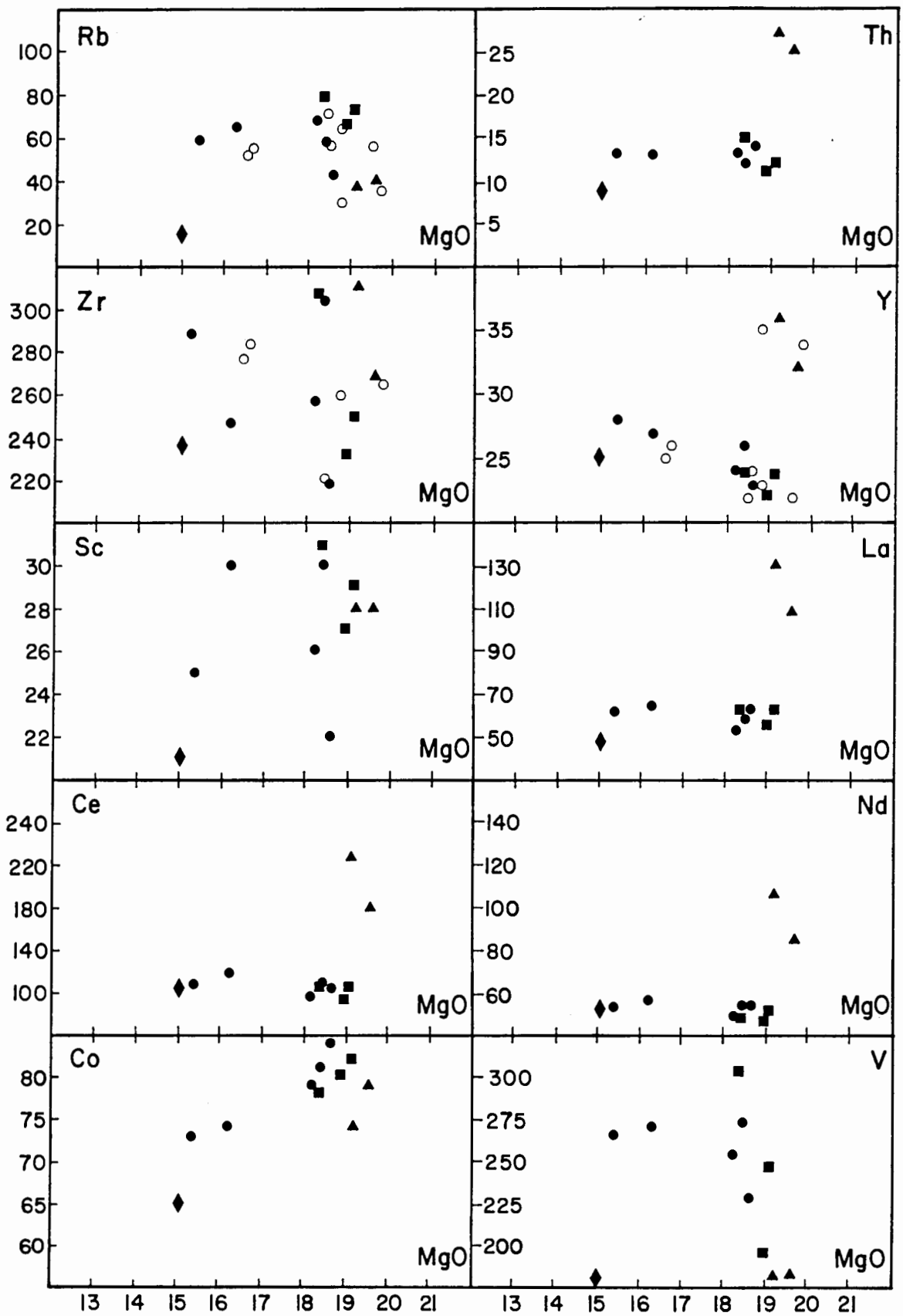

Figure 7.2 (continued)

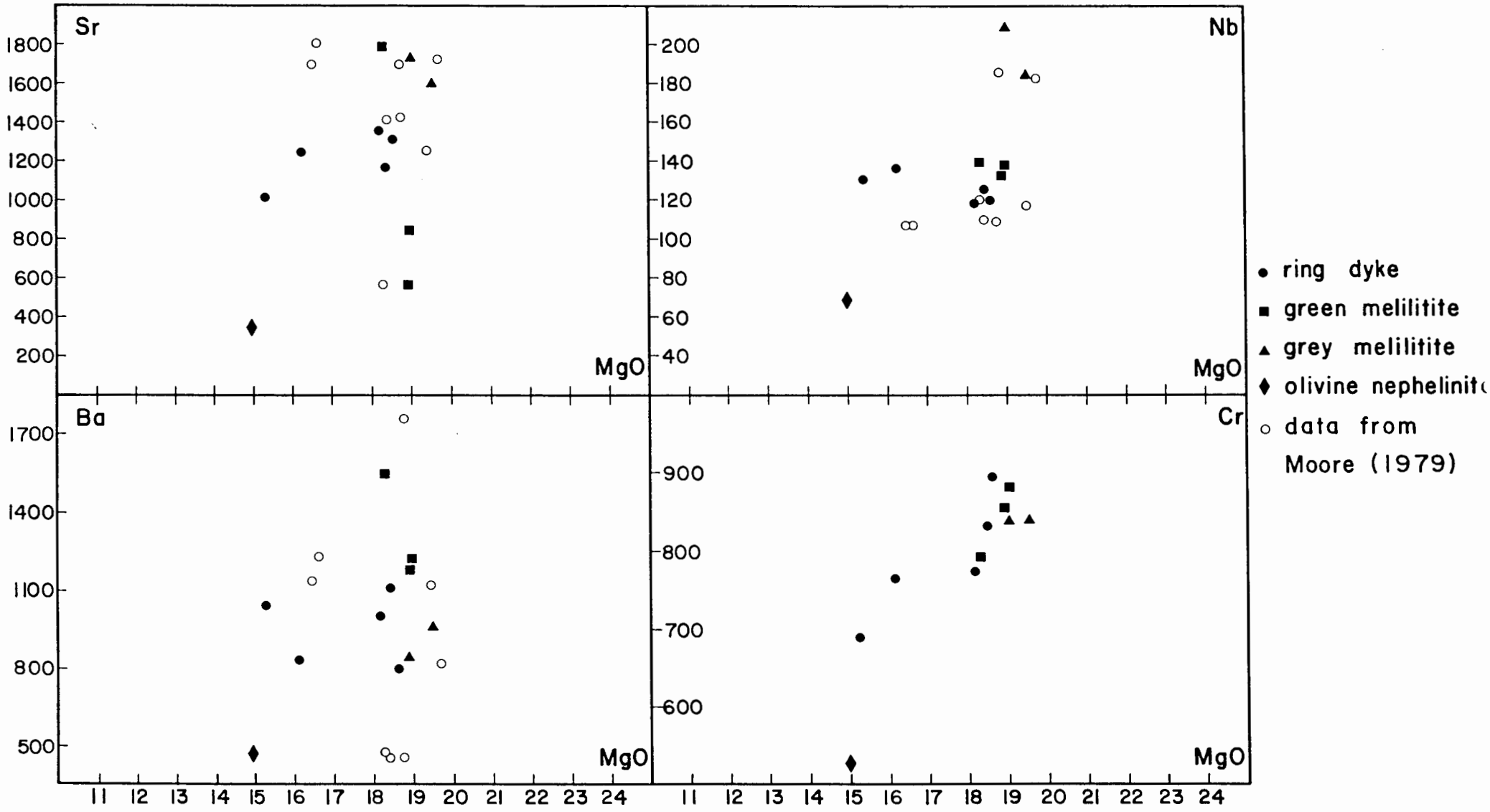

of the intrusions, while the olivine nephelinite is enriched in SiO_2, Al_2O_3 and Na_2O. The trace element variation diagrams indicate that the grey melilitite has elevated levels of Ce, Th, Y, La and Nb while the olivine nephelinite is depleted in virtually all the trace elements analysed for in this study. Analyses of rock samples from the ring dyke and the green melilitite occupy an intermediate position between these two extremes for both major and trace elements.

7.2.2 Strontium isotopes

Strontium isotope compositions of the individual samples are plotted on an isochron diagram in figure 7.3. Most of the samples plot in the vicinity of a 74.9 Ma reference line which was calculated from the K-Ar age data of Duncan (et al., 1978).

The relatively wide scatter displayed by the samples when plotted in figure 7.3 could be ascribed to contamination by assimilated crustal material. However, when the samples are plotted on a mixing diagram (Cox et al., 1979) they do not show any clear linear trend which can be easily explained by a mixing model (figure 7.4). A more likely scenario is that circulating meteoric water leached Rb (and possibly also Sr) from the rock shortly after intrusion and therefore caused a change in the resultant $^{87}Sr/^{86}Sr$ ratio with time. Barrett and Berg (1973) considered that groundwater contamination may best account for variable $^{87}Sr/^{86}Sr$ initial ratio's in kimberlites.

7.2.3 Discussion

Figure 7.3 Strontium isotope ratio plot for the Commonage melilitites

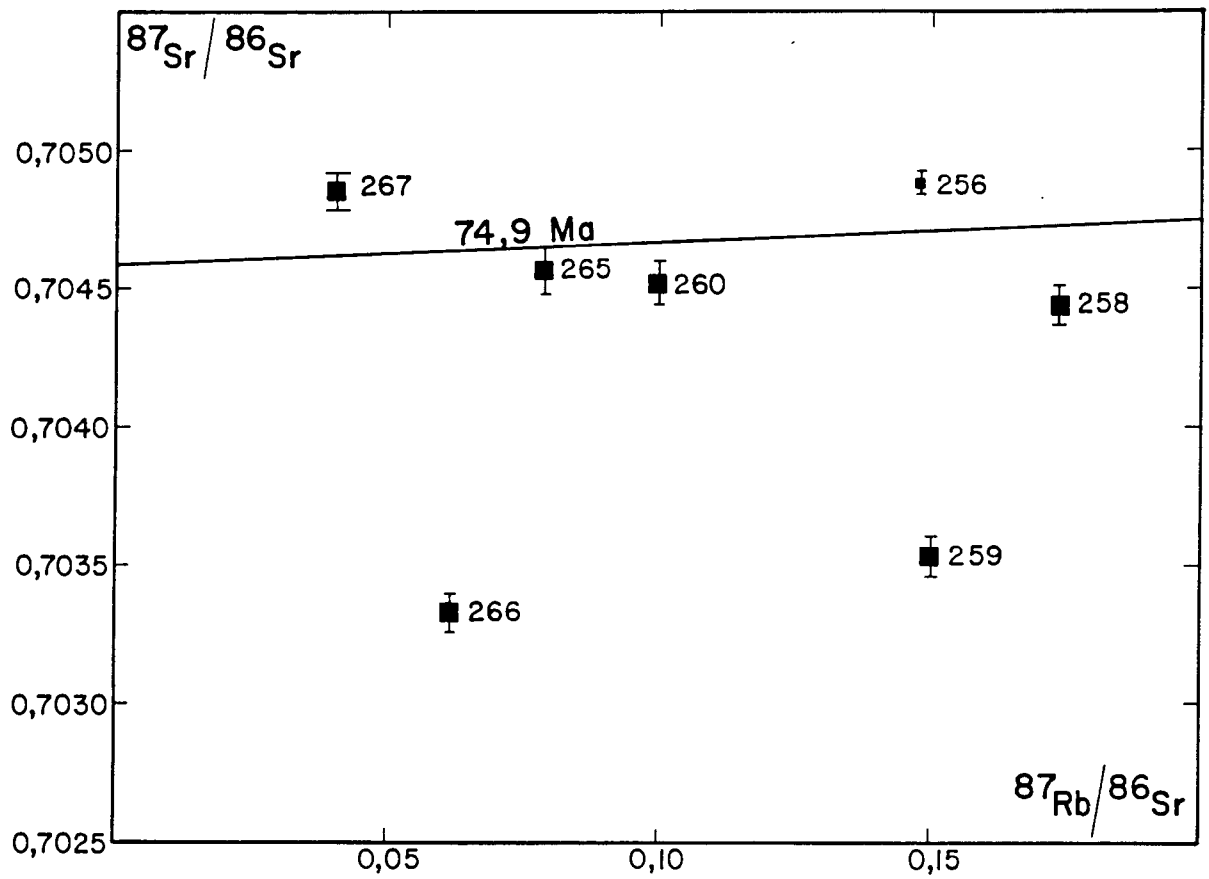

Figure 7.4 Plot of $^{87}Sr/^{86}Sr$ versus Sr content for the Commonage melilitites

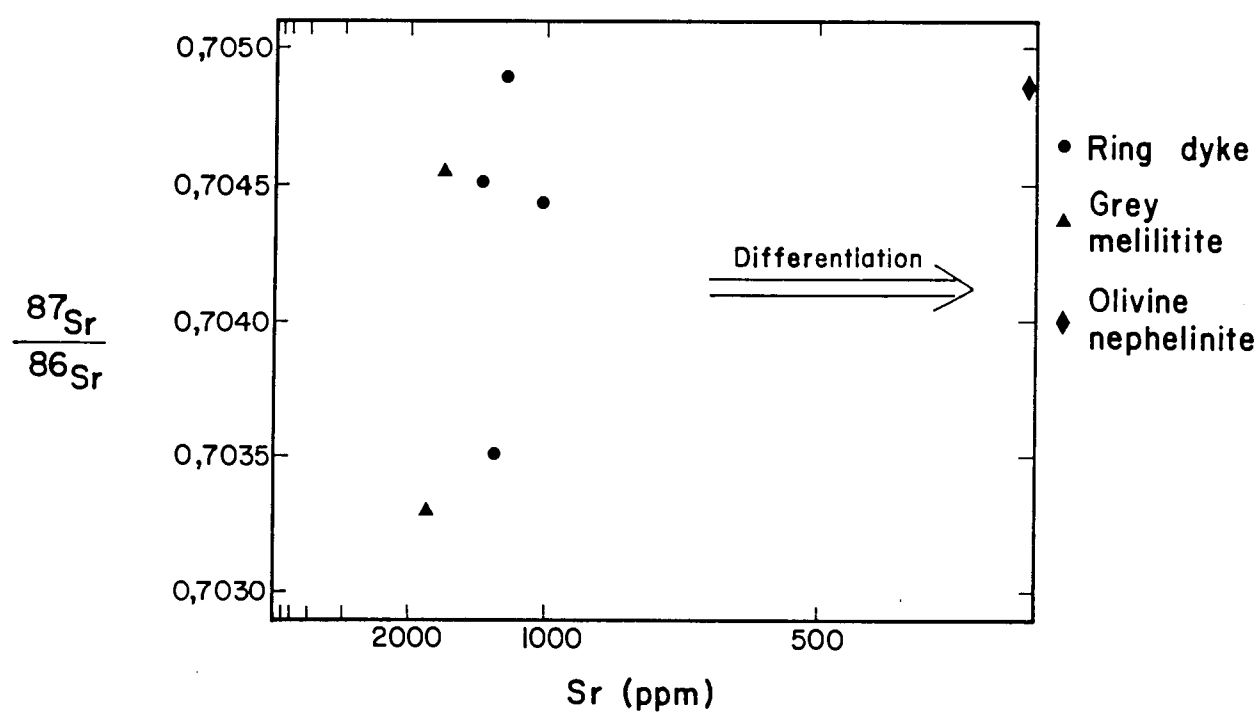

Inspection of figure 7.1 indicates that some of the variation in major element composition within the suite can be explained by the modal variation in olivine, clinopyroxene and magnetite content. However, it is clear that distinct chemical differences exist between the grey melilitite as well as the olivine nephelinite and the rest of the intrusives and that these differences cannot be attributed simply to accumulation or removal of various mineral types.

The unique chemical character of the grey melilitite is clearly apparent in terms of relative abundances of incompatible trace elements and is reflected in the geochemical patterns (figure 7.5). The chemical differences between the grey melilitite and the rest of the intrusives (excepting the olivine nephelinite) could indicate that (i) a parent magma common to all the intrusives evolved by high-pressure fractionation to produce different intrusive pulses of varying composition or (ii) the various rock types are related by varying degrees of melting of the same source region. The higher incompatible trace element content of the grey melilitite suggests that it is more differentiated than the rest of the intrusives. This, however, is at odds with the major elements which show that the grey melilitite is the most primitive rock type. It is therefore likely that the grey melilitite is related to the other rock types by a lower degree of melting of the same source region. Clinopyroxene is the dominant host for CaO in a plagioclase-free peridotite; consequently, the enrichment of CaO in the grey melilitite magma must be from clinopyroxene. In addition, the low SiO_2 content of this melt requires that garnet and olivine

preferentially contribute to the melt, and that residual orthopyroxene increases as clinopyroxene melts incongruently (Clague and Frey, 1982). The higher Al_2O_3 content and Al_2O_3/CaO ratio of the other melilitites (on average 0.50 as opposed to 0.39 in the grey) suggests that an increased degree of melting in the source region led to a higher concentration of the garnet component in the melt(s) which intruded to form the green melilitite and the ring dyke respectively.

The olivine nephelinite on the other hand, shows a variety of chemical features which is characteristic of a highly evolved magma - the high SiO_2 and low MgO content as well as the differentiation trend in figure 7.4 being a particularly good indication of this. It is, however, also depleted in a variety of incompatible trace elements which would be expected to concentrate in an evolved liquid. Petrographic study (chapter 2) shows that phenocrystic and groundmass phases in the rock tend to occur in aggregates which are suspended in a matrix of nepheline. This emulsion texture is taken as evidence that the olivine nephelinite formed from a fairly crystalline rock (either the green or grey melilitite) which was disrupted and invaded by a residual liquid which could have formed by filter pressing due to the movement of the magma. This liquid must have been enriched in SiO_2, Al_2O_3 and Na_2O and would have "diluted" the chemistry of the original rock.

7.2.4 Comparative geochemistry

Geochemical patterns for the Commonage melilitites relative to the average of Namaqualand melilitites (Moore, 1979) have

been plotted in figure 7.6. Inspection of this diagram shows that there are notable differences between Sutherland and Namqualand melilitites. These differences are most apparant for TiO_2, Fe_2O_3, MgO and CaO.

Worldwide studies of melilite-rich ultramafic lamprophyres (Rock, 1986) have shown that they have comparatively low SiO_2 (average=32 wt%) and $FeO_{(t)}$ (m=14 wt%) contents and elevated CaO (m=16 wt%) and MgO (m=15 wt%) contents. The Sutherland Commonage rocks are therefore not all that different in major element composition to most other melilite-rich ultramafic rocks. Trace element data are too sparse and variable to warrant a detailed comparison. The Commonage rocks share the trace element characteristics of other melilitites, viz. combined high contents of both compatible and incompatible trace elements.

The strontium isotope chemistry of the Commonage melilitites is compatible with most other melilitites in that they all derive from an undepleted to slightly depleted mantle source (table 7.3 and figure 7.7).

7.3 A petrogenetic model

7.3.1 Magma chemistry

Problems relating to the petrogenesis of melilitic rock suites, and alkali volcanics in general are many since the abnormal abundances of elements such as Ti, K, Rb and Ba found in these rocks present problems with respect to mechanisms of trace element enrichment in either the primary mantle source

Figure 7.5 Trace element abundances normalised to estimated primitive mantle abundances (from Wood, 1979)

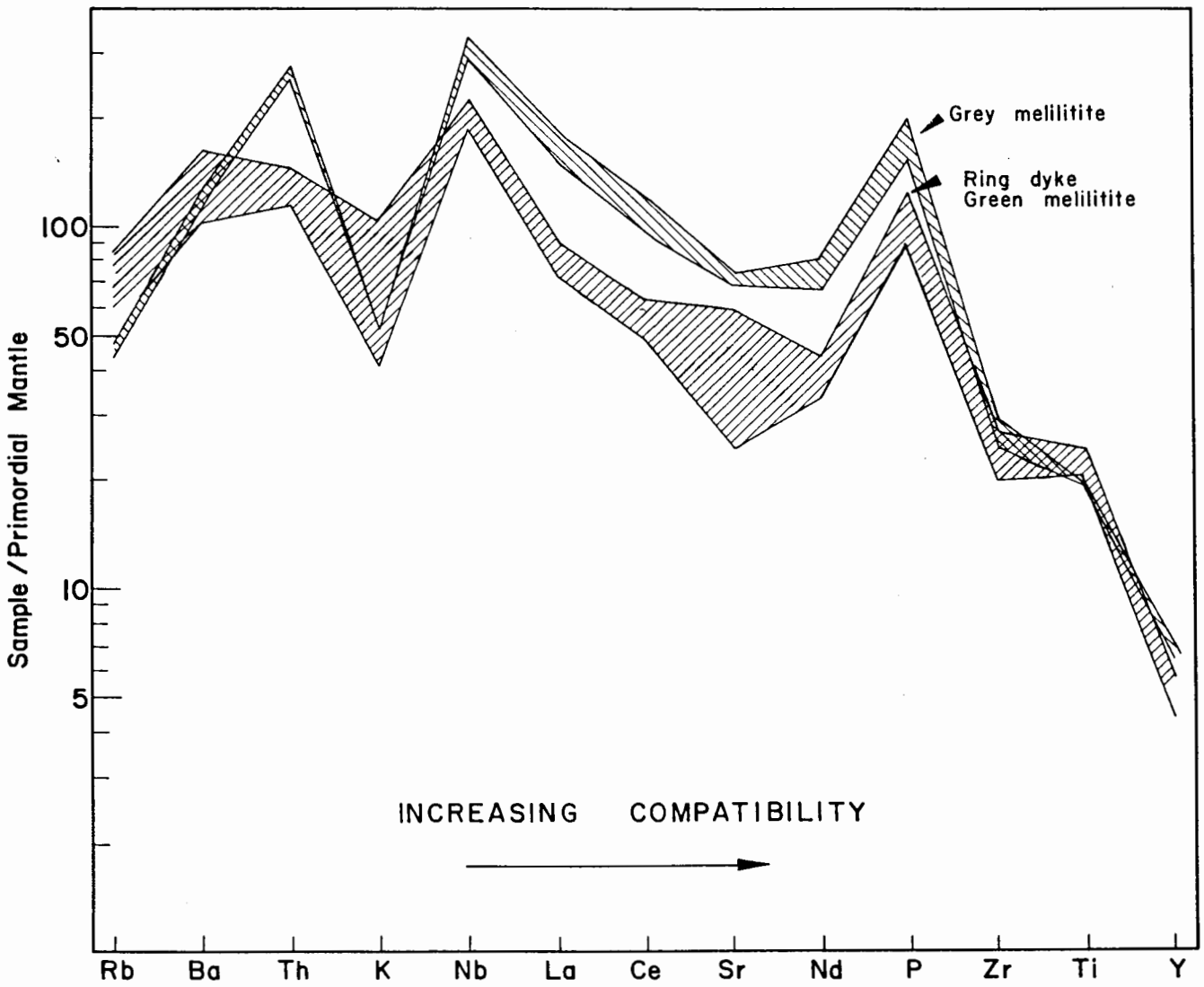

Figure 7.6 Major elements normalised to the average Namaqualand melilitite of Moore (1979)

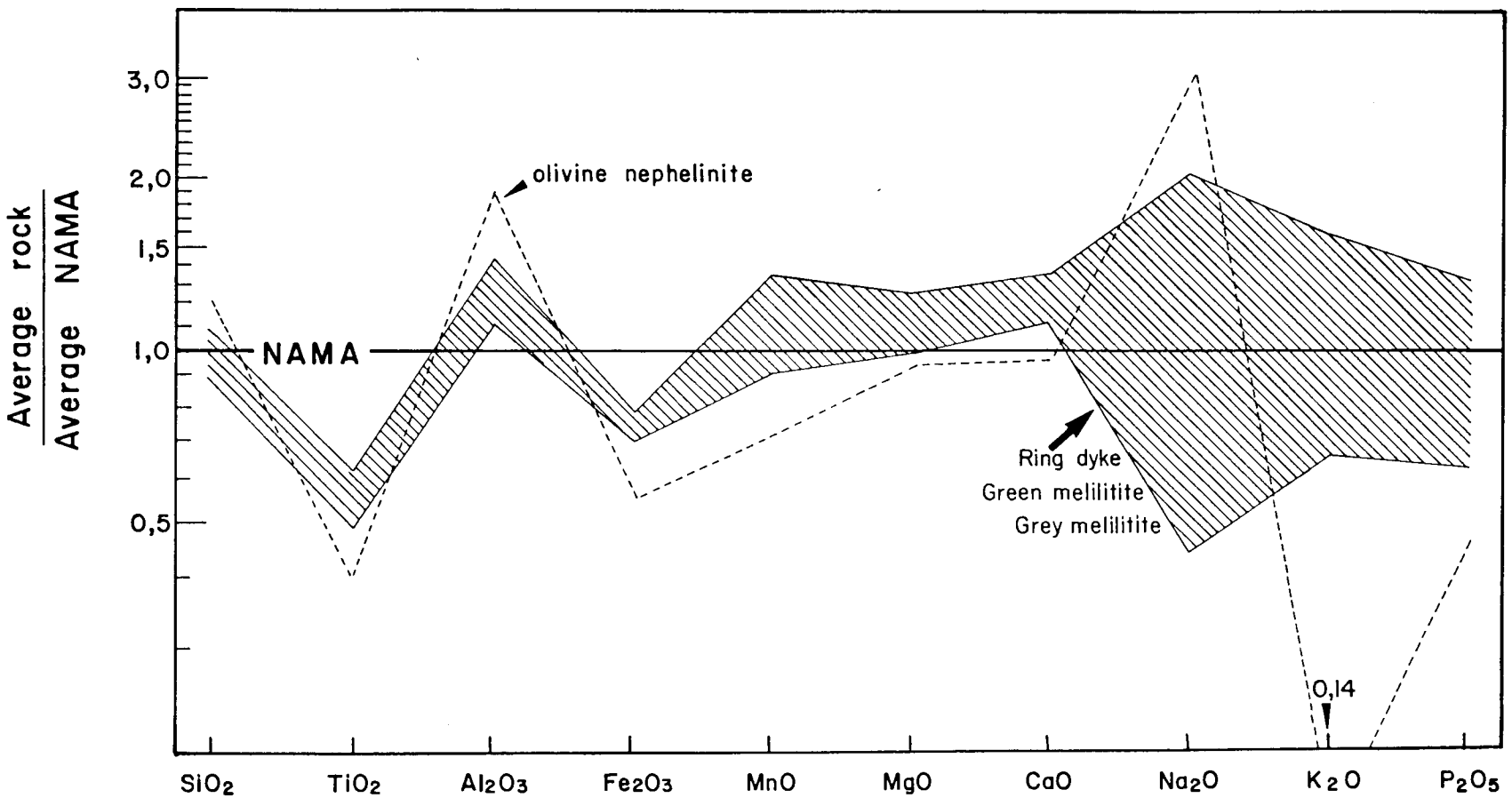

Table 7.3 Summary of selected strontium isotope data for melilitites and nephelinites

Locality	age/Ma, technique, reference	87Sr/86Sr initial ratio's	comments
1)Virunga volcanics, East Africa	0;----;(1)	0.70463-0.70475	nephelinites from Nyiragongo and Bushwaga
2)Kalihi, Hawaii	0.58;K-Ar;(2)	0.70338	nepheline-melilite basalt
3)Kahoehe Group, Hawaii	0.7;K-Ar;(2)	0.70332	"
4)West Eifel Group, West Germany	2;----;(3)	0.70413-0.70443	melilite nephelinites
5)Pyramid Rock, Hawaii	3.6;K-Ar;(2)	0.70327	melilite-nepheline basalt
6)Eifel 1 and 2, West Germany	5;K-Ar;(4)	0.70415-0.70433	melilitites
7)Polzen, West Germany	7;K-Ar;(4)	0.70378	melilitite
8)Hoher Berg, West Germany	9;K-Ar;(5)	0.70345	melilite-bearing olivine nephelinite
9)Westberg, West Germany	10;K-Ar;(5)	0.70354	"
10)Burgberg, East Germany	11;K-Ar;(5)	0.70343	"
11)Lützelberg, West Germany	14;K-Ar;(6)	0.70340	olivine-nephelinite
12)Bölle, West Germany	15;K-Ar;(6)	0.70385	olivine melilitite

Table 7.3 (Cont.)

Locality	age/Ma, technique, reference	87Sr/86Sr initial ratio's	comments
13)Niederhessische Senke, Urach and Hegau-West Germany	20;K-Ar;(3&4)	0.70354-0.70431	olivine melilitites (14 occurrences)
14)Götzenbrühl, West Germany	23;K-Ar;(6)	0.70362	olivine melilitite
15)Vosges, France	28;K-Ar;(4&6)	0.70342-0.70389	olivine nephelinites
16)Malaita, Solomon Islands	34;U-Pb;(7)	0.7045-0.70464	olivine melilitite
17)Klinghardt Mountains, Namibia	35;K-Ar;(8)	0.70406	olivine melilitite
18)Garies cluster, R.S.A.	40;----;(8)	0.70335	olivine melilitite, approximate age
19)Rozberg, West Germany	43;K-Ar;(6)	0.70359	olivine nephelinite
20)Messel, West Germany	49;K-Ar;(6)	0.70336	"
21)Forst, France	53;K-Ar;(6)	0.70391	"
22)Tannengrund, West Germany	60;K-Ar;(6)	0.70355	"
23)Gamoep Cluster, R.S.A.	60;----;(8)	0.70344-0.7039	olivine melilitite, approximate age
24)Uhlberg, West Germany	83;K-Ar;(6)	0.70393	olivine nephelinite

Table 7.3 (Cont.)

Locality	age/Ma, technique, reference	87Sr/86Sr initial ratio's	comments
25) Dyke, southern West Greenland	116;K-Ar;(9)	0.7056	olivine nephelinite
26) "	122;K-Ar;(9)	0.7049	"
27) "	138;K-Ar;(9)	0.70584	"
28) Alnö, Sweden	553;Rb-Sr;(10)	0.70281-0.70569	alnoite
29) Marathon dikes, Canada	1653;Rb-Sr;(11)	0.70167	melilite-bearing lamprophyre

References. 1, Volmer and Norry (1983);2, Lanphere and Dalrymple (1980);3, Wörner (et al., 1986); 4, Alibert and Albarede (1983);5, Mengel (et al., 1984);6, Calvez and Lippolt (1980); 7, Bielski-Zyskind (et al., 1984); 8, Moore (1979);9, Hansen (1981);10, Brueckner and Rex (1980);11, Platt (et al., 1983).

Figure 7.7 Variation of initial $^{87}Sr/^{86}Sr$ ratios with time for various melilitic and nephelinitic intrusives (see also table 7.3)

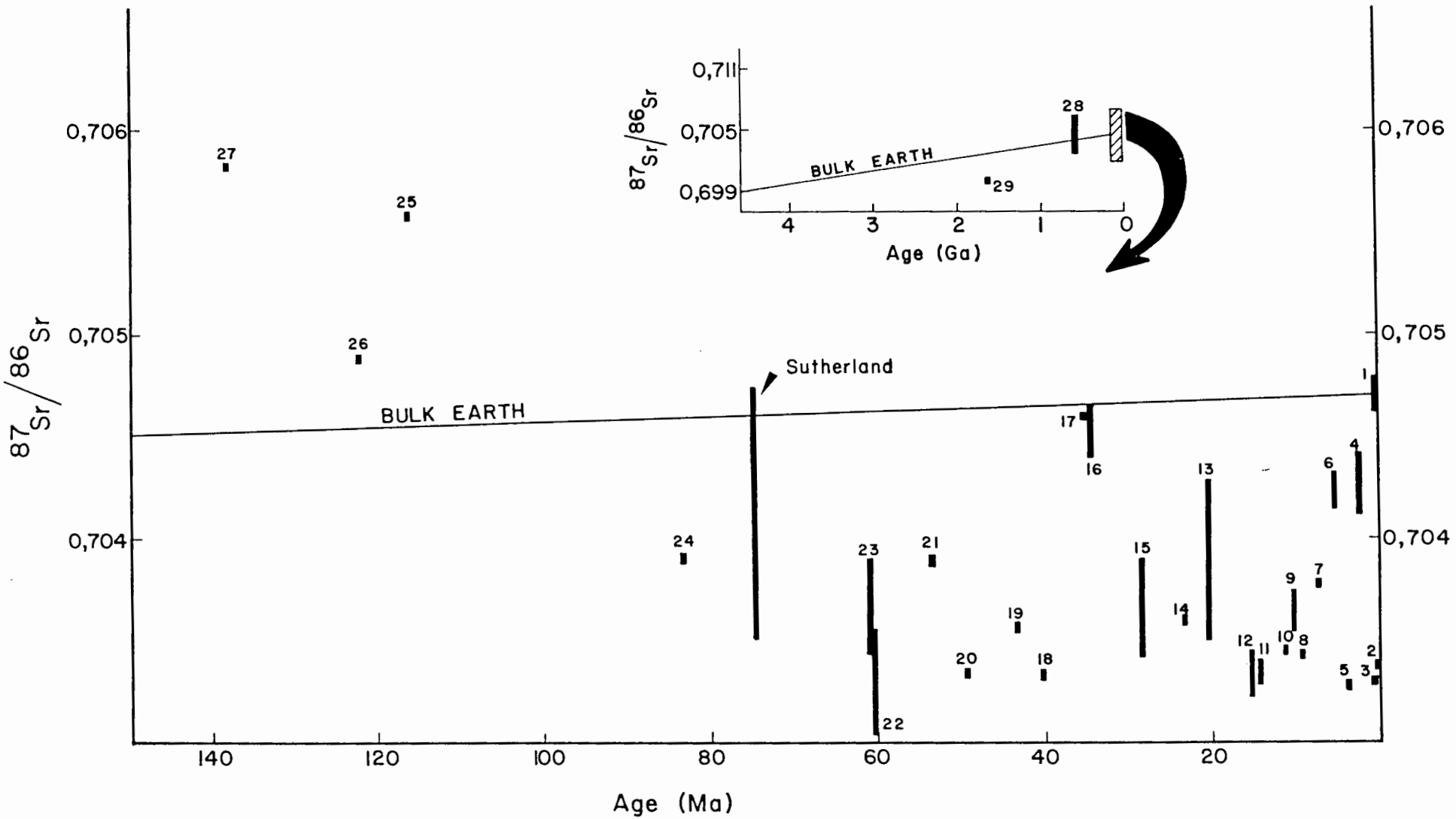

region or during the genesis of melilitites. In the past the petrogenesis of alkaline volcanics has been attributed to high-pressure fractionation (Bultitude and Green, 1968), differences in partial melting regimes (Green, 1971) or combinations of the above processes plus low-pressure fractionation (O'Hara, 1968). The inherent problem associated with almost all these models is that abundances of incompatible elements in alkali volcanics relative to those in other basic to ultrabasic magmas have been largely inexplicable in terms of the major processes proposed. Consideration of trace element abundances in alkali basalts (Gast, 1968) has led to the conclusion that the chemical characteristics of these rocks are best explained by small degrees of partial melting rather than by fractional crystallisation processes. However, recent studies (Menzies and Murthy, 1980) have shown that some degree of pre-enrichment of the mantle source area is necessary prior to or during the melting event that gives rise to alkaline rock suites. Considerable petrographic and geochemical evidence now exists in the literature which suggests that pervasive metasomatism, which leads to enrichment in LREE and incompatible elements of mantle material, precedes or accompanies the genesis of deep-seated alkali basaltic magmas. For example, ultramafic mantle xenoliths sampled by alkali lavas commonly exhibit evidence of metasomatic enrichment as do many xenoliths in kimberlites (Erlank et al., 1987). Apart from enriching portions of the mantle, it may also promote melting in the mantle by providing a source of CO_2, H_2O and other volatiles, as well as alkali-enriched low temperature melting phases e.g. phlogopite and amphibole.

A petrogenetic model in which mantle metasomatism played a role in source enrichment is therefore preferred since it eliminates the need for very small degrees of partial melting during the petrogenesis of the Commonage rocks. This enrichment must have occurred shortly before magma generation took place since the initial strontium isotope ratio of the Commonage melilitites do not reflect an enrichment event.

7.3.2 The role of carbon dioxide

Though it can be argued that the Commonage melilitites were derived from an enriched source, there remains the problem of accounting for their highly silica undersaturated nature. It is now widely accepted that carbonate species play a major role in the petrogenesis of these rock types (Fitton and Upton, 1987). More significant, however, is that experimental studies have shown that it is possible to produce silica-undersaturated compositions by melting peridotitic material in the presence of CO_2. During investigations of the synthetic system Mg_2SiO_4-SiO_2-H_2O-CO_2 (Eggler, 1974) and natural peridotites (e.g. Mysen and Boetcher, 1975) it was found that the effect of CO_2 on melting was the opposite of that of H_2O such that melting in the presence of CO_2-rich (low H_2O) vapour produced silica undersaturated liquids, whereas melting in an H_2O-rich (low CO_2) system produced more silica saturated liquids. Results obtained from these experimental studies have shown that CO_2 dissolves in silicate melts, thereby causing distinct changes in melt structure. The most notable of these changes is that the orthopyroxene field, and to a lesser extent the clinopyroxene field, expands in the

presence of CO_2 such that compositions of melts derived from CO_2 bearing peridotite sources are silica undersaturated.

7.3.3 Source region considerations

A consideration of the strontium isotope initial ratio's and incompatible element abundances (figures 7.8-7.10) of the Commonage melilitites indicate that the source region shares some of the characteristics of the mantle source for South African Group 1 kimberlites as well as various ocean islands in the central and south Atlantic ocean (data from Le Roux, 1986). Since the source of ocean island basalts are considered to be situated in the asthenosphere (Fitton and Upton, 1987), the observed chemical similarities between the Commonage source and that of ocean island basalt implies that the Commonage magma also derive from a similar (or the same) region of the mantle. Furthermore, the Commonage source region might even be related to the same mantle plume (or plumes) as that which gave rise to ocean islands situated to the south of the continent (and possibly also Group 1 kimberlites). Theories on the origin of these plumes are highly speculative. They have variously been ascribed to degassing of the core (Nicolaysen, 1985), upwelling of primordial or near-primordial mantle across the asthenosphere-mesosphere boundary (Le Roux, 1986) or the deep subduction (into the lower mantle) and subsequent melting of oceanic lithosphere (Hofmann and White, 1982; Weaver et al., 1987).

7.4 Conclusion

The geochemistry of the Commonage intrusives suggests the

Figure 7.8 Covariation of Ba/Nb and Zr/Nb ratios in South Atlantic basalts, Group I and Group II kimberlites and the Commonage melilitites

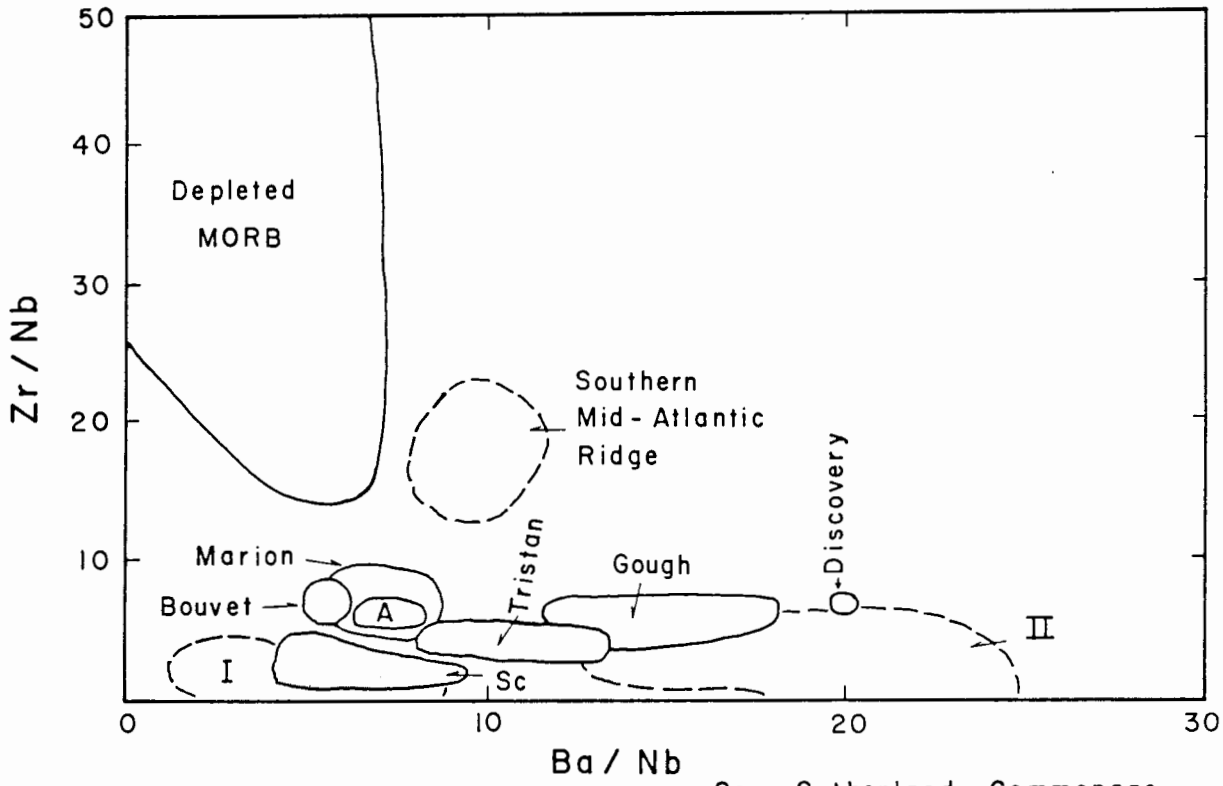

Sc = Sutherland Commonage
A = Ascension
I+II = Group I + Group II kimberlites

Figure 7.9 Covariation of Ba/Nb and La/Nb ratios in South Atlantic basalts, Group I and Group II kimberlites and the Commonage melilitites

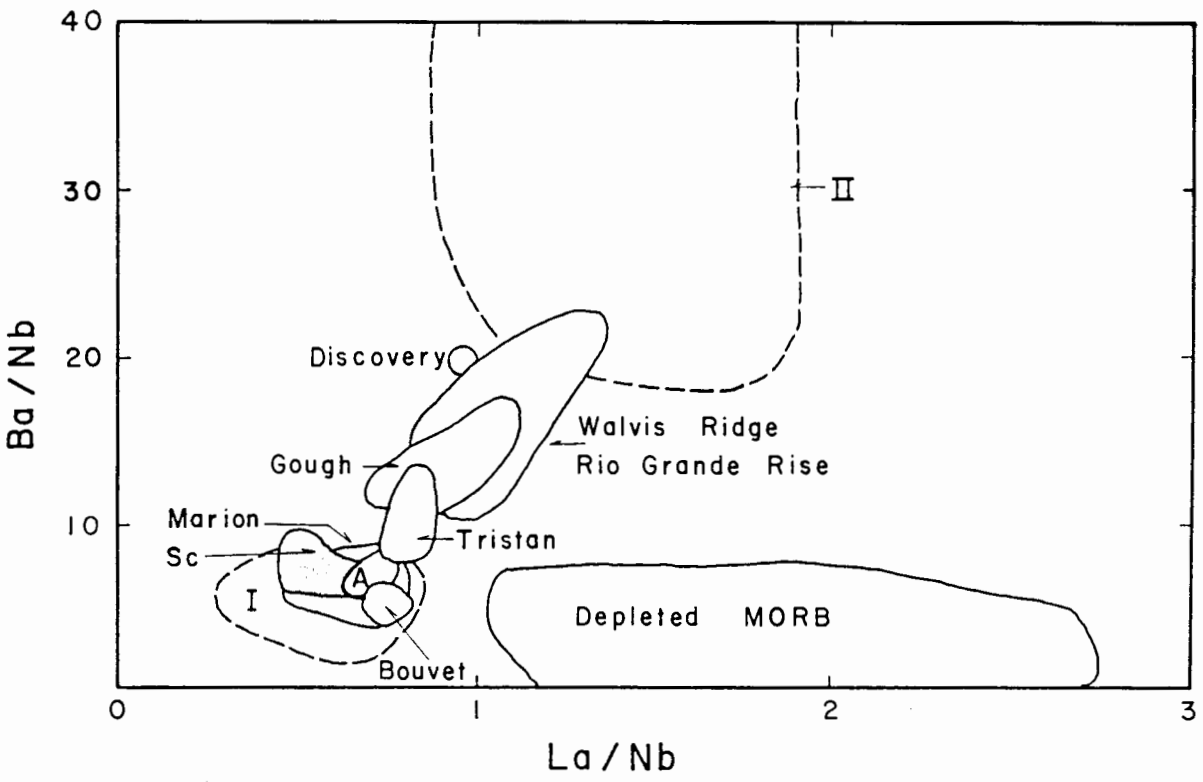

Figure 7.10 Correlation between Zr/Nb ratio and $^{87}Sr/^{86}Sr$ ratio in South Atlantic basalts, Group I and Group II kimberlites and the Commonage melilitites

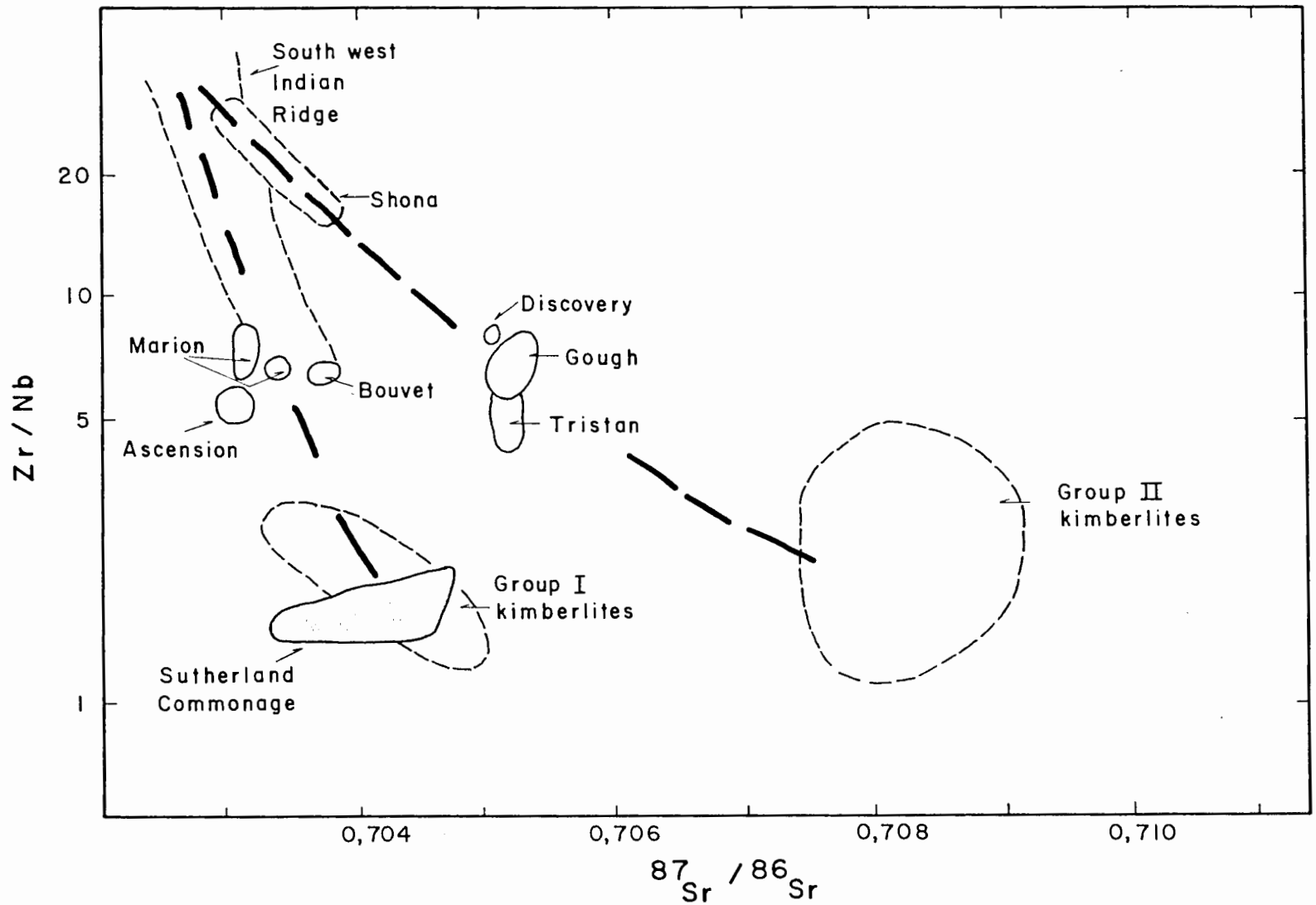

following:

1)The grey melilitite represents the most primitive magma at the Commonage. It probably formed by a lower degree of partial melting than the green melilitite and the ring dyke melilitite. The olivine nephelinite is a highly differentiated magma which formed by the post-intrusive accumulation of residual, evolved melt.

2)The Commonage melilitites represent partial melts of a CO_2-rich peridotite which was metasomatically enriched in incompatible elements prior to melting.

3)The Commonage magma source shows similarities to the source region of ocean island basalts. It is therefore considered that the source was situated in the asthenosphere and that it was plume related. This upwelling mantle plume presumably initially only caused metasomatism in the mantle above it. A gradual increase in the geothermal gradient due to the thermal effect of the plume ultimately led to the melting of the metasomatised mantle and the generation of the Commonage melilitite intrusives.

8 MINERALOGICAL VARIABILITY OF MELILITITES

8.1 Introduction

The groundmass mineralogy of melilite bearing rocks is highly variable and this has caused confusion in the classification of the melilitite clan of alkaline rocks (Rock, 1986). An attempt has therefore been made at the Kimberlite Petrology Unit (K.P.U.) of De Beers Consolidated Mines to define a sack term for this rock type in order to alleviate classification problems. Many of the ideas presented in this section resulted from the research of J. Robey and E.M.W. Skinner. The current philosophy at the K.P.U. is to group all rocks of the alnöite-melilitite-katungite-nephelinite series together, and to call them melnoites. It is an in-house petrographic term and is therefore not used in this thesis. Fortunately the Commonage rocks do not present any classification problems. However, the underlying petrological reasons for this classification is of relevance to the petrogenesis of the Commonage intrusives and is therefore discussed in some detail.

8.2 The melnoite clan

The term melnoite is used to encompass a suite of mantle-derived alkaline, basic to ultrabasic rocks including melilitites, nephelinites, alnoites and monticellite peridotites. They consist of ubiquitous olivine phenocrysts (and more rarely macrocrysts) set in a finer-grained matrix of the following non-essential minerals:- melilite, clinopyroxene, nepheline, monticellite and phlogopite (phlogopite may also be phenocrystal or macrocrystal).

Calcite, perovskite, Fe-Ti spinels, apatite, serpentine and andradite series garnets occur in accessory amounts. Melnoites may contain mantle-derived pyropic garnet, chrome diopside, chromite and ilmenite as well as ultramafic peridotite and crustal xenoliths. Macrocrysts of amphibole and magnetite are commonly present.

8.2.1 Physical and chemical influences on mineralogy

A common feature of the melnoite group is that it appear to consist of three main petrographic variants viz clinopyroxene-rich melnoites ("olivine nephelinites"), monticellitic melnoites ("monticellite peridotites") and melilitic melnoites ("melilitites"). If K_2O contents are ideal then phlogopitic melnoites result. These three major variants of the melnoite clan are considered to be closely related to each other and the presence or absence of minerals such as clinopyroxene and monticellite are largely controlled by cooling rates and volatile contents of the magma. This reasoning is based on experimental studies of melilite stability under varying conditions of pressure, temperature and CO_2 and H_2O contents (Yoder, 1973; Yoder, 1975). See figures 8.1 and 8.2.

Rapid chilling of a melnoite magma (under both H_2O or CO_2 rich conditions) leads to the crystallisation of a melilitic melnoite (the groundmass contains melilite and nepheline and the rock type is equivalent to melilitite).

During slower cooling of the same magma (e.g. in the centre of a sill) under H_2O rich conditions (figure 8.2) akermanite

Figure 8.1 Phase relations in the system akermanite - CO_2

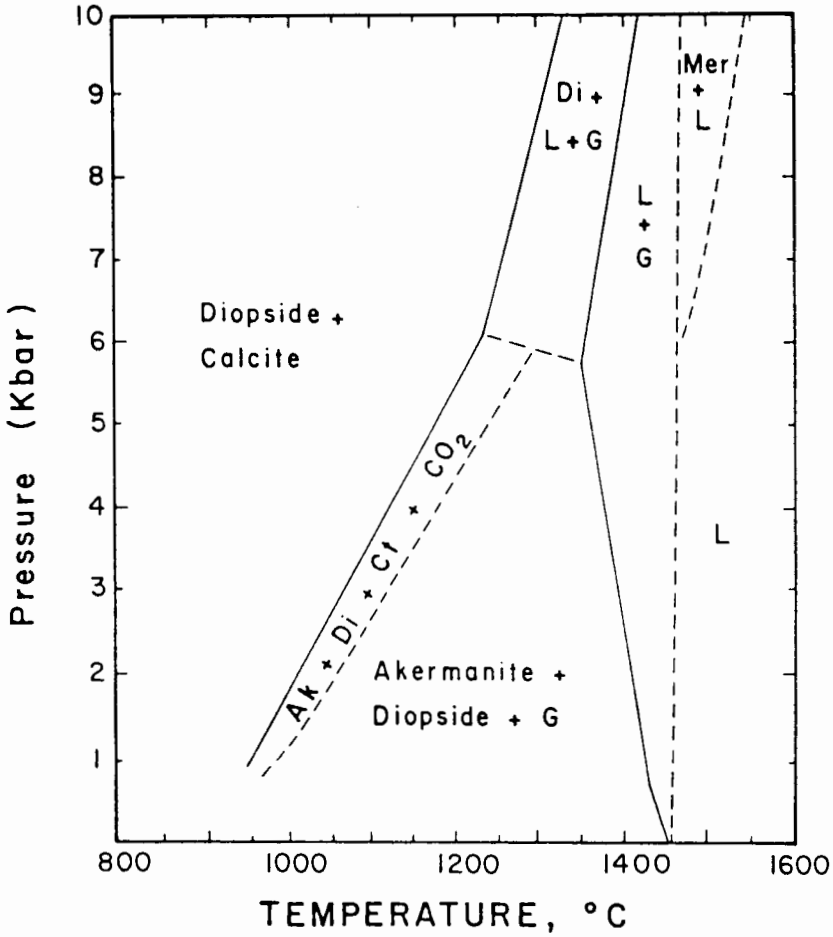

Data from Yoder (1973)

Figure 8.2 Phase relations in the system akermanite - H_2O

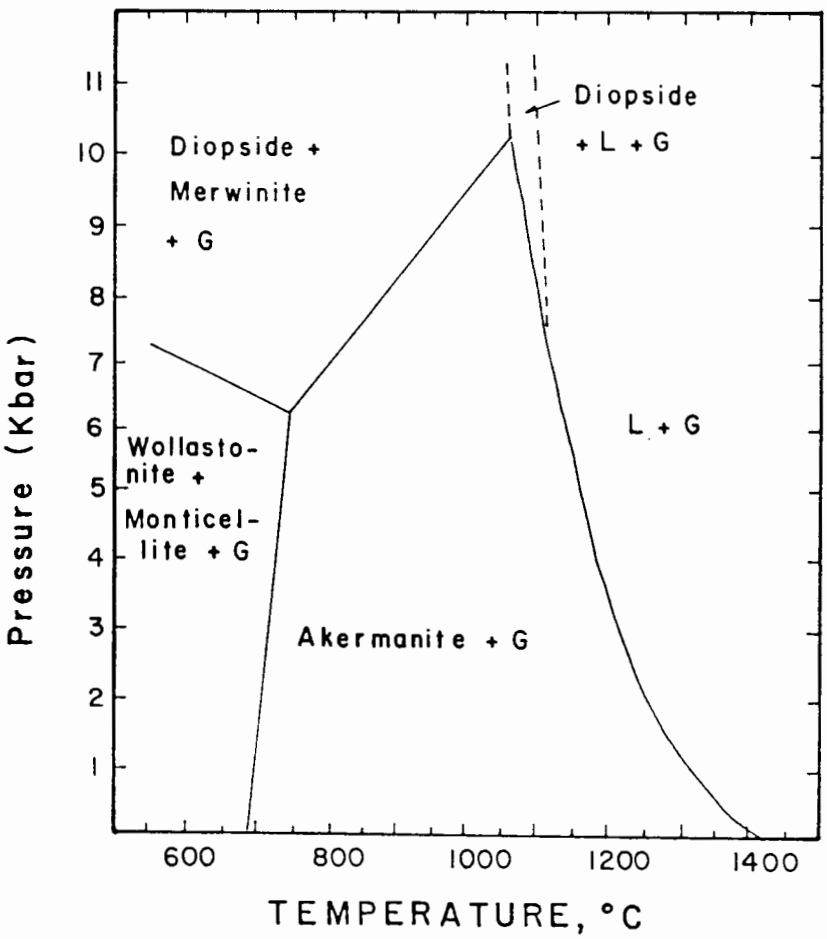

Data from Yoder (1973)

Figure 8.3 Diagrammatic representation of phase relations in the system $CaO - MgO - SiO_2 - CO_2$

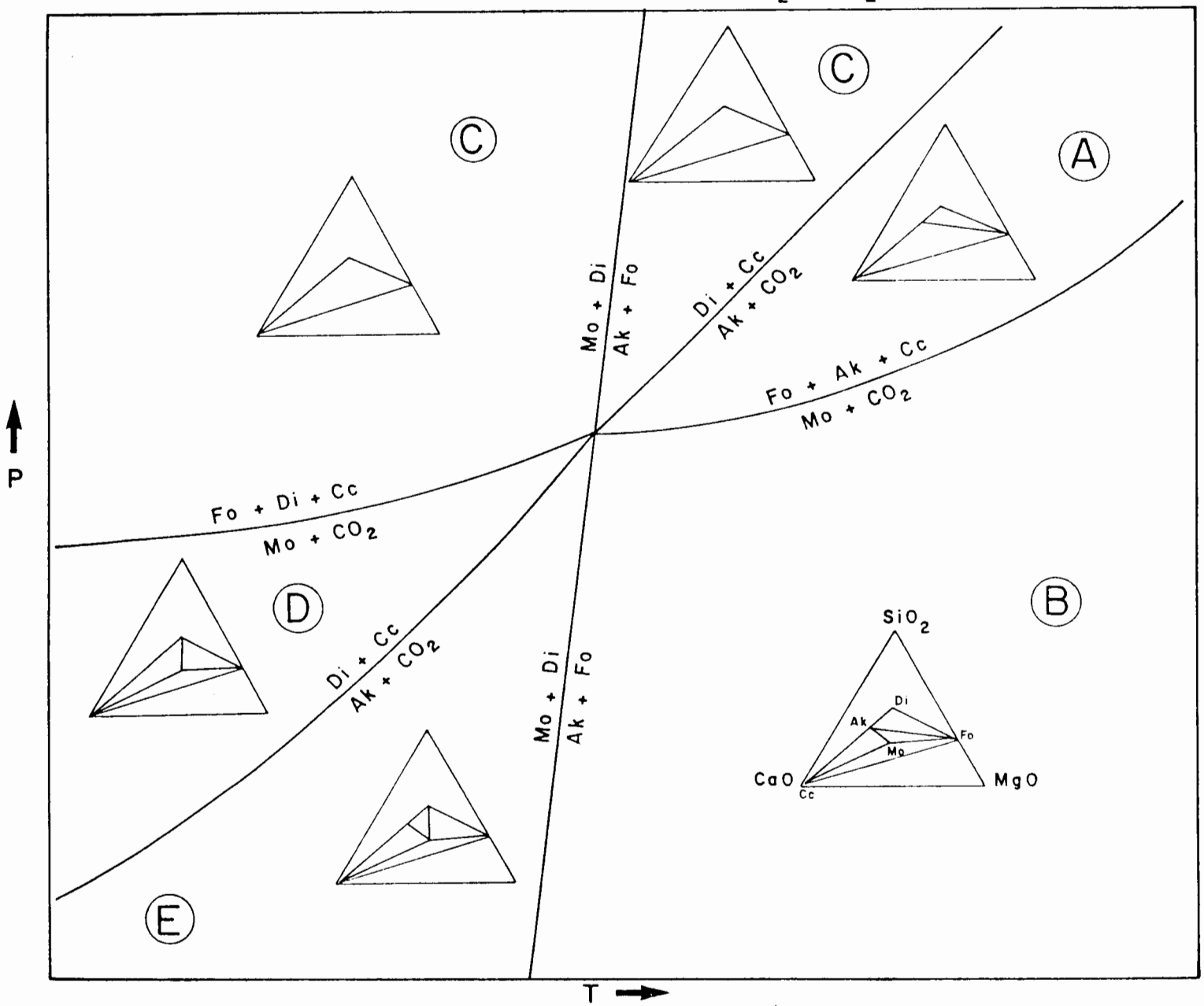

Diagram adapted from Walter (1963)

will react with the magma to produce monticellite and the resultant rock type will be a monticellitic melnoite (the groundmass contains monticellite and nepheline and the rock type is equivalent to monticellite peridotites). If excessive CO_2 is present then clinopyroxene will be produced from akermanite (figure 8.1) and the resultant clinopyroxene rich melnoite will be akin to olivine nephelinites.

It is, however, important to realise that this is a grossly simplified interpretation of stability relations in the systems akermanite-H_2O and akermanite-CO_2 and is as such only applicable to the natural rock system in very broad terms. It is therefore necessary to refine this line of thought to a large extent.

The primary chemical constituents of typical melnoites are silica, calcium, magnesium and iron. These elements usually make up the bulk (often 80%) of a typical chemical analysis and phase relations can therefore be adequately represented by the system SiO_2-CaO-MgO if iron is ignored. The system can be expanded to include CO_2 since it is considered to be an important volatile species in melnoites (M. Skinner, pers. comm.).

The SiO_2-CaO-MgO-CO_2 system contains the phases akermanite (a reasonable approximation of the composition of natural melilite-Yoder, 1973), forsterite, quartz, calcite, diopside, periclase and wollastonite. Free quartz, periclase and wollastonite are never seen in melnoites and are therefore excluded from the discussion. Walter (1963) presented a

theoretical thermodynamic analysis of the system. A modified version of his diagram is presented in figure 8.3.

Various stability relations are evident. High T-high P_{CO_2} conditions (plane A in figure 8.3) will stabilise the assemblages Di-Ak-Fo or Ak-Cc-Fo, depending on the bulk composition. High T-low P_{CO_2} conditions (plane B) will stabilise the assemblages Di-Ak-Fo, Ak-Mo-Fo, Ak-Mo-Cc or Mo-Fo-Cc. Lower T-high P_{CO_2} conditions (plane C) will stabilise the assemblage Di-Cc-Fo. Lower T-low P_{CO_2} (plane D) will stabilise the assemblages Di-Cc-Mo, Di-Mo-Fo or Mo-Fo-Cc and at slightly lower conditions of P_{CO_2} (plane E) the assemblages Di-Mo-Ak, Ak-Mo-Cc, Mo-Cc-Fo or Di-Mo-Fo will be stable.

Melilitic melnoites are therefore considered to represent high temperature disequilibrium assemblages which have been preserved by rapid chilling. It should also be noted that monticellitic assemblages can be stable at high temperatures if bulk compositions are ideal which suggest that monticellitic melnoites could represent primary assemblages which crystallised directly from a magma. However, the pressure sensitive univariant curves in figure 8.3 are seen to produce either monticellite or melilite upon CO_2 release. The vast majority of monticellitic melnoites therefore probably formed by the late stage, post intrusion reaction of olivine, diopside, calcite and melilite as a consequence of CO_2 loss.

The phase relations of clinopyroxene rich melnoites (consisting predominantly of olivine, calcite and diopside)

are far less complex. They simply form by the breakdown of melilite to clinopyroxene under CO_2-rich conditions.

8.3 Late processes in the grey melilitite

Striking petrographic features of the grey melilitite (see chapter 3) is the total absence of groundmass clinopyroxene and the abundance of monticellite. Since clinopyroxene is seen in corrosional hollows in olivine which have been protected in some way (often by a "plug" of phlogopite) it is assumed that it was originally present in the rock. Melilite is present but abundances are low. Conclusions which can be drawn from this is that melilite was probably more abundant and that diopside was originally present in the rock but that both minerals were lost due to reaction. It is therefore considered that olivine, melilite, clinopyroxene and calcite crystallised from the magma parental to the grey melilitite during and after intrusion. Subsequent degassing of CO_2 into the overlying sandstone horizon initiated a monticellite forming reaction which consumed most of the melilite and all the clinopyroxene. Reaction ceased after the elimination of clinopyroxene.

9 PETROGENETIC MODEL

From all the data on the Sutherland Commonage melilitite intrusives the following model is proposed for their petrogenesis.

(1)A region of the asthenosphere beneath Sutherland was metasomatised by fluids or melt emanating from a hot spot type source. During this stage the asthenospheric source region was enriched in volatiles and incompatible trace elements.

(2)Melting ensued due to the introduction of heat and volatiles associated with the metasomatic process. This melt coalesced, percolated upwards and accumulated in a magma chamber at the base of the lithosphere. Olivine started to crystallise in the chamber.

(3)The chamber ruptured (presumably due to a build-up of volatiles) and released a batch of magma which ascended to the surface. This early (primitive) magma intruded to form the grey melilitite in the sill complex (but must have reached the surface after the green melilitite due to a slow rate of ascent).

(4)Extrusion of the parent magma of the grey melilitite partially drained the chamber and intrusive activity ceased until continued melting in the source led to the accumulation of a sufficient volume of magma for magma ascent to be re-initiated. In this way two further batches of magma were released from the chamber. The first release produced the

green melilitite in the sill complex and the second produced the evolved parent magma of the ring dyke.

(5)A study of olivine mineral chemistry and zonation patterns shows that the ascent of magma through the cooler lithosphere led to a state of supercooling and an accelerated rate of olivine precipitation. This also initiated the start of chromite crystallisation.

(6)The ascending magmas disrupted a cumulate layer at the base of the crust which had formed by the fractionation of a basaltic magma. During this stage olivine and chromite crystallisation ceased and magnetite, perovskite and melilite started to crystallise.

(7)Clinopyroxene, apatite, phlogopite and nepheline crystallisation ensued after intrusion.

(8)In all the intrusions a volatile rich fluid formed either as a result of the separation of an immiscible liquid, or as a residual fluid after most of the constituent minerals had crystallised. From this fluid carbonate and a variety of zeolites crystallised.

(9)Separation of a nepheline rich differentiate from the crystallising green or grey melilitite in the sill complex led to the formation of the olivine nephelinite.

(10)Degassing of CO_2 from the grey melilitite initiated a monticellite forming reaction which consumed most of the

melilite and all the clinopyroxene which had previously crystallised.

REFERENCES

Alibert, C., Michard, A. and Albarede, F. (1983). The transition from alkali basalts to kimberlites: Isotope and trace element evidence from melilitites. Contrib. Mineral. Petrol. 82, 176-186.

Barret, D.R. and Berg, G.W. (1973). Complementary petrographic and strontium isotope ratio studies of South African kimberlite pipes. In: Ahrens, L.H., Dawson, J.B., Duncan, A.R. and Erlank, A.J. Eds. Physics and Chemistry of the Earth Vol. 9. p.619. Pergammon Press.

Barton, M. and Hamilton, D.L. (1982). Water-undersaturated melting experiments bearing upon the origin of potassium-rich magmas. Miner. Mag. 45, 267-278.

Bielski-Zyskind, M., Wasserburg, G.J. and Nixon, P.H. (1984). Sm-Nd and Rb-Sr systematics in volcanics and ultramafic xenoliths from Malaita, Solomon Islands, and the nature of the Ontong-Java plateau. J. Geophys. Res. 89, 2415-2424.

Boctor, N.Z. and Yoder, H.S. (1982). Distribution of rare earth elements in perovskite from melilite-bearing rocks. Carnegie Inst. Wash. Yb. 81, 369-371.

---------- (1986). Petrology of some melilite-bearing rocks from Cape Province, Republic of South Africa: Relationship to kimberlites. Am. J. Sci. 286, 513-539.

Bowen, N.L. (1982). Genetic features of alnoitic rocks at Ile Cadieux, Quebec. Am. J. Sci. 13, 1-34.

Boyd, F.R. and Clement, C.R. (1977. Compositional zoning of olivine in kimberlites from the De Beers mine, Kimberley, South Africa. Carnegie Inst. Wash. Yb. 76, 485-493.

Breuckner, H.K. and Rex, D.C. (1980). K-Ar and Rb-Sr geochronology and Sr isotopic study of the Alnö alkaline complex, Northeastern Sweden. Lithos 13, 111-119.

Buie, B.F. (1941). Igneous rocks of the Highwood Mountains, Montana. Bull. Geol. Soc. Am. 52, 1753-1808.

Bultitude, R.J. and Green, D.H. (1968). Experimental study at high pressure on the origin of olivine nephelinite and olivine melilitite-nephelinite magmas. Earth Planet. Sci. Lett. 3, 325-337.

Calvez, J.Y. and Lippolt, H.J. (1980). Strontium isotope constraints to the Rhine Graben volcanism. N. Jhb. Miner. Abh. 139, 59-81.

Carmichael, I.S.E., Nicholls, J.W. and Smith, A.L. (1970). Silica activity in igneous rocks. Amer. Mineral. 55, 246-263.

----------, Turner, F.J. and Verhoogen, J. (1974).

Igneous Petrology. McGraw-Hill, Inc. U.S.A.

Clague, D.A. and Frey, F.A. (1982). Petrology and trace element geochemistry of the Honolulu volcanics, Oahu: Implications for the oceanic mantle below Hawaii. J. Petrol. 23, 447-504.

Clement, C.R. (1982). A comparative geological study of some major kimberlite pipes in the Northern Cape and Orange Free State. Unpublished Ph.D. Thesis, University of Cape Town, South Africa.

Colgan, E.C., Clark, T.C. Bristow, J.W. and Allsop, H.L. (1988). Geological setting, petrography and petrogenesis of olivine melilitites of the Natal coast, South Africa. In Press.

Cooper, A.F. (1979). Petrology of ocellar lamprophyres from Western Otago, New Zealand. J. Petrol. 20, 139-163.

Cox, K.G., Bell, D. and Pankhurst, R.J. (1981). The interpretation of igneous rocks. George Allen and Unwin (Publishers) Ltd. London.

Dawson, J.B., Delaney, J.S. and Smith, J.V. (1978). Aspects of the mineralogy of alnoitic breccia, Malaita, Solomon Islands; comparison with continental kimberlites. Contrib. Min. Petrol. 67, 189-193.

Deer, W.A., Howie, R.A. and Zussman, J. (1982). Rock-forming minerals. Vol 1A. Orthosilicates. John Wiley and Sons, Inc. New York.

Donaldson, C.H. (1976). An experimental investigation of olivine morphology. Contrib. Min. Petrol. 57, 187-213.

Duncan, R.A., Hargraves, R.B. and Brey, G.P. (1978). Age, paleomagnetism and chemistry of melilite basalts in the Southern Cape, South Africa. Geol. Mag. 115, 317-327.

Durazzo, A., Taylor, A.T. and Shervais, J.W. (1984). Ultramafic lamprophyre in a carbonate platform environment, Mt. Queglia, Abruzzo, Italy. N. Jhb. Miner. Abh. 150, 199-217.

Eales, H.V., Marsh, J.S. and Cox, K.G. (1984). The Karoo igneous province: an introduction. Spec. Publ. Geol. Soc. S. Africa. 13, 1-26.

Eggler, D.H. (1974). Effect of CO_2 on the melting of peridotite. Carnegie Inst. Wash. Yb. 73, 215-223.

Erlank, A.J., Waters, F.G., Hawkesworth, C.J., Haggerty, S.E., Allsopp, H.L., Rickard, R.S. and Menzies, M.A. (1978). Evidence for mantle metasomatism in peridotite nodules from the Kimberley pipes, South Africa. In: Menzies, M.A. and Hawkesworth, C.J. Mantle metasomatism. Academic Press, London.

Ferguson, A.K. (1978). Ca-enrichment in olivines from volcanic rocks. Lithos. 11, 189-194.

Finger, L.W. (1972). The uncertainty in the calculated ferric iron content of a microprobe analysis. Carnegie Inst. Wash. Ybk. 71, 600-603.

Fisk, M.R. and Bence, A.E. (1980) Experimental crystallisation of chrome spinel in FAMOUS basalt 527-1-1. Earth Planet. Sci. Lett. 48, 111-123.

Fitton, J.G. and Upton, B.G.J. (1987) Alkaline igneous rocks. Geological Society Special Publication No. 30. Blackwell Scientific Publications. Oxford.

Fodor, R.V. and Keil, K. (1975). Contributions to the mineral chemistry of Hawaiian rocks. IV. Pyroxenes in rocks from Haleakala and West Maui, Hawaii. Contrib. Min. Petrol. 50, 173-195.

Foley, S.F. (1984). Liquid immiscibility and melt segregation in alkaline lamprophyres from Labrador. Lithos, 17, 127-137.

Frechen, J. (1963). Kristallisation, mineralbestand, mineralchemismus und forderfolge der mafitite vom Dreisen Weiher in der Eiffel. N. Jhb. Miner. MH. 7, 205-225.

Gast, P.W. (1968). Trace element fractionation and the origin of tholeiitic and alkaline magma types. Geochim. Cosmochim. Acta, 32, 1057-1087.

Gerard, I. (1958). The olivine melilitites from the Western Cape. Unpublished M.Sc. Thesis, University of Cape Town, South Africa.

Green, D.H. (1971). Composition of basaltic magmas as indicators of conditions of origin: applications to ocean volcanism. Phil. Trans. R. Soc. Lond. 268, 707-725.

Gupta, A.K., Onuma, K., Yagi, K. and Lidiak, E.G. (1973). Effects of silica concentration on the diopsidic pyroxenes in the system diopside-$CaTiAl_2O_6$-SiO_2. Contrib. Min. Petrol. 41, 336-344.

Gurney, J.J., Jakob, W.R.O. and Dawson, J.B. (1979). Megacrysts from the Monastery kimberlite pipe, South Africa. In: Boyd, F.R. and Meyer, H.O.A. The mantle sample: Inclusions in kimberlites and other volcanics. Proc. 2nd Int. Kimb. Conf. Sante Fe, A.G.U. Washington.

Haggerty, S.E. (1972). Luna 16. An opaque mineral study and a systematic examination of compositional variations of spinels from Mare Fecunditatis. Earth Planet. Sci. Lett. 13, 328-352.

---------- (1973). Spinels of unique composition associated with ilmenite reaction mantles in the Liqhobong Kimberlite pipe, Lesotho. In: Nixon, P.H. Lesotho

kimberlites. Lesotho National Development Corporation, Maseru, Lesotho.

---------- (1976). Opaque mineral oxides in terrestrial igneous rocks. In: Rumble, D. Oxide minerals. Mineralogical Society of America, Short course notes, 3.

Hansen, K. (1980). Lamprophyres and carbonatitic lamprophyres related to rifting in the Labrador Sea. Lithos, 13, 145-152.

---------- (1981). Systematic Sr-isotopic variation in alkaline rocks from West Greenland. Lithos, 14, 183-188.

Hart, S.R. and Davis, K.E. (1978). Nickel partitioning between olivine and silicate melt. Earth Planet. Sci. Lett. 40, 203-219.

Hearn, B.C. (1979). Preliminary map of diatremes and alkalic ultramafic intrusions, Missouri River Breaks and vicinity, North Central Montana. U.S.G.S. Open file report 79-1128.

Hernandez, J. (1976). Donnees nouvelles sur la composition mineralogique de la nephelinite de Marcoux (Forez.). Bull. Soc. Fr. Mineral. Cristallogr., 99, 61-66.

Hofmann, A.W. and White, W.M. (1982). Mantle plumes from ancient oceanic crust. Earth Planet. Sci. Lett. 57, 421-436.

Huckenholz, H.G. (1973). The origin of fassaitic augite in the alkali basalt suite of the Hocheifel area, West Germany. Contrib. Min. Petrol. 40, 315-326.

Irvine, T.N. (1965). Chromian spinels as a petrogenetic indicator. Part 1. Theory. Canadian Journal of Earth Sciences, 2, 648-672.

---------- (1967). Chromian spinel as a petrogenetic indicator. Part 2. Petrogenetic implications. Canadian Journal of Earth Sciences, 4, 71-103.

Jago, B.C. (1982). Mineralogy and petrology of the Ham kimberlite, Somerset Island, N.W.T., Canada. M.Sc. Thesis, Lakehead University, Thunder Bay, Canada.

Jones, A.P. and Wyllie, P.J. (1985). Paragenetic trends of oxide minerals in carbonate-rich kimberlites, with new analysis from the Benfontein sill, South Africa. J. Petrol. 26, 210-222.

Kushiro, I. (1960). Si-Al relations in clinopyroxenes from igneous rocks. Am. Jnl. Sci. 258, 548-554.

Lanphere, M.A. and Dalrymple, G.B. (1980). Age and strontium isotopic composition of the Honolulu volcanic series, Oahu, Hawaii. Am. Jnl. Sci. 280 A, 736-751.

Larsen, E.S., Hurlbut, C.S., Buie, B.F. and Burgess, C.H.

(1941). Igneous rocks of the Highwood mountains, Montana. Part VI. Miner. Bull. Geol. Soc. America. 52, 1841-1856.

Lawless, P.J. (1978). Some aspects of the mineral chemistry of peridotitic xenoliths from the Bultfontein mine. Unpublished Ph.D. Thesis, University of Cape Town, South Africa.

Le Roux, A.P. (1986). Geochemical correlation between Southern African kimberlites and South Atlantic hotspots. Nature. 324, 243-245.

Luth, W.C. (1967). Studies in the system $KAlSiO_4$-Mg_2SiO_4-SiO_2-H_2O: Inferred phase relations and petrologic applications. J. Petrol. 8, 372-416.

Maaløe, S. (1985). Principles of igneous petrology. Springer Verlag, Berlin.

---------- and Hansen, B. (1982). Olivine phenocrysts of Hawaiian tholeite and oceanite. Contrib. Min. Petrol. 81, 203-211.

Magonthier, M.C. and Velde, D. (1976). Mineralogy and petrology of some tertiary leucite-rhönite basanites from Central France. Miner. Mag. 40, 817-826.

Marsh, J.S,, Hawkesworth, C.J. and Moore, A.E. (1981). Sr and Nd isotopes in tertiary alkaline volcanics in South-Western Africa. Abstract Geocongress '81. Geological Society of Southern Africa.

Mathez, E.A. (1984). Influence of degassing on oxidation states of basaltic magmas. Nature. 310, 371-375.

McIver, J.R. (1981). Aspects of ultrabasic and basic alkaline intrusive rocks from Bitterfontein, South Africa. Contrib. Min. Petrol. 78, 1-11.

---------- and Ferguson, J. (1979). Kimberlitic, melilitic, trachytic and carbonatite eruptives at Saltpetre Kop, Sutherland, South Africa. In: Boyd, F.R. and Meyer, H.O.A. Eds. Kimberlites, Diatremes and Diamonds. Proc. 2nd. Int. Kimb. Conf. A.G.U. Washington.

Mengel, K., Kramm, U., Wedepohl, K.H. and Gohn, E. (1984). Sr isotopes in peridotite xenoliths and their basaltic host rocks from the Northern Hessian Depression (NW Germany). Contrib. Min. Petrol. 87, 369-375.

Menzies, M. and Murthy, V.R. (1980). Mantle metasomatism as a precursor to the genesis of alkaline magmas - isotopic evidence. Am. Jnl. Sci. 280-A, 622-638.

Meyer, H.O.A. and Villar, L.M. (1984). An alnoite in the Sierras Subandinas, Northern Argentina. J. Geol. 92, 741-751.

Mitchell, R.H. (1980). Pyroxenes of the Fen alkaline

complex, Norway. Am. Miner. 65, 45-54.

---------- (1983). The Ile Bizard intrusion, Montreal, Quebec-kimberlite or lamprophyre? Discussion. Canadian Jnl. Earth Sci. 20, 1493-1496.

---------- (1985). A review of the mineralogy of lamproites. Trans. Geol. Soc. South Africa. 88, 411-438.

---------- (1986). Kimberlites: mineralogy, geochemistry and petrology. Plenum Press, New York.

Moore, A.E. (1979). The geochemistry of the olivine melilitites and related rocks of Namaqualand-Bushmanland, South Africa. Unpublished Ph.D. Thesis, University of Cape Town, South Africa.

---------- (1981). Unusual perovskite textural relationships in olivine melilitites from Namaqualand-Bushmanland, South Africa. Miner. Mag. 44, 147-150.

---------- (1983). A note on the occurrence of melilite in olivine melilitites and kimberlites. Miner. Mag. 47, 404-406.

---------- and Erlank, A.J. (1979). Unusual olivine zoning - evidence for complex physico chemical changes during the evolution of olivine melilitite and kimberlite magmas. Contrib. Min. Petrol. 70, 391-405.

---------- and Duncan, A.R. (1982). The evolution of olivine melilitites and kimberlite magmas. Terra Cognita. 2, 214.

Mysen, B.O. and Boettcher, A.L. (1975). Melting of a hydrous mantle: 2. Geochemistry of crystals and liquids formed by anatexis of mantle peridotite at high pressures and high temperatures as a function of controlled activities of water, hydrogen and carbon dioxide. J. Petrol. 16, 549-593.

Nicolaysen, L.O. (1985). Renewed ferment in the Earth Science-especially about power supplies for the core, for the mantle and for crises in the faunal record. South African Jnl. Sci. 81, 120-132.

Nielsen, T.F.D. (1980). The petrology of a melilitolite, melteigite, carbonatite and syenite ring dyke system, in the Gardiner Complex, East Greenland. Lithos. 13, 181-197.

Nixon, P.H. and Boyd, F.R. (1979). Garnet bearing lherzolites and discrete nodule suites from the Malaita alnoite, Solomon Islands, S.W. Pacific, and their bearing on oceanic mantle composition and geotherm. In: Boyd, F.R. and Meyer, H.O.A. Eds. The mantle sample: Inclusions in kimberlites and other volcanics. Proc. 2nd Int. Kimb. Conf. A.G.U. Washington.

----------, Mitchell, R.H. and Rogers, N.W. (1980). Petrogenesis of alnoitic rocks from Malaita, Solomon Islands, Melanesia. Miner. Mag. 43, 587-596.

Norrish, K. and Hutton, J.T. (1969). An accurate X-ray spectrographic method for the analysis of a wide range of geological samples. Geochim et Cosmochim Acta. 33, 431-453.

O'Hara, M.J. (1968). The bearing of phase equilibria studies in synthetic and natural systems on the origin and evolution of basic and ultrabasic rocks. Earth Sci. Rev. 4, 69-133.

Ohta, K., Onuma, K. and Yagi, K. (1977). The system $NaFe^{3+}Si_2O_6$-$CaFe^{2+}Si_2O_6$ at low oxygen fugacity. Jnl. Fac. Sci. Hokkaido Univ. Ser IV. 17, 487-504.

O'Nions, R.K., Hamilton, P.J. and Evenson, N.M. (1977). Variations in $^{143}Nd/^{144}Nd$ and $^{87}Sr/^{86}Sr$ ratios in oceanic basalts. Earth Planet. Sci. Lett. 34, 13-22.

Onuma, K. (1983). Effect of oxygen fugacity on fassaitic pyroxene. Jnl. Fac. Sci. Hokkaido Univ. Ser IV. 20, 185-194.

--------- and Yagi, K. (1971). The join $CaMgSi_2O_6$-$Ca_2MgSi_2O_7$-$CaTiAl_2O_6$ in the system CaO-MgO-Al_2O_3-TiO_2-SiO_2 and its bearing on titanpyroxenes. Miner. Mag. 38, 471-480.

---------- (1975). The join $CaMgSi_2O_6$-$CaAl_2SiO_6$-$CaFe^{3+}AlSiO_6$ in air and its bearing on fassaitic pyroxene. Jnl. Fac. Sci. Hokkaido Univ. Ser IV. 16, 343-356.

--------- and Akasaka, M. (1980). Clinopyroxene with $Si<Al_{IV}$ in the join $CaFeAlSiO_6$-$CaTiAl_2O_6$. Miner. Mag. 43, 851-856.

Pasteris, J.D. (1980). Opaque oxide phases of the De Beers pipe kimberlite (Kimberley, South Africa) and their petrologic significance. Unpublished Ph.D. Thesis, Yale University, U.S.A.

Platt, R.G. and Mitchell, R.H. (1979). The Marathon dikes. I: Zirconium rich titanian garnets and manganoan magnesian ulvospinel-magnetite spinels. Am. Miner. 64, 546-550.

---------- (1982). The Marathon dykes: Ultrabasic lamprophyres from the vicinity of McKellar Harbour, N.W. Ontario. Am. Miner. 67, 907-916.

---------- and Holm, P.M. (1983). Maraton dykes: Rb-Sr and K-Ar geochronology of ultrabasic lamprophyres from the vicinity of McKellar Harbour, Northwestern Ontario, Canada. Canadian Jnl. Earth Sci. 20, 961-967.

Poldervaart, A. and Hess, H.H. (1951). Pyroxenes in the crystallisation of basaltic magma. J. Geol. 59, 472-489.

Raeside, P.R. and Helmstaedt, H. (1982). The Ile Bizard intrusion, Montreal, Quebec-kimberlite or lamprophyre? Canadian Jnl. Earth Sci. 19, 1996-2011.

Ridley, W.I. (1977). The crystallisation trends of spinels in tertiary basalts from Rhum and Muck and their petrogenetic significance. Contrib. Min. Petrol. 64, 243-255.

Robey, J.v.A., Bristow, J.W., Marx, M.R., Joyce, J.J., Danchin, R.V. and Arnott, F. (1988) Alkaline ultrabasic dykes of the south-eastern Yilgarn craton margin, Western Australia. In Press.

Rock, N.M.S. (1986). The nature and origin of ultramafic lamprophyres: Alnoites and allied rocks. J. Petrol. 27, 155-196.

Roeder, P.L. and Emslie, R.F. (1970). Olivine-liquid equilibrium. Contrib. Min. Petrol. 29, 275-289.

----------, Campbell, I.H. and Jamieson, H.E. (1979). A re-evaluation of the olivine-spinel geothermometer. Contrib. Min. Petrol. 68, 325-334.

Rogers, A.W. and Du Toit, A.L. (1903). Volcanic pipes of Sutherland. Ann. Rept. Cape Geol. Comm. p.43.

---------- (1904) The Sutherland volcanic pipes and their relationship to other vents in South Africa. Trans. South African Phil. Soc. 15, 61-83.

Ross, C.S. (1926). Nephelite-hauynite alnoite from Winnett, Montana. Am. Jnl. Sci. 63, 218-227.

Sack, R.O. (1982). Spinels as petrogenetic indicators: Activity-composition relations at low pressure. Contrib. Min. Petrol. 79, 169-186.

SACS (The South African Commitee for stratigraphy), (1980). Stratigraphy of South Africa. Part 1 (Comp. L.E. Kent). Lithostratigraphy of the Republic of South Africa, South West Africa/Namibia, and the Republics of Bophuthatswana, Transkei and Venda. Handbk. Geol. Surv. S. Africa. 8, 690pp.

Scott, P.W. (1976). Crystallisation trends of pyroxenes from the alkaline volcanic rocks on Tenerife, Canary Islands. Miner. Mag. 40, 805-816.

Segalstadt, T.V. (1979). Petrology of the Skien basaltic rocks, South-Western Oslo region, Norway. Lithos. 221-239.

Shee, S.R. (1986). The petrogenesis of the Wesselton mine kimberlites, Cape Province, R.S.A. Unpublished Ph.D.

Thesis, University of Cape Town, South Africa.

Shrbeny, O. and Machacek, V. (1974). Microelements in melilitic rocks of Northern Bohemia. Casopis Pro Mineralogii a Geologii. 19, 15-25.

Sigurdsson H. and Schilling, J.G. (1976). Spinels in Mid-Atlantic ridge basalts: Chemistry and occurrence. Earth Planet. Sci. Lett. 29, 7-20.

Skinner, E.M.W. (1988). Contrasting Group 2 and Group 1 kimberlite petrology: Towards a genetic model for kimberlites. In Press.

Smith, C.B. (1983). Rb/Sr, U/Pb and Sm/Nd isotopic studies of kimberlites and selected mantle derived xenoliths. Unpublished Ph.D. Thesis, University of the Witwatersrand, South Africa.

Stormer, J.C. (1973). Calcium zoning in olivine and its relation to silica activity and pressure. Geochim. et Cosmochim. Acta. 37, 1815-1821.

Takahashi, E. and Scarfe, C.M. (1985). Melting of peridotite to 14 GPa and the genesis of komatiite. Nature, 315, 566-568.

Taljaard, M.S. (1937). South African melilite basalts and their relations. Trans. Geol. Soc. South Africa. 39, 281-316.

Thy, P. (1983). Spinel minerals in transitional and alkali basaltic glasses from Iceland. Contrib. Min. Petrol. 83, 141-149.

Tompkins, L.A. and Haggerty, S.E. (1985). Groundmass oxide minerals in the Koidu kimberlite dykes, Sierra Leone, West Africa. Contrib. Min. Petrol. 91, 245-263.

Tracy, R.J. and Robinson, P. (1977). Zoned titanian augite in alkali olivine basalt from Tahiti and the nature of titanium substitutions in augite. Am. Miner. 62, 634-645.

Velde, D. and Thiebault, J. (1973). Quelques precisions sur la constitution mineralogique de la nephelinite a olivine et melilite d'Essey-la-Cote (Meurthe-et-Mosette). Bulle. Soc. Fr. Mineral. Cristallogr. 96, 298-302.

Volmer, R. and Norry, M.J. (1983). Unusual isotopic variations in Nyiragongo nephelinites. Nature. 301, 141-143.

Walter, L.S. (1963). Experimental studies on Bowens decarbonation series: P-T univariant equilibria of the monticellite and ackermanite reactions. Am. J. Sci. 261, 488-500.

Wass, S. (1979). Multiple origins of clinopyroxenes in alkali basaltic rocks. Lithos. 12, 115-132.

Weaver, B.L., Wood, D.A., Tarney, J. and Joron, J.L. (1987). Geochemistry of ocean island basalts from the South Atlantic: Ascension, Bouvet, St. Helena, Gough and Tristan da Cunha. In: Fitton, J.G. and Upton, B.G.J. Eds. Alkaline Igneous Rocks. Geological Society Special Publication No. 30.

Wilkinson, J.F.G. and Stolz, A.J. (1983). Low-pressure fractionation of strongly undersaturated alkaline ultrabasic magma: The olivine melilitite at Moiliili, Oahu, Hawaii. Contrib. Min. Petrol. 83, 363-374.

Wimmernauer, W. (1967). Igneous rocks of the Rhine Graben. The Rhine Graben Progress Report. Abh. Geol. Landesamt Baden - Wurtemberg 6, 144-148.

Wood, D.A. (1979). A variably veined suboceanic upper mantle - genetic significance for mid-ocean ridge basalts from geochemical evidence. Geology. 7, 499-503.

Worner, G., Zindler, A., Staudigel, H. and Schimke, H.-U. (1986). Sr, Nd and Pb isotope geochemistry of tertiary and quaternary alkaline volcanics from West Germany. Earth Planet. Sci. Lett. 79, 107-119.

Wyllie, P.J. (1971). The Dynamic Earth. John Wyllie & Sons Inc. New York.

Yoder, H.S. (1968). Akermanite and related melilite-bearing assemblages. Carnegie Inst. Wash. Ybook. 66,471-477.

---------- (1973). Melilite stability and paragenesis. Fortschr. Mineral. 50, 140-173.

---------- (1975). Relationship of melilite-bearing rocks to kimberlite: A preliminary report on the system akermanite-CO_2. In: Ahrens, L.H., Dawson, J.B., Duncan, A.R. and Erlank, A.J. Eds. Physics and Chemistry of the Earth Vol. 9. p.883. Pergammon Press.

---------- (1976). Generation of basaltic magma. National Academy of Science, Washington.

Yoshikawa, K. (1977). Phase relations and the nature of clinopyroxene solid solutions in the system $NaFe^{3+}Si_2O_6$-$CaMgSi_2O_6$-$CaAl_2SiO_6$. Jnl. Fac. Sci. Hokkaido Univ. Ser IV. 17, 451-485.

APPENDIX 1

ANALYTICAL CONDITIONS FOR MICROPROBE ANALYSIS

All mineral analyses in this study were done on a Cameca/Camebax Microbeam electron microprobe. Standards used and statistical data are listed in tables 1a-c.

A finely focussed beam was used for all analyses. In general counting times of 10 seconds were used. Longer counts were done on Ni in olivine because lower detection limits was necessitated by low nickel concentrations.

Nominal concentrations were calculated prior to applying corrections for interelement and matrix effects. The ZAF correction procedure was used. Results are expressed as weight per cent of the oxides and atomic proportions are calculated to fit the structural formula.

All iron is reported as FeO, except in the case of spinels where Fe_2O_3 and FeO have been estimated assuming perfect spinel stoichiometry (Finger, 1972).

TABLE 1-A
OLIVINE

EL	STANDARD	COUNTING TIME(sec)	LLD	Wt.% OXIDE (STANDARD)
Si	Marjalahti Olivine	10	.04	40.24
Ti	Synthetic Rutile	10	.04	100.00
Al	Kakanui Pyrope	10	.03	23.73
Cr	Chromite 52NL11	10	.04	44.50
Fe	Marjalahti Olivine	10	.07	11.53
Mn	Rhodonite	10	.07	40.76
Mg	Marjalahti Olivine	10	.03	48.08
Ca	Kakanui Pyrope	10	.03	5.16
Ni	Synthetic Ni_2SO_4	30	.05	71.30

TABLE 1-B
CLINOPYROXENE

EL	STANDARD	COUNTING TIME(sec)	LLD	Wt.% OXIDE (STANDARD)
Si	Synthetic Diopside	10	.04	55.47
Ti	Synthetic Rutile	10	.04	100.00
Al	Kakanui Pyrope	10	.03	23.73
Cr	Chromite 52NL11	10	.05	44.50
Fe	Kakanui Pyrope	10	.08	10.68
Mn	Rhodonite	10	.07	40.76
Mg	Synthetic Diopside	10	.03	18.62
Ca	Synthetic Diopside	10	.03	25.90
Na	Kakanui Hornblende	10	.03	2.60
K	Kakanui Hornblende	10	.02	2.05

TABLE 1-C
CHROMITE/MAGNETITE

EL	STANDARD	COUNTING TIME(sec)	LLD	Wt.% OXIDE (STANDARD)
Si	Kakanui Pyrope	10	ND	41.46
Ti	Synthetic Rutile	10	.04	100.00
Al	Chromite 52NL11	10	.05	19.41
Cr	Chromite 52NL11	10	.05	44.50
Fe	Ilmenite (Ilm.Mts., USSR)	10	.09	46.53
Mn	Rhodonite	10	.08	40.76
Mg	Chromite 52NL11	10	.04	12.30
Ca	Kakanui Pyrope	10	.03	51.60

APPENDIX 2

WHOLE ROCK XRF ANALYSIS

Samples were selected for analysis on the basis of petrographic examination of thin sections. Relatively large samples (1-2 kg) were used. Samples were prepared for chemical analysis by splitting with a sledge hammer, crushing in a jaw crusher with Mn-steel jaws and grinding in a carbon steel vessel on a Siebtechnik swing mill to -300 mesh.

All samples were analysed on the Philips PW 1400 machine at UCT. Major elements were determined on duplicate fusion discs, prepared after the method of Norrish and Hutton (1969). Na_2O and trace elements were determined on pressed powder briquettes.

Standard computer programs for data reduction included corrections for position factors, dead time, background, drift and spectral line interferences. Mass absorption coefficients were calculated by the Mo K Compton Peak method.

Precision on major element analysis (2 sigma counting error) is typically better than 2% relative. Errors on trace element analysis (2 sigma error) are typically better than 5% relative (table 2a).

TABLE 2-A
TYPICAL COUNTING STATISTICS FOR TRACE ELEMENT ANALYSIS

ELEMENT	PRECISION (2 SIGMA)	LLD(PPM)
Ba	3	4
Sc	1	1.2
La	2	2.5
Ce	4	5
Nd	2	4
Co	2	4
Cr	2	2
V	3	5
Nb	1	1
Zr	2	2
Y	1.5	2
Sr	1.8	.6
Rb	.6	.6
Th	1	1.5

Long counting times (200 seconds) were used for La, Ce, Nd, Rb, Sr and Th.

APPENDIX 3

ISOTOPE ANALYSIS

Samples for isotope analysis were selected after petrographic examination in order to ensure that only the freshest material available are used. Samples from the green melilitite were excluded from this study since analyses from this intrusive type would probably have produced meaningless results due to the pervasive deuteric alteration present. Aliquots of approximately 0.2g of seven of the samples selected for whole rock analysis was prepared for Sr isotope analysis. Total Rb and Sr analyses were obtained by XRF methods at UCT and the respective $^{87}Rb/^{86}Sr$ ratios calculated accordingly.

Samples were dissolved in clean teflon beakers with five mls of double distilled hydrofluoric acid. A few drops of double distilled nitric acid were added in order to retard the formation of insoluble fluorides. Beakers were then covered with teflon cover slips and heated on a hot plate for approximately 24 hrs after which the cover slips were removed in order to allow the sample to dry down. Each sample was then dissolved again in 6N double distilled HCl in order to convert the sample to a chloride for ion exchange chemistry. Samples were again dried down and the procedure repeated with 2.59N HCl. Following this each sample was then redissolved in 2.59N HCl and centrifuged in 1.5ml centrifuge tubes in order to prevent clogging of the ion exchange columns.

Samples were pipetted onto precleaned and pre-conditioned

Dowex 50 x 8 exchange resin contained in glass columns which accept about 10g resin. About 75 mls of acid is passed through these columns before strontium is eluted. After elution Sr is dried, converted to nitrate with a few drops of double distilled HNO_3, and dried again prior to loading onto filaments for mass spectrometric analysis.

Sr isotope determinations were performed on a V.G. Micromass 30 mass spectrometer. The Micromass 30 (MM30) has a 30cm radius of curvature (90° field sector). The instrument is equipped with on-line data collection and reduction and peak switching capabilities. Ion detection and signal amplification on the MM30 is with a Daly detector and a Faraday cup. Accelerating voltage is 8000V and peak measurement times and delay times between peaks are 4.7 and 5.0 seconds respectively.

Samples were loaded using clean pyrex glass pipettes and double distilled HNO_3. A single tantalum filament configuration was used. Prior to loading filaments were cleaned in an ultrasonic bath by succesive immersion in Contrad, distilled water, alcohol and acetone followed by outgassing. This consists of passing successive 2.5, 4.0-4.5 and 2.0 ampere currents through each filament under high vacuum in three 15 minute pulses.

Each filament were coated with a small amount of phosphoric acid before addition of sample. This oxidises the surface layer of the Ta and so increases the work function for thermionic emmision of Sr.

Running of samples were accomplished under filament currents of 2.4-2.8A. The sequence of peak measurements for a natural Sr run are baseline, 85(Rb), 86, 87, baseline respectively and an 88/86 rato of 8.375 are used to correct for thermal isotopic fractionation effects. Each block of data comprises 9 cycles through the sequence.

Analyses consisted of a number of individual block means and standard deviations (about 7 to 10 per sample) from which a combined mean and standard deviation were calculated. An upper limit of .0003 for the standard deviation was used as a means of selecting blocks suitable for inclusion in final data reduction.

APPENDIX 4, 5 & 6

MINERAL ANALYSES

INDEX

OBS = Observation number
NO = Sample number (refer to OBS)
MINSPENO = Mineral ID/grain number/analysis number
ANALPOS = Analytical position
WO = Mole% wollastonite
DI = Mole% diopside
FS = Mole% ferrosilite
FO = Mole% forsterite
FFM = $Fe^{2+}/(Fe^{2+}+Mg)$
CCA = Cr/(Cr+Al)
2TAC = 2Ti/(2Ti+Al+Cr)

ANALPOS indicates crystal type:
S = Single or simple crystal
K = Kernal of crystal which has mantle
M = Mantle
The above symbols are only used in zonation studies.
For spot analyses on simple crystals:
C = Core
I = Position intermediate between core and rim
R = Rim
All measurements are in microns and were measured from the core of the grain towards the analytical position.
For example:
SI/C-1333 indicates an intermediate position 1333 microns away from the core of a simple crystal.

APPENDIX 4

CLINOPYROXENE ANALYSES

INDEX

Sample	Clinopyroxene	Description
83	1-10	cpx in vesicle
160	35-39;41-42	cpx in vesicle

APPENDIX 4
CLINOPYROXENE ANALYSES

OBS	1	2	3	4	5	6	7	8
SIO2	51.33	51.47	51.04	50.92	51.26	50.95	49.83	50.38
TIO2	1.67	1.52	1.55	1.60	1.58	1.64	2.14	1.92
AL2O3	1.21	0.79	1.13	1.51	1.17	1.45	1.89	1.51
CR2O3	0.00	0.00	0.00	0.00	0.00	0.00	0.00	0.00
FEOT	5.26	5.27	5.57	5.17	6.00	5.78	7.04	5.40
MNO	0.13	0.16	0.18	0.13	0.18	0.17	0.18	0.15
MGO	15.26	15.13	14.97	15.20	15.06	14.94	13.83	15.29
CAO	23.57	23.42	23.89	23.79	23.66	23.48	23.08	23.65
NA2O	0.62	0.73	0.58	0.60	0.58	0.59	0.76	0.59
K2O	0.00	0.06	0.03	0.05	0.02	0.00	0.03	0.00
TOTAL	99.05	98.55	98.94	98.97	99.51	99.00	98.78	98.89

** ATOMIC PROPORTIONS BASED ON SELECTED NO. OF OXYGENS **

OXYGN	6	6	6	6	6	6	6	6
SI	1.920	1.936	1.917	1.908	1.916	1.912	1.888	1.893
TI	0.047	0.043	0.044	0.045	0.044	0.046	0.061	0.054
AL	0.053	0.035	0.050	0.067	0.052	0.064	0.084	0.067
CR	0.000	0.000	0.000	0.000	0.000	0.000	0.000	0.000
FE	0.165	0.166	0.175	0.162	0.188	0.181	0.223	0.170
MN	0.004	0.005	0.006	0.004	0.006	0.005	0.006	0.005
MG	0.851	0.848	0.838	0.849	0.839	0.835	0.781	0.856
CA	0.945	0.944	0.962	0.955	0.948	0.944	0.937	0.952
NA	0.045	0.053	0.042	0.044	0.042	0.043	0.056	0.043
K	0.000	0.003	0.001	0.002	0.001	0.000	0.001	0.000
WO	48.10	48.09	48.56	48.48	47.86	48.01	48.13	48.02
DI	43.31	43.21	42.32	43.08	42.37	42.49	40.11	43.18
FS	8.59	8.71	9.13	8.43	9.76	9.50	11.76	8.80

**** SAMPLE DIRECTORY ****

OBS	NO	MINSPENO	ANALPOS	OBS	NO	MINSPENO	ANALPOS
1	30	CPX/001/001	C	2	30	CPX/001/002	R
3	30	CPX/002/001	I	4	30	CPX/003/001	R
5	30	CPX/004/001	C	6	30	CPX/005/001	C
7	30	CPX/006/001	C	8	30	CPX/007/001	I

APPENDIX 4
CLINOPYROXENE ANALYSES

OBS	9	10	11	12	13	14	15	16
SIO2	48.44	48.03	50.52	45.16	47.27	49.66	52.61	47.31
TIO2	2.84	3.24	1.63	4.87	3.66	2.34	0.66	3.23
AL2O3	2.79	3.11	1.30	6.04	4.00	2.32	0.27	3.67
CR2O3	0.00	0.00	0.00	0.00	0.00	0.00	0.00	0.00
FEOT	7.47	7.59	6.55	8.44	7.48	7.40	4.95	7.46
MNO	0.17	0.18	0.20	0.12	0.16	0.24	0.15	0.16
MGO	13.64	13.29	14.62	12.08	12.85	13.87	15.71	13.05
CAO	22.84	22.57	23.50	22.91	23.06	23.25	24.14	23.13
NA2O	0.83	0.92	0.59	0.81	0.84	0.86	0.56	0.79
K2O	0.00	0.00	0.00	0.00	0.00	0.00	0.00	0.00
TOTAL	99.02	98.93	98.91	100.43	99.32	99.94	99.05	98.80

** ATOMIC PROPORTIONS BASED ON SELECTED NO. OF OXYGENS **

OXYGN	6	6	6	6	6	6	6	6
SI	1.839	1.826	1.907	1.706	1.793	1.865	1.963	1.804
TI	0.081	0.093	0.046	0.138	0.104	0.066	0.019	0.093
AL	0.125	0.139	0.058	0.269	0.179	0.103	0.012	0.165
CR	0.000	0.000	0.000	0.000	0.000	0.000	0.000	0.000
FE	0.237	0.241	0.207	0.267	0.237	0.232	0.154	0.238
MN	0.005	0.006	0.006	0.004	0.005	0.008	0.005	0.005
MG	0.772	0.753	0.822	0.680	0.726	0.776	0.874	0.742
CA	0.929	0.919	0.950	0.927	0.937	0.936	0.965	0.945
NA	0.061	0.068	0.043	0.059	0.062	0.063	0.041	0.058
K	0.000	0.000	0.000	0.000	0.000	0.000	0.000	0.000
WO	47.81	47.90	47.86	49.38	49.17	47.93	48.31	48.97
DI	39.71	39.23	41.41	36.22	38.11	39.77	43.73	38.43
FS	12.48	12.87	10.73	14.40	12.72	12.30	7.97	12.60

**** SAMPLE DIRECTORY ****

OBS	NO	MINSPENO	ANALPOS	OBS	NO	MINSPENO	ANALPOS
9	30	CPX/008/001	C	10	30	CPX/009/001	I
11	30	CPX/010/001	C	12	83	CPX/001/001	C
13	83	CPX/001/002	R	14	83	CPX/002/001	C
15	83	CPX/002/002	R	16	83	CPX/003/001	C

APPENDIX 4
CLINOPYROXENE ANALYSES

OBS	17	18	19	20	21	22	23	24
SIO2	48.44	51.24	51.39	46.91	48.72	49.85	51.46	52.04
TIO2	2.78	1.24	1.50	3.52	2.55	2.25	1.81	1.15
AL2O3	2.90	1.37	0.89	4.04	2.61	1.92	0.96	0.63
CR2O3	0.00	0.00	0.00	0.00	0.00	0.00	0.00	0.00
FEOT	7.55	6.17	6.16	7.63	7.26	6.98	6.12	5.78
MNO	0.10	0.20	0.19	0.13	0.17	0.15	0.23	0.23
MGO	13.48	14.94	14.93	12.86	13.56	14.20	15.04	15.23
CAO	23.26	24.01	23.65	23.04	23.11	23.08	23.21	23.69
NA2O	0.72	0.45	0.65	0.80	0.71	0.89	0.84	0.54
K2O	0.00	0.00	0.00	0.00	0.00	0.00	0.02	0.00
TOTAL	99.23	99.62	99.36	98.93	98.69	99.32	99.69	99.29

** ATOMIC PROPORTIONS BASED ON SELECTED NO. OF OXYGENS **

OXYGN	6	6	6	6	6	6	6	6
SI	1.836	1.915	1.925	1.788	1.853	1.879	1.921	1.945
TI	0.079	0.035	0.042	0.101	0.073	0.064	0.051	0.032
AL	0.130	0.060	0.039	0.182	0.117	0.085	0.042	0.028
CR	0.000	0.000	0.000	0.000	0.000	0.000	0.000	0.000
FE	0.239	0.193	0.193	0.243	0.231	0.220	0.191	0.181
MN	0.003	0.006	0.006	0.004	0.005	0.005	0.007	0.007
MG	0.761	0.832	0.834	0.731	0.769	0.798	0.837	0.848
CA	0.945	0.962	0.949	0.941	0.942	0.932	0.928	0.949
NA	0.053	0.033	0.047	0.059	0.052	0.065	0.061	0.039
K	0.000	0.000	0.000	0.000	0.000	0.000	0.001	0.000
WO	48.48	48.25	47.90	49.04	48.38	47.69	47.28	47.79
DI	39.08	41.76	42.06	38.07	39.48	40.81	42.62	42.74
FS	12.45	10.00	10.04	12.89	12.14	11.50	10.10	9.47

**** SAMPLE DIRECTORY ****

OBS	NO	MINSPENO	ANALPOS	OBS	NO	MINSPENO	ANALPOS
17	83	CPX/003/002	R	18	83	CPX/004/001	C
19	83	CPX/005/001	C	20	83	CPX/006/001	C
21	83	CPX/007/001	C	22	83	CPX/008/001	I
23	83	CPX/009/001	I	24	83	CPX/010/001	C

APPENDIX 4
CLINOPYROXENE ANALYSES

OBS	25	26	27	28	29	30	31	32
SIO2	48.66	52.72	50.17	52.48	48.38	50.03	52.76	52.40
TIO2	3.55	1.19	2.29	1.11	2.75	2.43	1.34	1.55
AL2O3	3.15	0.45	1.32	0.30	3.63	2.71	0.25	0.55
CR2O3	0.00	0.06	0.00	0.00	0.18	0.20	0.00	0.00
FEOT	5.65	4.78	5.50	5.18	4.88	4.99	5.20	5.53
MNO	0.08	0.00	0.14	0.13	0.09	0.00	0.08	0.09
MGO	14.59	15.86	15.02	15.60	14.66	15.11	15.32	15.26
CAO	23.57	23.80	23.54	23.82	23.68	23.60	23.32	23.52
NA2O	0.54	0.39	0.57	0.46	0.37	0.44	0.59	0.55
K2O	0.00	0.06	0.00	0.00	0.00	0.00	0.00	0.00
TOTAL	99.79	99.31	98.55	99.08	98.62	99.51	98.86	99.45

** ATOMIC PROPORTIONS BASED ON SELECTED NO. OF OXYGENS **

OXYGN	6	6	6	6	6	6	6	6
SI	1.819	1.957	1.893	1.958	1.823	1.863	1.969	1.949
TI	0.100	0.033	0.065	0.031	0.078	0.068	0.038	0.043
AL	0.139	0.020	0.059	0.013	0.161	0.119	0.011	0.024
CR	0.000	0.002	0.000	0.000	0.005	0.006	0.000	0.000
FE	0.177	0.148	0.174	0.162	0.154	0.155	0.162	0.172
MN	0.003	0.000	0.004	0.004	0.003	0.000	0.003	0.003
MG	0.813	0.877	0.845	0.867	0.823	0.838	0.852	0.846
CA	0.944	0.947	0.952	0.952	0.956	0.942	0.932	0.938
NA	0.039	0.028	0.042	0.033	0.027	0.032	0.043	0.040
K	0.000	0.003	0.000	0.000	0.000	0.000	0.000	0.000
WO	48.76	47.99	48.20	47.96	49.38	48.65	47.84	47.87
DI	41.98	44.48	42.78	43.69	42.52	43.32	43.71	43.20
FS	9.25	7.52	9.02	8.35	8.09	8.03	8.46	8.93

**** SAMPLE DIRECTORY ****

OBS	NO	MINSPENO	ANALPOS	OBS	NO	MINSPENO	ANALPOS
25	155	CPX/001/001	C	26	155	CPX/001/002	R
27	155	CPX/002/001	C	28	155	CPX/002/002	R
29	155	CPX/003/001	C	30	155	CPX/003/002	R
31	155	CPX/004/001	C	32	155	CPX/004/002	R

APPENDIX 4
CLINOPYROXENE ANALYSES

OBS	33	34	35	36	37	38	39	40
SIO2	51.60	52.97	51.19	53.09	53.88	50.94	52.03	50.99
TIO2	2.46	1.48	2.21	0.54	0.41	1.69	2.18	2.13
AL2O3	1.06	0.21	1.37	0.43	0.13	1.44	0.56	1.67
CR2O3	0.05	0.00	0.00	0.00	0.08	0.10	0.00	0.00
FEOT	4.53	3.94	5.22	4.41	4.06	5.03	4.84	6.01
MNO	0.11	0.12	0.08	0.00	0.08	0.08	0.12	0.17
MGO	15.91	16.26	15.30	16.15	16.27	15.56	15.52	14.43
CAO	23.09	23.26	22.76	24.26	23.96	24.02	23.35	23.92
NA2O	0.63	0.69	0.61	0.39	0.37	0.31	0.58	0.69
K2O	0.00	0.00	0.00	0.00	0.00	0.03	0.00	0.00
TOTAL	99.44	98.93	98.74	99.27	99.24	99.20	99.18	100.01

** ATOMIC PROPORTIONS BASED ON SELECTED NO. OF OXYGENS **

OXYGN	6	6	6	6	6	6	6	6
SI	1.914	1.965	1.916	1.968	1.990	1.903	1.937	1.899
TI	0.069	0.041	0.062	0.015	0.011	0.047	0.061	0.060
AL	0.046	0.009	0.060	0.019	0.006	0.063	0.025	0.073
CR	0.001	0.000	0.000	0.000	0.002	0.003	0.000	0.000
FE	0.141	0.122	0.163	0.137	0.125	0.157	0.151	0.187
MN	0.003	0.004	0.003	0.000	0.003	0.003	0.004	0.005
MG	0.879	0.899	0.853	0.892	0.896	0.866	0.861	0.801
CA	0.918	0.924	0.913	0.963	0.948	0.962	0.931	0.955
NA	0.045	0.050	0.044	0.028	0.026	0.022	0.042	0.050
K	0.000	0.000	0.000	0.000	0.000	0.001	0.000	0.000
WO	47.28	47.43	47.24	48.36	48.09	48.38	47.84	49.00
DI	45.31	46.11	44.17	44.78	45.42	43.59	44.23	41.11
FS	7.42	6.46	8.59	6.86	6.49	8.03	7.93	9.88

**** SAMPLE DIRECTORY ****

OBS	NO	MINSPENO	ANALPOS	OBS	NO	MINSPENO	ANALPOS
33	155	CPX/005/001	C	34	155	CPX/005/002	R
35	155	CPX/006/001	C	36	155	CPX/007/001	C
37	155	CPX/008/001	I	38	155	CPX/009/001	C
39	155	CPX/010/001	C	40	160	CPX/001/001	C

APPENDIX 4
CLINOPYROXENE ANALYSES

OBS	41	42	43	44	45	46	47	48
SIO2	51.21	51.12	53.23	48.18	43.48	48.55	52.58	46.03
TIO2	1.88	2.04	1.06	3.10	4.69	2.58	1.40	3.83
AL2O3	1.23	1.64	0.44	3.62	6.49	3.34	0.75	4.60
CR2O3	0.00	0.00	0.00	0.00	0.00	0.00	0.00	0.00
FEOT	5.96	6.00	4.86	6.69	7.83	6.49	5.36	7.51
MNO	0.13	0.15	0.14	0.17	0.12	0.14	0.16	0.15
MGO	14.61	14.40	15.58	13.44	12.01	13.62	15.40	12.93
CAO	23.58	23.70	24.09	23.57	23.24	23.75	23.99	23.66
NA2O	0.76	0.68	0.65	0.64	0.69	0.60	0.69	0.67
K2O	0.00	0.00	0.00	0.00	0.00	0.00	0.00	0.05
TOTAL	99.36	99.73	100.05	99.41	98.55	99.07	100.33	99.43

** ATOMIC PROPORTIONS BASED ON SELECTED NO. OF OXYGENS **

OXYGN	6	6	6	6	6	6	6	6
SI	1.917	1.907	1.963	1.817	1.676	1.835	1.941	1.752
TI	0.053	0.057	0.029	0.088	0.136	0.073	0.039	0.110
AL	0.054	0.072	0.019	0.161	0.295	0.149	0.033	0.206
CR	0.000	0.000	0.000	0.000	0.000	0.000	0.000	0.000
FE	0.187	0.187	0.150	0.211	0.252	0.205	0.165	0.239
MN	0.004	0.005	0.004	0.005	0.004	0.004	0.005	0.005
MG	0.815	0.800	0.856	0.756	0.690	0.767	0.847	0.733
CA	0.946	0.947	0.952	0.953	0.960	0.962	0.949	0.965
NA	0.055	0.049	0.046	0.047	0.052	0.044	0.049	0.049
K	0.000	0.000	0.000	0.000	0.000	0.000	0.000	0.002
WO	48.46	48.84	48.51	49.50	50.36	49.61	48.25	49.68
DI	41.76	41.27	43.63	39.26	36.20	39.57	43.08	37.76
FS	9.77	9.89	7.86	11.25	13.45	10.81	8.67	12.56

**** SAMPLE DIRECTORY ****

OBS	NO	MINSPENO	ANALPOS	OBS	NO	MINSPENO	ANALPOS
41	160	CPX/001/002	R	42	160	CPX/002/001	C
43	160	CPX/002/002	R	44	160	CPX/003/001	C
45	160	CPX/004/001	C	46	160	CPX/005/001	C
47	160	CPX/005/002	R	48	160	CPX/006/001	I

APPENDIX 4
CLINOPYROXENE ANALYSES

OBS	49	50	51	52	53	54	55	56
SIO2	50.03	51.83	48.37	51.67	46.31	48.20	48.29	50.02
TIO2	2.13	1.30	3.09	1.64	3.61	3.09	3.06	2.11
AL2O3	1.62	0.94	3.26	1.06	4.65	3.25	2.94	2.14
CR2O3	0.00	0.00	0.00	0.00	0.00	0.00	0.00	0.00
FEOT	5.85	5.12	6.72	5.74	7.13	6.76	6.91	6.27
MNO	0.16	0.14	0.15	0.15	0.15	0.17	0.16	0.19
MGO	14.70	15.34	13.58	14.67	12.95	13.60	13.57	14.34
CAO	23.63	24.28	23.47	23.67	23.62	23.61	23.46	23.97
NA2O	0.70	0.52	0.69	0.71	0.70	0.73	0.71	0.66
K2O	0.00	0.00	0.00	0.04	0.00	0.00	0.02	0.00
TOTAL	98.82	99.47	99.33	99.35	99.12	99.41	99.12	99.70

** ATOMIC PROPORTIONS BASED ON SELECTED NO. OF OXYGENS **

OXYGN	6	6	6	6	6	6	6	6
SI	1.887	1.931	1.826	1.931	1.763	1.820	1.830	1.875
TI	0.060	0.036	0.088	0.046	0.103	0.088	0.087	0.059
AL	0.072	0.041	0.145	0.047	0.209	0.145	0.131	0.095
CR	0.000	0.000	0.000	0.000	0.000	0.000	0.000	0.000
FE	0.185	0.160	0.212	0.179	0.227	0.214	0.219	0.197
MN	0.005	0.004	0.005	0.005	0.005	0.005	0.005	0.006
MG	0.826	0.852	0.764	0.817	0.735	0.765	0.766	0.801
CA	0.955	0.969	0.949	0.948	0.963	0.955	0.952	0.963
NA	0.051	0.038	0.050	0.051	0.052	0.053	0.052	0.048
K	0.000	0.000	0.000	0.002	0.000	0.000	0.001	0.000
WO	48.45	48.83	49.18	48.63	49.92	49.25	49.02	48.96
DI	41.92	42.91	39.58	41.92	38.07	39.46	39.44	40.74
FS	9.62	8.26	11.24	9.45	12.01	11.29	11.53	10.30

**** SAMPLE DIRECTORY ****

OBS	NO	MINSPENO	ANALPOS	OBS	NO	MINSPENO	ANALPOS
49	160	CPX/007/001	I	50	160	CPX/008/001	R
51	160	CPX/009/001	I	52	160	CPX/010/001	C
53	160	CPX/011/001	C	54	160	CPX/012/001	C
55	160	CPX/013/001	I	56	160	CPX/014/001	C

APPENDIX 4
CLINOPYROXENE ANALYSES

OBS	57	58	59	60	61	62	63	64
SIO2	49.83	53.32	50.81	52.39	52.68	49.22	51.96	45.81
TIO2	2.51	0.42	2.14	1.14	1.03	2.84	1.28	3.98
AL2O3	2.04	0.16	1.54	0.69	0.56	2.52	0.86	5.21
CR2O3	0.00	0.00	0.00	0.00	0.00	0.00	0.00	0.00
FEOT	6.20	4.00	6.02	5.32	5.49	6.51	5.53	7.57
MNO	0.15	0.11	0.18	0.24	0.15	0.14	0.18	0.14
MGO	14.36	16.16	14.62	15.16	15.28	14.03	15.39	12.50
CAO	23.68	24.47	23.69	24.13	24.14	23.73	24.19	23.30
NA2O	0.76	0.61	0.68	0.54	0.59	0.66	0.42	0.64
K2O	0.00	0.03	0.03	0.00	0.00	0.00	0.00	0.00
TOTAL	99.53	99.28	99.71	99.61	99.92	99.65	99.81	99.15

** ATOMIC PROPORTIONS BASED ON SELECTED NO. OF OXYGENS **

OXYGN	6	6	6	6	6	6	6	6
SI	1.870	1.976	1.898	1.948	1.953	1.849	1.932	1.745
TI	0.071	0.012	0.060	0.032	0.029	0.080	0.036	0.114
AL	0.090	0.007	0.068	0.030	0.024	0.112	0.038	0.234
CR	0.000	0.000	0.000	0.000	0.000	0.000	0.000	0.000
FE	0.195	0.124	0.188	0.165	0.170	0.205	0.172	0.241
MN	0.005	0.003	0.006	0.008	0.005	0.004	0.006	0.005
MG	0.803	0.893	0.814	0.840	0.844	0.786	0.853	0.710
CA	0.952	0.972	0.948	0.962	0.959	0.955	0.964	0.951
NA	0.055	0.044	0.049	0.039	0.042	0.048	0.030	0.047
K	0.000	0.001	0.001	0.000	0.000	0.000	0.000	0.000
WO	48.71	48.79	48.48	48.69	48.48	48.99	48.33	49.89
DI	41.09	44.81	41.61	42.55	42.68	40.29	42.76	37.22
FS	10.20	6.40	9.91	8.76	8.84	10.72	8.91	12.89

**** SAMPLE DIRECTORY ****

OBS	NO	MINSPENO	ANALPOS	OBS	NO	MINSPENO	ANALPOS
57	160	CPX/015/001	C	58	160	CPX/015/002	R
59	160	CPX/016/001	I	60	160	CPX/017/001	I
61	160	CPX/018/001	C	62	160	CPX/019/001	C
63	160	CPX/019/002	R	64	160	CPX/020/001	I

APPENDIX 4
CLINOPYROXENE ANALYSES

OBS	65	66	67	68	69	70	71	72
SIO2	48.96	51.37	49.49	52.14	52.02	51.29	51.50	48.98
TIO2	2.73	1.49	1.74	1.35	1.13	1.58	1.65	2.79
AL2O3	2.55	1.22	1.78	1.22	0.59	1.35	1.02	2.89
CR2O3	0.00	0.00	0.00	0.00	0.00	0.00	0.00	0.00
FEOT	6.53	5.61	6.12	5.33	5.20	5.75	5.41	6.42
MNO	0.15	0.20	0.22	0.11	0.17	0.20	0.16	0.13
MGO	13.94	14.88	14.50	15.05	15.25	14.64	15.01	13.87
CAO	23.63	24.26	24.29	24.41	24.25	24.25	23.88	23.47
NA2O	0.77	0.51	0.44	0.46	0.56	0.46	0.69	0.65
K2O	0.00	0.00	0.00	0.00	0.00	0.00	0.00	0.00
TOTAL	99.26	99.54	98.58	100.07	99.17	99.52	99.32	99.20

** ATOMIC PROPORTIONS BASED ON SELECTED NO. OF OXYGENS **

OXYGN	6	6	6	6	6	6	6	6
SI	1.848	1.918	1.878	1.931	1.944	1.917	1.924	1.846
TI	0.077	0.042	0.050	0.038	0.032	0.044	0.046	0.079
AL	0.113	0.054	0.080	0.053	0.026	0.059	0.045	0.128
CR	0.000	0.000	0.000	0.000	0.000	0.000	0.000	0.000
FE	0.206	0.175	0.194	0.165	0.163	0.180	0.169	0.202
MN	0.005	0.006	0.007	0.003	0.005	0.006	0.005	0.004
MG	0.784	0.828	0.820	0.830	0.849	0.815	0.836	0.779
CA	0.956	0.971	0.988	0.968	0.971	0.971	0.956	0.948
NA	0.056	0.037	0.032	0.033	0.041	0.033	0.050	0.048
K	0.000	0.000	0.000	0.000	0.000	0.000	0.000	0.000
WO	48.99	49.02	49.16	49.22	48.84	49.23	48.63	49.02
DI	40.20	41.82	40.82	42.21	42.72	41.34	42.51	40.30
FS	10.81	9.17	10.02	8.56	8.44	9.43	8.86	10.68

**** SAMPLE DIRECTORY ****

OBS	NO	MINSPENO	ANALPOS	OBS	NO	MINSPENO	ANALPOS
65	160	CPX/021/001	I	66	160	CPX/022/001	C
67	160	CPX/023/001	I	68	160	CPX/024/001	I
69	160	CPX/025/001	C	70	160	CPX/026/001	C
71	160	CPX/026/002	R	72	160	CPX/027/001	C

APPENDIX 4
CLINOPYROXENE ANALYSES

OBS	73	74	75	76	77	78	79	80
SIO2	48.75	52.55	49.24	42.62	51.16	45.38	43.19	52.10
TIO2	2.70	0.98	2.46	4.95	1.71	4.09	5.13	1.26
AL2O3	2.63	0.50	3.35	6.95	1.67	6.09	6.99	0.87
CR2O3	0.00	0.00	0.00	0.00	0.00	0.00	0.00	0.00
FEOT	6.83	5.29	6.35	8.20	5.73	7.56	8.14	5.55
MNO	0.11	0.17	0.15	0.11	0.13	0.13	0.14	0.15
MGO	13.91	15.29	13.67	11.65	14.73	12.27	11.78	15.35
CAO	23.83	24.36	23.76	23.54	23.99	23.47	23.35	24.42
NA2O	0.67	0.54	0.64	0.61	0.53	0.62	0.64	0.42
K2O	0.00	0.00	0.00	0.00	0.00	0.00	0.00	0.00
TOTAL	99.43	99.68	99.62	98.63	99.65	99.61	99.36	100.12

** ATOMIC PROPORTIONS BASED ON SELECTED NO. OF OXYGENS **

CXYGN	6	6	6	6	6	6	6	6
SI	1.840	1.953	1.847	1.649	1.908	1.722	1.655	1.931
TI	0.077	0.027	0.069	0.144	0.048	0.117	0.148	0.035
AL	0.117	0.022	0.148	0.317	0.073	0.272	0.316	0.038
CR	0.000	0.000	0.000	0.000	0.000	0.000	0.000	0.000
FE	0.216	0.164	0.199	0.265	0.179	0.240	0.261	0.172
MN	0.004	0.005	0.005	0.004	0.004	0.004	0.005	0.005
MG	0.783	0.847	0.764	0.672	0.819	0.694	0.673	0.848
CA	0.964	0.970	0.955	0.976	0.958	0.954	0.959	0.970
NA	0.049	0.039	0.047	0.046	0.038	0.046	0.048	0.030
K	0.000	0.000	0.000	0.000	0.000	0.000	0.000	0.000
WO	49.04	48.83	49.66	50.92	48.91	50.43	50.54	48.63
DI	39.81	42.63	39.74	35.05	41.77	36.67	35.47	42.51
FS	11.15	8.55	10.61	14.03	9.33	12.90	13.99	8.86

**** SAMPLE DIRECTORY ****

OBS	NO	MINSPENO	ANALPOS	OBS	NO	MINSPENO	ANALPOS
73	160	CPX/028/001	E	74	160	CPX/029/001	C
75	160	CPX/030/001	I	76	160	CPX/031/001	C
77	160	CPX/031/002	R	78	160	CPX/032/001	C
79	160	CPX/033/001	C	80	160	CPX/034/001	C

APPENDIX 4
CLINOPYROXENE ANALYSES

OBS	81	82	83	84	85	86	87	88
SIO2	51.91	51.87	51.43	52.13	50.87	51.43	46.77	47.04
TIO2	1.11	0.99	1.59	1.18	1.46	1.50	3.55	3.42
AL2O3	0.87	2.92	1.48	0.84	1.59	1.61	4.71	4.53
CR2O3	0.00	0.05	0.00	0.00	0.00	0.00	0.00	0.00
FEOT	7.70	4.94	5.99	5.66	5.48	5.79	6.71	6.59
MNO	0.17	0.13	0.22	0.21	0.17	0.12	0.15	0.18
MGO	13.79	14.42	14.67	14.86	14.86	14.63	13.01	13.04
CAO	23.23	23.42	23.84	24.15	24.10	24.05	23.36	23.49
NA2O	0.86	0.62	0.64	0.50	0.50	0.54	0.66	0.73
K2O	0.00	0.00	0.00	0.00	0.00	0.00	0.00	0.00
TOTAL	99.64	99.36	99.86	99.53	99.03	99.67	98.92	99.02

** ATOMIC PROPORTIONS BASED ON SELECTED NO. OF OXYGENS **

OXYGN	6	6	6	6	6	6	6	6
SI	1.948	1.923	1.916	1.943	1.908	1.917	1.776	1.784
TI	0.031	0.028	0.045	0.033	0.041	0.042	0.101	0.098
AL	0.038	0.128	0.065	0.037	0.070	0.071	0.211	0.203
CR	0.000	0.001	0.000	0.000	0.000	0.000	0.000	0.000
FE	0.242	0.153	0.187	0.176	0.172	0.180	0.213	0.209
MN	0.005	0.004	0.007	0.007	0.005	0.004	0.005	0.006
MG	0.771	0.797	0.814	0.826	0.831	0.813	0.736	0.737
CA	0.934	0.930	0.951	0.965	0.969	0.960	0.950	0.955
NA	0.063	0.045	0.046	0.036	0.036	0.039	0.049	0.054
K	0.000	0.000	0.000	0.000	0.000	0.000	0.000	0.000
WO	47.84	49.37	48.56	48.88	49.00	49.07	49.90	50.07
DI	39.50	42.28	41.56	41.84	42.03	41.52	38.66	38.66
FS	12.65	8.35	9.88	9.28	8.97	9.41	11.44	11.27

**** SAMPLE DIRECTORY ****

OBS	NO	MINSPENO	ANALPOS	OBS	NO	MINSPENO	ANALPOS
81	160	CPX/035/001	C	82	160	CPX/035/002	R
83	160	CPX/036/001	C	84	160	CPX/036/002	R
85	160	CPX/037/001	C	86	160	CPX/037/002	R
87	160	CPX/038/001	I	88	160	CPX/038/002	R

APPENDIX 4
CLINOPYROXENE ANALYSES

OBS	89	90	91	92	93	94	95	96
SIO2	49.92	51.90	52.37	51.87	51.88	50.86	52.07	52.64
TIO2	2.64	1.30	1.31	1.32	1.37	2.10	1.55	1.48
AL2O3	1.97	1.23	0.84	0.89	0.92	1.42	1.03	0.83
CR2O3	0.00	0.00	0.00	0.00	0.00	0.00	0.00	0.00
FEOT	7.22	5.58	5.82	5.70	5.95	6.34	5.85	5.54
MNO	0.21	0.16	0.24	0.14	0.21	0.18	0.15	0.14
MGO	13.42	14.85	14.76	14.71	14.73	14.35	14.86	14.95
CAO	23.18	24.05	24.19	24.13	24.19	23.77	23.94	23.92
NA2O	0.88	0.56	0.52	0.54	0.60	0.78	0.65	0.66
K2O	0.00	0.00	0.00	0.00	0.00	0.00	0.00	0.00
TOTAL	99.44	99.63	100.05	99.30	99.85	99.80	100.10	100.16

** ATOMIC PROPORTIONS BASED ON SELECTED NO. OF OXYGENS **

OXYGN	6	6	6	6	6	6	6	6
SI	1.881	1.932	1.943	1.939	1.933	1.902	1.932	1.946
TI	0.075	0.036	0.037	0.037	0.038	0.059	0.043	0.041
AL	0.088	0.054	0.037	0.039	0.040	0.063	0.045	0.036
CR	0.000	0.000	0.000	0.000	0.000	0.000	0.000	0.000
FE	0.228	0.174	0.181	0.178	0.185	0.198	0.181	0.171
MN	0.007	0.005	0.008	0.004	0.007	0.006	0.005	0.004
MG	0.754	0.824	0.816	0.820	0.818	0.800	0.822	0.824
CA	0.936	0.959	0.962	0.967	0.966	0.952	0.952	0.948
NA	0.064	0.040	0.037	0.039	0.043	0.057	0.047	0.047
K	0.000	0.000	0.000	0.000	0.000	0.000	0.000	0.000
WO	48.65	48.90	48.92	49.10	48.88	48.69	48.57	48.67
DI	39.17	41.99	41.51	41.63	41.40	40.88	41.93	42.31
FS	12.18	9.11	9.57	9.28	9.72	10.43	9.50	9.02

**** SAMPLE DIRECTORY ****

OBS	NO	MINSPENO	ANALPOS	OBS	NO	MINSPENO	ANALPOS
89	160	CPX/039/001	I	90	160	CPX/039/002	R
91	160	CPX/040/001	KC/C-000	92	160	CPX/040/002	KI/C-016
93	160	CPX/040/003	KI/C-032	94	160	CPX/040/004	KB/C-048
95	160	CPX/040/005	MB/C-064	96	160	CPX/040/006	MI/C-080

APPENDIX 4
CLINOPYROXENE ANALYSES

OBS	97	98	99	100	101	102	103	104
SIO2	52.39	52.88	47.42	48.35	50.66	50.17	52.42	53.56
TIO2	1.48	1.11	3.62	3.27	2.30	2.42	1.32	0.44
AL2O3	0.71	0.69	4.31	3.78	1.83	1.88	0.68	0.13
CR2O3	0.00	0.00	0.00	0.00	0.00	0.00	0.00	0.00
FEOT	5.50	4.70	7.26	7.01	6.23	6.44	5.25	3.86
MNO	0.14	0.19	0.13	0.16	0.15	0.17	0.14	0.09
MGO	15.06	15.13	13.04	13.20	14.26	14.19	15.00	15.94
CAO	23.76	24.25	23.15	23.23	23.43	23.38	23.90	24.30
NA2O	0.72	0.71	0.78	0.80	0.78	0.80	0.76	0.67
K2O	0.00	0.00	0.00	0.00	0.00	0.00	0.00	0.00
TOTAL	99.76	99.66	99.71	99.80	99.66	99.45	99.47	98.99

** ATOMIC PROPORTIONS BASED ON SELECTED NO. OF OXYGENS **

OXYGN	6	6	6	6	6	6	6	6
SI	1.945	1.959	1.788	1.817	1.894	1.884	1.951	1.987
TI	0.041	0.031	0.103	0.092	0.065	0.068	0.037	0.012
AL	0.031	0.030	0.192	0.167	0.081	0.083	0.030	0.006
CR	0.000	0.000	0.000	0.000	0.000	0.000	0.000	0.000
FE	0.171	0.146	0.229	0.220	0.195	0.202	0.163	0.120
MN	0.004	0.006	0.004	0.005	0.005	0.005	0.004	0.003
MG	0.833	0.835	0.733	0.739	0.796	0.794	0.832	0.881
CA	0.945	0.963	0.936	0.936	0.939	0.941	0.953	0.966
NA	0.052	0.051	0.057	0.058	0.057	0.058	0.055	0.048
K	0.000	0.000	0.000	0.000	0.000	0.000	0.000	0.000
WO	48.38	49.38	49.20	49.23	48.54	48.43	48.80	49.04
DI	42.65	42.85	38.54	38.91	41.14	40.88	42.60	44.74
FS	8.97	7.78	12.26	11.86	10.32	10.69	8.59	6.22

**** SAMPLE DIRECTORY ****

OBS	NO	MINSPENO	ANALPOS	OBS	NO	MINSPENO	ANALPOS
97	160	CPX/040/007	MI/C-096	98	160	CPX/040/008	ME/C-112
99	160	CPX/041/001	SC/C-000	100	160	CPX/041/002	SI/C-050
101	160	CPX/041/003	SI/C-100	102	160	CPX/041/004	SI/C-150
103	160	CPX/041/005	SI/C-200	104	160	CPX/041/006	SR/C-250

APPENDIX 4
CLINOPYROXENE ANALYSES

OBS	105	106	107	108	109	110	111	112
SIO2	48.96	49.52	50.85	51.12	51.83	51.69	51.32	51.66
TIO2	2.49	2.39	2.03	1.96	1.53	1.51	1.43	1.56
AL2O3	2.62	2.19	1.50	1.42	0.85	1.17	1.22	1.23
CR2O3	0.00	0.00	0.00	0.00	0.00	0.00	0.00	0.00
FEOT	6.29	6.30	5.59	5.92	5.39	5.50	5.64	5.76
MNO	0.16	0.12	0.18	0.13	0.15	0.24	0.21	0.16
MGO	13.76	14.02	14.54	14.35	14.86	14.89	14.81	14.82
CAO	23.49	23.67	23.53	23.75	23.88	24.10	23.92	24.02
NA2O	0.75	0.74	0.71	0.79	0.77	0.53	0.53	0.56
K2O	0.00	0.00	0.00	0.00	0.00	0.00	0.00	0.00
TOTAL	98.52	98.95	98.93	99.44	99.26	99.63	99.08	99.77

** ATOMIC PROPORTIONS BASED ON SELECTED NO. OF OXYGENS **

OXYGN	6	6	6	6	6	6	6	6
SI	1.858	1.870	1.909	1.913	1.937	1.926	1.924	1.923
TI	0.071	0.068	0.057	0.055	0.043	0.042	0.040	0.044
AL	0.117	0.098	0.066	0.063	0.037	0.051	0.054	0.054
CR	0.000	0.000	0.000	0.000	0.000	0.000	0.000	0.000
FE	0.200	0.199	0.176	0.185	0.168	0.171	0.177	0.179
MN	0.005	0.004	0.006	0.004	0.005	0.008	0.007	0.005
MG	0.778	0.789	0.814	0.800	0.827	0.827	0.827	0.822
CA	0.955	0.958	0.947	0.952	0.956	0.962	0.961	0.958
NA	0.055	0.054	0.052	0.057	0.056	0.038	0.039	0.040
K	0.000	0.000	0.000	0.000	0.000	0.000	0.000	0.000
WO	49.28	49.13	48.76	49.04	48.86	48.89	48.73	48.77
DI	40.15	40.47	41.91	41.21	42.29	42.01	41.96	41.85
FS	10.57	10.40	9.34	9.75	8.85	9.09	9.31	9.38

**** SAMPLE DIRECTORY ****

OBS	NO	MINSPENO	ANALPOS	OBS	NO	MINSPENO	ANALPOS
105	160	CPX/042/001	SC/C-000	106	160	CPX/042/002	SI/C-32.5
107	160	CPX/042/003	SI/C-065	108	160	CPX/042/004	SI/C-97.5
109	160	CPX/042/005	SR/C-130	110	160	CPX/043/001	SC/C-0000
111	160	CPX/043/002	SI/C-0040	112	160	CPX/043/003	SI/C-0080

APPENDIX 4
CLINOPYROXENE ANALYSES

OBS	113	114	115	116	117	118	119	120
SIO2	50.30	51.53	50.16	50.07	49.74	51.63	52.43	46.09
TIO2	2.31	1.80	2.15	2.35	2.22	1.48	1.24	3.45
AL2O3	1.84	1.02	2.00	2.04	1.83	0.79	0.53	6.65
CR2O3	0.00	0.00	0.00	0.00	0.00	0.00	0.00	0.00
FEOT	5.94	5.49	5.85	6.08	6.14	5.11	4.86	6.66
MNO	0.20	0.17	0.17	0.15	0.17	0.17	0.18	0.08
MGO	14.38	14.92	14.23	14.28	14.24	14.98	15.28	13.26
CAO	23.78	23.63	23.71	23.60	23.47	23.82	23.95	23.98
NA2O	0.78	0.79	0.65	0.74	0.82	0.69	0.78	0.29
K2O	0.00	0.00	0.00	0.00	0.00	0.00	0.03	0.16
TOTAL	99.53	99.35	98.92	99.31	98.63	98.67	99.28	100.62

** ATOMIC PROPORTIONS BASED ON SELECTED NO. OF OXYGENS **

OXYGN	6	6	6	6	6	6	6	6
SI	1.885	1.925	1.888	1.880	1.883	1.938	1.953	1.722
TI	0.065	0.051	0.061	0.066	0.063	0.042	0.035	0.097
AL	0.081	0.045	0.089	0.090	0.082	0.035	0.023	0.293
CR	0.000	0.000	0.000	0.000	0.000	0.000	0.000	0.000
FE	0.186	0.172	0.184	0.191	0.194	0.160	0.151	0.208
MN	0.006	0.005	0.005	0.005	0.005	0.005	0.006	0.003
MG	0.803	0.831	0.798	0.799	0.803	0.838	0.848	0.738
CA	0.955	0.946	0.956	0.950	0.952	0.958	0.956	0.960
NA	0.057	0.057	0.047	0.054	0.060	0.050	0.056	0.021
K	0.000	0.000	0.000	0.000	0.000	0.000	0.001	0.008
WO	48.96	48.42	49.19	48.84	48.69	48.83	48.74	50.29
DI	41.17	42.52	41.06	41.10	41.09	42.71	43.25	38.68
FS	9.87	9.06	9.75	10.07	10.22	8.45	8.01	11.03

**** SAMPLE DIRECTORY ****

OBS	NO	MINSPENO	ANALPOS	OBS	NO	MINSPENO	ANALPOS
113	160	CPX/043/004	SI/C-0120	114	160	CPX/043/005	SI/C-0160
115	160	CPX/044/001	SC/C-0000	116	160	CPX/044/002	SI/C-0019
117	160	CPX/044/003	SI/C-0036	118	160	CPX/044/004	SI/C-0055
119	160	CPX/044/005	SR/C-0074	120	267	CPX/001/001	C

APPENDIX 4
CLINOPYROXENE ANALYSES

OBS	121	122	123	124	125	126	127	128
SIO2	42.18	51.13	52.66	52.74	50.16	50.06	53.32	45.95
TIO2	4.39	0.85	1.11	0.96	1.77	2.10	0.67	3.36
AL2O3	10.99	0.98	1.33	1.08	3.51	3.61	0.70	7.41
CR2O3	0.00	0.00	0.00	0.00	0.00	0.08	0.06	0.00
FEOT	8.40	5.98	6.06	5.78	6.00	5.28	5.76	6.89
MNO	0.00	0.17	0.19	0.17	0.18	0.11	0.15	0.16
MGO	12.80	15.43	14.91	15.04	14.37	14.56	14.86	12.49
CAO	21.75	23.93	23.59	23.89	23.26	23.61	24.01	23.45
NA2O	0.40	0.37	0.46	0.37	0.48	0.33	0.44	0.44
K2O	0.07	0.00	0.00	0.00	0.00	0.00	0.00	0.00
TOTAL	100.98	98.84	100.31	100.03	99.73	99.74	99.97	100.15

** ATOMIC PROPORTIONS BASED ON SELECTED NO. OF OXYGENS **

OXYGN	6	6	6	6	6	6	6	6
SI	1.579	1.924	1.944	1.951	1.867	1.859	1.972	1.722
TI	0.124	0.024	0.031	0.027	0.050	0.059	0.019	0.095
AL	0.485	0.043	0.058	0.047	0.154	0.158	0.031	0.327
CR	0.000	0.000	0.000	0.000	0.000	0.002	0.002	0.000
FE	0.263	0.188	0.187	0.179	0.187	0.164	0.178	0.216
MN	0.000	0.005	0.006	0.005	0.006	0.003	0.005	0.005
MG	0.714	0.866	0.820	0.829	0.797	0.806	0.819	0.697
CA	0.873	0.965	0.933	0.947	0.928	0.939	0.952	0.942
NA	0.029	0.027	0.033	0.027	0.035	0.024	0.032	0.032
K	0.003	0.000	0.000	0.000	0.000	0.000	0.000	0.000
WO	47.17	47.68	47.94	48.31	48.39	49.12	48.71	50.62
DI	38.61	42.76	42.14	42.30	41.58	42.13	41.93	37.50
FS	14.22	9.57	9.92	9.39	10.04	8.75	9.36	11.88

**** SAMPLE DIRECTORY ****

OBS	NO	MINSPENO	ANALPOS	OBS	NO	MINSPENO	ANALPOS
121	267	CPX/001/002	R	122	267	CPX/002/001	C
123	267	CPX/003/001	C	124	267	CPX/004/001	C
125	267	CPX/004/002	R	126	267	CPX/005/001	C
127	267	CPX/006/001	C	128	267	CPX/007/001	C

APPENDIX 4
CLINOPYROXENE ANALYSES

OBS	129	130	131	132	133	134	135	136
SIO2	47.76	50.48	48.90	48.00	45.89	47.17	45.68	48.49
TIO2	2.97	1.94	2.70	3.20	3.37	3.22	3.80	2.78
AL2O3	6.01	3.11	4.24	5.16	7.76	5.81	6.89	4.34
CR2O3	0.00	0.00	0.12	0.08	0.00	0.12	0.00	0.00
FEOT	6.69	5.71	5.71	6.33	7.39	6.05	7.65	7.52
MNO	0.18	0.13	0.11	0.00	0.18	0.12	0.13	0.15
MGO	13.14	14.60	13.91	13.50	11.94	13.31	12.34	12.74
CAO	22.85	23.84	24.10	24.12	23.72	23.80	23.89	23.67
NA2O	0.49	0.35	0.38	0.41	0.44	0.38	0.38	0.44
K2O	0.00	0.00	0.00	0.00	0.00	0.00	0.00	0.00
TOTAL	100.09	100.16	100.17	100.80	100.69	99.98	100.76	100.13

** ATOMIC PROPORTIONS BASED ON SELECTED NO. OF OXYGENS **

OXYGN	6	6	6	6	6	6	6	6
SI	1.781	1.871	1.819	1.781	1.715	1.764	1.712	1.818
TI	0.083	0.054	0.076	0.089	0.095	0.091	0.107	0.078
AL	0.264	0.136	0.186	0.226	0.342	0.256	0.304	0.192
CR	0.000	0.000	0.004	0.002	0.000	0.004	0.000	0.000
FE	0.209	0.177	0.178	0.196	0.231	0.189	0.240	0.236
MN	0.006	0.004	0.003	0.000	0.006	0.004	0.004	0.005
MG	0.730	0.806	0.771	0.747	0.665	0.742	0.689	0.712
CA	0.913	0.947	0.961	0.959	0.950	0.954	0.959	0.951
NA	0.035	0.025	0.027	0.030	0.032	0.028	0.028	0.032
K	0.000	0.000	0.000	0.000	0.000	0.000	0.000	0.000
WO	49.15	48.95	50.22	50.42	51.30	50.50	50.69	49.96
DI	39.31	41.69	40.31	39.25	35.92	39.28	36.42	37.40
FS	11.54	9.36	9.47	10.33	12.78	10.22	12.89	12.64

**** SAMPLE DIRECTORY ****

OBS	NO	MINSPENO	ANALPOS	OBS	NO	MINSPENO	ANALPOS
129	267	CPX/007/002	R	130	267	CPX/008/001	C
131	267	CPX/009/001	C	132	267	CPX/010/001	C
133	267	CPX/010/002	R	134	267	CPX/011/001	C
135	267	CPX/012/001	I	136	267	CPX/013/001	C

APPENDIX 4
CLINOPYROXENE ANALYSES

OBS	137	138	139	140	141	142	143	144
SIO2	45.53	45.36	46.23	45.58	45.40	52.37	52.21	52.66
TIO2	3.66	3.96	3.58	3.75	3.72	1.12	1.38	1.10
AL2O3	7.11	7.47	6.72	7.36	7.45	1.29	1.79	1.38
CR2O3	0.00	0.00	0.00	0.00	0.00	0.20	0.12	0.14
FEOT	7.55	7.16	6.75	6.52	6.69	6.07	6.14	5.34
MNO	0.10	0.10	0.00	0.00	0.12	0.14	0.10	0.13
MGO	12.31	12.58	13.12	12.63	12.83	15.72	15.85	16.21
CAO	23.72	24.17	24.04	24.23	24.14	23.18	23.13	23.15
NA2O	0.37	0.33	0.38	0.30	0.31	0.39	0.42	0.41
K2O	0.00	0.00	0.00	0.00	0.03	0.00	0.00	0.00
TOTAL	100.35	101.13	100.82	100.37	100.69	100.48	101.14	100.52

** ATOMIC PROPORTIONS BASED ON SELECTED NO. OF OXYGENS **

OXYGN	6	6	6	6	6	6	6	6
SI	1.711	1.691	1.722	1.706	1.696	1.930	1.912	1.932
TI	0.103	0.111	0.100	0.106	0.105	0.031	0.038	0.030
AL	0.315	0.328	0.295	0.325	0.328	0.056	0.077	0.060
CR	0.000	0.000	0.000	0.000	0.000	0.006	0.003	0.004
FE	0.237	0.223	0.210	0.204	0.209	0.187	0.188	0.164
MN	0.003	0.003	0.000	0.000	0.004	0.004	0.003	0.004
MG	0.689	0.699	0.728	0.704	0.714	0.864	0.865	0.886
CA	0.955	0.966	0.960	0.972	0.967	0.915	0.908	0.910
NA	0.027	0.024	0.027	0.022	0.022	0.028	0.030	0.029
K	0.000	0.000	0.000	0.000	0.001	0.000	0.000	0.000
WO	50.67	51.06	50.55	51.68	51.03	46.46	46.22	46.33
DI	36.57	36.96	38.37	37.47	37.73	43.82	44.05	45.12
FS	12.76	11.97	11.08	10.85	11.24	9.72	9.73	8.55

**** SAMPLE DIRECTORY ****

OBS	NO	MINSPENO	ANALPOS	OBS	NO	MINSPENO	ANALPOS
137	267	CPX/013/002	R	138	267	CPX/014/001	C
139	267	CPX/015/001	C	140	267	CPX/016/001	I
141	267	CPX/017/001	C	142	267	CPX/018/001	C
143	267	CPX/019/001	C	144	267	CPX/020/001	C

APPENDIX 4
CLINOPYROXENE ANALYSES

OBS	145	146	147	148	149	150	151	152
SIO2	51.88	52.31	52.30	52.52	51.76	51.88	50.98	53.39
TIO2	1.11	1.24	0.99	1.15	1.39	1.25	1.55	0.43
AL2O3	1.42	1.63	1.46	1.18	2.06	1.30	2.16	0.40
CR2O3	0.11	0.00	0.00	0.00	0.00	0.05	0.06	0.00
FEOT	6.44	6.94	6.67	6.27	6.24	6.32	6.58	5.80
MNO	0.15	0.16	0.15	0.10	0.16	0.14	0.17	0.14
MGO	16.32	15.75	16.04	15.53	14.76	15.55	14.88	15.85
CAO	22.26	21.76	22.39	23.36	23.23	23.67	22.57	23.78
NA2O	0.40	0.39	0.35	0.38	0.44	0.35	0.44	0.38
K2O	0.00	0.00	0.00	0.00	0.10	0.00	0.27	0.00
TOTAL	100.09	100.18	100.35	100.49	100.14	100.51	99.66	100.17

** ATOMIC PROPORTIONS BASED ON SELECTED NO. OF OXYGENS **

OXYGN	6	6	6	6	6	6	6	6
SI	1.920	1.932	1.930	1.936	1.917	1.918	1.902	1.970
TI	0.031	0.034	0.027	0.032	0.039	0.035	0.043	0.012
AL	0.062	0.071	0.064	0.051	0.090	0.057	0.095	0.017
CR	0.003	0.000	0.000	0.000	0.000	0.001	0.002	0.000
FE	0.199	0.214	0.206	0.193	0.193	0.195	0.205	0.179
MN	0.005	0.005	0.005	0.003	0.005	0.004	0.005	0.004
MG	0.900	0.867	0.882	0.853	0.815	0.857	0.828	0.872
CA	0.883	0.861	0.885	0.923	0.922	0.938	0.902	0.940
NA	0.029	0.028	0.025	0.027	0.032	0.025	0.032	0.027
K	0.000	0.000	0.000	0.000	0.005	0.000	0.013	0.000
WO	44.43	44.22	44.76	46.78	47.65	47.02	46.50	47.12
DI	45.30	44.52	44.60	43.26	42.11	42.96	42.64	43.69
FS	10.27	11.26	10.64	9.96	10.25	10.02	10.86	9.19

**** SAMPLE DIRECTORY ****

OBS	NO	MINSPENO	ANALPOS	OBS	NO	MINSPENO	ANALPOS
145	267	CPX/021/001	C	146	267	CPX/021/002	R
147	267	CPX/022/001	C	148	267	CPX/023/001	C
149	267	CPX/023/002	R	150	267	CPX/024/001	C
151	267	CPX/025/001	C	152	267	CPX/026/001	C

APPENDIX 4
CLINOPYROXENE ANALYSES

OBS	153	154	155	156	157	158	159	160
SIO2	53.96	42.81	41.05	45.73	42.00	51.89	49.22	49.18
TIO2	0.54	4.33	5.35	3.46	5.42	1.49	2.43	2.42
AL2O3	0.55	9.17	10.88	7.20	9.51	1.78	3.92	3.91
CR2O3	0.00	0.00	0.00	0.00	0.00	0.05	0.10	0.12
FEOT	5.81	6.94	7.73	6.20	7.95	5.28	6.29	6.97
MNO	0.12	0.08	0.00	0.07	0.11	0.10	0.13	0.00
MGO	15.97	11.96	11.22	12.98	11.44	15.63	14.18	13.60
CAO	23.34	24.05	23.86	24.11	22.47	24.11	23.27	23.74
NA2O	0.45	0.32	0.32	0.31	0.58	0.41	0.46	0.47
K2O	0.00	0.00	0.02	0.00	0.11	0.00	0.00	0.00
TOTAL	100.74	99.66	100.43	100.06	99.59	100.74	100.00	100.41

** ATOMIC PROPORTIONS BASED ON SELECTED NO. OF OXYGENS **

OXYGN	6	6	6	6	6	6	6	6
SI	1.975	1.624	1.554	1.714	1.600	1.907	1.834	1.832
TI	0.015	0.124	0.152	0.098	0.155	0.041	0.068	0.068
AL	0.024	0.410	0.486	0.318	0.427	0.077	0.172	0.172
CR	0.000	0.000	0.000	0.000	0.000	0.001	0.003	0.004
FE	0.178	0.220	0.245	0.194	0.253	0.162	0.196	0.217
MN	0.004	0.003	0.000	0.002	0.004	0.003	0.004	0.000
MG	0.871	0.676	0.633	0.725	0.650	0.856	0.787	0.755
CA	0.915	0.978	0.968	0.968	0.917	0.949	0.929	0.948
NA	0.032	0.024	0.023	0.023	0.043	0.029	0.033	0.034
K	0.000	0.000	0.001	0.000	0.005	0.000	0.000	0.000
WO	46.51	52.10	52.44	51.23	50.30	48.17	48.47	49.36
DI	44.26	36.03	34.30	38.36	35.62	43.44	41.08	39.33
FS	9.23	11.87	13.26	10.40	14.08	8.39	10.44	11.31

**** SAMPLE DIRECTORY ****

OBS	NO	MINSPENO	ANALPOS	OBS	NO	MINSPENO	ANALPOS
153	267	CPX/027/001	C	154	267	CPX/028/001	C
155	267	CPX/028/002	R	156	267	CPX/029/001	C
157	267	CPX/030/001	C	158	267	CPX/031/001	I
159	267	CPX/032/001	C	160	267	CPX/033/001	C

APPENDIX 4
CLINOPYROXENE ANALYSES

OBS	161	162	163	164	165	166	167	168
SIO2	46.19	50.45	47.75	49.41	52.62	49.48	50.77	50.78
TIO2	3.40	2.17	2.78	2.71	1.06	2.43	1.89	2.11
AL2O3	6.81	2.67	5.12	3.60	0.70	3.16	1.73	2.36
CR2O3	0.00	0.06	0.08	0.06	0.05	0.09	0.10	0.11
FEOT	7.51	6.51	6.73	6.81	6.37	6.51	6.54	6.55
MNO	0.15	0.00	0.15	0.15	0.12	0.14	0.12	0.11
MGO	12.41	14.25	13.55	13.59	14.87	14.02	14.70	14.58
CAO	23.68	23.66	23.13	23.28	24.11	23.53	23.65	23.48
NA2O	0.43	0.47	0.43	0.49	0.38	0.46	0.40	0.45
K2O	0.00	0.00	0.00	0.00	0.00	0.00	0.00	0.00
TOTAL	100.58	100.24	99.72	100.10	100.28	99.82	99.90	100.53

** ATOMIC PROPORTIONS BASED ON SELECTED NO. OF OXYGENS **

OXYGN	6	6	6	6	6	6	6	6
SI	1.730	1.875	1.791	1.843	1.950	1.851	1.895	1.882
TI	0.096	0.061	0.078	0.076	0.030	0.068	0.053	0.059
AL	0.301	0.117	0.226	0.158	0.031	0.139	0.076	0.103
CR	0.000	0.002	0.002	0.002	0.001	0.003	0.003	0.003
FE	0.235	0.202	0.211	0.212	0.197	0.204	0.204	0.203
MN	0.005	0.000	0.005	0.005	0.004	0.004	0.004	0.003
MG	0.693	0.789	0.757	0.756	0.821	0.781	0.818	0.805
CA	0.950	0.942	0.930	0.931	0.957	0.943	0.946	0.932
NA	0.031	0.034	0.031	0.035	0.027	0.033	0.029	0.032
K	0.000	0.000	0.000	0.000	0.000	0.000	0.000	0.000
WO	50.47	48.72	48.85	48.89	48.36	48.80	47.98	47.96
DI	36.79	40.81	39.80	39.70	41.48	40.44	41.48	41.42
FS	12.75	10.46	11.34	11.41	10.16	10.77	10.55	10.62

**** SAMPLE DIRECTORY ****

OBS	NO	MINSPENO	ANALPOS	OBS	NO	MINSPENO	ANALPOS
161	267	CPX/034/001	I	162	267	CPX/035/001	C
163	267	CPX/036/001	C	164	267	CPX/036/002	R
165	267	CPX/037/001	C	166	267	CPX/038/001	C
167	267	CPX/039/001	C	168	267	CPX/039/002	R

APPENDIX 4
CLINOPYROXENE ANALYSES

OBS	169	170	171	172	173	174	175	176
SIO2	47.50	48.62	51.57	47.53	47.18	45.89	49.68	50.02
TIO2	2.57	2.61	1.55	3.29	3.69	3.57	2.29	2.49
AL2O3	5.46	4.67	2.28	5.50	6.00	6.63	4.17	3.45
CR2O3	0.00	0.08	0.00	0.00	0.00	0.07	0.11	0.00
FEOT	7.50	6.86	6.72	6.88	7.21	7.22	5.70	6.16
MNO	0.11	0.12	0.12	0.08	0.21	0.09	0.10	0.14
MGO	12.96	13.65	14.15	13.23	12.44	12.43	14.25	14.13
CAO	23.82	23.45	23.34	22.72	22.26	23.15	23.06	22.72
NA2O	0.39	0.42	0.56	0.57	0.80	0.50	0.44	0.51
K2O	0.00	0.00	0.00	0.00	0.00	0.00	0.00	0.00
TOTAL	100.31	100.48	100.29	99.80	99.79	99.55	99.80	99.62

** ATOMIC PROPORTIONS BASED ON SELECTED NO. OF OXYGENS **

OXYGN	6	6	6	6	6	6	6	6
SI	1.780	1.809	1.912	1.780	1.770	1.733	1.845	1.863
TI	0.072	0.073	0.043	0.093	0.104	0.101	0.064	0.070
AL	0.241	0.205	0.100	0.243	0.265	0.295	0.183	0.152
CR	0.000	0.002	0.000	0.000	0.000	0.002	0.003	0.000
FE	0.235	0.213	0.208	0.216	0.226	0.228	0.177	0.192
MN	0.003	0.004	0.004	0.003	0.007	0.003	0.003	0.004
MG	0.724	0.757	0.782	0.739	0.696	0.700	0.789	0.785
CA	0.957	0.935	0.927	0.912	0.895	0.937	0.918	0.907
NA	0.028	0.030	0.040	0.041	0.058	0.037	0.032	0.037
K	0.000	0.000	0.000	0.000	0.000	0.000	0.000	0.000
WO	49.85	48.97	48.26	48.80	49.08	50.17	48.64	48.04
DI	37.72	39.65	40.70	39.53	38.15	37.47	41.81	41.56
FS	12.43	11.38	11.04	11.67	12.77	12.37	9.55	10.40

**** SAMPLE DIRECTORY ****

OBS	NO	MINSPENO	ANALPOS	OBS	NO	MINSPENO	ANALPOS
169	267	CPX/040/001	C	170	267	CPX/040/002	R
171	267	CPX/041/001	R	172	267	CPX/042/001	R
173	267	CPX/043/001	R	174	267	CPX/044/001	R
175	267	CPX/045/001	R	176	267	CPX/046/001	R

APPENDIX 4
CLINOPYROXENE ANALYSES

OBS	177	178	179	180	181	182	183	184
SIO2	53.02	52.77	50.15	49.26	46.83	47.23	46.71	47.05
TIO2	0.84	1.34	1.93	2.53	3.29	3.04	2.90	2.99
AL2O3	1.01	1.14	3.02	4.14	6.31	6.38	7.24	7.15
CR2O3	0.05	0.14	0.00	0.00	0.00	0.06	0.00	0.00
FEOT	5.59	5.39	6.68	6.49	5.64	6.06	6.30	6.06
MNO	0.00	0.13	0.12	0.12	0.09	0.07	0.17	0.19
MGO	15.10	15.48	14.32	14.15	13.54	13.43	12.88	12.89
CAO	23.45	23.29	22.75	22.94	23.63	24.03	23.63	23.15
NA2O	0.40	0.45	0.57	0.49	0.33	0.36	0.46	0.60
K2O	0.00	0.00	0.00	0.00	0.00	0.00	0.00	0.00
TOTAL	99.46	100.13	99.54	100.12	99.66	100.66	100.29	100.08

** ATOMIC PROPORTIONS BASED ON SELECTED NO. OF OXYGENS **

OXYGN	6	6	6	6	6	6	6	6
SI	1.966	1.945	1.875	1.832	1.752	1.753	1.741	1.753
TI	0.023	0.037	0.054	0.071	0.093	0.085	0.081	0.084
AL	0.044	0.050	0.133	0.182	0.278	0.279	0.318	0.314
CR	0.001	0.004	0.000	0.000	0.000	0.002	0.000	0.000
FE	0.173	0.166	0.209	0.202	0.176	0.188	0.196	0.189
MN	0.000	0.004	0.004	0.004	0.003	0.002	0.005	0.006
MG	0.834	0.850	0.798	0.784	0.755	0.743	0.716	0.716
CA	0.932	0.920	0.911	0.914	0.947	0.956	0.944	0.924
NA	0.029	0.032	0.041	0.035	0.024	0.026	0.033	0.043
K	0.000	0.000	0.000	0.000	0.000	0.000	0.000	0.000
WO	48.04	47.40	47.42	48.01	50.35	50.60	50.71	50.37
DI	43.02	43.82	41.52	41.19	40.12	39.33	38.45	39.01
FS	8.94	8.77	11.07	10.80	9.53	10.08	10.84	10.62

**** SAMPLE DIRECTORY ****

OBS	NO	MINSPENO	ANALPOS	OBS	NO	MINSPENO	ANALPOS
177	267	CPX/047/001	R	178	267	CPX/048/001	R
179	267	CPX/049/001	R	180	267	CPX/050/001	R
181	267	CPX/051/001	SC/C-000	182	267	CPX/051/002	SI/C-22.5
183	267	CPX/051/003	SI/C-045	184	267	CPX/051/004	SI/C-67.5

APPENDIX 4
CLINOPYROXENE ANALYSES

OBS 185

SIO2	47.03
TIO2	3.06
AL2O3	7.59
CR2O3	0.00
FEOT	6.23
MNO	0.14
MGO	12.59
CAO	22.86
NA2O	0.69
K2C	0.00
TOTAL	100.19

** ATOMIC PROPORTIONS BASED ON SELECTED NO. OF OXYGENS **

OXYGN 6

SI	1.749
TI	0.086
AL	0.333
CR	0.000
FE	0.194
MN	0.004
MG	0.698
CA	0.911
NA	0.050
K	0.000

WO	50.41
DI	38.62
FS	10.97

**** SAMPLE DIRECTORY ****

OBS	NO	MINSPENC	ANALPOS
185	267	CPX/051/005	SI/C-090

APPENDIX 5

OLIVINE ANALYSES

INDEX

Sample	Olivine	Description
9	5-6;8	HILN olivine
14	7	HILN olivine
26	1-5	HILN olivine
30	1	HILN olivine
205	16	HILN olivine
9	10	complex phenocryst
14	8	complex phenocryst
205	15	complex phenocryst
256	3-4;10;17; 26-27;41;44-50	complex phenocryst
259	4	complex phenocryst
205	1	hopper olivine
256	13;15;16	hopper olivine

APPENDIX 5
OLIVINE ANALYSES

OBS	1	2	3	4	5	6	7	8
SIO2	39.66	39.26	39.01	39.19	37.13	36.94	39.66	38.37
TIO2	0.00	0.00	0.00	0.04	0.00	0.00	0.00	0.00
AL2O3	0.06	0.07	0.04	0.06	0.00	0.00	0.06	0.00
CR2O3	0.00	0.08	0.00	0.00	0.00	0.00	0.06	0.00
FEOT	11.77	10.31	10.93	10.65	25.46	22.42	12.14	22.05
MNO	0.14	0.13	0.15	0.14	0.57	0.53	0.12	0.50
NIO	0.21	0.25	0.23	0.40	0.00	0.00	0.26	0.00
MGO	47.14	48.35	47.89	48.26	37.28	38.85	46.83	39.52
CAO	0.24	0.19	0.19	0.19	0.04	0.13	0.18	0.11
TOTAL	99.22	98.64	98.44	98.93	100.48	98.87	99.31	100.55

** ATOMIC PROPORTIONS BASED ON SELECTED NO. OF OXYGENS **

OXYGN	4	4	4	4	4	4	4	4
SI	0.991	0.982	0.981	0.980	0.979	0.978	0.992	0.993
FE	0.246	0.216	0.230	0.223	0.562	0.496	0.254	0.477
MN	0.003	0.003	0.003	0.003	0.013	0.012	0.003	0.011
NI	0.004	0.005	0.005	0.008	0.000	0.000	0.005	0.000
MG	1.756	1.802	1.794	1.798	1.466	1.533	1.745	1.524
CA	0.006	0.005	0.005	0.005	0.001	0.004	0.005	0.003
FO	87.71	89.31	88.65	88.98	72.29	75.54	87.30	76.16

**** SAMPLE DIRECTORY ****

OBS	NO	MINSPENO	ANALPOS	OBS	NO	MINSPENO	ANALPOS
1	9	OLI/001/001	C	2	9	OLI/002/001	C
3	9	OLI/003/001	C	4	9	OLI/004/001	C
5	9	OLI/005/001	C	6	9	OLI/006/001	C
7	9	OLI/007/001	C	8	9	OLI/008/001	C

APPENDIX 5
OLIVINE ANALYSES

OBS	9	10	11	12	13	14	15	16
SIO2	39.49	39.93	39.88	39.84	40.65	40.20	40.25	40.11
TIO2	0.06	0.00	0.00	0.00	0.00	0.00	0.00	0.00
AL2O3	0.06	0.08	0.00	0.04	0.05	0.05	0.07	0.07
CR2O3	0.07	0.10	0.06	0.07	0.05	0.00	0.06	0.06
FEOT	10.16	10.47	10.93	11.83	11.25	11.00	11.07	10.47
MNO	0.13	0.16	0.15	0.17	0.15	0.18	0.15	0.16
NIO	0.36	0.25	0.29	0.37	0.24	0.31	0.27	0.31
MGO	48.24	47.99	47.97	46.82	48.12	47.99	47.58	47.88
CAO	0.18	0.21	0.18	0.15	0.19	0.18	0.22	0.19
TOTAL	98.75	99.19	99.46	99.29	100.70	99.91	99.67	99.25

** ATOMIC PROPORTIONS BASED ON SELECTED NO. OF OXYGENS **

OXYGN	4	4	4	4	4	4	4	4
SI	0.986	0.992	0.991	0.995	0.997	0.994	0.997	0.996
FE	0.212	0.218	0.227	0.247	0.231	0.227	0.229	0.217
MN	0.003	0.003	0.003	0.004	0.003	0.004	0.003	0.003
NI	0.007	0.005	0.006	0.007	0.005	0.006	0.005	0.006
MG	1.795	1.777	1.776	1.743	1.759	1.768	1.757	1.772
CA	0.005	0.006	0.005	0.004	0.005	0.005	0.006	0.005
FO	89.43	89.09	88.66	87.58	88.40	88.60	88.45	89.07

**** SAMPLE DIRECTORY ****

OBS	NO	MINSPENO	ANALPOS	CBS	NO	MINSPENO	ANALPOS
9	9	OLI/009/001	C	10	9	OLI/010/001	C
11	9	OLI/011/001	C	12	14	OLI/001/001	C
13	14	OLI/001/002	R	14	14	OLI/002/001	C
15	14	OLI/003/001	C	16	14	OLI/004/001	C

APPENDIX 5
OLIVINE ANALYSES

OBS	17	18	19	20	21	22	23	24
SIO2	39.79	39.71	37.98	39.80	39.59	39.54	40.09	40.25
TIO2	0.00	0.00	0.00	0.00	0.00	0.00	0.00	0.00
AL2O3	0.05	0.04	0.00	0.04	0.03	0.04	0.06	0.03
CR2O3	0.00	0.05	0.00	0.00	0.00	0.00	0.08	0.07
FEOT	11.09	10.10	23.34	11.06	12.04	12.21	11.83	10.29
MNO	0.08	0.09	0.62	0.17	0.14	0.22	0.16	0.10
NIO	0.40	0.28	0.00	0.27	0.21	0.13	0.35	0.32
MGO	47.38	48.05	38.39	47.81	46.72	46.53	47.21	48.23
CAO	0.15	0.20	0.07	0.19	0.20	0.38	0.15	0.20
TOTAL	98.94	98.52	100.40	99.34	98.93	99.05	99.93	99.49

** ATOMIC PROPORTIONS BASED ON SELECTED NO. OF OXYGENS **

OXYGN	4	4	4	4	4	4	4	4
SI	0.994	0.992	0.991	0.990	0.993	0.992	0.995	0.996
FE	0.232	0.211	0.509	0.230	0.253	0.256	0.245	0.213
MN	0.002	0.002	0.014	0.004	0.003	0.005	0.003	0.002
NI	0.008	0.006	0.000	0.005	0.004	0.003	0.007	0.006
MG	1.764	1.789	1.493	1.773	1.747	1.740	1.746	1.778
CA	0.004	0.005	0.002	0.005	0.005	0.010	0.004	0.005
FO	88.39	89.45	74.56	88.51	87.37	87.16	87.67	89.31

**** SAMPLE DIRECTORY ****

OBS	NO	MINSPENO	ANALPOS	OBS	NO	MINSPENO	ANALPOS
17	14	OLI/005/001	C	18	14	OLI/006/001	C
19	14	OLI/007/001	C	20	14	OLI/008/001	C
21	14	OLI/009/001	C	22	14	OLI/009/002	R
23	14	OLI/010/001	C	24	14	OLI/011/001	C

APPENDIX 5
OLIVINE ANALYSES

OBS	25	26	27	28	29	30	31	32
SIO2	37.92	37.83	37.61	38.76	39.93	38.11	39.02	39.78
TIO2	0.00	0.00	0.00	0.00	0.00	0.00	0.00	0.00
AL2O3	0.00	0.00	0.00	0.00	0.00	0.00	0.00	0.00
CR2O3	0.00	0.00	0.00	0.00	0.05	0.00	0.00	0.00
FEOT	25.82	25.88	25.60	21.51	12.32	25.44	19.77	15.01
MNO	0.60	0.56	0.53	0.29	0.21	0.48	0.31	0.48
NIO	0.00	0.00	0.00	0.00	0.00	0.00	0.03	0.00
MGO	37.00	36.75	36.68	40.01	46.34	37.23	41.75	44.20
CAO	0.04	0.00	0.07	0.09	0.47	0.03	0.10	0.72
TOTAL	101.38	101.02	100.49	100.66	99.32	101.29	100.98	100.19

** ATOMIC PROPORTIONS BASED ON SELECTED NO. OF OXYGENS **

OXYGN	4	4	4	4	4	4	4	4
SI	0.991	0.992	0.991	0.997	0.998	0.994	0.993	1.000
FE	0.564	0.568	0.564	0.463	0.258	0.555	0.421	0.315
MN	0.013	0.012	0.012	0.006	0.004	0.011	0.007	0.010
NI	0.000	0.000	0.000	0.000	0.000	0.000	0.001	0.000
MG	1.440	1.436	1.440	1.534	1.727	1.447	1.583	1.655
CA	0.001	0.000	0.002	0.002	0.013	0.001	0.003	0.019
FO	71.86	71.68	71.86	76.82	87.02	72.28	79.01	83.99

**** SAMPLE DIRECTORY ****

OBS	NO	MINSPENO	ANALPOS	OBS	NO	MINSPENO	ANALPOS
25	26	OLI/001/001	C	26	26	OLI/001/002	I
27	26	OLI/001/003	R	28	26	OLI/002/001	C
29	26	OLI/002/002	R	30	26	OLI/003/001	C
31	26	OLI/004/001	C	32	26	OLI/005/001	R

APPENDIX 5
OLIVINE ANALYSES

OBS	33	34	35	36	37	38	39	40
SIO2	38.19	39.15	39.22	39.63	39.11	39.48	39.78	39.61
TIO2	0.00	0.05	0.10	0.00	0.12	0.00	0.05	0.04
AL2O3	0.00	0.00	0.07	0.05	0.04	0.05	0.05	0.00
CR2O3	0.00	0.00	0.00	0.07	0.00	0.05	0.00	0.00
FEOT	19.40	13.25	12.86	11.57	12.24	11.18	12.49	12.27
MNO	0.28	0.18	0.24	0.13	0.20	0.15	0.21	0.17
NIO	0.00	0.22	0.10	0.18	0.10	0.24	0.25	0.14
MGO	41.70	46.02	46.01	47.34	46.63	47.49	46.75	46.82
CAO	0.09	0.27	0.56	0.14	0.66	0.19	0.18	0.31
TOTAL	99.66	99.14	99.16	99.11	99.10	98.83	99.76	99.36

** ATOMIC PROPORTIONS BASED ON SELECTED NO. OF OXYGENS **

OXYGN	4	4	4	4	4	4	4	4
SI	0.985	0.987	0.987	0.990	0.983	0.989	0.992	0.991
FE	0.418	0.279	0.271	0.242	0.257	0.234	0.260	0.257
MN	0.006	0.004	0.005	0.003	0.004	0.003	0.004	0.004
NI	0.000	0.004	0.002	0.004	0.002	0.005	0.005	0.003
MG	1.603	1.729	1.726	1.763	1.747	1.772	1.737	1.745
CA	0.002	0.007	0.015	0.004	0.018	0.005	0.005	0.008
FO	79.30	86.09	86.44	87.94	87.16	88.33	86.96	87.18

**** SAMPLE DIRECTORY ****

OBS	NO	MINSPENO	ANALPOS	OBS	NO	MINSPENO	ANALPOS
33	30	OLI/001/001	SC/C-000	34	30	OLI/001/002	SI/C-3300
35	30	OLI/001/003	SR/C-4000	36	205	OLI/001/001	C
37	205	OLI/001/002	R	38	205	OLI/002/001	C
39	205	OLI/003/001	C	40	205	OLI/004/001	C

APPENDIX 5
OLIVINE ANALYSES

OBS	41	42	43	44	45	46	47	48
SIO2	39.37	39.94	39.75	39.82	38.90	39.26	39.61	39.83
TIO2	0.00	0.05	0.00	0.04	0.00	0.04	0.00	0.00
AL2O3	0.00	0.00	0.05	0.12	0.00	0.00	0.06	0.06
CR2O3	0.00	0.00	0.00	0.08	0.00	0.06	0.06	0.10
FEOT	13.23	12.34	10.94	12.07	14.99	12.00	11.71	10.78
MNO	0.19	0.26	0.14	0.11	0.00	0.24	0.19	0.16
NIO	0.22	0.09	0.27	0.34	0.09	0.09	0.26	0.30
MGO	46.13	46.43	47.64	47.04	44.75	46.46	47.00	47.80
CAO	0.20	0.55	0.19	0.18	0.07	0.51	0.17	0.18
TOTAL	99.34	99.66	98.98	99.80	98.98	98.66	99.06	99.21

** ATOMIC PROPORTIONS BASED ON SELECTED NO. OF OXYGENS **

OXYGN	4	4	4	4	4	4	4	4
SI	0.990	0.996	0.992	0.991	0.990	0.989	0.992	0.991
FE	0.278	0.257	0.228	0.251	0.319	0.253	0.245	0.224
MN	0.004	0.005	0.003	0.002	0.000	0.005	0.004	0.003
NI	0.004	0.002	0.005	0.007	0.002	0.002	0.005	0.006
MG	1.728	1.726	1.772	1.744	1.697	1.745	1.753	1.773
CA	0.005	0.015	0.005	0.005	0.002	0.014	0.005	0.005
FO	86.14	87.02	88.58	87.41	84.18	87.34	87.73	88.77

**** SAMPLE DIRECTORY ****

OBS	NO	MINSPENO	ANALPOS	OBS	NO	MINSPENO	ANALPOS
41	205	OLI/005/001	C	42	205	OLI/005/002	R
43	205	OLI/006/001	C	44	205	OLI/007/001	C
45	205	OLI/008/001	C	46	205	OLI/008/002	R
47	205	OLI/009/001	C	48	205	OLI/010/001	C

APPENDIX 5
OLIVINE ANALYSES

OBS	49	50	51	52	53	54	55	56
SIO2	40.30	39.60	40.38	39.85	39.84	39.94	38.07	38.12
TIO2	0.09	0.00	0.00	0.00	0.04	0.00	0.00	0.00
AL2O3	0.04	0.05	0.04	0.05	0.04	0.00	0.00	0.00
CR2O3	0.00	0.05	0.10	0.07	0.05	0.00	0.00	0.00
FEOT	12.33	11.02	10.70	10.52	11.44	11.92	19.37	19.38
MNO	0.26	0.08	0.14	0.15	0.14	0.18	0.22	0.23
NIO	0.13	0.29	0.28	0.34	0.21	0.38	0.05	0.00
MGO	46.89	47.61	47.43	48.05	47.33	46.86	41.35	41.72
CAO	0.36	0.20	0.18	0.18	0.19	0.15	0.05	0.04
TOTAL	100.40	98.90	99.25	99.21	99.28	99.43	99.11	99.49

** ATOMIC PROPORTIONS BASED ON SELECTED NO. OF OXYGENS **

OXYGN	4	4	4	4	4	4	4	4
SI	0.997	0.990	1.002	0.991	0.993	0.997	0.987	0.985
FE	0.255	0.230	0.222	0.219	0.238	0.249	0.420	0.419
MN	0.005	0.002	0.003	0.003	0.003	0.004	0.005	0.005
NI	0.003	0.006	0.006	0.007	0.004	0.008	0.001	0.000
MG	1.729	1.773	1.755	1.781	1.758	1.743	1.598	1.606
CA	0.010	0.005	0.005	0.005	0.005	0.004	0.001	0.001
FO	87.14	88.50	88.76	89.06	88.06	87.51	79.18	79.32

**** SAMPLE DIRECTORY ****

OBS	NO	MINSPENO	ANALPOS	OBS	NO	MINSPENO	ANALPOS
49	205	OLI/010/002	R	50	205	OLI/011/001	C
51	205	OLI/012/001	C	52	205	OLI/013/001	C
53	205	OLI/014/001	C	54	205	OLI/015/001	C
55	205	OLI/016/001	SC/C-000	56	205	OLI/016/002	SI/C-1333

APPENDIX 5
OLIVINE ANALYSES

OBS	57	58	59	60	61	62	63	64
SIO2	38.32	38.40	39.70	39.29	40.12	40.47	39.87	38.55
TIO2	0.00	0.00	0.05	0.09	0.00	0.04	0.07	0.00
AL2O3	0.00	0.00	0.05	0.00	0.04	0.04	0.03	0.00
CR2O3	0.00	0.00	0.00	0.04	0.00	0.05	0.00	0.00
FEOT	19.10	17.44	13.20	12.45	12.37	12.02	12.06	16.99
MNO	0.31	0.17	0.15	0.23	0.16	0.18	0.32	0.22
NIO	0.00	0.07	0.20	0.13	0.23	0.27	0.06	0.06
MGO	41.81	43.35	46.44	46.34	47.01	47.06	47.21	44.01
CAO	0.06	0.12	0.23	0.54	0.18	0.23	1.50	0.06
TOTAL	99.60	99.55	100.02	99.11	100.11	100.36	101.12	99.89

** ATOMIC PROPORTIONS BASED ON SELECTED NO. OF OXYGENS **

OXYGN	4	4	4	4	4	4	4	4
SI	0.987	0.983	0.990	0.988	0.995	1.000	0.983	0.981
FE	0.412	0.373	0.275	0.262	0.257	0.248	0.249	0.362
MN	0.007	0.004	0.003	0.005	0.003	0.004	0.007	0.005
NI	0.000	0.001	0.004	0.003	0.005	0.005	0.001	0.001
MG	1.605	1.653	1.727	1.736	1.738	1.732	1.734	1.669
CA	0.002	0.003	0.006	0.015	0.005	0.006	0.040	0.002
FO	79.60	81.58	86.24	86.90	87.13	87.46	87.46	82.19

**** SAMPLE DIRECTORY ****

OBS	NO	MINSPENO	ANALPOS	OBS	NO	MINSPENO	ANALPOS
57	205	OLI/016/003	SI/C-2666	58	205	OLI/016/004	SI/C-3110
59	205	OLI/016/005	SI/C-3555	60	205	OLI/016/006	SR/C-4000
61	256	OLI/001/001	C	62	256	OLI/001/002	I
63	256	OLI/001/003	R	64	256	OLI/002/001	C

APPENDIX 5
OLIVINE ANALYSES

OBS	65	66	67	68	69	70	71	72
SIO2	39.05	39.31	39.78	40.03	39.90	39.67	39.68	38.95
TIO2	0.00	0.00	0.00	0.00	0.00	0.00	0.00	0.04
AL2O3	0.00	0.00	0.04	0.05	0.06	0.00	0.00	0.00
CR2O3	0.00	0.00	0.00	0.06	0.07	0.00	0.00	0.00
FEOT	17.23	16.68	11.80	12.60	11.73	13.61	12.94	15.04
MNO	0.25	0.48	0.13	0.14	0.18	0.44	0.16	0.44
NIO	0.00	0.06	0.23	0.21	0.27	0.07	0.19	0.08
MGO	44.03	43.36	47.53	46.73	47.49	44.97	46.50	44.28
CAO	0.06	0.75	0.20	0.26	0.20	1.22	0.24	0.99
TOTAL	100.62	100.64	99.71	100.08	99.90	99.98	99.71	99.82

** ATOMIC PROPORTIONS BASED ON SELECTED NO. OF OXYGENS **

OXYGN	4	4	4	4	4	4	4	4
SI	0.986	0.992	0.989	0.995	0.990	0.995	0.992	0.986
FE	0.364	0.352	0.245	0.262	0.243	0.285	0.271	0.318
MN	0.005	0.010	0.003	0.003	0.004	0.009	0.003	0.009
NI	0.000	0.001	0.005	0.004	0.005	0.001	0.004	0.002
MG	1.657	1.631	1.762	1.731	1.757	1.681	1.732	1.670
CA	0.002	0.020	0.005	0.007	0.005	0.033	0.006	0.027
FO	81.99	82.25	87.77	86.86	87.83	85.48	86.49	83.99

**** SAMPLE DIRECTORY ****

OBS	NO	MINSPENO	ANALPOS	OBS	NO	MINSPENO	ANALPOS
65	256	OLI/002/002	I	66	256	OLI/002/003	R
67	256	OLI/003/001	C	68	256	OLI/003/002	R
69	256	OLI/004/001	C	70	256	OLI/004/002	R
71	256	OLI/005/001	C	72	256	OLI/005/002	R

APPENDIX 5
OLIVINE ANALYSES

OBS	73	74	75	76	77	78	79	80
SIO2	39.70	39.51	39.48	39.19	39.21	39.49	39.67	39.17
TIO2	0.05	0.06	0.05	0.05	0.00	0.04	0.08	0.00
AL2O3	0.00	0.04	0.04	0.06	0.07	0.04	0.05	0.06
CR2O3	0.00	0.00	0.06	0.08	0.00	0.00	0.00	0.06
FEOT	12.52	11.78	12.25	11.89	13.37	12.75	13.23	13.52
MNO	0.13	0.22	0.17	0.11	0.43	0.19	0.33	0.14
NIO	0.21	0.07	0.23	0.29	0.00	0.13	0.08	0.17
MGO	46.86	46.95	47.20	47.62	45.41	46.10	45.29	46.07
CAO	0.24	0.79	0.23	0.19	1.26	0.44	0.90	0.20
TOTAL	99.71	99.42	99.71	99.48	99.75	99.18	99.63	99.39

** ATOMIC PROPORTIONS BASED ON SELECTED NO. OF OXYGENS **

CXYGN	4	4	4	4	4	4	4	4
SI	0.991	0.987	0.985	0.979	0.986	0.992	0.995	0.986
FE	0.261	0.246	0.256	0.248	0.281	0.268	0.278	0.285
MN	0.003	0.005	0.004	0.002	0.009	0.004	0.007	0.003
NI	0.004	0.001	0.005	0.006	0.000	0.003	0.002	0.003
MG	1.742	1.748	1.755	1.773	1.701	1.726	1.694	1.728
CA	0.006	0.021	0.006	0.005	0.034	0.012	0.024	0.005
FO	86.96	87.66	87.29	87.71	85.82	86.56	85.92	85.86

**** SAMPLE DIRECTORY ****

OBS	NO	MINSPENO	ANALPOS	OBS	NO	MINSPENO	ANALPOS
73	256	OLI/006/001	C	74	256	OLI/006/002	R
75	256	OLI/007/001	C	76	256	OLI/008/001	C
77	256	OLI/008/002	R	78	256	OLI/009/001	C
79	256	OLI/009/002	R	80	256	OLI/010/001	C

APPENDIX 5
OLIVINE ANALYSES

OBS	81	82	83	84	85	86	87	88
SIO2	39.35	39.77	39.44	39.11	39.27	39.78	39.66	39.63
TIO2	0.06	0.00	0.05	0.10	0.00	0.08	0.04	0.11
AL2O3	0.00	0.05	0.04	0.04	0.05	0.04	0.05	0.08
CR2O3	0.00	0.05	0.00	0.00	0.05	0.00	0.00	0.00
FEOT	12.17	12.07	12.84	12.36	12.81	12.79	12.70	12.76
MNO	0.25	0.14	0.13	0.37	0.16	0.18	0.13	0.25
NIO	0.10	0.23	0.17	0.08	0.20	0.12	0.22	0.12
MGO	46.09	46.92	46.31	45.85	46.24	46.13	46.38	45.79
CAO	0.76	0.24	0.22	1.12	0.17	0.46	0.22	0.51
TOTAL	98.78	99.47	99.20	99.03	98.95	99.58	99.40	99.25

** ATOMIC PROPORTIONS BASED ON SELECTED NO. OF OXYGENS **

OXYGN	4	4	4	4	4	4	4	4
SI	0.991	0.993	0.991	0.986	0.989	0.995	0.993	0.995
FE	0.256	0.252	0.270	0.261	0.270	0.268	0.266	0.268
MN	0.005	0.003	0.003	0.008	0.003	0.004	0.003	0.005
NI	0.002	0.005	0.003	0.002	0.004	0.002	0.004	0.002
MG	1.731	1.745	1.733	1.722	1.736	1.719	1.731	1.713
CA	0.021	0.006	0.006	0.030	0.005	0.012	0.006	0.014
FO	87.09	87.39	86.54	86.86	86.55	86.54	86.68	86.48

**** SAMPLE DIRECTORY ****

OBS	NO	MINSPENO	ANALPOS	OBS	NO	MINSPENO	ANALPOS
81	256	OLI/010/002	R	82	256	OLI/011/001	C
83	256	OLI/012/001	C	84	256	OLI/012/002	R
85	256	OLI/013/001	C	86	256	OLI/013/002	R
87	256	OLI/014/001	C	88	256	OLI/014/002	R

APPENDIX 5
OLIVINE ANALYSES

OBS	89	90	91	92	93	94	95	96
SIO2	39.74	39.78	39.74	40.18	40.20	39.81	39.76	39.80
TIO2	0.00	0.04	0.00	0.00	0.09	0.00	0.00	0.00
AL2O3	0.06	0.04	0.04	0.05	0.04	0.04	0.00	0.05
CR2O3	0.00	0.07	0.00	0.00	0.00	0.06	0.00	0.04
FEOT	11.29	11.74	11.98	11.85	13.22	12.14	13.07	11.98
MNO	0.17	0.14	0.25	0.13	0.23	0.15	0.23	0.16
NIO	0.34	0.31	0.09	0.30	0.08	0.27	0.14	0.26
MGO	47.08	47.14	46.26	47.07	45.76	46.66	46.00	46.77
CAO	0.19	0.17	0.81	0.19	0.51	0.23	0.38	0.24
TOTAL	98.87	99.43	99.17	99.77	100.13	99.36	99.58	99.30

** ATOMIC PROPORTIONS BASED ON SELECTED NO. OF OXYGENS **

OXYGN	4	4	4	4	4	4	4	4
SI	0.995	0.992	0.996	0.998	1.001	0.995	0.996	0.995
FE	0.236	0.245	0.251	0.246	0.275	0.254	0.274	0.250
MN	0.004	0.003	0.005	0.003	0.005	0.003	0.005	0.003
NI	0.007	0.006	0.002	0.006	0.002	0.005	0.003	0.005
MG	1.756	1.752	1.727	1.742	1.698	1.738	1.717	1.742
CA	0.005	0.005	0.022	0.005	0.014	0.006	0.010	0.006
FO	88.14	87.74	87.31	87.62	86.05	87.26	86.25	87.43

**** SAMPLE DIRECTORY ****

OBS	NO	MINSPENO	ANALPOS	OBS	NO	MINSPENO	ANALPOS
89	256	OLI/015/001	C	90	256	OLI/015/002	I
91	256	OLI/015/003	R	92	256	OLI/016/001	C
93	256	OLI/016/002	R	94	256	OLI/017/001	C
95	256	OLI/017/002	R	96	256	OLI/018/001	C

APPENDIX 5
OLIVINE ANALYSES

OBS	97	98	99	100	101	102	103	104
SIO2	39.86	40.11	39.89	39.99	39.78	39.79	39.92	39.96
TIO2	0.00	0.00	0.04	0.05	0.09	0.00	0.05	0.00
AL2O3	0.00	0.07	0.04	0.04	0.04	0.00	0.00	0.00
CR2O3	0.00	0.08	0.00	0.00	0.00	0.05	0.00	0.00
FEOT	12.39	11.72	12.95	12.97	12.09	11.94	12.04	11.69
MNO	0.25	0.12	0.17	0.18	0.27	0.11	0.26	0.14
NIO	0.07	0.38	0.18	0.13	0.11	0.32	0.10	0.29
MGO	46.39	47.25	46.19	46.03	46.09	47.03	46.40	47.17
CAO	0.67	0.19	0.33	0.25	0.94	0.15	0.88	0.20
TOTAL	99.63	99.92	99.79	99.64	99.41	99.39	99.65	99.45

** ATOMIC PROPORTIONS BASED ON SELECTED NO. OF OXYGENS **

OXYGN	4	4	4	4	4	4	4	4
SI	0.995	0.995	0.996	0.999	0.995	0.993	0.996	0.996
FE	0.259	0.243	0.270	0.271	0.253	0.249	0.251	0.244
MN	0.005	0.003	0.004	0.004	0.006	0.002	0.005	0.003
NI	0.001	0.008	0.004	0.003	0.002	0.006	0.002	0.006
MG	1.726	1.747	1.719	1.714	1.718	1.750	1.725	1.751
CA	0.018	0.005	0.009	0.007	0.025	0.004	0.024	0.005
FO	86.97	87.78	86.41	86.35	87.17	87.53	87.29	87.79

**** SAMPLE DIRECTORY ****

OBS	NO	MINSPENO	ANALPOS	OBS	NO	MINSPENO	ANALPOS
97	256	OLI/018/002	R	98	256	OLI/019/001	C
99	256	OLI/019/002	R	100	256	OLI/020/001	C
101	256	OLI/020/002	R	102	256	OLI/021/001	C
103	256	OLI/021/002	R	104	256	OLI/022/001	C

APPENDIX 5
OLIVINE ANALYSES

OBS	105	106	107	108	109	110	111	112
SIO2	39.64	40.08	39.55	39.89	39.73	40.05	39.92	39.66
TIO2	0.05	0.00	0.04	0.06	0.07	0.00	0.00	0.08
AL2O3	0.04	0.04	0.00	0.03	0.03	0.00	0.04	0.04
CR2O3	0.00	0.00	0.00	0.00	0.00	0.06	0.00	0.00
FEOT	11.86	11.80	12.29	12.94	11.65	11.86	13.07	12.38
MNO	0.23	0.20	0.19	0.20	0.20	0.10	0.17	0.21
NIO	0.07	0.20	0.10	0.12	0.00	0.27	0.17	0.09
MGO	46.28	47.16	46.29	45.98	46.27	46.93	45.63	46.38
CAO	0.77	0.19	0.58	0.38	0.95	0.25	0.27	0.74
TOTAL	98.94	99.67	99.04	99.60	98.90	99.52	99.27	99.58

** ATOMIC PROPORTIONS BASED ON SELECTED NO. OF OXYGENS **

OXYGN	4	4	4	4	4	4	4	4
SI	0.995	0.996	0.993	0.998	0.996	0.998	1.002	0.991
FE	0.249	0.245	0.258	0.271	0.244	0.247	0.274	0.259
MN	0.005	0.004	0.004	0.004	0.004	0.002	0.004	0.004
NI	0.001	0.004	0.002	0.002	0.000	0.005	0.003	0.002
MG	1.731	1.747	1.732	1.714	1.729	1.742	1.706	1.728
CA	0.021	0.005	0.016	0.010	0.026	0.007	0.007	0.020
FO	87.43	87.69	87.03	86.36	87.62	87.58	86.15	86.97

**** SAMPLE DIRECTORY ****

OBS	NO	MINSPENO	ANALPOS	OBS	NO	MINSPENO	ANALPOS
105	256	OLI/022/002	R	106	256	OLI/023/001	C
107	256	OLI/023/002	R	108	256	OLI/024/001	C
109	256	OLI/024/002	R	110	256	OLI/025/001	C
111	256	OLI/026/001	C	112	256	OLI/026/002	R

APPENDIX 5
OLIVINE ANALYSES

OBS	113	114	115	116	117	118	119	120
SIO2	39.53	39.52	39.95	40.02	39.56	39.29	39.82	39.75
TIO2	0.00	0.11	0.00	0.08	0.10	0.08	0.05	0.06
AL2O3	0.00	0.36	0.04	0.03	0.07	0.00	0.04	0.00
CR2O3	0.00	0.00	0.00	0.00	0.00	0.00	0.05	0.00
FEOT	13.53	13.24	12.41	11.84	12.75	14.04	11.73	13.11
MNO	0.22	0.40	0.18	0.28	0.13	0.47	0.18	0.14
NIO	0.18	0.08	0.17	0.10	0.14	0.06	0.20	0.14
MGO	46.01	43.94	46.15	46.20	46.55	44.08	46.78	45.69
CAO	0.25	1.44	0.26	0.84	0.23	1.30	0.24	0.29
TOTAL	99.72	99.09	99.16	99.39	99.53	99.32	99.09	99.18

** ATOMIC PROPORTIONS BASED ON SELECTED NO. OF OXYGENS **

OXYGN	4	4	4	4	4	4	4	4
SI	0.991	0.998	1.001	0.999	0.990	0.995	0.996	0.999
FE	0.284	0.280	0.260	0.247	0.267	0.297	0.245	0.276
MN	0.005	0.009	0.004	0.006	0.003	0.010	0.004	0.003
NI	0.004	0.002	0.003	0.002	0.003	0.001	0.004	0.003
MG	1.719	1.654	1.723	1.719	1.735	1.663	1.744	1.711
CA	0.007	0.039	0.007	0.022	0.006	0.035	0.006	0.008
FO	85.84	85.54	86.89	87.43	86.68	84.84	87.66	86.13

**** SAMPLE DIRECTORY ****

OBS	NO	MINSPENO	ANALPOS	OBS	NO	MINSPENO	ANALPOS
113	256	OLI/027/001	C	114	256	OLI/027/002	R
115	256	OLI/028/001	C	116	256	OLI/028/002	R
117	256	OLI/029/001	C	118	256	OLI/029/002	R
119	256	OLI/030/001	C	120	256	OLI/031/001	C

APPENDIX 5
OLIVINE ANALYSES

OBS	121	122	123	124	125	126	127	128
SIO2	40.46	39.88	39.80	39.97	40.07	39.97	39.51	39.84
TIO2	0.08	0.06	0.07	0.06	0.10	0.00	0.00	0.00
AL2O3	0.06	0.00	0.00	0.04	0.07	0.00	0.00	0.05
CR2O3	0.00	0.06	0.07	0.00	0.08	0.06	0.12	0.11
FEOT	13.64	12.80	11.69	12.95	11.95	11.62	12.85	12.07
MNO	0.36	0.15	0.35	0.26	0.15	0.16	0.14	0.14
NIO	0.00	0.19	0.00	0.12	0.21	0.32	0.26	0.27
MGO	45.48	46.26	45.96	46.08	46.17	46.56	46.03	46.46
CAO	1.22	0.24	1.38	0.43	0.23	0.23	0.14	0.20
TOTAL	101.30	99.64	99.32	99.91	99.03	98.92	99.05	99.14

** ATOMIC PROPORTIONS BASED ON SELECTED NO. OF OXYGENS **

OXYGN	4	4	4	4	4	4	4	4
SI	0.999	0.996	0.996	0.997	1.003	1.001	0.994	0.997
FE	0.282	0.267	0.245	0.270	0.250	0.243	0.270	0.253
MN	0.008	0.003	0.007	0.005	0.003	0.003	0.003	0.003
NI	0.000	0.004	0.000	0.002	0.004	0.006	0.005	0.005
MG	1.674	1.722	1.714	1.713	1.722	1.737	1.726	1.733
CA	0.032	0.006	0.037	0.011	0.006	0.006	0.004	0.005
FO	85.59	86.56	87.51	86.38	87.32	87.72	86.46	87.28

**** SAMPLE DIRECTORY ****

OBS	NO	MINSPENO	ANALPOS	OBS	NO	MINSPENO	ANALPOS
121	256	OLI/031/002	R	122	256	OLI/032/001	C
123	256	CLI/032/002	R	124	256	OLI/033/001	C
125	256	OLI/034/001	C	126	256	OLI/035/001	C
127	256	OLI/036/001	I	128	256	OLI/037/001	I

APPENDIX 5
OLIVINE ANALYSES

OBS	129	130	131	132	133	134	135	136
SIO2	39.73	39.66	39.84	39.96	39.19	39.46	39.84	40.17
TIO2	0.00	0.00	0.00	0.00	0.07	0.00	0.00	0.00
AL2O3	0.04	0.05	0.04	0.04	0.04	0.03	0.11	0.04
CR2O3	0.14	0.10	0.00	0.15	0.00	0.08	0.05	0.08
FEOT	12.09	12.46	11.93	12.63	12.54	12.13	12.25	12.29
MNO	0.14	0.15	0.12	0.18	0.20	0.09	0.11	0.09
NIO	0.33	0.21	0.26	0.25	0.10	0.25	0.21	0.26
MGO	46.55	46.30	46.52	46.39	46.85	47.30	47.07	47.14
CAO	0.25	0.24	0.24	0.18	0.60	0.19	0.19	0.19
TOTAL	99.27	99.17	98.95	99.78	99.59	99.53	99.83	100.26

** ATOMIC PROPORTIONS BASED ON SELECTED NO. OF OXYGENS **

OXYGN	4	4	4	4	4	4	4	4
SI	0.994	0.995	0.998	0.996	0.981	0.985	0.991	0.995
FE	0.253	0.261	0.250	0.263	0.263	0.253	0.255	0.255
MN	0.003	0.003	0.003	0.004	0.004	0.002	0.002	0.002
NI	0.007	0.004	0.005	0.005	0.002	0.005	0.004	0.005
MG	1.736	1.730	1.737	1.724	1.748	1.760	1.745	1.740
CA	0.007	0.006	0.006	0.005	0.016	0.005	0.005	0.005
FO	87.28	86.88	87.42	86.75	86.94	87.42	87.26	87.24

**** SAMPLE DIRECTORY ****

OBS	NO	MINSPENO	ANALPOS	OBS	NO	MINSPENO	ANALPOS
129	256	OLI/038/001	I	130	256	OLI/038/002	I
131	256	OLI/038/003	C	132	256	OLI/039/001	I
133	256	OLI/040/001	SR/R+000	134	256	OLI/040/002	SI/R+57
135	256	OLI/040/003	SI/R+114	136	256	OLI/040/004	SI/R+171

APPENDIX 5
OLIVINE ANALYSES

OBS	137	138	139	140	141	142	143	144
SIO2	39.57	39.28	39.36	39.40	39.70	39.98	39.77	39.47
TIO2	0.05	0.00	0.00	0.05	0.00	0.05	0.00	0.00
AL2O3	0.05	0.04	0.00	0.05	0.04	0.06	0.04	0.04
CR2O3	0.08	0.00	0.00	0.00	0.08	0.00	0.07	0.05
FEOT	12.15	12.29	12.46	12.55	11.73	11.23	11.38	11.47
MNO	0.15	0.12	0.14	0.27	0.14	0.16	0.13	0.16
NIO	0.27	0.26	0.26	0.00	0.27	0.32	0.37	0.38
MGO	47.13	47.51	47.18	46.07	46.99	47.34	47.36	47.79
CAO	0.18	0.18	0.21	1.13	0.24	0.17	0.17	0.18
TOTAL	99.63	99.68	99.61	99.52	99.19	99.31	99.29	99.54

** ATOMIC PROPORTIONS BASED ON SELECTED NO. OF OXYGENS **

OXYGN	4	4	4	4	4	4	4	4
SI	0.987	0.981	0.984	0.988	0.993	0.995	0.992	0.984
FE	0.254	0.257	0.261	0.263	0.245	0.234	0.237	0.239
MN	0.003	0.003	0.003	0.006	0.003	0.003	0.003	0.003
NI	0.005	0.005	0.005	0.000	0.005	0.006	0.007	0.008
MG	1.752	1.768	1.758	1.721	1.751	1.757	1.760	1.775
CA	0.005	0.005	0.006	0.030	0.006	0.005	0.005	0.005
FO	87.36	87.32	87.09	86.74	87.71	88.25	88.12	88.13

**** SAMPLE DIRECTORY ****

OBS	NO	MINSPENO	ANALPOS	OBS	NO	MINSPENO	ANALPOS
137	256	OLI/040/005	SC/R+228	138	256	OLI/040/006	SI/R+286
139	256	OLI/040/007	SI/R+343	140	256	OLI/040/008	SR/R+400
141	256	OLI/041/001	SR/R+000	142	256	OLI/041/002	SI/R+083
143	256	OLI/041/003	SI/R+166	144	256	OLI/041/004	SR/R+240

APPENDIX 5
OLIVINE ANALYSES

OBS	145	146	147	148	149	150	151	152
SIO2	39.76	39.41	39.99	39.46	39.20	39.16	38.91	38.82
TIO2	0.00	0.00	0.00	0.09	0.07	0.00	0.00	0.00
AL2O3	0.04	0.04	0.04	0.00	0.04	0.00	0.03	0.00
CR2O3	0.05	0.08	0.05	0.00	0.00	0.00	0.00	0.00
FEOT	11.21	11.41	11.78	12.64	13.13	12.15	15.04	16.84
MNO	0.16	0.12	0.16	0.34	0.35	0.22	0.18	0.25
NIO	0.38	0.39	0.31	0.07	0.06	0.00	0.15	0.14
MGO	47.40	47.40	47.39	45.50	45.87	47.04	45.09	43.58
CAO	0.18	0.18	0.19	1.25	1.32	0.73	0.30	0.27
TOTAL	99.18	99.03	99.91	99.35	100.04	99.30	99.70	99.90

** ATOMIC PROPORTIONS BASED ON SELECTED NO. OF OXYGENS **

OXYGN	4	4	4	4	4	4	4	4
SI	0.992	0.987	0.992	0.992	0.982	0.982	0.984	0.987
FE	0.234	0.239	0.244	0.266	0.275	0.255	0.318	0.358
MN	0.003	0.003	0.003	0.007	0.007	0.005	0.004	0.005
NI	0.008	0.008	0.006	0.001	0.001	0.000	0.003	0.003
MG	1.763	1.768	1.753	1.705	1.712	1.758	1.699	1.652
CA	0.005	0.005	0.005	0.034	0.035	0.020	0.008	0.007
FC	88.28	88.10	87.76	86.51	86.16	87.34	84.23	82.18

**** SAMPLE DIRECTORY ****

OBS	NO	MINSPENO	ANALPOS	OBS	NO	MINSPENO	ANALPOS
145	256	OLI/041/005	SR/R+258	146	256	OLI/041/006	SI/R+332
147	256	OLI/041/007	SI/R+443	148	256	OLI/041/008	SR/R+498
149	256	OLI/042/001	SR/R+000	150	256	OLI/042/002	SI/R+042
151	256	OLI/042/003	SI/R+082	152	256	OLI/042/004	SI/R+123

APPENDIX 5
OLIVINE ANALYSES

OBS	153	154	155	156	157	158	159	160
SIO2	38.56	38.03	37.29	39.43	40.17	39.77	39.81	39.76
TIO2	0.00	0.00	0.05	0.06	0.00	0.00	0.00	0.00
AL2O3	0.05	0.00	0.04	0.00	0.04	0.04	0.08	0.07
CR2O3	0.00	0.00	0.00	0.00	0.05	0.07	0.05	0.05
FEOT	17.47	17.33	17.91	12.41	12.23	11.56	11.69	12.11
MNO	0.30	0.23	0.23	0.20	0.14	0.15	0.16	0.14
NIO	0.15	0.12	0.10	0.10	0.30	0.32	0.27	0.21
MGO	43.21	43.57	43.22	46.38	46.23	46.92	46.77	46.55
CAO	0.26	0.26	0.27	0.54	0.16	0.18	0.23	0.24
TOTAL	100.00	99.54	99.11	99.12	99.32	99.01	99.06	99.13

** ATOMIC PROPORTIONS BASED ON SELECTED NO. OF OXYGENS **

OXYGN	4	4	4	4	4	4	4	4
SI	0.983	0.975	0.964	0.990	1.003	0.995	0.996	0.996
FE	0.373	0.371	0.387	0.261	0.256	0.242	0.245	0.254
MN	0.006	0.005	0.005	0.004	0.003	0.003	0.003	0.003
NI	0.003	0.002	0.002	0.002	0.006	0.006	0.005	0.004
MG	1.642	1.664	1.666	1.736	1.721	1.750	1.744	1.737
CA	0.007	0.007	0.007	0.015	0.004	0.005	0.006	0.006
FO	81.51	81.75	81.13	86.94	87.07	87.85	87.70	87.26

**** SAMPLE DIRECTORY ****

OBS	NO	MINSPENO	ANALPOS	OBS	NO	MINSPENO	ANALPOS
153	256	OLI/042/005	SC/R+164	154	256	OLI/042/006	SI/R+205
155	256	OLI/042/007	SI/R+246	156	256	OLI/042/008	SR/R+280
157	256	OLI/043/001	SC/C-000	158	256	OLI/043/002	SI/C-140
159	256	OLI/043/003	SI/C-163	160	256	OLI/043/004	SI/C-186

APPENDIX 5
OLIVINE ANALYSES

OBS	161	162	163	164	165	166	167	168
SIO2	39.82	40.08	39.89	39.66	39.89	39.82	39.82	39.74
TIO2	0.04	0.00	0.00	0.00	0.00	0.08	0.07	0.05
AL2O3	0.03	0.05	0.03	0.04	0.05	0.00	0.00	0.03
CR2O3	0.05	0.00	0.00	0.00	0.00	0.00	0.00	0.00
FEOT	12.57	12.98	13.32	13.16	12.88	12.30	12.06	13.26
MNO	0.15	0.15	0.18	0.20	0.17	0.26	0.28	0.39
NIO	0.23	0.19	0.15	0.12	0.11	0.10	0.06	0.05
MGO	46.10	45.97	45.78	45.71	45.80	46.10	45.74	44.73
CAO	0.26	0.28	0.28	0.31	0.42	0.66	0.98	1.02
TOTAL	99.25	99.70	99.63	99.20	99.32	99.32	99.01	99.27

** ATOMIC PROPORTIONS BASED ON SELECTED NO. OF OXYGENS **

OXYGN	4	4	4	4	4	4	4	4
SI	0.998	1.001	0.999	0.997	1.000	0.997	1.000	1.001
FE	0.263	0.271	0.279	0.277	0.270	0.258	0.253	0.279
MN	0.003	0.003	0.004	0.004	0.004	0.006	0.006	0.008
NI	0.005	0.004	0.003	0.002	0.002	0.002	0.001	0.001
MG	1.722	1.711	1.708	1.713	1.711	1.720	1.711	1.679
CA	0.007	0.007	0.008	0.008	0.011	0.018	0.026	0.028
FO	86.73	86.32	85.96	86.09	86.37	86.98	87.11	85.74

**** SAMPLE DIRECTORY ****

OBS	NO	MINSPENO	ANALPOS	OBS	NO	MINSPENO	ANALPOS
161	256	OLI/043/005	SI/C-209	162	256	OLI/043/006	SI/C-232
163	256	OLI/043/007	SI/C-255	164	256	OLI/043/008	SI/C-278
165	256	OLI/043/009	SI/C-301	166	256	OLI/043/010	SI/C-324
167	256	OLI/043/011	SR/C-347	168	256	OLI/044/001	SR/R+000

APPENDIX 5
OLIVINE ANALYSES

OBS	169	170	171	172	173	174	175	176
SIO2	39.69	39.82	39.65	39.94	41.07	39.71	39.55	39.73
TIO2	0.00	0.00	0.00	0.00	0.05	0.00	0.00	0.00
AL2O3	0.00	0.04	0.04	0.03	0.47	0.00	0.00	0.00
CR2O3	0.05	0.00	0.07	0.05	0.00	0.00	0.00	0.00
FEOT	11.98	12.17	11.95	11.82	12.79	12.21	15.09	14.72
MNO	0.13	0.14	0.18	0.20	0.29	0.21	0.23	0.19
NIO	0.28	0.28	0.27	0.26	0.26	0.17	0.14	0.14
MGO	46.58	46.68	46.62	46.56	43.98	46.47	44.55	45.21
CAO	0.20	0.22	0.23	0.22	1.28	0.47	0.03	0.08
TOTAL	98.91	99.35	99.01	99.08	100.19	99.24	99.59	100.07

** ATOMIC PROPORTIONS BASED ON SELECTED NO. OF OXYGENS **

OXYGN	4	4	4	4	4	4	4	4
SI	0.996	0.995	0.994	0.999	1.020	0.995	0.998	0.996
FE	0.251	0.254	0.251	0.247	0.266	0.256	0.319	0.309
MN	0.003	0.003	0.004	0.004	0.006	0.004	0.005	0.004
NI	0.006	0.006	0.005	0.005	0.005	0.003	0.003	0.003
MG	1.742	1.739	1.742	1.736	1.627	1.735	1.676	1.690
CA	0.005	0.006	0.006	0.006	0.034	0.013	0.001	0.002
FO	87.39	87.24	87.42	87.53	85.97	87.15	84.03	84.55

**** SAMPLE DIRECTORY ****

OBS	NO	MINSPENO	ANALPOS	OBS	NO	MINSPENO	ANALPOS
169	256	OLI/044/002	SI/R+200	170	256	OLI/044/003	SI/R+400
171	256	OLI/044/004	SI/R+430	172	256	OLI/044/005	SR/R+480
173	256	OLI/045/001	SR/R+520	174	256	OLI/045/002	SI/R+730
175	256	OLI/045/003	SI/R+970	176	256	OLI/045/004	SI/R+1235

APPENDIX 5
OLIVINE ANALYSES

OBS	177	178	179	180	181	182	183	184
SIO2	40.05	39.62	39.21	39.76	39.84	39.96	40.05	39.71
TIO2	0.05	0.00	0.00	0.00	0.00	0.00	0.00	0.05
AL2O3	0.00	0.00	0.00	0.00	0.00	0.05	0.00	0.04
CR2O3	0.00	0.00	0.00	0.00	0.05	0.06	0.05	0.00
FEOT	12.30	13.40	12.81	14.74	14.00	12.36	11.90	11.75
MNO	0.18	0.16	0.14	0.15	0.15	0.08	0.13	0.23
NIO	0.18	0.17	0.12	0.13	0.18	0.25	0.28	0.10
MGO	45.48	46.01	46.30	44.84	45.62	46.34	46.64	46.26
CAO	1.31	0.13	0.12	0.07	0.14	0.20	0.23	0.86
TOTAL	99.55	99.49	98.70	99.69	99.98	99.30	99.28	99.00

** ATOMIC PROPORTIONS BASED ON SELECTED NO. OF OXYGENS **

OXYGN	4	4	4	4	4	4	4	4
SI	1.002	0.994	0.990	1.000	0.997	0.999	1.000	0.996
FE	0.257	0.281	0.270	0.310	0.293	0.258	0.248	0.246
MN	0.004	0.003	0.003	0.003	0.003	0.002	0.003	0.005
NI	0.004	0.003	0.002	0.003	0.004	0.005	0.006	0.002
MG	1.695	1.720	1.742	1.681	1.701	1.727	1.736	1.729
CA	0.035	0.003	0.003	0.002	0.004	0.005	0.006	0.023
FO	86.82	85.95	86.56	84.43	85.31	86.98	87.48	87.52

**** SAMPLE DIRECTORY ****

OBS	NO	MINSPENO	ANALPOS	OBS	NO	MINSPENO	ANALPOS
177	256	CLI/045/005	SR/R+1480	178	256	OLI/046/001	R
179	256	CLI/046/002	C	180	256	OLI/047/001	C
181	256	OLI/048/001	C	182	256	OLI/049/001	C
183	256	OLI/050/001	C	184	256	OLI/050/002	R

APPENDIX 5
OLIVINE ANALYSES

OBS	185	186	187	188	189	190	191	192
SIO2	40.15	39.86	40.06	39.89	39.48	39.46	39.83	39.98
TIO2	0.00	0.05	0.00	0.04	0.00	0.04	0.00	0.00
AL2O3	0.04	0.05	0.04	0.00	0.00	0.00	0.05	0.04
CR2O3	0.07	0.16	0.08	0.13	0.22	0.00	0.23	0.07
FEOT	12.32	11.88	12.00	12.32	13.13	13.59	12.44	12.36
MNO	0.12	0.13	0.15	0.17	0.10	0.18	0.13	0.14
NIO	0.29	0.32	0.28	0.22	0.12	0.19	0.19	0.34
MGO	46.51	47.26	47.35	46.45	46.63	46.15	46.59	47.01
CAO	0.18	0.20	0.17	0.26	0.21	0.19	0.25	0.17
TOTAL	99.68	99.91	100.13	99.48	99.89	99.80	99.71	100.11

** ATOMIC PROPORTIONS BASED ON SELECTED NO. OF OXYGENS **

OXYGN	4	4	4	4	4	4	4	4
SI	1.000	0.990	0.993	0.996	0.986	0.989	0.993	0.993
FE	0.257	0.247	0.249	0.257	0.274	0.285	0.259	0.257
MN	0.003	0.003	0.003	0.004	0.002	0.004	0.003	0.003
NI	0.006	0.006	0.006	0.004	0.002	0.004	0.004	0.007
MG	1.726	1.750	1.749	1.729	1.736	1.723	1.732	1.740
CA	0.005	0.005	0.005	0.007	0.006	0.005	0.007	0.005
FO	87.06	87.64	87.55	87.04	86.35	85.82	86.97	87.14

**** SAMPLE DIRECTORY ****

OBS	NO	MINSPENO	ANALPOS	OBS	NO	MINSPENO	ANALPOS
185	259	OLI/001/001	C	186	259	OLI/002/001	I
187	259	OLI/002/002	C	188	259	OLI/003/001	I
189	259	OLI/004/001	I	190	259	OLI/004/002	C
191	259	OLI/005/001	R	192	259	OLI/005/002	C

APPENDIX 5
OLIVINE ANALYSES

OBS	193	194	195	196	197	198	199	200
SIO2	39.63	39.71	38.15	40.01	39.79	39.84	39.73	39.27
TIO2	0.06	0.00	0.06	0.00	0.00	0.00	0.00	0.00
AL2O3	0.04	0.06	0.05	0.06	0.04	0.04	0.06	0.00
CR2O3	0.18	0.07	0.11	0.11	0.11	0.11	0.00	0.06
FEOT	12.76	11.10	17.12	11.51	11.60	13.00	13.23	12.58
MNO	0.20	0.16	0.36	0.13	0.14	0.18	0.15	0.18
NIO	0.12	0.33	0.15	0.33	0.20	0.23	0.23	0.35
MGO	46.48	47.64	43.05	47.83	47.56	46.75	46.65	46.93
CAO	0.38	0.15	0.33	0.20	0.25	0.23	0.28	0.19
TOTAL	99.85	99.22	99.38	100.18	99.69	100.38	100.33	99.56

** ATOMIC PROPORTIONS BASED ON SELECTED NO. OF OXYGENS **

OXYGN	4	4	4	4	4	4	4	4
SI	0.989	0.990	0.979	0.989	0.989	0.990	0.989	0.984
FE	0.266	0.231	0.367	0.238	0.241	0.270	0.275	0.264
MN	0.004	0.003	0.008	0.003	0.003	0.004	0.003	0.004
NI	0.002	0.007	0.003	0.007	0.004	0.005	0.005	0.007
MG	1.729	1.770	1.647	1.763	1.762	1.731	1.730	1.752
CA	0.010	0.004	0.009	0.005	0.007	0.006	0.007	0.005
FO	86.65	88.44	81.76	88.10	87.96	86.50	86.27	86.92

**** SAMPLE DIRECTORY ****

OBS	NO	MINSPENO	ANALPOS	OBS	NO	MINSPENO	ANALPOS
193	259	OLI/006/001	C	194	267	OLI/001/001	C
195	267	OLI/001/002	R	196	267	OLI/002/001	C
197	267	OLI/002/002	I	198	267	OLI/003/001	C
199	267	OLI/003/002	R	200	267	OLI/004/001	C

APPENDIX 5
OLIVINE ANALYSES

OBS	201	202	203	204	205	206	207	208
SIO2	39.82	39.62	39.56	39.62	39.98	39.71	40.03	39.64
TIO2	0.00	0.00	0.00	0.00	0.00	0.00	0.00	0.04
AL2O3	0.04	0.00	0.04	0.04	0.00	0.04	0.06	0.05
CR2O3	0.06	0.05	0.08	0.05	0.00	0.00	0.06	0.00
FEOT	11.31	12.12	12.40	12.06	12.49	13.07	12.59	11.30
MNO	0.16	0.17	0.14	0.15	0.15	0.15	0.17	0.10
NIO	0.34	0.39	0.35	0.39	0.22	0.33	0.35	0.35
MGO	47.69	47.38	47.47	47.40	47.28	46.61	47.58	47.67
CAO	0.19	0.17	0.23	0.17	0.19	0.17	0.16	0.16
TOTAL	99.61	99.90	100.27	99.88	100.31	100.08	101.00	99.31

** ATOMIC PROPORTIONS BASED ON SELECTED NO. OF OXYGENS **

OXYGN	4	4	4	4	4	4	4	4
SI	0.990	0.986	0.983	0.986	0.991	0.990	0.987	0.988
FE	0.235	0.252	0.258	0.251	0.259	0.272	0.260	0.236
MN	0.003	0.004	0.003	0.003	0.003	0.003	0.004	0.002
NI	0.007	0.008	0.007	0.008	0.004	0.007	0.007	0.007
MG	1.767	1.758	1.757	1.758	1.747	1.732	1.748	1.771
CA	0.005	0.005	0.006	0.005	0.005	0.005	0.004	0.004
FO	88.25	87.45	87.22	87.51	87.09	86.40	87.07	88.26

**** SAMPLE DIRECTORY ****

OBS	NO	MINSPENO	ANALPOS	OBS	NO	MINSPENO	ANALPOS
201	267	OLI/005/001	C	202	267	OLI/006/001	C
203	267	OLI/006/002	R	204	267	OLI/007/001	C
205	267	OLI/008/001	C	206	267	OLI/009/001	C
207	267	OLI/010/001	C	208	267	CLI/011/001	C

APPENDIX 5
OLIVINE ANALYSES

OBS	209	210	211	212	213	214
SIO2	39.91	39.43	38.70	39.20	39.09	39.57
TIO2	0.00	0.00	0.05	0.06	0.00	0.00
AL2O3	0.05	0.00	0.04	0.00	0.00	0.04
CR2O3	0.00	0.00	0.00	0.05	0.04	0.00
FEOT	11.94	15.99	17.83	13.63	13.36	13.30
MNO	0.17	0.26	0.33	0.17	0.17	0.18
NIO	0.26	0.19	0.14	0.20	0.21	0.23
MGO	47.18	44.39	43.26	46.39	46.45	46.57
CAO	0.19	0.28	0.18	0.17	0.17	0.23
TOTAL	99.70	100.54	100.53	99.87	99.49	100.12

** ATOMIC PROPORTIONS BASED ON SELECTED NO. OF OXYGENS **

OXYGN	4	4	4	4	4	4
SI	0.993	0.992	0.983	0.983	0.983	0.987
FE	0.248	0.336	0.379	0.286	0.281	0.278
MN	0.004	0.006	0.007	0.004	0.004	0.004
NI	0.005	0.004	0.003	0.004	0.004	0.005
MG	1.749	1.664	1.637	1.733	1.740	1.732
CA	0.005	0.008	0.005	0.005	0.005	0.006
FO	87.56	83.18	81.22	85.85	86.10	86.19

**** SAMPLE DIRECTORY ****

OBS	NO	MINSPENO	ANALPOS	OBS	NO	MINSPENO	ANALPOS
209	267	OLI/012/001	C	210	267	OLI/013/001	I
211	267	OLI/014/001	C	212	267	OLI/015/001	C
213	267	OLI/015/002	I	214	267	OLI/015/003	R

APPENDIX 6

SPINEL ANALYSES

INDEX

Sample	Spinel	Description
14	3-4;10;22	red chromite
205	2	red chromite
213	15-18;25-26	red chromite

Olivine/Spinel pairs

Sample	Pair
256	spi1-oli36;spi2-oli37;spi3-oli38; spi4-oli38;spi5-oli39
259	spi21-oli2;spi22-oli3;spi23-oli4; spi24-oli5;spi25-oli6

APPENDIX 6
SPINEL ANALYSES

OBS	1	2	3	4	5	6	7	8
SIO2	0.11	0.06	0.07	0.10	0.00	0.00	0.00	0.00
TIO2	5.89	10.08	6.35	6.85	3.27	1.98	1.81	2.98
AL2O3	0.49	4.14	0.48	1.07	27.17	33.64	32.80	22.47
CR2O3	0.00	0.11	0.00	0.00	26.86	24.34	26.48	32.46
FEOT	85.56	73.22	85.17	80.18	24.72	20.39	19.61	24.37
MNO	0.38	0.65	0.34	0.51	0.25	0.28	0.22	0.39
MGO	2.09	7.23	2.00	5.40	15.59	16.96	17.10	14.92
CAO	0.00	0.10	0.00	0.34	0.00	0.12	0.05	0.07
TOTAL	94.52	95.59	94.41	94.45	97.86	97.71	98.07	97.66
FEO	33.25	29.45	33.74	28.55	14.70	12.21	11.96	14.43
FE2O3	58.14	48.64	57.16	57.38	11.13	9.09	8.51	11.04
TOTAL	100.35	100.46	100.14	100.20	98.98	98.62	98.92	98.77

** ATOMIC PROPORTIONS BASED ON SELECTED NO. OF OXYGENS **

OXYGN	4	4	4	4	4	4	4	4
TI	0.166	0.267	0.179	0.188	0.074	0.043	0.040	0.069
AL	0.022	0.172	0.021	0.046	0.962	1.154	1.125	0.816
CR	0.000	0.003	0.000	0.000	0.638	0.560	0.609	0.790
FE2+	1.041	0.867	1.059	0.869	0.369	0.297	0.291	0.372
FE3+	1.638	1.288	1.615	1.572	0.252	0.199	0.186	0.256
MN	0.012	0.019	0.011	0.016	0.006	0.007	0.005	0.010
MG	0.117	0.379	0.112	0.293	0.698	0.736	0.742	0.685
FFM	0.90	0.70	0.90	0.75	0.35	0.29	0.28	0.35
CCA	0.00	0.02	0.00	0.00	0.40	0.33	0.35	0.49
2TAC	0.94	0.75	0.94	0.89	0.08	0.05	0.04	0.08

**** SAMPLE DIRECTORY ****

OBS	NO	MINSPENO	ANALPOS	OBS	NO	MINSPENO	ANALPOS
1	9	SPI/001/001	C	2	9	SPI/001/002	R
3	9	SPI/002/001	C	4	9	SPI/002/002	R
5	9	SPI/003/001	C	6	9	SPI/004/001	C
7	9	SPI/005/001	C	8	9	SPI/006/001	C

APPENDIX 6
SPINEL ANALYSES

OBS	9	10	11	12	13	14	15	16
SIO2	0.00	0.01	0.00	0.05	0.00	0.00	0.07	0.13
TIO2	2.32	3.05	5.41	5.59	11.97	11.17	5.67	7.33
AL2O3	20.47	19.32	0.53	0.51	2.26	1.47	0.47	8.58
CR2O3	39.96	36.19	0.00	0.00	0.30	0.14	0.00	0.17
FEOT	19.52	24.28	86.55	81.23	72.25	74.80	85.20	68.47
MNO	0.23	0.23	0.37	0.49	0.75	0.58	0.34	0.59
MGO	15.28	14.47	1.06	6.38	7.57	6.78	1.95	8.71
CAO	0.01	0.01	0.00	0.00	0.14	0.19	0.00	0.23
TOTAL	97.79	97.55	93.92	94.25	95.24	95.13	93.70	94.21
FEO	13.18	14.89	34.08	26.19	29.97	30.45	32.98	24.96
FE2O3	7.04	10.43	58.32	61.17	46.99	49.29	58.03	48.35
TOTAL	98.50	98.60	99.76	100.38	99.95	100.07	99.52	99.06

** ATOMIC PROPORTIONS BASED ON SELECTED NO. OF OXYGENS **

OXYGN	4	4	4	4	4	4	4	4
TI	0.054	0.072	0.155	0.152	0.320	0.301	0.161	0.190
AL	0.748	0.714	0.024	0.022	0.095	0.062	0.021	0.349
CR	0.979	0.896	0.000	0.000	0.008	0.004	0.000	0.005
FE2+	0.342	0.390	1.083	0.794	0.891	0.914	1.043	0.721
FE3+	0.164	0.246	1.667	1.670	1.257	1.331	1.651	1.256
MN	0.006	0.006	0.012	0.015	0.023	0.018	0.011	0.017
MG	0.706	0.676	0.060	0.345	0.401	0.363	0.110	0.448
FFM	0.33	0.37	0.95	0.70	0.69	0.72	0.90	0.62
CCA	0.57	0.56	0.00	0.00	0.08	0.06	0.00	0.01
2TAC	0.06	0.08	0.93	0.93	0.86	0.90	0.94	0.52

**** SAMPLE DIRECTORY ****

OBS	NO	MINSPENO	ANALPOS	OBS	NO	MINSPENO	ANALPOS
9	11	SPI/001/001		10	11	SPI/002/001	
11	11	SPI/003/001	C	12	11	SPI/003/002	I
13	11	SPI/003/003	R	14	14	SPI/001/001	MI
15	14	SPI/002/001	C	16	14	SPI/002/002	R

APPENDIX 6
SPINEL ANALYSES

OBS	17	18	19	20	21	22	23	24
SIO2	0.00	0.00	0.00	0.00	0.00	0.00	0.00	0.00
TIO2	1.70	1.78	1.63	2.06	1.96	1.86	2.61	2.05
AL2O3	31.58	31.35	33.42	27.82	26.52	32.23	23.08	25.94
CR2O3	28.47	28.06	25.84	31.56	29.18	26.66	33.83	33.80
FEOT	19.15	18.86	18.88	20.65	24.66	20.52	23.13	20.11
MNO	0.16	0.14	0.10	0.33	0.38	0.23	0.21	0.14
MGO	17.17	17.04	17.54	15.67	15.20	16.49	14.89	15.86
CAO	0.00	0.00	0.00	0.06	0.04	0.04	0.03	0.04
TOTAL	98.23	97.23	97.41	98.15	97.94	98.03	97.78	97.94
FEO	11.73	11.66	11.19	13.48	13.88	12.84	14.49	13.03
FE2O3	8.25	8.01	8.55	7.97	11.98	8.54	9.61	7.87
TOTAL	99.06	98.03	98.27	98.95	99.14	98.89	98.74	98.73

** ATOMIC PROPORTIONS BASED ON SELECTED NO. OF OXYGENS **

OXYGN	4	4	4	4	4	4	4	4
TI	0.037	0.039	0.036	0.046	0.044	0.041	0.060	0.047
AL	1.087	1.090	1.147	0.981	0.943	1.113	0.836	0.922
CR	0.657	0.654	0.595	0.747	0.696	0.617	0.822	0.806
FE2+	0.286	0.287	0.272	0.337	0.350	0.314	0.372	0.329
FE3+	0.181	0.178	0.187	0.179	0.272	0.188	0.222	0.179
MN	0.004	0.003	0.002	0.008	0.010	0.006	0.005	0.004
MG	0.747	0.749	0.761	0.699	0.683	0.720	0.682	0.713
FFM	0.28	0.28	0.26	0.33	0.34	0.30	0.35	0.32
CCA	0.38	0.38	0.34	0.43	0.42	0.36	0.50	0.47
2TAC	0.04	0.04	0.04	0.05	0.05	0.05	0.07	0.05

**** SAMPLE DIRECTORY ****

OBS	NO	MINSPENO	ANALPOS	OBS	NO	MINSPENO	ANALPOS
17	14	SPI/003/001	C	18	14	SPI/003/002	R
19	14	SPI/004/001	C	20	14	SPI/005/001	C
21	14	SPI/006/001	C	22	14	SPI/007/001	C
23	14	SPI/008/001	C	24	14	SPI/009/001	C

APPENDIX 6
SPINEL ANALYSES

OBS	25	26	27	28	29	30	31	32
SIO2	0.00	0.00	0.05	0.00	0.00	0.05	0.09	0.00
TIO2	1.87	8.63	8.99	7.14	8.35	9.24	9.85	3.45
AL2O3	29.17	6.30	6.76	2.66	5.02	6.47	5.85	26.89
CR2O3	30.53	2.76	0.19	0.33	0.70	0.20	0.95	25.13
FEOT	20.01	67.32	68.74	75.61	71.71	69.45	68.23	27.30
MNO	0.24	0.67	0.70	0.69	0.69	0.68	0.84	0.27
MGO	16.33	8.82	8.84	7.15	8.39	9.22	9.29	14.45
CAO	0.07	0.13	0.14	0.44	0.17	0.10	0.15	0.05
TOTAL	98.22	94.63	94.41	94.02	95.03	95.41	95.25	97.54
FEO	12.62	25.58	25.91	25.78	25.92	25.91	26.01	16.40
FE2O3	8.22	46.39	47.60	55.38	50.89	48.39	46.92	12.12
TOTAL	99.04	99.28	99.18	99.57	100.13	100.26	99.95	98.75

** ATOMIC PROPORTIONS BASED ON SELECTED NO. OF OXYGENS **

OXYGN	4	4	4	4	4	4	4	4
TI	0.042	0.226	0.235	0.192	0.219	0.239	0.256	0.079
AL	1.019	0.258	0.277	0.112	0.206	0.262	0.238	0.962
CR	0.715	0.076	0.005	0.009	0.019	0.005	0.026	0.603
FE2+	0.313	0.744	0.753	0.773	0.756	0.745	0.751	0.416
FE3+	0.183	1.214	1.245	1.493	1.336	1.251	1.219	0.277
MN	0.006	0.020	0.021	0.021	0.020	0.020	0.025	0.007
MG	0.721	0.457	0.458	0.382	0.436	0.472	0.478	0.654
FFM	0.30	0.62	0.62	0.67	0.63	0.61	0.61	0.39
CCA	0.41	0.23	0.02	0.08	0.09	0.02	0.10	0.39
2TAC	0.05	0.57	0.62	0.76	0.66	0.64	0.66	0.09

**** SAMPLE DIRECTORY ****

OBS	NO	MINSPENO	ANALPOS	OBS	NO	MINSPENO	ANALPOS
25	14	SPI/010/001	C	26	14	SPI/011/001	C
27	14	SPI/012/001	I	28	14	SPI/013/001	C
29	14	SPI/014/001	C	30	14	SPI/015/001	C
31	14	SPI/016/001	M	32	14	SPI/016/002	C

APPENDIX 6
SPINEL ANALYSES

OBS	33	34	35	36	37	38	39	40
SIO2	0.00	0.00	0.00	0.00	0.06	0.00	0.00	0.00
TIO2	7.81	9.48	9.11	10.11	9.57	1.56	3.70	3.70
AL2O3	6.31	6.58	11.24	2.57	3.41	37.23	21.40	21.56
CR2O3	0.29	0.19	15.19	0.97	1.24	23.39	30.36	29.36
FEOT	70.91	68.10	48.76	72.09	71.90	17.43	29.05	28.56
MNO	0.65	0.67	0.73	0.63	0.68	0.21	0.24	0.34
MGO	8.78	9.14	11.87	8.17	8.32	17.77	13.18	13.56
CAO	0.12	0.14	0.07	0.07	0.07	0.06	0.07	0.17
TOTAL	94.87	94.30	96.97	94.61	95.25	97.65	98.00	97.25
FEO	25.09	25.79	22.59	27.47	27.13	11.24	17.86	16.85
FE2O3	50.93	47.02	29.09	49.59	49.76	6.88	12.43	13.01
TOTAL	99.97	99.01	99.88	99.58	100.24	98.34	99.25	98.55

** ATOMIC PROPORTIONS BASED ON SELECTED NO. OF OXYGENS **

OXYGN	4	4	4	4	4	4	4	4
TI	0.203	0.248	0.225	0.270	0.253	0.034	0.087	0.087
AL	0.258	0.270	0.436	0.108	0.141	1.256	0.787	0.795
CR	0.008	0.005	0.395	0.027	0.034	0.529	0.748	0.726
FE2+	0.727	0.749	0.621	0.816	0.797	0.269	0.466	0.441
FE3+	1.327	1.230	0.719	1.325	1.315	0.148	0.292	0.306
MN	0.019	0.020	0.020	0.019	0.020	0.005	0.006	0.009
MG	0.453	0.473	0.581	0.432	0.435	0.758	0.612	0.632
FFM	0.62	0.61	0.52	0.65	0.65	0.26	0.43	0.41
CCA	0.03	0.02	0.48	0.20	0.20	0.30	0.49	0.48
2TAC	0.61	0.64	0.35	0.80	0.74	0.04	0.10	0.10

**** SAMPLE DIRECTORY ****

OBS	NO	MINSPENO	ANALPOS	OBS	NO	MINSPENO	ANALPOS
33	14	SPI/017/001	C	34	14	SPI/018/001	C
35	14	SPI/019/001	C	36	14	SPI/020/001	C
37	14	SPI/021/001	C	38	14	SPI/022/001	C
39	14	SPI/023/001	C	40	14	SPI/023/002	R

APPENDIX 6
SPINEL ANALYSES

OBS	41	42	43	44	45	46	47	48
SIO2	0.07	0.05	0.00	0.00	0.05	0.06	0.05	0.00
TIO2	6.15	6.87	1.71	1.84	6.53	10.42	9.91	8.51
AL2O3	1.35	2.26	27.33	30.92	0.53	4.26	5.56	4.22
CR2O3	0.00	0.00	32.99	27.87	0.00	0.14	2.65	0.25
FEOT	79.69	77.98	19.68	20.29	83.24	72.80	67.89	72.38
MNO	0.53	0.55	0.17	0.20	0.51	0.68	0.68	0.67
MGO	6.40	6.57	15.91	15.97	3.73	6.91	9.28	8.28
CAO	0.07	0.13	0.00	0.14	0.00	0.12	0.07	0.14
TOTAL	94.26	94.41	97.79	97.23	94.59	95.39	96.09	94.45
FEO	26.66	27.08	12.83	13.05	31.13	30.13	26.50	25.98
FE2O3	58.93	56.56	7.61	8.04	57.91	47.42	46.00	51.56
TOTAL	100.17	100.08	98.55	98.04	100.39	100.14	100.70	99.62

** ATOMIC PROPORTIONS BASED ON SELECTED NO. OF OXYGENS **

OXYGN	4	4	4	4	4	4	4	4
TI	0.167	0.186	0.039	0.041	0.181	0.277	0.256	0.225
AL	0.058	0.096	0.968	1.083	0.023	0.177	0.225	0.175
CR	0.000	0.000	0.783	0.655	0.000	0.004	0.072	0.007
FE2+	0.806	0.814	0.322	0.324	0.962	0.890	0.761	0.765
FE3+	1.603	1.529	0.172	0.180	1.610	1.261	1.188	1.367
MN	0.016	0.017	0.004	0.005	0.016	0.020	0.020	0.020
MG	0.345	0.352	0.712	0.707	0.205	0.364	0.475	0.435
FFM	0.70	0.70	0.31	0.31	0.82	0.71	0.62	0.64
CCA	0.00	0.00	0.45	0.38	0.00	0.02	0.24	0.04
2TAC	0.85	0.80	0.04	0.05	0.94	0.75	0.63	0.71

**** SAMPLE DIRECTORY ****

OBS	NO	MINSPENO	ANALPOS	OBS	NO	MINSPENO	ANALPOS
41	14	SPI/024/001	C	42	14	SPI/024/002	R
43	14	SPI/025/001	C	44	14	SPI/025/002	R
45	14	SPI/026/001	C	46	14	SPI/026/002	R
47	14	SPI/027/001	C	48	14	SPI/027/002	R

APPENDIX 6
SPINEL ANALYSES

OBS	49	50	51	52	53	54	55	56
SIO2	0.00	0.06	0.07	0.06	0.09	0.08	0.06	0.06
TIO2	12.73	8.41	6.59	6.44	6.42	6.41	6.40	6.51
AL2O3	6.64	3.49	0.55	0.51	0.52	0.53	0.52	0.54
CR2O3	0.94	0.14	0.00	0.00	0.00	0.06	0.05	0.00
FEOT	65.04	73.50	85.77	84.90	85.26	85.29	85.74	84.94
MNO	0.75	0.62	0.32	0.34	0.36	0.33	0.36	0.40
MGO	10.20	7.78	2.02	1.94	1.97	2.04	2.24	2.50
CAO	0.11	0.28	0.00	0.00	0.00	0.00	0.00	0.00
TOTAL	96.41	94.28	95.32	94.19	94.62	94.74	95.37	94.95
FEO	27.64	26.46	34.25	33.82	33.92	33.86	33.71	33.23
FE2O3	41.56	52.28	57.26	56.77	57.06	57.15	57.83	57.47
TOTAL	100.58	99.52	101.06	99.88	100.34	100.47	101.17	100.71

** ATOMIC PROPORTIONS BASED ON SELECTED NO. OF OXYGENS **

OXYGN	4	4	4	4	4	4	4	4
TI	0.325	0.225	0.184	0.182	0.181	0.180	0.179	0.182
AL	0.265	0.146	0.024	0.023	0.023	0.023	0.023	0.024
CR	0.025	0.004	0.000	0.000	0.000	0.002	0.001	0.000
FE2+	0.784	0.786	1.065	1.065	1.063	1.059	1.046	1.033
FE3+	1.060	1.397	1.602	1.608	1.609	1.608	1.614	1.608
MN	0.022	0.019	0.010	0.011	0.011	0.010	0.011	0.013
MG	0.515	0.412	0.112	0.109	0.110	0.114	0.124	0.139
FFM	0.60	0.66	0.90	0.91	0.91	0.90	0.89	0.88
CCA	0.09	0.03	0.00	0.00	0.00	0.07	0.06	0.00
2TAC	0.69	0.75	0.94	0.94	0.94	0.93	0.94	0.94

**** SAMPLE DIRECTORY ****

OBS	NO	MINSPENO	ANALPOS	OBS	NO	MINSPENO	ANALPOS
49	14	SPI/028/001	C	50	14	SPI/028/002	R
51	14	SPI/029/001	SC/C-0000	52	14	SPI/029/002	SI/C-625
53	14	SPI/029/003	SI/C-1250	54	14	SPI/029/004	SI/C-1875
55	14	SPI/029/005	SI/C-1979	56	14	SPI/029/006	SI/C-2083

APPENDIX 6
SPINEL ANALYSES

OBS	57	58	59	60	61	62	63	64
SIO2	0.07	0.06	0.09	0.00	0.10	0.05	0.04	0.06
TIO2	6.53	6.77	7.43	8.78	6.74	7.86	3.95	3.18
AL2O3	0.53	0.66	1.64	4.23	0.55	5.02	20.84	20.12
CR2O3	0.00	0.00	0.00	0.06	0.00	0.12	30.11	33.21
FEOT	83.82	83.15	80.70	76.29	83.68	73.47	27.96	26.53
MNO	0.42	0.52	0.50	0.54	0.32	0.59	0.32	0.30
MGO	3.63	4.09	4.67	5.95	2.00	6.59	14.04	14.10
CAO	0.00	0.04	0.07	0.10	0.00	0.14	0.09	0.11
TOTAL	95.00	95.29	95.10	95.95	93.39	93.84	97.35	97.61
FEO	31.53	31.00	30.78	30.44	33.80	28.04	16.43	15.62
FE2O3	58.11	57.96	55.48	50.95	55.44	50.49	12.82	12.12
TOTAL	100.82	101.10	100.66	101.06	98.95	98.90	98.63	98.82

** ATOMIC PROPORTIONS BASED ON SELECTED NO. OF OXYGENS **

OXYGN	4	4	4	4	4	4	4	4
TI	0.181	0.186	0.203	0.233	0.192	0.211	0.093	0.075
AL	0.023	0.028	0.070	0.176	0.025	0.212	0.767	0.741
CR	0.000	0.000	0.000	0.002	0.000	0.003	0.743	0.820
FE2+	0.971	0.948	0.935	0.900	1.073	0.839	0.429	0.408
FE3+	1.610	1.595	1.517	1.355	1.583	1.359	0.301	0.285
MN	0.013	0.016	0.015	0.016	0.010	0.018	0.008	0.008
MG	0.199	0.223	0.253	0.313	0.113	0.351	0.653	0.657
FFM	0.83	0.81	0.79	0.74	0.90	0.70	0.40	0.38
CCA	0.00	0.00	0.00	0.01	0.00	0.02	0.49	0.53
2TAC	0.94	0.93	0.85	0.72	0.94	0.66	0.11	0.09

**** SAMPLE DIRECTORY ****

OBS	NO	MINSPENO	ANALPOS	OBS	NO	MINSPENO	ANALPOS
57	14	SPI/029/007	SI/C-2187	58	14	SPI/029/008	SI/C-2291
59	14	SPI/029/009	SI/C-2395	60	14	SPI/029/010	SR/C-2500
61	26	SPI/001/001	C	62	26	SPI/001/002	C
63	30	SPI/001/001	C	64	30	SPI/002/001	C

APPENDIX 6
SPINEL ANALYSES

OBS	65	66	67	68	69	70	71	72
SIO2	0.07	0.05	0.05	0.16	0.04	0.03	0.14	0.02
TIO2	2.54	3.27	2.98	4.36	3.35	3.61	15.66	14.10
AL2O3	23.90	21.70	18.10	17.86	22.53	20.72	1.98	2.46
CR2O3	32.40	31.09	38.05	26.65	28.82	25.15	3.14	6.69
FEOT	22.89	26.11	23.32	36.11	29.95	35.45	69.12	65.53
MNO	0.15	0.24	0.14	0.60	0.59	0.60	1.08	0.99
MGO	15.59	14.71	15.17	11.04	11.98	11.22	4.46	5.75
CAO	0.08	0.09	0.05	0.16	0.14	0.15	0.17	0.17
TOTAL	97.62	97.26	97.86	96.94	97.40	96.93	95.75	95.71
FEO	13.54	14.98	13.76	20.65	18.98	19.99	37.79	34.40
FE2O3	10.40	12.37	10.62	17.18	12.19	17.18	34.82	34.60
TOTAL	98.66	98.50	98.92	98.66	98.62	98.65	99.24	99.18

** ATOMIC PROPORTIONS BASED ON SELECTED NO. OF OXYGENS **

OXYGN	4	4	4	4	4	4	4	4
TI	0.058	0.076	0.070	0.106	0.079	0.087	0.429	0.382
AL	0.859	0.793	0.667	0.680	0.835	0.779	0.085	0.105
CR	0.781	0.762	0.940	0.680	0.716	0.634	0.091	0.191
FE2+	0.345	0.389	0.360	0.558	0.499	0.533	1.152	1.037
FE3+	0.239	0.289	0.250	0.418	0.288	0.412	0.955	0.939
MN	0.004	0.006	0.004	0.016	0.016	0.016	0.033	0.030
MG	0.709	0.680	0.707	0.531	0.561	0.533	0.242	0.309
FFM	0.33	0.36	0.34	0.51	0.47	0.50	0.83	0.77
CCA	0.48	0.49	0.59	0.50	0.46	0.45	0.52	0.65
2TAC	0.07	0.09	0.08	0.13	0.09	0.11	0.83	0.72

**** SAMPLE DIRECTORY ****

OBS	NO	MINSPENO	ANALPOS	OBS	NO	MINSPENO	ANALPOS
65	30	SPI/003/001	C	66	30	SPI/004/001	C
67	30	SPI/005/001	C	68	30	SPI/006/001	C
69	30	SPI/007/001	C	70	30	SPI/008/001	C
71	30	SPI/009/001	C	72	30	SPI/010/001	C

APPENDIX 6
SPINEL ANALYSES

OBS	73	74	75	76	77	78	79	80
SIO2	0.03	0.03	0.05	0.04	0.05	0.05	0.01	0.06
TIO2	14.76	16.95	16.66	16.86	16.40	15.69	14.64	15.39
AL2O3	1.65	0.94	0.89	1.27	1.12	1.78	3.23	0.99
CR2O3	4.59	0.47	0.82	0.66	1.03	2.70	3.26	2.85
FEOT	68.96	70.82	71.09	70.44	71.19	69.07	66.99	71.20
MNO	1.08	1.20	1.13	1.07	1.10	1.11	0.92	1.18
MGO	3.87	4.44	3.89	4.43	4.24	4.60	5.94	3.34
CAO	0.26	0.15	0.39	0.31	0.28	0.24	0.21	0.41
TOTAL	95.20	95.00	94.92	95.08	95.41	95.24	95.20	95.42
FEO	37.40	38.35	38.71	38.31	38.30	37.18	34.59	38.53
FE2O3	35.07	36.08	35.99	35.70	36.55	35.44	36.01	36.31
TOTAL	98.71	98.62	98.53	98.66	99.07	98.79	98.81	99.06

** ATOMIC PROPORTIONS BASED ON SELECTED NO. OF OXYGENS **

OXYGN	4	4	4	4	4	4	4	4
TI	0.409	0.471	0.465	0.467	0.453	0.432	0.397	0.429
AL	0.072	0.041	0.039	0.055	0.049	0.077	0.137	0.043
CR	0.134	0.014	0.024	0.019	0.030	0.078	0.093	0.083
FE2+	1.154	1.184	1.200	1.180	1.178	1.139	1.042	1.193
FE3+	0.973	1.002	1.004	0.989	1.011	0.977	0.976	1.012
MN	0.034	0.038	0.035	0.033	0.034	0.034	0.028	0.037
MG	0.213	0.244	0.215	0.243	0.232	0.251	0.319	0.184
FFM	0.84	0.83	0.85	0.83	0.84	0.82	0.77	0.87
CCA	0.65	0.25	0.38	0.26	0.38	0.50	0.40	0.66
2TAC	0.80	0.95	0.94	0.93	0.92	0.85	0.78	0.87

**** SAMPLE DIRECTORY ****

OBS	NO	MINSPENO	ANALPOS	OBS	NO	MINSPENO	ANALPOS
73	30	SPI/011/001	C	74	30	SPI/012/001	C
75	30	SPI/013/001	C	76	30	SPI/014/001	C
77	30	SPI/015/001	C	78	30	SPI/016/001	C
79	30	SPI/017/001	C	80	30	SPI/018/001	C

APPENDIX 6
SPINEL ANALYSES

OBS	81	82	83	84	85	86	87	88
SIO2	0.34	0.06	0.08	0.03	0.04	0.11	0.00	0.00
TIO2	14.81	16.68	15.63	14.97	15.60	16.48	2.87	3.33
AL2O3	2.16	1.04	3.76	1.03	2.53	0.87	23.69	24.43
CR2O3	4.41	0.22	1.38	3.38	1.03	1.36	30.58	26.45
FEOT	67.90	71.82	66.83	70.19	68.77	71.05	26.57	30.57
MNO	1.02	1.09	0.89	1.10	0.99	1.16	0.43	0.60
MGO	4.46	3.90	7.00	3.83	5.72	3.20	13.41	12.00
CAO	0.52	0.35	0.26	0.37	0.32	1.02	0.04	0.06
TOTAL	95.62	95.16	95.83	94.90	95.00	95.25	97.59	97.44
FEO	36.91	38.92	34.21	37.33	35.47	39.00	16.81	19.28
FE2O3	34.45	36.56	36.26	36.52	37.01	35.62	10.85	12.54
TOTAL	99.07	98.82	99.46	98.56	98.71	98.82	98.68	98.70

** ATOMIC PROPORTIONS BASED ON SELECTED NO. OF OXYGENS **

OXYGN	4	4	4	4	4	4	4	4
TI	0.406	0.464	0.416	0.417	0.425	0.460	0.067	0.078
AL	0.093	0.045	0.157	0.045	0.108	0.038	0.865	0.898
CR	0.127	0.006	0.039	0.099	0.030	0.040	0.749	0.652
FE2+	1.124	1.203	1.013	1.158	1.075	1.210	0.435	0.503
FE3+	0.944	1.017	0.966	1.019	1.009	0.994	0.253	0.294
MN	0.031	0.034	0.027	0.035	0.030	0.036	0.011	0.016
MG	0.242	0.215	0.369	0.212	0.309	0.177	0.619	0.557
FFM	0.82	0.85	0.73	0.85	0.78	0.87	0.41	0.47
CCA	0.58	0.12	0.20	0.69	0.21	0.51	0.46	0.42
2TAC	0.79	0.95	0.81	0.85	0.86	0.92	0.08	0.09

**** SAMPLE DIRECTORY ****

OBS	NO	MINSPENO	ANALPOS	OBS	NO	MINSPENO	ANALPOS
81	30	SPI/019/001	C	82	30	SPI/020/001	C
83	30	SPI/021/001	C	84	30	SPI/022/001	C
85	30	SPI/023/001	C	86	30	SPI/024/001	C
87	30	SPI/025/001	C	88	30	SPI/026/001	C

APPENDIX 6
SPINEL ANALYSES

OBS	89	90	91	92	93	94	95	96
SIO2	0.00	0.00	0.00	0.00	0.00	0.00	0.00	0.06
TIO2	2.77	9.60	7.04	10.66	3.17	15.63	14.92	13.83
AL2O3	24.23	8.21	11.77	7.77	24.45	3.05	4.70	4.13
CR2O3	29.74	13.53	16.55	10.13	27.32	0.65	0.00	1.39
FEOT	26.77	59.86	51.57	60.93	27.30	70.73	70.19	70.12
MNO	0.45	0.85	0.79	0.82	0.23	1.00	1.03	0.95
MGO	13.29	5.97	8.02	7.01	14.72	4.99	4.79	4.70
CAO	0.06	0.06	0.05	0.06	0.04	0.09	0.14	0.11
TOTAL	97.31	98.08	95.97	97.38	97.23	96.14	95.77	95.29
FEO	16.86	31.87	26.27	31.00	15.32	37.27	36.99	36.11
FE2O3	11.02	31.11	28.12	33.26	13.31	37.18	36.90	37.80
TOTAL	98.41	101.20	98.79	100.71	98.56	99.87	99.47	99.08

** ATOMIC PROPORTIONS BASED ON SELECTED NO. OF OXYGENS **

OXYGN	4	4	4	4	4	4	4	4
TI	0.065	0.248	0.180	0.275	0.073	0.423	0.403	0.376
AL	0.885	0.332	0.473	0.315	0.884	0.129	0.199	0.176
CR	0.729	0.367	0.446	0.275	0.662	0.018	0.000	0.040
FE2+	0.437	0.915	0.749	0.890	0.393	1.121	1.110	1.092
FE3+	0.257	0.804	0.721	0.860	0.307	1.006	0.996	1.028
MN	0.012	0.025	0.023	0.024	0.006	0.030	0.031	0.029
MG	0.614	0.306	0.407	0.359	0.673	0.268	0.256	0.253
FFM	0.42	0.75	0.65	0.71	0.37	0.81	0.81	0.81
CCA	0.45	0.52	0.49	0.47	0.43	0.13	0.00	0.18
2TAC	0.07	0.41	0.28	0.48	0.09	0.85	0.80	0.78

**** SAMPLE DIRECTORY ****

OBS	NO	MINSPENO	ANALPOS	OBS	NO	MINSPENO	ANALPOS
89	30	SPI/027/001	C	90	83	SPI/001/001	C
91	83	SPI/002/001	C	92	83	SPI/003/001	C
93	83	SPI/004/001	C	94	83	SPI/005/001	C
95	83	SPI/006/001	C	96	83	SPI/007/001	C

APPENDIX 6
SPINEL ANALYSES

OBS	97	98	99	100	101	102	103	104
SIO2	0.00	0.07	0.25	0.06	0.07	0.06	0.11	0.11
TIO2	14.09	16.46	15.37	15.41	4.51	4.62	3.98	3.22
AL2O3	3.60	1.16	2.79	2.52	23.67	24.40	23.59	19.40
CR2O3	2.40	0.00	1.19	0.17	26.17	25.79	28.16	34.21
FEOT	69.33	72.38	68.20	71.90	26.12	25.66	24.64	25.07
MNO	1.08	1.14	0.92	1.02	0.31	0.32	0.27	0.47
MGO	4.89	3.63	6.15	4.25	16.60	16.91	16.85	15.13
CAO	0.06	0.20	0.15	0.26	0.06	0.07	0.05	0.16
TOTAL	95.45	95.04	95.02	95.59	97.51	97.83	97.65	97.77
FEO	35.86	39.27	35.19	37.82	13.61	13.41	12.88	13.86
FE2O3	37.20	36.80	36.69	37.88	13.90	13.61	13.07	12.46
TOTAL	99.18	98.73	98.70	99.39	98.90	99.19	98.96	99.02

** ATOMIC PROPORTIONS BASED ON SELECTED NO. OF OXYGENS **

OXYGN	4	4	4	4	4	4	4	4
TI	0.383	0.459	0.417	0.422	0.103	0.105	0.091	0.075
AL	0.153	0.051	0.119	0.108	0.846	0.866	0.841	0.711
CR	0.069	0.000	0.034	0.005	0.627	0.614	0.673	0.840
FE2+	1.084	1.217	1.061	1.152	0.345	0.338	0.326	0.360
FE3+	1.012	1.026	0.996	1.038	0.317	0.308	0.298	0.291
MN	0.033	0.036	0.028	0.031	0.008	0.008	0.007	0.012
MG	0.263	0.201	0.331	0.231	0.750	0.758	0.760	0.701
FFM	0.80	0.86	0.76	0.83	0.32	0.31	0.30	0.34
CCA	0.31	0.00	0.22	0.04	0.43	0.41	0.44	0.54
2TAC	0.78	0.95	0.85	0.88	0.12	0.12	0.11	0.09

**** SAMPLE DIRECTORY ****

OBS	NO	MINSPENO	ANALPOS	OBS	NO	MINSPENO	ANALPOS
97	83	SPI/008/001	C	98	83	SPI/009/001	C
99	83	SPI/010/001	C	100	83	SPI/011/001	C
101	191	SPI/001/001	C	102	191	SPI/002/001	C
103	191	SPI/003/001	C	104	191	SPI/004/001	C

APPENDIX 6
SPINEL ANALYSES

OBS	105	106	107	108	109	110	111	112
SIO2	0.03	0.06	0.06	0.06	0.06	0.06	0.04	0.08
TIO2	1.81	2.16	2.48	2.06	1.95	1.86	2.17	3.26
AL2O3	27.59	23.66	22.15	23.61	24.15	27.09	20.27	21.23
CR2O3	28.92	33.74	26.81	32.90	29.98	28.93	28.08	32.66
FEOT	22.96	21.33	32.69	23.19	26.44	24.26	33.70	24.73
MNO	0.42	0.25	0.56	0.52	0.51	0.52	0.62	0.24
MGO	15.86	16.91	13.29	15.25	14.86	15.07	12.66	15.26
CAO	0.06	0.09	0.06	0.11	0.11	0.12	0.13	0.05
TOTAL	97.65	98.20	98.10	97.70	98.06	97.91	97.67	97.51
FEO	12.77	11.21	16.60	13.19	13.95	13.90	16.70	14.21
FE2O3	11.32	11.25	17.88	11.11	13.88	11.51	18.89	11.69
TOTAL	98.78	99.33	99.89	98.81	99.45	99.06	99.56	98.68

** ATOMIC PROPORTIONS BASED ON SELECTED NO. OF OXYGENS **

OXYGN	4	4	4	4	4	4	4	4
TI	0.041	0.049	0.058	0.047	0.045	0.042	0.051	0.076
AL	0.975	0.840	0.808	0.851	0.867	0.962	0.751	0.774
CR	0.686	0.803	0.656	0.795	0.722	0.689	0.697	0.798
FE2+	0.320	0.282	0.430	0.337	0.355	0.350	0.439	0.367
FE3+	0.256	0.255	0.416	0.256	0.318	0.261	0.447	0.272
MN	0.011	0.006	0.015	0.013	0.013	0.013	0.017	0.006
MG	0.709	0.759	0.613	0.695	0.674	0.677	0.593	0.703
FFM	0.31	0.27	0.41	0.33	0.35	0.34	0.43	0.34
CCA	0.41	0.49	0.45	0.48	0.45	0.42	0.48	0.51
2TAC	0.05	0.06	0.07	0.05	0.05	0.05	0.07	0.09

**** SAMPLE DIRECTORY ****

OBS	NO	MINSPENO	ANALPOS	OBS	NO	MINSPENO	ANALPOS
105	191	SPI/005/001	C	106	191	SPI/006/001	C
107	191	SPI/007/001	C	108	191	SPI/008/001	C
109	191	SPI/009/001	C	110	191	SPI/010/001	C
111	191	SPI/011/001	C	112	191	SPI/012/001	C

APPENDIX 6
SPINEL ANALYSES

OBS	113	114	115	116	117	118	119	120
SIO2	0.14	0.29	0.15	0.13	0.01	0.24	0.20	0.05
TIO2	4.06	2.09	3.43	5.02	3.51	22.21	21.86	21.97
AL2O3	22.20	21.06	19.66	16.05	20.23	1.06	1.08	1.40
CR2O3	28.83	30.25	34.26	27.09	29.12	0.09	0.08	0.08
FEOT	26.72	30.55	23.96	39.64	34.78	70.26	70.64	70.84
MNO	0.14	0.56	0.32	0.30	0.29	1.02	1.07	0.98
MGO	15.02	13.17	15.68	8.76	9.36	1.81	1.63	1.81
CAO	0.06	0.15	0.08	0.07	0.07	0.33	0.29	0.18
TOTAL	97.17	98.12	97.54	97.06	97.37	97.02	96.85	97.31
FEO	15.52	16.43	13.46	24.85	23.12	47.84	47.70	47.75
FE2O3	12.44	15.70	11.67	16.44	12.95	24.92	25.49	25.66
TOTAL	98.42	99.69	98.71	98.71	98.67	99.52	99.40	99.88

** ATOMIC PROPORTIONS BASED ON SELECTED NO. OF OXYGENS **

OXYGN	4	4	4	4	4	4	4	4
TI	0.094	0.049	0.080	0.125	0.085	0.619	0.611	0.610
AL	0.809	0.773	0.719	0.625	0.770	0.046	0.047	0.061
CR	0.704	0.744	0.840	0.708	0.744	0.003	0.002	0.002
FE2+	0.401	0.427	0.349	0.687	0.625	1.483	1.483	1.475
FE3+	0.289	0.368	0.272	0.409	0.315	0.695	0.713	0.713
MN	0.004	0.015	0.008	0.008	0.008	0.032	0.034	0.031
MG	0.692	0.611	0.725	0.431	0.451	0.100	0.090	0.100
FFM	0.37	0.41	0.33	0.61	0.58	0.94	0.94	0.94
CCA	0.47	0.49	0.54	0.53	0.49	0.05	0.05	0.04
2TAC	0.11	0.06	0.09	0.16	0.10	0.96	0.96	0.95

**** SAMPLE DIRECTORY ****

OBS	NO	MINSPENO	ANALPOS	OBS	NO	MINSPENO	ANALPOS
113	191	SPI/013/001	C	114	191	SPI/014/001	C
115	191	SPI/015/001	C	116	192	SPI/001/001	C
117	192	SPI/002/001	C	118	192	SPI/003/001	C
119	192	SPI/004/001	C	120	192	SPI/005/001	C

APPENDIX 6
SPINEL ANALYSES

OBS	121	122	123	124	125	126	127	128
SIO2	0.54	0.11	0.51	0.65	0.19	0.26	0.03	0.01
TIO2	21.26	21.26	21.30	20.92	21.38	21.38	18.12	17.87
AL2O3	1.13	1.21	1.57	1.40	1.48	1.27	2.48	3.49
CR2O3	0.09	0.09	0.09	0.19	0.15	0.12	2.61	4.61
FEOT	70.60	71.58	69.74	70.13	70.78	70.03	71.28	67.73
MNO	0.98	0.99	0.96	0.97	0.82	0.77	0.59	0.53
MGO	1.55	1.56	1.86	1.99	1.89	1.78	2.17	3.86
CAO	0.53	0.17	0.48	0.58	0.27	0.45	0.13	0.06
TOTAL	96.68	96.97	96.51	96.83	96.96	96.06	97.41	98.16
FEO	47.49	47.46	47.10	46.70	47.24	47.01	44.43	42.12
FE2O3	25.69	26.81	25.17	26.04	26.16	25.59	29.84	28.47
TOTAL	99.25	99.66	99.03	99.44	99.58	98.62	100.40	101.01

** ATOMIC PROPORTIONS BASED ON SELECTED NO. OF OXYGENS **

OXYGN	4	4	4	4	4	4	4	4
TI	0.594	0.594	0.594	0.581	0.595	0.601	0.498	0.479
AL	0.050	0.053	0.069	0.061	0.065	0.056	0.107	0.147
CR	0.003	0.003	0.003	0.006	0.004	0.004	0.075	0.130
FE2+	1.477	1.473	1.461	1.442	1.461	1.469	1.357	1.256
FE3+	0.719	0.749	0.702	0.724	0.728	0.719	0.820	0.764
MN	0.031	0.031	0.030	0.030	0.026	0.024	0.018	0.016
MG	0.086	0.086	0.103	0.110	0.104	0.099	0.118	0.205
FFM	0.95	0.94	0.93	0.93	0.93	0.94	0.92	0.86
CCA	0.05	0.05	0.04	0.08	0.06	0.06	0.41	0.47
2TAC	0.96	0.96	0.94	0.95	0.95	0.95	0.85	0.78

**** SAMPLE DIRECTORY ****

OBS	NO	MINSPENO	ANALPOS	OBS	NO	MINSPENO	ANALPOS
121	192	SPI/006/001	C	122	192	SPI/007/001	C
123	192	SPI/008/001	C	124	192	SPI/009/001	C
125	192	SPI/010/001	C	126	192	SPI/011/001	C
127	192	SPI/012/001	C	128	192	SPI/013/001	C

APPENDIX 6
SPINEL ANALYSES

OBS	129	130	131	132	133	134	135	136
SIO2	0.05	0.06	0.26	0.20	0.33	0.24	0.00	0.00
TIO2	16.49	21.80	20.27	20.28	20.36	19.81	1.85	1.66
AL2O3	4.14	0.88	3.22	3.13	3.22	3.41	27.48	32.63
CR2O3	7.51	0.00	0.32	0.39	0.29	0.28	32.16	27.46
FEOT	65.27	70.79	69.09	69.07	68.86	69.08	19.89	18.78
MNO	0.52	0.81	0.61	0.55	0.67	0.63	0.51	0.25
MGO	4.05	1.84	2.55	2.52	2.50	2.47	16.05	17.09
CAO	0.11	0.05	0.22	0.20	0.30	0.32	0.04	0.13
TOTAL	98.14	96.23	96.54	96.34	96.53	96.24	97.98	98.00
FEO	40.66	47.47	45.73	45.72	45.82	45.22	12.45	11.65
FE2O3	27.35	25.92	25.96	25.96	25.61	26.52	8.27	7.92
TOTAL	100.88	98.83	99.14	98.94	99.10	98.90	98.81	98.79

** ATOMIC PROPORTIONS BASED ON SELECTED NO. OF OXYGENS **

OXYGN	4	4	4	4	4	4	4	4
TI	0.441	0.613	0.558	0.560	0.561	0.547	0.042	0.036
AL	0.173	0.039	0.139	0.136	0.139	0.148	0.970	1.121
CR	0.211	0.000	0.009	0.011	0.008	0.008	0.761	0.633
FE2+	1.208	1.485	1.401	1.405	1.404	1.388	0.312	0.284
FE3+	0.731	0.730	0.716	0.718	0.706	0.733	0.186	0.174
MN	0.016	0.026	0.019	0.017	0.021	0.020	0.013	0.006
MG	0.214	0.103	0.139	0.138	0.137	0.135	0.716	0.742
FFM	0.85	0.94	0.91	0.91	0.91	0.91	0.30	0.28
CCA	0.55	0.00	0.06	0.08	0.06	0.05	0.44	0.36
2TAC	0.70	0.97	0.88	0.88	0.88	0.88	0.05	0.04

**** SAMPLE DIRECTORY ****

OBS	NO	MINSPENO	ANALPOS	OBS	NO	MINSPENO	ANALPOS
129	192	SPI/014/001	C	130	192	SPI/015/001	C
131	192	SPI/016/001	I	132	192	SPI/016/002	I
133	192	SPI/016/003	I	134	192	SPI/016/004	I
135	205	SPI/001/001	C	136	205	SPI/002/001	C

APPENDIX 6
SPINEL ANALYSES

OBS	137	138	139	140	141	142	143	144
SIO2	0.00	0.00	0.00	0.00	0.00	0.00	0.08	0.00
TIO2	1.85	1.86	3.17	1.78	1.78	9.00	9.01	1.65
AL2O3	33.32	25.92	28.49	30.32	27.44	1.52	0.36	23.45
CR2O3	25.87	33.68	16.18	29.69	32.60	2.40	0.41	36.66
FEOT	19.46	20.41	35.72	19.21	19.12	75.49	78.36	20.80
MNO	0.33	0.51	0.58	0.40	0.38	0.85	0.92	0.42
MGO	17.10	15.45	13.83	16.69	16.08	4.70	4.09	14.87
CAO	0.00	0.08	0.06	0.07	0.30	0.12	0.15	0.00
TOTAL	97.93	97.91	98.03	98.16	97.70	94.08	93.38	97.85
FEO	11.98	13.06	17.32	11.98	12.06	31.16	31.74	13.53
FE2O3	8.32	8.17	20.45	8.03	7.85	49.26	51.81	8.08
TOTAL	98.76	98.73	100.08	98.97	98.49	99.02	98.57	98.66

** ATOMIC PROPORTIONS BASED ON SELECTED NO. OF OXYGENS **

OXYGN	4	4	4	4	4	4	4	4
TI	0.040	0.042	0.072	0.039	0.040	0.249	0.254	0.038
AL	1.142	0.924	1.010	1.052	0.970	0.066	0.016	0.848
CR	0.595	0.805	0.384	0.691	0.773	0.070	0.012	0.889
FE2+	0.291	0.330	0.435	0.295	0.302	0.960	0.993	0.347
FE3+	0.182	0.186	0.463	0.178	0.177	1.365	1.459	0.186
MN	0.008	0.013	0.015	0.010	0.010	0.027	0.029	0.011
MG	0.741	0.696	0.620	0.732	0.719	0.258	0.228	0.680
FFM	0.28	0.32	0.41	0.29	0.30	0.79	0.81	0.34
CCA	0.34	0.47	0.28	0.40	0.44	0.51	0.43	0.51
2TAC	0.04	0.05	0.09	0.04	0.04	0.79	0.95	0.04

**** SAMPLE DIRECTORY ****

OBS	NO	MINSPENO	ANALPOS	OBS	NO	MINSPENO	ANALPOS
137	205	SPI/003/001	C	138	205	SPI/004/001	C
139	205	SPI/005/001	C	140	205	SPI/006/001	C
141	205	SPI/007/001	C	142	205	SPI/008/001	C
143	205	SPI/008/002	R	144	205	SPI/009/001	C

APPENDIX 6
SPINEL ANALYSES

OBS	145	146	147	148	149	150	151	152
SIO2	0.00	0.00	0.00	0.00	0.00	0.06	0.06	0.01
TIO2	1.70	1.86	1.51	1.90	1.88	3.20	1.71	2.17
AL2O3	30.51	30.73	34.15	21.71	28.48	19.52	18.31	30.18
CR2O3	29.74	29.32	25.33	38.60	31.12	33.14	42.92	27.25
FEOT	19.06	18.89	19.41	20.78	19.91	28.18	19.56	20.78
MNO	0.37	0.20	0.37	0.14	0.20	0.25	0.14	0.26
MGO	16.78	16.47	16.65	14.83	16.34	13.98	15.40	16.87
CAO	0.00	0.04	0.08	0.00	0.00	0.09	0.07	0.09
TOTAL	98.16	97.51	97.50	97.96	97.93	98.42	98.17	97.61
FEO	11.91	12.47	12.21	13.86	12.53	16.09	12.34	12.02
FE2O3	7.94	7.14	8.00	7.70	8.20	13.44	8.02	9.74
TOTAL	98.96	98.23	98.30	98.73	98.75	99.77	98.97	98.59

** ATOMIC PROPORTIONS BASED ON SELECTED NO. OF OXYGENS **

OXYGN	4	4	4	4	4	4	4	4
TI	0.038	0.041	0.033	0.044	0.042	0.075	0.040	0.048
AL	1.058	1.072	1.174	0.790	1.000	0.716	0.672	1.051
CR	0.691	0.686	0.584	0.942	0.732	0.815	1.056	0.636
FE2+	0.293	0.309	0.298	0.358	0.312	0.419	0.321	0.297
FE3+	0.176	0.159	0.176	0.179	0.184	0.315	0.188	0.216
MN	0.009	0.005	0.009	0.004	0.005	0.007	0.004	0.007
MG	0.735	0.726	0.724	0.683	0.725	0.648	0.714	0.742
FFM	0.28	0.30	0.29	0.34	0.30	0.39	0.31	0.29
CCA	0.40	0.39	0.33	0.54	0.42	0.53	0.61	0.38
2TAC	0.04	0.04	0.04	0.05	0.05	0.09	0.04	0.05

**** SAMPLE DIRECTORY ****

OBS	NO	MINSPENO	ANALPOS	OBS	NO	MINSPENO	ANALPOS
145	205	SPI/009/002	R	146	205	SPI/010/001	C
147	205	SPI/010/002	R	148	205	SPI/011/001	C
149	205	SPI/012/001	C	150	212	SPI/001/001	C
151	212	SPI/002/001	C	152	212	SPI/003/001	C

APPENDIX 6
SPINEL ANALYSES

OBS	153	154	155	156	157	158	159	160
SIO2	0.14	0.06	0.14	0.09	0.09	0.01	0.00	0.06
TIO2	1.87	3.11	2.00	1.94	2.13	1.91	4.67	1.86
AL2O3	26.71	19.62	29.62	24.15	21.19	28.78	13.94	23.93
CR2O3	32.05	35.63	28.21	34.06	38.03	30.17	32.32	35.73
FEOT	20.08	25.00	20.86	20.47	21.11	19.79	34.28	20.77
MNO	0.16	0.16	0.24	0.26	0.26	0.11	0.43	0.23
MGO	16.60	14.69	16.74	16.41	15.20	16.95	13.05	15.71
CAO	0.18	0.20	0.15	0.26	0.14	0.11	0.10	0.11
TOTAL	97.79	98.47	97.96	97.64	98.15	97.83	98.79	98.40
FEO	11.83	14.87	12.20	11.48	13.32	11.63	17.88	12.84
FE2O3	9.17	11.25	9.62	9.99	8.66	9.07	18.23	8.81
TOTAL	98.71	99.60	98.92	98.64	99.02	98.74	100.62	99.28

** ATOMIC PROPORTIONS BASED ON SELECTED NO. OF OXYGENS **

OXYGN	4	4	4	4	4	4	4	4
TI	0.042	0.072	0.044	0.044	0.049	0.043	0.112	0.042
AL	0.942	0.717	1.031	0.863	0.769	1.005	0.524	0.855
CR	0.758	0.873	0.658	0.816	0.926	0.707	0.815	0.856
FE2+	0.296	0.385	0.301	0.291	0.343	0.288	0.477	0.325
FE3+	0.207	0.262	0.214	0.228	0.201	0.202	0.437	0.201
MN	0.004	0.004	0.006	0.007	0.007	0.003	0.012	0.006
MG	0.740	0.678	0.736	0.741	0.698	0.748	0.620	0.709
FFM	0.29	0.36	0.29	0.28	0.33	0.28	0.43	0.31
CCA	0.45	0.55	0.39	0.49	0.55	0.41	0.61	0.50
2TAC	0.05	0.08	0.05	0.05	0.06	0.05	0.14	0.05

**** SAMPLE DIRECTORY ****

OBS	NO	MINSPENO	ANALPOS	OBS	NO	MINSPENO	ANALPOS
153	212	SPI/004/001	C	154	212	SPI/005/001	C
155	212	SPI/006/001	C	156	212	SPI/007/001	C
157	212	SPI/008/001	C	158	212	SPI/009/001	C
159	212	SPI/010/001	C	160	212	SPI/011/001	C

APPENDIX 6
SPINEL ANALYSES

OBS	161	162	163	164	165	166	167	168
SIO2	0.00	0.04	0.08	0.02	0.02	0.26	0.04	0.03
TIO2	3.15	3.14	1.75	9.79	12.40	9.45	9.71	10.19
AL2O3	23.89	19.93	22.23	5.57	5.23	4.33	4.69	4.96
CR2O3	29.49	32.92	37.52	0.29	0.48	0.42	0.93	0.47
FEOT	25.47	26.42	20.27	67.52	65.31	69.69	69.00	68.13
MNO	0.33	0.16	0.12	0.72	0.78	0.74	0.71	0.73
MGO	15.58	14.94	15.92	9.62	10.31	8.59	8.82	9.03
CAO	0.10	0.08	0.17	0.32	0.37	0.31	0.32	0.32
TOTAL	98.01	97.63	98.06	93.85	94.90	93.79	94.22	93.86
FEO	13.97	14.45	12.11	24.80	26.19	26.17	25.97	25.96
FE2O3	12.78	13.31	9.07	47.48	43.48	48.36	47.82	46.87
TOTAL	99.29	98.96	98.97	98.61	99.26	98.64	99.01	98.56

** ATOMIC PROPORTIONS BASED ON SELECTED NO. OF OXYGENS **

OXYGN	4	4	4	4	4	4	4	4
TI	0.072	0.073	0.040	0.257	0.322	0.251	0.257	0.269
AL	0.856	0.730	0.800	0.229	0.213	0.180	0.194	0.206
CR	0.708	0.809	0.906	0.008	0.013	0.012	0.026	0.013
FE2+	0.355	0.376	0.309	0.724	0.756	0.774	0.763	0.763
FE3+	0.292	0.311	0.208	1.247	1.129	1.287	1.264	1.240
MN	0.008	0.004	0.003	0.021	0.023	0.022	0.021	0.022
MG	0.705	0.692	0.725	0.500	0.530	0.453	0.462	0.473
FFM	0.33	0.35	0.30	0.59	0.59	0.63	0.62	0.62
CCA	0.45	0.53	0.53	0.03	0.06	0.06	0.12	0.06
2TAC	0.08	0.09	0.04	0.68	0.74	0.72	0.70	0.71

**** SAMPLE DIRECTORY ****

OBS	NO	MINSPENO	ANALPOS	OBS	NO	MINSPENO	ANALPOS
161	212	SPI/012/001	C	162	212	SPI/013/001	C
163	212	SPI/014/001	C	164	212	SPI/015/001	C
165	212	SPI/016/001	C	166	212	SPI/017/001	C
167	212	SPI/018/001	C	168	212	SPI/019/001	C

APPENDIX 6
SPINEL ANALYSES

OBS	169	170	171	172	173	174	175	176
SIO2	0.00	0.02	0.00	0.00	0.02	1.28	0.00	0.04
TIO2	8.30	10.74	11.00	10.56	11.45	10.53	10.27	11.53
AL2O3	3.00	1.27	5.07	6.39	5.10	3.10	7.21	5.15
CR2O3	0.80	0.44	0.80	0.23	0.54	0.40	0.25	0.54
FEOT	72.59	72.19	67.10	66.31	66.74	66.57	65.46	65.94
MNO	0.66	0.73	0.77	0.73	0.76	0.62	0.72	0.77
MGO	7.61	8.74	9.94	10.15	9.89	7.83	10.38	10.02
CAO	0.50	0.13	0.17	0.20	0.23	3.64	0.21	0.27
TOTAL	93.46	94.26	94.85	94.57	94.73	93.97	94.50	94.26
FEO	25.90	26.72	25.72	25.12	26.11	25.61	24.60	25.80
FE2O3	51.89	50.53	45.99	45.78	45.15	45.52	45.41	44.61
TOTAL	98.66	99.32	99.46	99.16	99.25	98.53	99.05	98.73

** ATOMIC PROPORTIONS BASED ON SELECTED NO. OF OXYGENS **

OXYGN	4	4	4	4	4	4	4	4
TI	0.224	0.288	0.286	0.274	0.299	0.280	0.265	0.302
AL	0.127	0.053	0.207	0.260	0.208	0.129	0.292	0.211
CR	0.023	0.012	0.022	0.006	0.015	0.011	0.007	0.015
FE2+	0.778	0.797	0.745	0.724	0.757	0.756	0.706	0.751
FE3+	1.402	1.356	1.198	1.187	1.178	1.210	1.172	1.168
MN	0.020	0.022	0.023	0.021	0.022	0.019	0.021	0.023
MG	0.407	0.465	0.513	0.521	0.511	0.412	0.531	0.520
FFM	0.66	0.63	0.59	0.58	0.60	0.65	0.57	0.59
CCA	0.15	0.19	0.10	0.02	0.07	0.08	0.02	0.07
2TAC	0.75	0.90	0.71	0.67	0.73	0.80	0.64	0.73

**** SAMPLE DIRECTORY ****

OBS	NO	MINSPENO	ANALPOS	OBS	NO	MINSPENO	ANALPOS
169	212	SPI/020/001	C	170	212	SPI/021/001	C
171	212	SPI/022/001	C	172	212	SPI/023/001	C
173	212	SPI/024/001	C	174	212	SPI/025/001	C
175	212	SPI/026/001	C	176	212	SPI/027/001	C

APPENDIX 6
SPINEL ANALYSES

OBS	177	178	179	180	181	182	183	184
SIO2	0.08	0.05	0.06	0.00	0.06	0.00	0.07	0.06
TIO2	11.72	10.64	10.05	10.10	10.64	9.52	10.88	10.38
AL2O3	1.25	1.02	1.20	0.84	1.17	2.15	6.21	0.79
CR2O3	0.24	1.30	0.76	1.26	0.57	4.61	4.04	0.42
FEOT	74.13	75.66	77.21	75.71	76.36	72.07	61.97	77.20
MNO	0.76	0.83	0.81	0.81	0.79	0.76	0.67	0.88
MGO	7.55	5.21	4.51	4.69	5.03	5.77	9.65	4.76
CAO	0.15	0.19	0.11	0.35	0.22	0.28	1.55	0.15
TOTAL	95.88	94.90	94.71	93.76	94.84	95.16	95.04	94.64
FEO	29.94	32.03	32.69	31.72	32.34	30.29	24.76	32.40
FE2O3	49.11	48.49	49.48	48.89	48.92	46.43	41.35	49.79
TOTAL	100.80	99.76	99.67	98.66	99.74	99.81	99.18	99.63

** ATOMIC PROPORTIONS BASED ON SELECTED NO. OF OXYGENS **

OXYGN	4	4	4	4	4	4	4	4
TI	0.313	0.292	0.277	0.281	0.292	0.258	0.281	0.287
AL	0.052	0.044	0.052	0.037	0.050	0.091	0.252	0.034
CR	0.007	0.037	0.022	0.037	0.016	0.131	0.110	0.012
FE2+	0.888	0.977	1.003	0.983	0.988	0.914	0.712	0.995
FE3+	1.310	1.331	1.367	1.363	1.344	1.260	1.070	1.376
MN	0.023	0.026	0.025	0.025	0.024	0.023	0.020	0.027
MG	0.399	0.283	0.247	0.259	0.274	0.310	0.495	0.261
FFM	0.69	0.78	0.80	0.79	0.78	0.75	0.59	0.79
CCA	0.11	0.46	0.30	0.50	0.25	0.59	0.30	0.26
2TAC	0.91	0.88	0.88	0.88	0.90	0.70	0.61	0.93

**** SAMPLE DIRECTORY ****

OBS	NO	MINSPENO	ANALPOS	OBS	NO	MINSPENO	ANALPOS
177	212	SPI/028/001	C	178	213	SPI/001/001	C
179	213	SPI/002/001	M	180	213	SPI/003/001	C
181	213	SPI/004/001	I	182	213	SPI/005/001	C
183	213	SPI/006/001	C	184	213	SPI/007/001	C

APPENDIX 6
SPINEL ANALYSES

OBS	185	186	187	188	189	190	191	192
SIO2	0.00	0.00	0.00	0.06	0.07	0.05	0.00	0.00
TIO2	7.72	8.78	10.46	10.07	10.49	10.55	1.81	1.76
AL2O3	6.47	5.56	0.98	0.61	1.31	1.28	27.87	33.26
CR2O3	10.08	4.13	1.02	0.29	0.56	0.54	29.47	26.05
FEOT	64.35	68.27	76.44	76.99	75.69	75.17	21.25	18.99
MNO	0.73	0.77	0.82	0.80	0.77	0.79	0.57	0.15
MGO	7.10	7.23	5.09	4.47	5.18	5.44	16.24	17.47
CAO	0.09	0.09	0.12	0.15	0.15	0.12	0.08	0.03
TOTAL	96.54	94.83	94.93	93.44	94.22	93.94	97.29	97.71
FEO	27.92	28.01	32.10	32.23	31.91	31.46	11.89	11.40
FE2O3	40.49	44.74	49.28	49.74	48.66	48.58	10.40	8.44
TOTAL	100.60	99.31	99.87	98.43	99.10	98.81	98.33	98.56

** ATOMIC PROPORTIONS BASED ON SELECTED NO. OF OXYGENS **

OXYGN	4	4	4	4	4	4	4	4
TI	0.201	0.233	0.287	0.282	0.289	0.291	0.041	0.038
AL	0.264	0.231	0.042	0.027	0.057	0.055	0.985	1.140
CR	0.276	0.115	0.029	0.009	0.016	0.016	0.699	0.599
FE2+	0.810	0.826	0.980	1.005	0.979	0.966	0.298	0.277
FE3+	1.057	1.188	1.354	1.395	1.343	1.342	0.235	0.185
MN	0.021	0.023	0.025	0.025	0.024	0.025	0.014	0.004
MG	0.367	0.380	0.277	0.248	0.283	0.298	0.726	0.757
FFM	0.69	0.68	0.78	0.80	0.78	0.76	0.29	0.27
CCA	0.51	0.33	0.41	0.24	0.22	0.22	0.41	0.34
2TAC	0.43	0.57	0.89	0.94	0.89	0.89	0.05	0.04

**** SAMPLE DIRECTORY ****

OBS	NO	MINSPENO	ANALPOS	OBS	NO	MINSPENO	ANALPOS
185	213	SPI/008/001	M	186	213	SPI/009/001	C
187	213	SPI/010/001	R	188	213	SPI/011/001	C
189	213	SPI/012/001	C	190	213	SPI/013/001	C
191	213	SPI/014/001	C	192	213	SPI/015/001	C

APPENDIX 6
SPINEL ANALYSES

OBS	193	194	195	196	197	198	199	200
SIO2	0.00	0.00	0.00	0.00	0.00	0.00	0.00	0.06
TIO2	1.90	1.77	1.96	1.78	1.89	3.76	10.86	10.27
AL2O3	32.69	29.62	28.96	29.32	26.38	18.82	1.14	0.89
CR2O3	25.88	29.98	30.64	30.67	33.15	30.22	0.30	0.88
FEOT	19.10	18.56	19.81	19.27	20.51	28.84	76.66	76.01
MNO	0.26	0.23	0.11	0.16	0.17	0.56	0.73	0.69
MGO	17.77	17.26	16.49	16.45	15.78	14.37	5.37	4.73
CAO	0.09	0.10	0.03	0.05	0.00	0.11	0.07	0.46
TOTAL	97.69	97.52	98.00	97.70	97.88	96.68	95.13	93.99
FEO	10.80	10.93	12.53	12.31	13.08	14.94	32.27	31.96
FE2O3	9.23	8.48	8.10	7.74	8.26	15.44	49.33	48.95
TOTAL	98.61	98.37	98.81	98.48	98.71	98.23	100.07	98.90

** ATOMIC PROPORTIONS BASED ON SELECTED NO. OF OXYGENS **

OXYGN	4	4	4	4	4	4	4	4
TI	0.042	0.039	0.044	0.040	0.043	0.089	0.297	0.285
AL	1.120	1.032	1.013	1.027	0.937	0.700	0.049	0.039
CR	0.595	0.701	0.719	0.720	0.790	0.754	0.009	0.026
FE2+	0.262	0.270	0.311	0.306	0.330	0.395	0.981	0.987
FE3+	0.202	0.189	0.181	0.173	0.187	0.367	1.349	1.361
MN	0.006	0.006	0.003	0.004	0.004	0.015	0.022	0.022
MG	0.770	0.760	0.729	0.728	0.709	0.676	0.291	0.260
FFM	0.25	0.26	0.30	0.30	0.32	0.37	0.77	0.79
CCA	0.35	0.40	0.42	0.41	0.46	0.52	0.15	0.40
2TAC	0.05	0.04	0.05	0.04	0.05	0.11	0.91	0.90

**** SAMPLE DIRECTORY ****

OBS	NO	MINSPENO	ANALPOS	OBS	NO	MINSPENO	ANALPOS
193	213	SPI/015/002	R	194	213	SPI/016/001	C
195	213	SPI/017/001	C	196	213	SPI/017/002	R
197	213	SPI/018/001	C	198	213	SPI/019/001	C
199	213	SPI/020/001	C	200	213	SPI/021/001	C

APPENDIX 6
SPINEL ANALYSES

OBS	201	202	203	204	205	206	207	208
SIO2	0.00	0.05	0.14	0.00	0.00	0.00	0.00	0.00
TIO2	3.68	10.88	10.46	1.71	1.70	1.72	2.71	2.83
AL2O3	18.78	1.27	1.11	25.26	30.49	29.99	29.04	23.70
CR2O3	31.58	1.06	2.17	35.04	29.78	30.15	27.69	32.24
FEOT	27.97	75.52	73.67	19.23	18.86	18.72	22.25	24.14
MNO	0.53	0.69	0.69	0.27	0.25	0.21	0.18	0.20
MGO	14.54	5.40	6.05	15.74	17.17	16.93	15.93	14.81
CAO	0.09	0.11	1.14	0.07	0.03	0.00	0.00	0.00
TOTAL	97.17	94.98	95.43	97.32	98.28	97.72	97.80	97.92
FEO	14.80	32.25	29.90	12.43	11.44	11.64	13.99	15.01
FE2O3	14.63	48.09	48.65	7.56	8.24	7.87	9.18	10.15
TOTAL	98.64	99.80	100.31	98.08	99.11	98.51	98.72	98.94

** ATOMIC PROPORTIONS BASED ON SELECTED NO. OF OXYGENS **

OXYGN	4	4	4	4	4	4	4	4
TI	0.087	0.298	0.283	0.039	0.037	0.038	0.061	0.065
AL	0.696	0.054	0.047	0.906	1.053	1.044	1.020	0.855
CR	0.784	0.030	0.062	0.843	0.690	0.704	0.652	0.780
FE2+	0.389	0.981	0.899	0.316	0.280	0.288	0.349	0.384
FE3+	0.346	1.316	1.316	0.173	0.182	0.175	0.206	0.234
MN	0.014	0.021	0.021	0.007	0.006	0.005	0.005	0.005
MG	0.681	0.293	0.324	0.714	0.750	0.745	0.708	0.676
FFM	0.36	0.77	0.73	0.31	0.27	0.28	0.33	0.36
CCA	0.53	0.36	0.57	0.48	0.40	0.40	0.39	0.48
2TAC	0.11	0.88	0.84	0.04	0.04	0.04	0.07	0.07

**** SAMPLE DIRECTORY ****

OBS	NO	MINSPENO	ANALPOS	OBS	NO	MINSPENO	ANALPOS
201	213	SPI/022/001	C	202	213	SPI/023/001	C
203	213	SPI/024/001	C	204	213	SPI/025/001	C
205	213	SPI/026/001	C	206	213	SPI/026/002	R
207	256	SPI/001/001	C	208	256	SPI/002/001	C

APPENDIX 6
SPINEL ANALYSES

OBS	209	210	211	212	213	214	215	216
SIO2	0.00	0.00	0.00	0.00	0.00	0.09	0.00	0.00
TIO2	2.85	3.09	3.19	2.38	2.26	19.60	18.11	16.40
AL2O3	23.68	21.47	21.07	27.35	25.33	0.95	1.02	0.99
CR2O3	32.36	32.64	33.24	28.66	31.38	0.00	0.00	0.00
FEOT	24.43	25.69	25.90	24.58	23.79	68.93	70.36	71.93
MNO	0.22	0.27	0.19	0.29	0.23	1.03	1.07	0.96
MGO	14.77	13.98	13.97	15.15	14.83	6.61	6.29	5.83
CAO	0.00	0.00	0.00	0.00	0.00	0.14	0.15	0.28
TOTAL	98.31	97.14	97.56	98.41	97.82	97.35	97.00	96.39
FEO	15.19	15.85	16.11	14.73	14.66	38.40	37.32	36.29
FE2O3	10.27	10.94	10.88	10.94	10.15	33.93	36.72	39.61
TOTAL	99.34	98.24	98.65	99.51	98.84	100.75	100.68	100.36

** ATOMIC PROPORTIONS BASED ON SELECTED NO. OF OXYGENS **

OXYGN	4	4	4	4	4	4	4	4
TI	0.065	0.073	0.075	0.054	0.052	0.524	0.486	0.443
AL	0.852	0.791	0.775	0.967	0.909	0.040	0.043	0.042
CR	0.781	0.806	0.820	0.679	0.755	0.000	0.000	0.000
FE2+	0.388	0.414	0.420	0.369	0.373	1.141	1.113	1.091
FE3+	0.236	0.257	0.256	0.247	0.233	0.907	0.986	1.071
MN	0.006	0.007	0.005	0.007	0.006	0.031	0.032	0.029
MG	0.672	0.651	0.650	0.677	0.673	0.350	0.334	0.312
FFM	0.37	0.39	0.39	0.35	0.36	0.77	0.77	0.78
CCA	0.48	0.50	0.51	0.41	0.45	0.00	0.00	0.00
2TAC	0.07	0.08	0.09	0.06	0.06	0.96	0.96	0.95

**** SAMPLE DIRECTORY ****

OBS	NO	MINSPENO	ANALPOS	OBS	NO	MINSPENO	ANALPOS
209	256	SPI/002/002	I	210	256	SPI/003/001	R
211	256	SPI/004/001	C	212	256	SPI/005/001	C
213	256	SPI/005/002	R	214	259	SPI/001/001	C
215	259	SPI/001/002	I	216	259	SPI/001/003	R

APPENDIX 6
SPINEL ANALYSES

OBS	217	218	219	220	221	222	223	224
SIO2	0.00	0.00	0.00	0.00	0.00	0.00	0.00	0.00
TIO2	3.58	2.45	2.55	3.52	3.38	2.57	2.58	2.86
AL2O3	19.86	21.29	22.25	18.95	17.70	21.60	21.99	21.40
CR2O3	29.82	34.85	31.78	32.48	26.69	32.50	32.72	30.15
FEOT	33.29	27.66	29.84	31.67	39.95	29.84	28.71	31.86
MNO	0.79	0.72	0.75	0.70	0.78	0.67	0.70	0.84
MGO	10.10	11.36	10.65	10.13	9.19	10.55	11.12	10.49
CAO	0.04	0.00	0.00	0.03	0.05	0.04	0.00	0.03
TOTAL	97.48	98.33	97.82	97.48	97.74	97.77	97.82	97.63
FEO	21.55	19.16	20.31	21.38	22.61	20.40	19.62	20.55
FE2O3	13.05	9.45	10.59	11.43	19.27	10.49	10.10	12.57
TOTAL	98.79	99.28	98.88	98.63	99.67	98.82	98.83	98.89

** ATOMIC PROPORTIONS BASED ON SELECTED NO. OF OXYGENS **

OXYGN	4	4	4	4	4	4	4	4
TI	0.087	0.058	0.061	0.086	0.083	0.061	0.061	0.068
AL	0.753	0.791	0.831	0.722	0.678	0.809	0.819	0.803
CR	0.758	0.869	0.796	0.829	0.686	0.817	0.818	0.759
FE2+	0.580	0.505	0.538	0.578	0.614	0.542	0.519	0.547
FE3+	0.316	0.224	0.252	0.278	0.471	0.251	0.240	0.301
MN	0.022	0.019	0.020	0.019	0.021	0.018	0.019	0.023
MG	0.484	0.534	0.503	0.488	0.445	0.500	0.524	0.498
FFM	0.54	0.49	0.52	0.54	0.58	0.52	0.50	0.52
CCA	0.50	0.52	0.49	0.53	0.50	0.50	0.50	0.49
2TAC	0.10	0.07	0.07	0.10	0.11	0.07	0.07	0.08

**** SAMPLE DIRECTORY ****

OBS	NO	MINSPENO	ANALPOS	OBS	NO	MINSPENO	ANALPOS
217	259	SPI/002/001	C	218	259	SPI/003/001	C
219	259	SPI/004/001	C	220	259	SPI/005/001	C
221	259	SPI/006/001	C	222	259	SPI/007/001	C
223	259	SPI/008/001	C	224	259	SPI/009/001	C

APPENDIX 6
SPINEL ANALYSES

OBS	225	226	227	228	229	230	231	232
SIO2	0.00	0.00	0.00	0.00	0.07	0.00	0.00	0.00
TIO2	3.36	2.96	14.14	12.53	14.79	11.94	12.30	2.36
AL2O3	22.52	18.86	1.08	1.11	0.89	1.42	1.26	23.82
CR2O3	29.78	30.45	2.94	6.85	0.73	8.34	7.81	33.36
FEOT	30.88	34.62	71.09	68.68	72.00	66.91	67.69	24.08
MNO	0.64	0.80	0.90	1.01	0.93	0.90	0.90	0.28
MGO	11.23	9.61	5.54	5.61	5.58	5.74	5.60	13.96
CAO	0.00	0.00	0.07	0.12	0.20	0.07	0.09	0.06
TOTAL	98.41	97.30	95.76	95.91	95.19	95.32	95.65	97.92
FEO	20.51	21.59	34.84	33.15	35.07	32.43	33.03	15.74
FE2O3	11.52	14.48	40.29	39.49	41.05	38.32	38.52	9.27
TOTAL	99.56	98.75	99.80	99.87	99.30	99.16	99.51	98.85

** ATOMIC PROPORTIONS BASED ON SELECTED NO. OF OXYGENS **

OXYGN	4	4	4	4	4	4	4	4
TI	0.079	0.072	0.385	0.341	0.405	0.326	0.335	0.055
AL	0.832	0.721	0.046	0.047	0.038	0.061	0.054	0.864
CR	0.738	0.781	0.084	0.196	0.021	0.239	0.224	0.812
FE2+	0.538	0.586	1.056	1.003	1.068	0.985	1.002	0.405
FE3+	0.272	0.354	1.099	1.075	1.125	1.047	1.051	0.215
MN	0.017	0.022	0.028	0.031	0.029	0.028	0.028	0.007
MG	0.525	0.465	0.299	0.302	0.303	0.311	0.303	0.640
FFM	0.51	0.56	0.78	0.77	0.78	0.76	0.77	0.39
CCA	0.47	0.52	0.65	0.81	0.35	0.80	0.81	0.48
2TAC	0.09	0.09	0.86	0.74	0.93	0.68	0.71	0.06

**** SAMPLE DIRECTORY ****

OBS	NO	MINSPENO	ANALPOS	OBS	NO	MINSPENO	ANALPOS
225	259	SPI/010/001	C	226	259	SPI/011/001	C
227	259	SPI/011/002	MI	228	259	SPI/012/001	C
229	259	SPI/013/001	C	230	259	SPI/014/001	C
231	259	SPI/015/001	C	232	259	SPI/016/001	C

APPENDIX 6
SPINEL ANALYSES

OBS	233	234	235	236	237	238	239	240
SIO2	0.00	0.00	0.00	0.00	0.00	0.00	0.07	0.00
TIO2	3.13	2.71	3.09	2.18	3.11	14.96	14.81	2.28
AL2O3	22.98	22.24	24.04	24.47	25.42	0.89	0.86	24.54
CR2O3	29.10	31.60	26.76	34.14	27.87	0.32	0.23	33.77
FEOT	30.28	29.34	31.42	22.98	29.23	73.02	73.16	22.81
MNO	0.64	0.67	0.69	0.27	0.61	0.93	0.89	0.18
MGO	11.60	11.01	11.49	14.25	12.10	5.48	5.42	14.51
CAO	0.00	0.00	0.04	0.00	0.00	0.11	0.20	0.00
TOTAL	97.73	97.57	97.53	98.29	98.34	95.71	95.64	98.09
FEO	19.60	19.90	19.76	15.42	19.41	35.56	35.52	15.15
FE2O3	11.87	10.49	12.96	8.40	10.91	41.63	41.83	8.51
TOTAL	98.92	98.62	98.83	99.13	99.43	99.88	99.83	98.94

** ATOMIC PROPORTIONS BASED ON SELECTED NO. OF OXYGENS **

OXYGN	4	4	4	4	4	4	4	4
TI	0.074	0.065	0.073	0.050	0.072	0.408	0.404	0.052
AL	0.850	0.830	0.887	0.882	0.924	0.038	0.037	0.884
CR	0.722	0.791	0.662	0.825	0.679	0.009	0.007	0.816
FE2+	0.514	0.527	0.517	0.394	0.500	1.079	1.079	0.387
FE3+	0.280	0.250	0.305	0.193	0.253	1.136	1.143	0.196
MN	0.017	0.018	0.018	0.007	0.016	0.029	0.027	0.005
MG	0.542	0.520	0.536	0.649	0.556	0.296	0.293	0.661
FFM	0.49	0.50	0.49	0.38	0.47	0.78	0.79	0.37
CCA	0.46	0.49	0.43	0.48	0.42	0.19	0.15	0.48
2TAC	0.09	0.07	0.09	0.06	0.08	0.95	0.95	0.06

**** SAMPLE DIRECTORY ****

OBS	NO	MINSPENO	ANALPOS	OBS	NO	MINSPENO	ANALPOS
233	259	SPI/016/002	R	234	259	SPI/017/001	C
235	259	SPI/017/002	R	236	259	SPI/018/001	C
237	259	SPI/018/002	R	238	259	SPI/019/001	C
239	259	SPI/019/002	R	240	259	SPI/021/001	C

APPENDIX 6
SPINEL ANALYSES

OBS	241	242	243	244	245	246	247	248
SIO2	0.00	0.00	0.00	0.00	0.00	0.00	0.00	0.00
TIO2	2.16	2.17	3.61	3.67	2.53	2.43	2.25	2.61
AL2O3	24.32	23.77	22.30	23.96	25.17	23.90	24.75	23.81
CR2O3	33.39	32.89	30.59	28.35	26.96	27.94	33.44	30.44
FEOT	23.73	25.20	28.19	27.98	28.31	28.07	22.73	27.33
MNO	0.21	0.24	0.24	0.25	0.29	0.30	0.28	0.50
MGO	14.54	13.76	13.62	13.98	15.18	15.07	14.63	13.29
CAO	0.00	0.04	0.00	0.00	0.00	0.03	0.00	0.00
TOTAL	98.35	98.07	98.55	98.19	98.44	97.74	98.08	97.98
FEO	15.03	15.99	17.50	17.14	14.56	14.17	14.87	16.89
FE2O3	9.67	10.23	11.88	12.05	15.28	15.45	8.73	11.60
TOTAL	99.32	99.10	99.74	99.40	99.97	99.29	98.96	99.14

** ATOMIC PROPORTIONS BASED ON SELECTED NO. OF OXYGENS **

OXYGN	4	4	4	4	4	4	4	4
TI	0.050	0.050	0.084	0.085	0.057	0.056	0.052	0.061
AL	0.874	0.862	0.811	0.866	0.895	0.860	0.890	0.867
CR	0.805	0.800	0.746	0.687	0.643	0.674	0.806	0.743
FE2+	0.383	0.412	0.451	0.439	0.367	0.362	0.379	0.436
FE3+	0.222	0.237	0.276	0.278	0.347	0.355	0.200	0.269
MN	0.005	0.006	0.006	0.006	0.007	0.008	0.007	0.013
MG	0.661	0.631	0.626	0.639	0.683	0.685	0.665	0.611
FFM	0.37	0.39	0.42	0.41	0.35	0.35	0.36	0.42
CCA	0.48	0.48	0.48	0.44	0.42	0.44	0.48	0.46
2TAC	0.06	0.06	0.10	0.10	0.07	0.07	0.06	0.07

**** SAMPLE DIRECTORY ****

OBS	NO	MINSPENO	ANALPOS	OBS	NO	MINSPENO	ANALPOS
241	259	SPI/021/002	R	242	259	SPI/022/001	I
243	259	SPI/023/001	C	244	259	SPI/023/002	R
245	259	SPI/024/001	C	246	259	SPI/024/002	R
247	259	SPI/025/001	C	248	259	SPI/025/002	R

APPENDIX 6
SPINEL ANALYSES

OBS	249	250	251	252	253	254	255	256
SIO2	0.00	0.06	0.00	0.00	0.00	0.00	0.00	0.00
TIO2	8.48	16.69	12.25	12.41	15.89	2.10	7.02	12.19
AL2O3	13.25	4.64	9.64	9.68	6.71	21.31	11.23	6.75
CR2O3	14.59	1.39	6.79	7.73	1.35	30.13	22.57	9.06
FEOT	54.29	68.40	63.22	61.53	67.73	34.94	49.10	62.42
MNO	0.70	0.82	0.73	0.75	0.73	0.58	0.75	0.89
MGO	5.74	3.72	4.36	4.61	3.91	8.68	6.17	4.81
CAO	0.00	0.13	0.00	0.06	0.14	0.08	0.03	0.04
TOTAL	97.05	95.85	96.99	96.77	96.46	97.82	96.87	96.16
FEO	31.80	40.44	36.76	36.34	39.95	22.90	29.31	35.10
FE2O3	25.00	31.07	29.41	28.00	30.87	13.38	21.99	30.36
TOTAL	99.56	98.96	99.94	99.58	99.55	99.16	99.07	99.20

** ATOMIC PROPORTIONS BASED ON SELECTED NO. OF OXYGENS **

OXYGN	4	4	4	4	4	4	4	4
TI	0.217	0.455	0.322	0.326	0.426	0.051	0.181	0.326
AL	0.532	0.198	0.397	0.399	0.282	0.808	0.455	0.283
CR	0.393	0.040	0.187	0.213	0.038	0.766	0.613	0.254
FE2+	0.906	1.226	1.073	1.062	1.191	0.616	0.842	1.043
FE3+	0.641	0.848	0.773	0.736	0.828	0.324	0.569	0.812
MN	0.020	0.025	0.022	0.022	0.022	0.016	0.022	0.027
MG	0.291	0.201	0.227	0.240	0.208	0.416	0.316	0.255
FFM	0.76	0.86	0.83	0.82	0.85	0.60	0.73	0.80
CCA	0.42	0.17	0.32	0.35	0.12	0.49	0.57	0.47
2TAC	0.32	0.79	0.52	0.52	0.73	0.06	0.25	0.55

**** SAMPLE DIRECTORY ****

OBS	NO	MINSPENO	ANALPOS	OBS	NO	MINSPENO	ANALPOS
249	267	SPI/001/001	C	250	267	SPI/001/002	R
251	267	SPI/002/001	C	252	267	SPI/003/001	C
253	267	SPI/003/002	R	254	267	SPI/004/001	C
255	267	SPI/004/002	I	256	267	SPI/004/003	R

APPENDIX 6
SPINEL ANALYSES

OBS	257	258	259	260	261	262	263	264
SIO2	0.00	0.00	0.00	0.00	0.00	0.00	0.05	0.00
TIO2	9.45	1.97	3.41	8.82	15.12	2.47	17.35	1.85
AL2O3	10.22	25.02	21.75	9.00	6.48	22.31	5.78	22.64
CR2O3	17.33	31.28	30.30	18.39	5.18	34.81	0.19	30.99
FEOT	54.01	24.77	29.13	54.18	63.08	25.46	68.07	32.12
MNO	0.74	0.24	0.20	0.61	0.75	0.21	0.67	0.50
MGO	5.95	14.45	12.92	6.19	5.56	13.19	4.30	9.86
CAO	0.04	0.04	0.05	0.11	0.00	0.00	0.05	0.08
TOTAL	97.74	97.77	97.76	97.30	96.17	98.45	96.46	98.04
FEO	31.99	14.87	18.04	30.80	36.72	17.09	40.74	21.21
FE2O3	24.47	11.00	12.33	25.99	29.30	9.30	30.37	12.13
TOTAL	100.19	98.87	99.00	99.90	99.11	99.38	99.50	99.26

** ATOMIC PROPORTIONS BASED ON SELECTED NO. OF OXYGENS **

OXYGN	4	4	4	4	4	4	4	4
TI	0.243	0.045	0.080	0.229	0.402	0.058	0.466	0.044
AL	0.413	0.901	0.801	0.366	0.270	0.815	0.243	0.846
CR	0.469	0.755	0.749	0.502	0.145	0.853	0.005	0.777
FE2+	0.917	0.380	0.471	0.889	1.087	0.443	1.217	0.562
FE3+	0.631	0.253	0.290	0.675	0.780	0.217	0.816	0.289
MN	0.021	0.006	0.005	0.018	0.022	0.006	0.020	0.013
MG	0.304	0.658	0.602	0.318	0.293	0.609	0.229	0.466
FFM	0.75	0.37	0.44	0.74	0.79	0.42	0.84	0.55
CCA	0.53	0.46	0.48	0.58	0.35	0.51	0.02	0.48
2TAC	0.36	0.05	0.09	0.35	0.66	0.06	0.79	0.05

**** SAMPLE DIRECTORY ****

OBS	NO	MINSPENO	ANALPOS	OBS	NO	MINSPENO	ANALPOS
257	267	SPI/005/001	C	258	267	SPI/006/001	C
259	267	SPI/007/001	C	260	267	SPI/008/001	C
261	267	SPI/009/001	M	262	267	SPI/010/001	C
263	267	SPI/011/001	C	264	267	SPI/012/001	C

APPENDIX 6
SPINEL ANALYSES

OBS	265	266	267	268	269	270	271	272
SIO2	0.57	0.00	0.00	0.00	0.00	0.21	0.00	0.10
TIO2	19.22	16.27	12.10	11.10	18.52	22.13	13.59	18.56
AL2O3	3.50	5.59	6.96	7.62	4.38	2.09	4.38	2.71
CR2O3	0.22	4.42	14.45	16.87	3.75	0.19	14.56	0.32
FEOT	66.94	66.02	57.71	55.78	65.84	67.69	59.29	71.21
MNO	0.78	0.70	0.77	0.78	0.79	1.10	0.70	0.83
MGO	3.90	4.40	4.72	4.86	4.17	2.65	4.95	2.75
CAO	0.68	0.17	0.18	0.14	0.25	0.20	0.09	0.33
TOTAL	95.81	97.57	96.89	97.15	97.70	96.26	97.56	96.81
FEO	42.24	39.69	35.29	34.38	41.69	46.41	36.27	43.41
FE2O3	27.45	29.26	24.92	23.79	26.84	23.65	25.58	30.89
TOTAL	98.56	100.50	99.39	99.53	100.39	98.63	100.12	99.91

** ATOMIC PROPORTIONS BASED ON SELECTED NO. OF OXYGENS **

OXYGN	4	4	4	4	4	4	4	4
TI	0.526	0.433	0.322	0.293	0.496	0.615	0.363	0.509
AL	0.150	0.233	0.290	0.316	0.184	0.091	0.183	0.117
CR	0.006	0.124	0.404	0.469	0.106	0.006	0.408	0.009
FE2+	1.284	1.173	1.043	1.010	1.241	1.435	1.076	1.325
FE3+	0.751	0.778	0.663	0.629	0.719	0.658	0.683	0.848
MN	0.024	0.021	0.023	0.023	0.024	0.034	0.021	0.026
MG	0.211	0.232	0.249	0.255	0.221	0.146	0.262	0.150
FFM	0.86	0.84	0.81	0.80	0.85	0.91	0.80	0.90
CCA	0.04	0.35	0.58	0.60	0.36	0.06	0.69	0.07
2TAC	0.87	0.71	0.48	0.43	0.77	0.93	0.55	0.89

**** SAMPLE DIRECTORY ****

OBS	NO	MINSPENO	ANALPOS	OBS	NO	MINSPENO	ANALPOS
265	267	SPI/013/001	C	266	267	SPI/014/001	C
267	267	SPI/015/001	I	268	267	SPI/015/002	R
269	267	SPI/016/001	C	270	267	SPI/017/001	C
271	267	SPI/018/001	C	272	267	SPI/019/001	C

APPENDIX 6
SPINEL ANALYSES

OBS	273	274	275	276	277	278	279	280
SIO2	0.81	0.00	0.00	0.15	0.00	0.09	0.29	0.00
TIO2	18.83	2.44	16.41	19.89	7.11	15.13	21.64	12.88
AL2O3	4.42	24.18	5.65	0.79	9.48	4.79	2.55	5.86
CR2O3	0.00	31.47	1.20	0.00	26.72	12.17	0.24	14.72
FEOT	66.89	25.22	68.13	72.97	47.99	60.12	67.23	58.96
MNO	0.74	0.18	0.81	1.10	0.62	0.63	0.88	0.68
MGO	4.19	13.92	4.42	1.43	5.53	4.46	2.95	4.02
CAO	0.36	0.00	0.04	0.19	0.06	0.11	0.39	0.19
TOTAL	96.24	97.41	96.66	96.52	97.51	97.50	96.17	97.31
FEO	42.46	15.95	39.59	46.18	30.36	38.59	45.66	37.09
FE2O3	27.15	10.30	31.72	29.78	19.60	23.93	23.97	24.30
TOTAL	98.96	98.44	99.84	99.50	99.47	99.90	98.57	99.75

** ATOMIC PROPORTIONS BASED ON SELECTED NO. OF OXYGENS **

OXYGN	4	4	4	4	4	4	4	4
TI	0.510	0.057	0.439	0.559	0.185	0.405	0.599	0.345
AL	0.187	0.880	0.237	0.035	0.387	0.201	0.111	0.246
CR	0.000	0.768	0.034	0.000	0.732	0.342	0.007	0.414
FE2+	1.278	0.412	1.179	1.442	0.879	1.148	1.405	1.104
FE3+	0.735	0.239	0.850	0.837	0.511	0.641	0.664	0.651
MN	0.023	0.005	0.024	0.035	0.018	0.019	0.027	0.020
MG	0.225	0.640	0.235	0.080	0.285	0.237	0.162	0.213
FFM	0.85	0.39	0.83	0.95	0.75	0.83	0.90	0.84
CCA	0.00	0.47	0.12	0.00	0.65	0.63	0.06	0.63
2TAC	0.84	0.06	0.76	0.97	0.25	0.60	0.91	0.51

**** SAMPLE DIRECTORY ****

OBS	NO	MINSPENO	ANALPOS	OBS	NO	MINSPENO	ANALPOS
273	267	SPI/020/001	C	274	267	SPI/021/001	C
275	267	SPI/022/001	C	276	267	SPI/040/001	C
277	267	SPI/041/001	C	278	267	SPI/042/001	C
279	267	SPI/043/001	C	280	267	SPI/044/001	C

APPENDIX 6
SPINEL ANALYSES

OBS 281

SIO2	0.18
TIO2	22.40
AL2O3	1.76
CR2O3	0.16
FEOT	68.21
MNO	0.92
MGO	2.27
CAO	0.15
TOTAL	96.05
FEO	47.31
FE2O3	23.23
TOTAL	98.38

** ATOMIC PROPORTIONS BASED ON SELECTED NO. OF OXYGENS **

OXYGN 4

TI	0.627
AL	0.077
CR	0.005
FE2+	1.473
FE3+	0.651
MN	0.029
MG	0.126

FFM	0.92
CCA	0.06
2TAC	0.94

**** SAMPLE DIRECTORY ****

OBS	NO	MINSPENO	ANALPOS
281	267	SPI/045/001	C

APPENDIX 7

DETAILS OF SAMPLES COLLECTED FROM SUTHERLAND COMMONAGE

A RING DYKE

AREA 1

SAMPLE	DESCRIPTION
154	Highly vesicular
155	Glassy chill

AREA 2

SAMPLE	DESCRIPTION
156	Highly vesicular
256	Chill
257	Highly vesicular

AREA 3

SAMPLE	DESCRIPTION
159	Highly vesicular
160	Highly vesicular
258	Highly vesicular

AREA 4

SAMPLE	DESCRIPTION
161	Highly vesicular
162	Slightly vesicular
163	Chill

AREA 5

SAMPLE	DESCRIPTION
164	Chill
259	Chill

AREA 6

SAMPLE	DESCRIPTION
102	Slightly vesicular
103	Slightly vesicular
260	Slightly vesicular

AREA 7

SAMPLE	DESCRIPTION
92	Slightly vesicular
100	Slightly vesicular

AREA 8

SAMPLE	DESCRIPTION
73	Glassy chill
80	Slightly vesicular
83	Highly vesicular

AREA 9

SAMPLE	DESCRIPTION
30	Chill
33	Slightly vesicular
38	Highly vesicular
55	Chill
59	Chill
69	Chill

AREA 10

SAMPLE	DESCRIPTION
167	Chill
169	Chill

B SILL COMPLEX

SAMPLE	DESCRIPTION
9	Grey melilitite. De Beers collection
11	Grey melilitite. De Beers collection
14	Grey melilitite. De Beers collection
26	Grey melilitite. De Beers collection

AREA 11

SAMPLE	DESCRIPTION
178	Grey melilitite
179	Chill
180	Metasomatised siltstone

AREA 12

SAMPLE	DESCRIPTION
176	Grey melilitite

AREA 13

SAMPLE	DESCRIPTION
172	Grey melilitite
173	Baked shale

AREA 14

SAMPLE	DESCRIPTION
171	Grey melilitite

AREA 15

SAMPLE	DESCRIPTION
182	Grey melilitite
183	Green melilitite at contact with grey
185	Partially melted country rock
188	Partially melted country rock
191	Green melilitite
192	Olivine nephelinite
193	Green melilitite
195	Chill
196	Chill
197	Chill
267	Olivine nephelinite

AREA 16

SAMPLE	DESCRIPTION
205	Green melilitite
206	Green melilitite at contact with grey
207	Green melilitite at contact with grey
208	Green melilitite at contact with grey
209	Green melilitite at contact with grey
210	Grey melilitite
211	Grey melilitite
212	Grey melilitite
213	Green melilitite
261	Green melilitite
262	Green melilitite
263	Green melilitite at contact with grey

264	Green melilitite
265	Grey melilitite
266	Grey melilitite

5 JUN 1989

OUTCROP MAP OF THE SUTHERLAND COMMONAGE ALKALINE ULTRABASIC ROCKS

(MODIFIED FROM GERARD, 1958)

25 0 25 50 75 100 125 150 175 200 Metres

LEGEND

- Outcrop
- Loose float
- Brecciation
- Country rock
- Contact
- Concealed contact
- 102 Sample position

TOPOGRAPHICAL DATA

- Sandstone terrace
- Watercourse
- Road
- Marsh
- Bh1 Borehole

INSET MAP OF AREA 16

0 2 4 6 8 10 Metres

LEGEND

- Grey melilitite
- Green melilitite

AREA 1 154 155

AREA 2 156 256 257

AREA 3 159 160 258

AREA 4 163 161 162

AREA 5 164 259

AREA 6 102 103 260

AREA 7 92 100

AREA 8 73 80 83

AREA 9 30 33 38 55 59 69

AREA 10 167 169

AREA 11 178 179 180

AREA 12 176

AREA 13 173 172

AREA 14 171

AREA 15 182 183 192 267 185 188 191 193 195 196 197

AREA 16

Bh 1

Bh 2

FENCE

DAM